

THE GEOLOGY OF THE COUNTRY AROUND  
NETTOSETER, HÖYDALEN, NORWAY

by

D. R. COWAN, B.Sc.

THESIS TO BE SUMMITTED TO THE UNIVERSITY OF  
NOTTINGHAM FOR THE DEGREE OF DOCTOR OF  
PHILOSOPHY APRIL 1966



## **IMAGING SERVICES NORTH**

Boston Spa, Wetherby

West Yorkshire, LS23 7BQ

[www.bl.uk](http://www.bl.uk)

**BEST COPY AVAILABLE.**

**VARIABLE PRINT QUALITY**





## **IMAGING SERVICES NORTH**

Boston Spa, Wetherby

West Yorkshire, LS23 7BQ

[www.bl.uk](http://www.bl.uk)

**CONTAINS  
PULLOUTS**

# CONTENTS

## PART I

### CHAPTER 1

#### Introduction

	<u>Page</u>
(a) Location of area and topography	1
(b) Geological setting and history of research	2
(c) Aims of the present study	4
(d) Methods of working	4

### CHAPTER 2

#### Stratigraphy

(a) Introduction	6
(b) N. W. Basal Gneisses	8
(c) Sparagmite Group	8
(d) Eugeosynclinal succession	9
(e) Feldspathic quartzite Group	11
(f) Upper Jotun Nappe	12

### CHAPTER 3

#### Description of the Rock Groups

(a) Basal Gneiss Complex	13
(b) Sparagmite Group	17
(c) Psammite Group	20
(d) Lower Limestone-Pelite Group	27
(e) The Greenstone Group Part I	31
(f) The Greenstone Group Part II	47
(g) Thrust Rock Anorthosite	60

(h) The Upper Pelite Group	61
(i) The Upper Limestone Pelite Group	65
(j) The Feldspathic Quartzite Group	72
(k) The Upper Jotun Nappe	75
(l) Dunite Serpentinities	80

## PART II

	<u>Page</u>
<u>CHAPTER 4</u>	
<u>Structural Analysis</u>	101
(a) Introduction	101
(b) Pre-Cambrian	104
(c) 1st Caledonian De formation	105
(d) 2nd Caledonian De formation	109
(e) 3rd Caledonian De formation	113
(f) 4th Caledonian De formation	115
(g) 5th Caledonian De formation	115
(h) De formation of pre-existing structures by later folds	117
(i) Jointing	119
<u>CHAPTER 5</u>	
Phacoidal Quartzites	121
<u>CHAPTER 6</u>	
Quantitative Study of Fold Styles	136
<u>CHAPTER 7</u>	
Movement Picture and Tectonic synthesis	145
<u>CHAPTER 8</u>	
Theoretical	150
<u>CHAPTER 9</u>	
Metamorphic history	156
1. Metamorphic facies	156
2. Relations of metamorphism and structure	159
<u>CHAPTER 10</u>	
Geological History	162

CHAPTER 11

Regional Correlations	166
-----------------------	-----

PART III

CHAPTER 12

Mineralogy	175
------------	-----

CHAPTER 13

Laboratory Methods	182
--------------------	-----

BIBLIOGRAPHY	187
--------------	-----

ACKNOWLEDGEMENTS	193
------------------	-----

## CHAPTER 1.

## INTRODUCTION

### Location of area and topography

The Nettoseter area forms a part of the North-West Jotunheim mountains of Central Southern Norway. It is situated between the latitude of  $61^{\circ}37'$  and  $61^{\circ}47'$  north, longitude  $8^{\circ}05'40''$  and  $8^{\circ}20'$  east as shown in the locality map (fig. 1). The area mapped is approximately 80 sq. kms.

The area lies astride the main Lom-Sogndal road (route 55) and a small road runs along Høydalen.

The area mapped is covered by sheets 1518, 1 (Skjåk) and 1518, 11 (Vest Jotunheim) of the A. M. S. series 711 maps on a scale of 1:50,000. In addition aerial photograph coverage is provided on a scale of 1:48,000 by military aerial photographs.

The northern part of the area is within the Basal Gneiss Complex which consists here of foliated granites and gneisses. In the south of the area the Bergen-Jotun kindred of the Upper Jotun Nappe occurs. Between the Basal Gneisses and the Upper Jotun Nappe occur supracrustal rocks of probable Eo-Cambrian to Ordovician (?Silurian) age.

The Basal Gneiss Complex forms a mountainous region with peaks rising to over 2,000 metres (East Hestbrepiggan 2,100 metres). Several glaciers with large moraines and a large permafrost block-field occur in the area, but otherwise exposure is good.

The supracrustal rocks form an area of lower relief than the Basal Gneisses, although the topography is still rugged. Steep sided valleys and high cliffs occur and several high-level plateaus are found in the north. Exposure is variable on the valley sides; quite good on the high ground, but rather poor on the plateaus.

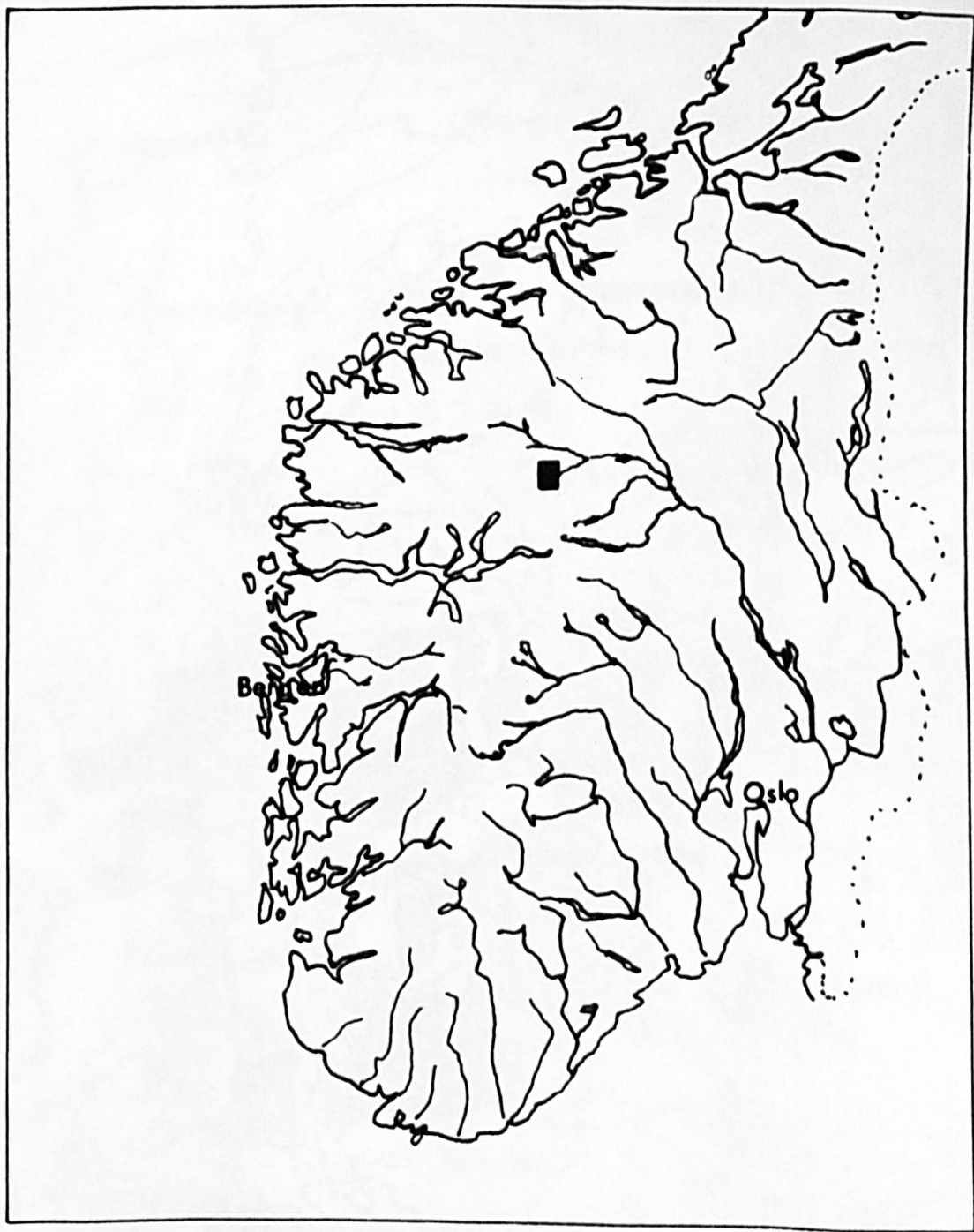


Fig.1. Location of the area. The black rectangle indicates the Skjåk and Vest Jotunheim map areas.



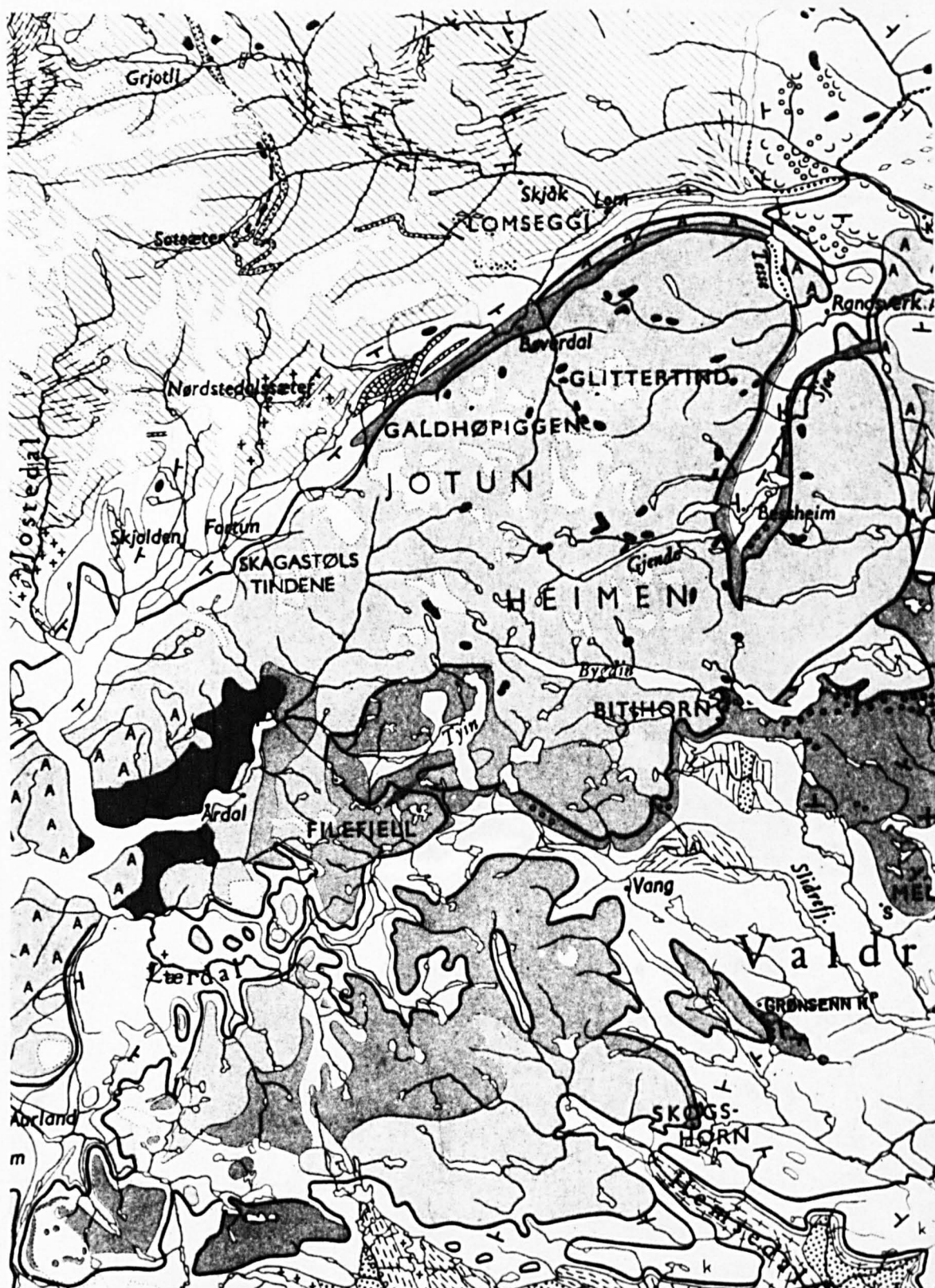


Fig 2 (from Holtedahl & Dons 1953).



Fig. 3 . General view of the area from Loftet, looking north. The Hestbrepiggan ridge is in the far distance.

The Upper Jotun Nappe forms the highest mountains in Norway. The granites, gabbros and gneisses have been eroded to a steep, rocky mountainous area with good exposure. The peaks rise to over 2,000 metres. Loftet is 2,170 metres.

Much of the area has been glaciated in historical times. Glacial retreat has been noted during the time the writer worked in the area.

### Geological setting and history of research

Briefly the Nettoseter area occupies a position between the N. W. Basal Gneiss Group and the "Internal Crystallines" of the Upper Jotun Nappe. This is part of a complex marginal thrust zone which is called the "Jotun Thrust Zone" by the present writer. A section from north to south in the area mapped, begins in the Basal Gneiss Complex, passes into the Eo-Cambrian Sparagmite, then a succession of Cambro-Ordovician rocks of western facies - eugeosynclinal (Trondheim facies), followed by feldspathic quartzites which may represent the Valdres Group and finally up into rocks of the Upper Jotun Nappe.

Prior to work by Nottingham students under Dr. R.B. Elliott the state of knowledge of the north-Jotunheim was portrayed by the 1:1,000,000 map of Norway (Holtedahl and Dons 1953) shown in fig. 2. The area was thought to consist of Basal Gneisses overlain by Sparagmite, then mica-schist of eastern (miogeosynclinal) facies, Valdres Group and Upper Jotun Nappe.

The present work has confirmed the presence of meta-volcanic rocks and demonstrated intrusion of alpine-type serpentinites and gabbros in the Cambro-Ordovician succession. Hence the Cambro-Ordovician succession has affinities with the western eugeosynclinal (Trondheim) facies rather than the miogeosynclinal facies as suggested by Strand (1964).

To the north and west of the present area occurs the



Fig. 4 . General view of the area, looking east.  
Holleindalen is in the middle distance.



Fig. 5 . Storhoe from the north-west. The joint  
pattern is shown by the nicks in the main ridge and  
the snow-filled gullies.

large area of the N. W. Basal Gneiss area and approximately 40 kms to the E. N. E. occurs the south-westerly extension of the Trondheim synclinorium into Gudbrandsdalen (Strand 1951).

Previous workers in the vicinity were Rekstad, Landmark, Strand and Gjelsvik.

Rekstad (1914) mapped a large area between Lysterfjord and Boverdalen. He divided the area into granite-gneisses, phyllites with limestone, sheared gneisses and gabbros. He also recorded the large ultrabasic body above Netto seter and described the Vassenden "conglomerate".

Landmark (1948) mapped between Luster i Sogn and Boverdalen. He recognised the following divisions from N. W. to S. E. across the area:

1. Granites and migmatites
2. Mica schist and limestone (presumably Cambro-Ordovician)
3. Highly deformed sparagmitic rocks (Valdres Sparagmite ?)
4. Eruptive rocks of the Bergen Jotun kindred. These were separated from the underlying divisions by a marked thrust plane.

In addition Landmark recognised that several phases of folding were involved. He described a N. E. - S. W. Caledonian main trend and a N. W. - S. E. "transverse trend" in the Groups 2 and 3 above. He thought that these structures were formed at the same time.

Strand (1949, 1951, 1964) mapped the Sel and Vågå<sup>o</sup> area, 40 kms to the east of the present area. He established a succession of meta-sedimentary and volcanic rocks lying between the Pre-Cambrian Gneiss area and the Upper Jotun Nappe. In 1964 he published a series of traverses towards the present area. Discussion of this work is considered in the chapter on regional correlations.

Peacey (in Strand 1964) undertook structural analysis of part of the Sel and Vågå area and found at least three phases of folding.

### Nottingham Workers

Three previous studies have been made in the Jotunheim by Nottingham workers.

1/M. M. Shouls (1958) The Sota synform several miles to the north of the present area. He found that the Sota synform was composed of thrust sheets and had a thrust at the base.

2/R. B. Elliott (1965) Høyøyen-Grønevatn area. He found a similar relationship to the above.

3/P. H. Banham (1962, 1965). Study of the Basal Gneisses and the contact with the supracrustal rocks to the north and west of the present area. Banham worked out the major structure of the Supracrustal rocks which he found to be isoclinal with an approximate N. E. - S. W. trend.

Studies by Nottingham workers had shown that the structure was complex and that several phases of folding were involved (Banham 1962, Banham and Elliott 1965), but no detailed structural analysis of the supracrustal rocks had been undertaken and nothing was known concerning the relationship of the Upper Jotun Nappe to the structure of the supracrustal rocks.

### Aims of the present study

The object of the present work was to study the structure, petrology and geochemistry of the rocks of the Jotun Thrust Zone around Netto seter-Boverdalen; in particular the relationship between the thrusting and folding and the relationship between the Basal Gneiss Thrust and the Upper Jotun Thrust.

### Methods of working

Field mapping was carried out in three consecutive field seasons. The summer season is short, but it was possible

to map for about 10-12 weeks so that a total of 32 weeks was spent in the field.

The major structure and the structural history of the area was determined using minor structures and modern structural techniques of fold interferences etc., such as those used by Ramsay (1957, 1958) and Turner and Weiss (1963).

A detailed study of several so-called 'quartzite conglomerates' was made.

#### Base Maps, etc.

As the existing maps were on too small a scale for detailed structural mapping, base maps had to be constructed. These were made by enlarging the 1:50,000 map optically to a scale of 1:20,000 and using the aerial photographs to correct the enlarged map.

The aerial photographs were used for location of outcrops.

## CHAPTER 2.



## STRATIGRAPHY

### Introduction

The rocks of the area mapped are an assemblage of medium to high grade gneisses, schists, quartzites and greenstones, in which no fossils have been found and from which no radiometric age determinations have been made. There is, therefore, no direct evidence of their age. However, correlation can be made with similar lithologies and sequences near Otta, where a rich Llanvirn fauna is recorded. From this and other geological considerations, it seems likely that rocks which range in age from Pre-Cambrian to Ordovician, or possibly Silurian, are represented here.

It has been found difficult to erect a stratigraphical succession which does not involve, in part, a structural succession; so that the sequence given below is based upon an interpretation of the tectonics which is fully discussed in the structural chapters.

The following units have been recognised:

### Pre-Cambrian

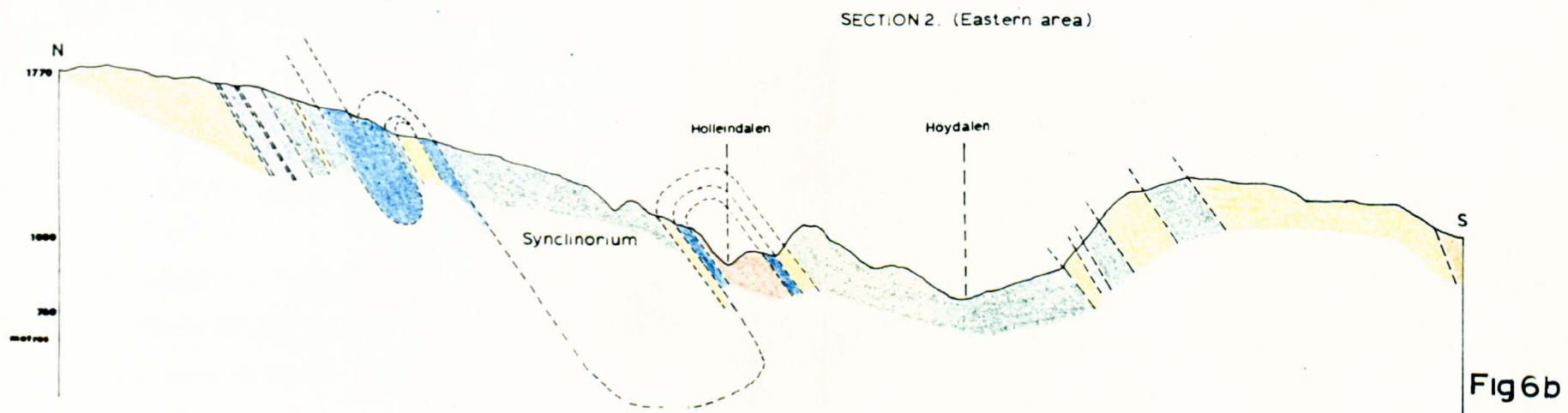
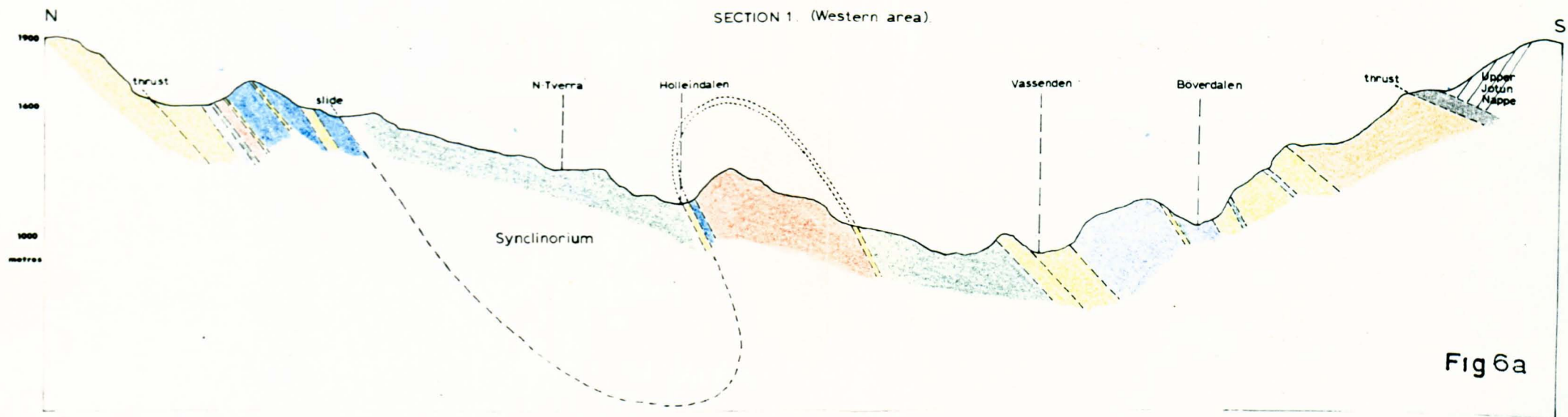
1. Granite-gneisses which outcrop in the north of the area and which constitute a basement complex.
2. Granites, gabbros, pyroxene-gneisses and ultramafics of the Bergen-Jotun kindred, occurring as the Upper Jotun Nappe in the south of the mapped area.

### Eq-Cambrian

3. Feldspathic quartzites, micaceous quartzites and mica-schists of the Sparagmite Group. The Sparagmite Group is separated from the underlying basement by a thrust plane.

### Cambro-Ordovician

- 4 (a). Quartzites and micaceous quartzites with an amphibolite band,



comprising the Psammite Group.

4 (b). Marbles and mica-schists of the Lower Limestone-pelite Group.

4 (c). Amphibolites and mica schists of the Holleindalen Greenstone Group.

4 (d). Phyllites and micaceous quartzites of the Upper Pelite Group

4 (e). "Conglomerates", phyllites, marbles and micaceous quartzites of the Upper Limestone-pelite Group.

The Cambro-Ordovician succession is eugeosynclinal and is separated from the underlying Sparagmite Group by the Gjeitaa thrust.

#### Ordovician ?

5. Feldspathic Quartzite Group, possibly equivalent to the Valdres Sparagmite Group.

The boundaries between the above groups are usually distinct and readily mappable.

The basal gneisses tend to strike approximately E-W and dip steeply to the south, whereas the supracrustal rocks have a regional N. E. -S. W. strike and dip at variable angles to the south.

The stratigraphy and its variations can best be illustrated by two approximately N-S sections and appropriate stratigraphical columns (Figs. 6 & 7 ).

Areal mapping reveals that the contact between the basal gneisses and the supracrustal rocks is discordant. The apparent conformity seen in some localities is a local phenomenon produced by the induced foliation parallel to the thrust in rocks adjacent to the main plane of movement.

The Gjeitaa thrust, separating miogeosynclinal rocks (Eo-Cambrian Sparagmite) from the main eugeosynclinal sequence above, is an important tectonic boundary and can be traced across the area.

Fig. 7. DIAGRAMMATIC CORRELATION (not to scale)

Lithologies as on geological map.

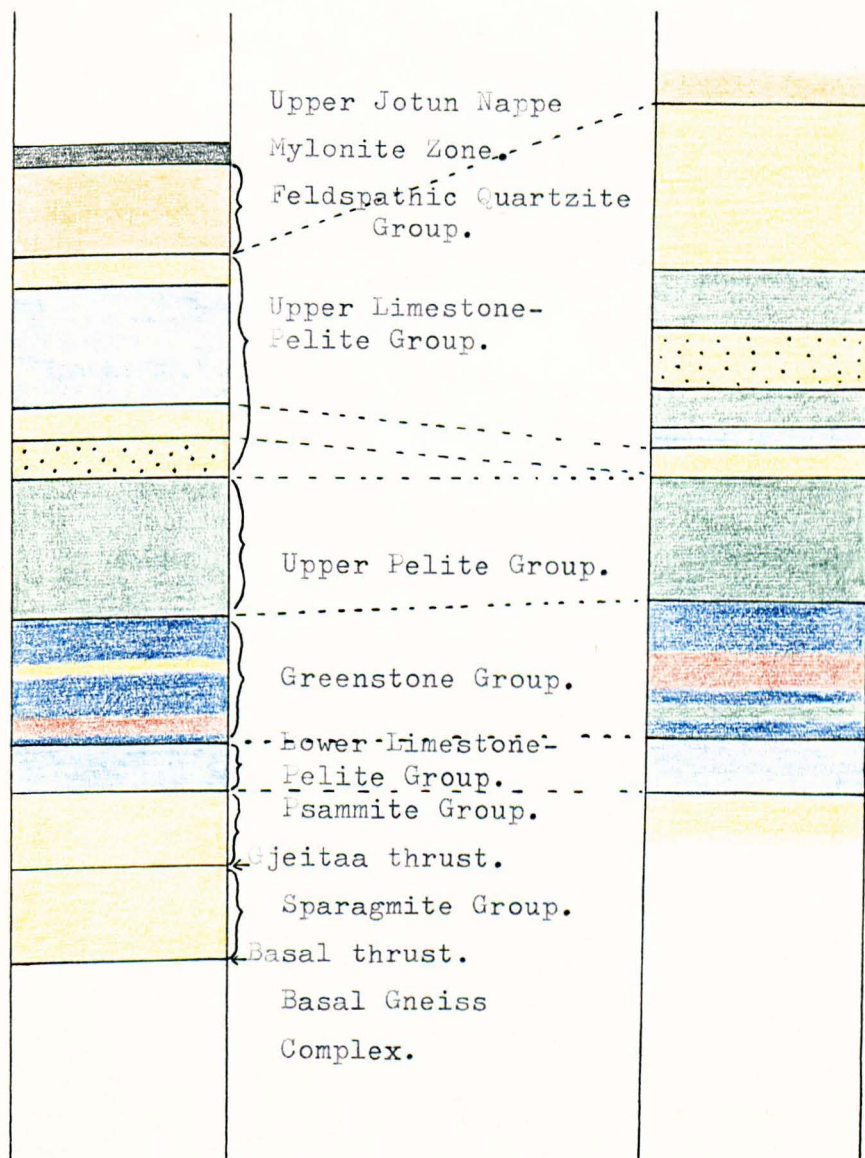
The sequence is generalised where facies variation is great.

Western area.

Near section 1.

Eastern area.

Near section 2.



The relationship of the eugeosynclinal rocks to the overlying Feldspathic Quartzite Group is obscure; on the meagre evidence available of absence of a dislocation, it is probably an unconformity. On the other hand, the contact between the Feldspathic Quartzite Group and the rocks of the Upper Jotun Nappe is a major thrust plane - the Upper Jotun Thrust. It is marked by a zone of mylonite and extends from Leirdalen across the north face of the subsidiary north-peak of Loftet.

Detailed measurements on thickness are difficult in view of the complex folding but nevertheless a few generalisations can be made from the lithological map and the N.-S. sections concerning sedimentary variation:

1. The Sparagmite Group thickens eastwards
2. There is a tendency for an increase eastwards of psammitic material at all horizons
3. The meta-volcanic rocks thin and finally disappear to the east.
4. There is an increase in width of outcrop of the supracrustal rocks to the east.

#### 1. N. W. Basal Gneisses

Lithologies within the basal gneisses in the area mapped are fairly constant and the dominant lithology is a foliated granite called the Hestbrepiggan granite. Towards the basal thrust, the granite becomes sheared out and develops a cross-cutting muscovite foliation, while in the basal gneiss thrust zone itself, rather flaggy muscovite-chlorite gneisses occur. For a detailed discussion of field relations of the basal gneisses, reference should be made to Banham (1962).

#### 2. Sparagmite Group

The Sparagmite Group rests discordantly upon the Basal Gneiss Complex; in particular upon the flaggy muscovite-chlorite

gneisses. As a result of movement associated with the basal thrust, an apparent structural conformity is produced; muscovite-chlorite gneisses and sparagmites having the same dip and strike. However, as previously stated, the discordant nature of the contact can be seen when a large portion of the basal thrust area is considered.

The Sparagmite Group strikes approximately N. E. - S. W. and dips at moderate angles to the south. Its thickness is variable; it is at a minimum thickness (around ? metres) in the west and thickens rapidly to the east, reaching a maximum thickness of about 300 metres. The thickening to the east is exaggerated by imbrication thrusting but there is little doubt that it is mainly sedimentary.

The dominant rock type is an arkosic quartzite, termed "sparagmite" by the Norwegians. Other lithologies include rather pure blue and white quartzites, quartz-mica schists and a garnet mica schist horizon.

The ratio of sparagmitic material within the group also increases eastwards.

In the north of the area, on Hesthoe, a so-called basal conglomerate is found. This is considered in detail in the structural section and it is concluded that the rock is tectonic in origin.

#### Eugeosynclinal succession

The rocks above the Gjeitaa thrust constitute a thrust slice of Cambro-Ordovician rocks, in turn overlain to the south by the Feldspathic Quartzite Group. Lithological mapping has shown that the eugeosynclinal succession can be divided into five groups separated by contacts which are, in the main, normal sedimentary, but which may occasionally be tectonic, as for example, the slide between the Holleindalen Greenstone Group and the Upper Pelite Group. On the evidence available, this slide appears to be pre-B2 major folding and

its significance is discussed fully in the structural section.

#### 4. (a) Psammite Group

This marks the base of the eugeosynclinal succession. The main lithologies are quartzites and psammitic schists; two pelitic horizons occur, now represented by garnet-mica-schist and a meta-volcanic horizon occurs towards the top of the succession.

The thickness of the Psammite Group is variable, at least 150 metres and the thickness increases to the east. Facies variation within this group is quite pronounced; for example, the amphibolite (meta-volcanic) horizon, when traced laterally, passes into garnet-mica schist. In several places, thin pelitic bands appear amongst the psammites but are impersistent.

#### 4. (b) Limestone-pelite Group

The Limestone-pelite Group consists essentially of a limestone formation with pelites above and below. It shows some facies variation and thickens to the east. Although some of the thickening may be tectonic, the increase in the limestone/pelite ratio indicates a sedimentary variation in that direction. Some evidence of thickening and thinning of the limestone formation due to flow, ie diapiric structures, has been obtained.

#### 4. (c) Holleindalen Greenstone Group

The Greenstone Group is rather variable. Basic volcanic rocks occur interbedded with pelitic and psammitic rocks and there is considerable facies variation. In consequence, the detailed successions of the two outcrops of meta-volcanic rocks differ. In particular the proportion of amphibolites is less in the southern outcrop and the proportion of pelitic material increased. The interbedding of basic lavas and sparagmites in the Gjeitaa-Runninge area is explained by the postulated presence of a delta depositing sand, while a volcano was located in the Gjeitaa region;

this has produced irregular lenses of "sparagmite" among basic lavas.

The basic volcanic rocks have a maximum thickness around Gjeitaabreen. Eastwards, there is an increase of psammitic and pelitic material and a thinning of the volcanics until in the extreme east of the area, the volcanics appear to die out, leaving a succession dominated by phyllites.

#### 4. (d) Upper Pelite Group

In view of their stratigraphic position, the Upper Pelite Group (4d) and the Upper Limestone-pelite Group (4e) have a large outcrop in the area mapped.

The Upper Pelite Group consists of phyllites, quartz-mica schists and some impersistent quartzite bands. Localised facies variation is quite marked and passage from phyllite through quartz-mica schist to quartzite can occur in a few metres.

#### 4. (e) Upper Limestone-pelite Group

The Upper Limestone-pelite Group consists mainly of marble with bands of quartz-mica schist, phyllite and micaceous quartzite in the west of the area; becoming more pelitic to the east. In addition, a possible "quartzite-conglomerate" is found near the base.

The marble thins rapidly eastwards and in the extreme east of the area is only about five metres thick.

The top of the succession is a rather quartzose quartz-mica schist which may represent a transition to the overlying feldspathic Quartzite Group.

#### 5. Feldspathic Quartzite Group

This group occurs above the Upper Limestone-pelite Group and is composed dominantly of feldspathic quartzites with some pure blue quartzites.

The contact of the Feldspathic Quartzite Group with the underlying rocks may prove to be an unconformity. A little evidence



of divergence of lithological boundaries between the feldspathic Quartzite Group and the underlying rocks has been obtained.

The lithologies are fairly constant, except that towards the Upper Jotun Nappe, the feldspathic quartzites have recrystallised to become a hard flaggy grey quartzite.

## 2. Upper Jotun Nappe

The Upper Jotun Nappe is the highest tectonic unit in the area mapped. The base of the Upper Jotun Nappe has been extensively mylonitised, so that cataclastites, mylonites and phyllonites are developed. Above the mylonite zone of the nappe is a thin sheet of granite, followed by a layer of gabbro. The higher part of the succession comprises pyroxene-gneisses (granulites) with ultramafic layers. Essentially the succession is a metamorphosed layered igneous complex.

More detailed descriptions of variation within the stratigraphical/structural units outlined above, can be found in the relevant parts of the next section.

## CHAPTER 3.

## BASAL GNEISS COMPLEX

### Introduction and Field Relations

The Basal Gneiss Complex has been investigated by Banham (1962) and the present writer was only concerned with the relationship between the basement and the overlying supracrustal rocks. In consequence, the complex was not studied in any detail; the contacts were mapped and one N-S geochemical traverse was made from foliated granite to micaceous quartzite of the sparagmite group.

Away from the contact, the dominant lithology is a foliated granite (Hestbrepiggan granite of (Banham (1962))). Near the thrust at the base of the supracrustals, the granite has developed a foliation parallel to the thrust plane and suffered retrograde metamorphism and is now a muscovite-chlorite gneiss. In the thrust zone, the quartzites and arkoses have also developed a foliation parallel to the thrust. The result is an apparent conformable passage from granite through flaggy gneiss to sparagmites. This phenomenon has been elsewhere ascribed to granitisation by some Norwegian geologists (Holtedahl 1950). In the present area, at least, it is only a structural conformity.

### Petrography

#### Hestbrepiggan granite

The granite consists, in order of abundance, of K feldspar, quartz, plagioclase and biotite. The grain size is medium-grained. A foliation defined by planar alignment of biotite flakes is present and strikes approximately E-W. Towards the basal thrust plane, a cross-cutting muscovite foliation develops and in the muscovite-chlorite gneiss of the thrust zone, this is the major foliation. Detailed petrography is not presented here since it

was adequately covered by Banham (1962). A few determinations of the plagioclase have been made, on the universal stage, using extinction in the zone perpendicular to 010: the composition is constant between  $An_4$  and  $An_5$ .

#### Muscovite-chlorite gneisses

Muscovite-chlorite gneisses occur immediately below the basal thrust, in a zone about one hundred metres wide. They consist of K feldspar, quartz, plagioclase ( $An_3$ ), muscovite and chlorite with small amounts of biotite, epidote and sphene. They are medium-grained and a muscovite foliation is present. This foliation can be seen to cut and displace the biotite foliation of the adjacent Hestbrepiggan granite.

#### Metamorphic facies of the Basal Gneiss Complex

##### (a) Hestbrepiggan granite

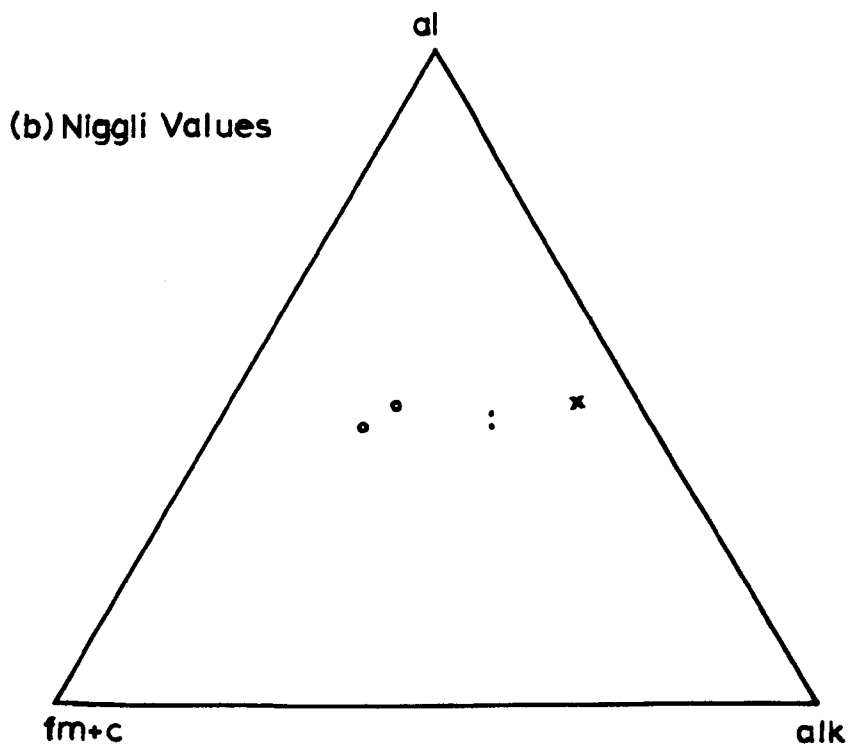
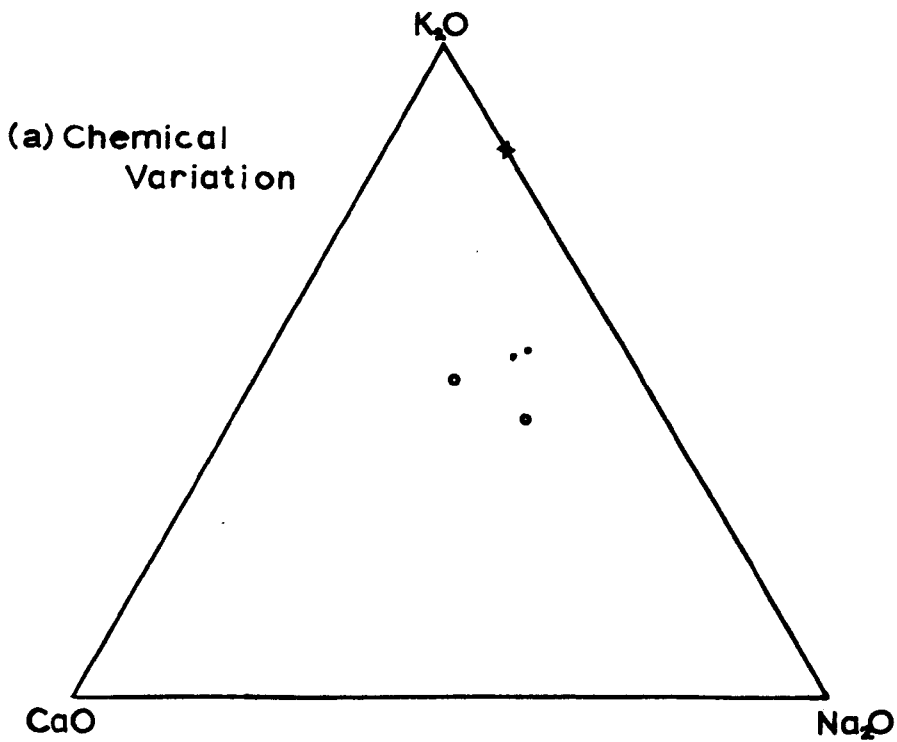
The mineral assemblage of essentially Quartz- K feldspar-plagioclase-biotite (muscovite-epidote) is one which is stable over quite a wide range, and it is necessary to use the anorthite content of the plagioclase to specify the facies (de Waard 1959). The plagioclase has a composition of  $An_4$  to  $An_5$  which suggests the highest sub-facies of the greenschist facies (Quartz-albite-epidote-almandine sub-facies). The chlorite occasionally found in these rocks is probably due to retrograde metamorphism.

##### (b) Muscovite-chlorite gneisses

The normal mineral assemblage is Quartz-K feldspar-plagioclase-muscovite-chlorite-(epidote-biotite). The plagioclase has a composition of about  $An_3$ . The muscovite chlorite gneisses are probably in the lowest sub-facies of the greenschist facies (Quartz-albite-muscovite-chlorite sub-facies).

Banham (1962) has presented evidence to demonstrate a sequence of crystallisations in the basal gneisses, involving an earlier crystallisation in the almandine-amphibolite facies (Pre-Cambrian)

**Fig.8.Basal Gneisses**



- × Micaceous Quartzites
- Foliated Granite
- Muscovite Chlorite Gneiss

and subsequent retrograde metamorphisms during the Caledonian orogeny. The greenschist facies event described above (upper greenschist event) accords with Banham's retrograde event, but in the writers opinion may prove to be Pre-Cambrian in age.

### Chemistry

A N-S geochemical traverse was made from foliated granite to micaceous quartzite. Two analyses of foliated granite, two analyses of muscovite-chlorite gneisses and one of somewhat arkosic micaceous quartzite are presented in Table 1.

Fig. 8a. shows a plot of  $\text{CaO}/\text{Na}_2\text{O}/\text{K}_2\text{O}$  for the five analyses and fig. 8b. is a plot of Niggli values  $\text{al}/\text{fm} + \text{c}/\text{alk}$ .

The results show that although there is a marked difference in composition between granite, muscovite-chlorite gneiss and micaceous quartzite, there is no gradual change from quartzite to granite which might be attributed to granitisation. Many more analyses would be required before any statement could be made concerning chemical variation within the basal gneiss complex. At present it can merely be suggested that if the few specimens are representative of wider formations, then the muscovite-chlorite gneisses are somewhat poorer in  $\text{K}_2\text{O}$  and  $\text{Na}_2\text{O}$  and richer in  $\text{Al}_2\text{O}_3$  and total iron than the foliated granites.

### Petrogenesis of the Basal Gneiss Complex

The first stage in the development of the Basal Gneiss Complex, which can be recognised, was crystallisation of foliated granites and granite-gneisses during Pre-Cambrian times. Banham (1962) has shown that this crystallisation was in the almandine-amphibolite facies. The dominant foliation was E.-W.

During the Caledonian orogeny (or earlier ?), the basal gneiss complex suffered a general metamorphism in the upper greenschist facies. Near the basal thrust plane, retrogressive

metamorphism occurred in the lowest sub-facies of the greenschist facies; chlorite being quite abundant. During this retrograde metamorphism, a muscovite foliation developed which cuts and displaces the earlier biotite foliation. Extensive strain shadows developed during quartz recrystallisation. This retrograde metamorphism may be due to movement along the basal thrust associated with the movement of the Upper Jotun Nappe, i. e. B2 or B3, but may be dominantly B1 in age.

#### Joint Mineralisation within the Basal Gneiss Group

A small amount of mineralisation on joint surfaces and in vugs is present within the basal gneiss complex. It is a late-stage phenomenon.

Joint mineralisation occurs in high angle joint zones, especially those with a strike of  $80^{\circ}\text{T}$  and  $140^{\circ}\text{T}$ . The normal minerals are quartz, epidote and clinoclre, with smaller amounts of galena, specularite and pyrite.

Vugs have a rare occurrence. Assemblages are similar to those of the joints, but one specimen containing an assemblage of epidote and aluminous hornblende has been collected.

Analyses of Basal Gneisses

TABLE 1

Sp.	94A	94B	94C	94D	110
	granite	granite	musc-chl gneiss	musc-chl gneiss	qtzite
SiO <sub>2</sub>	69.2	72.1	67.2	69.3	83.6
TiO <sub>2</sub>	0.26	0.19	0.31	0.26	0.11
Al <sub>2</sub> O <sub>3</sub>	14.6	13.92	16.41	15.96	8.08
Fe <sub>2</sub> O <sub>3</sub>	0.51	0.43	1.9	2.83	-
FeO	1.62	1.14	3.2	3.35	0.39
MgO	0.39	0.41	0.73	0.58	0.27
CaO	1.51	1.62	1.37	1.92	-
Na <sub>2</sub> O	3.73	3.39	2.86	2.12	1.02
K <sub>2</sub> O	5.81	5.30	3.14	3.71	5.55
P <sub>2</sub> O <sub>5</sub>	0.17	0.14	0.11	0.13	0.05
Total	97.80	98.55	97.23	99.16	99.00
CaO	14	16	19	25	-
Na <sub>2</sub> O	34	32	39	27	16
K <sub>2</sub> O	52	52	42	48	84
al	43	45	46	43	47
fm	12	10	25	27	7
c	8	10	7	9	-
alk	37	36	22	20	46
mg	0.26	0.31	0.20	0.16	0.06
k	0.51	0.51	0.42	0.54	0.78



## SPARAGMITE GROUP

### Lithologies and Field Relations

The Sparagmite Group is the lowest group of supra-crustal rocks which overlie the Basal Gneiss Complex; it is thought to be of Eo-Cambrian age.

Its thickness is variable and increases from west to east, probably reaching about 300 metres around Hestbreen. The true thickness is exaggerated by imbricate thrusting, especially in the west; in the east, evidence of imbrication is obscured.

The dominant lithology is an arkosic quartzite, termed "sparagmite" by Norwegian geologists. Other important lithologies include pure quartzites and semi-pelitic schists with garnets. In the extreme north of the area, on Hesthoe, a phacoidal quartzite occurs; the origin of this rock type is discussed in the structural section.

The base of the group is a thrust, adjacent to which the "sparagmites" have become sheared out, parallel to the thrust plane producing schistose and flaggy quartzites in structural conformity with the muscovite-chlorite gneisses of the underlying basement. Some low-grade metamorphism has accompanied the shearing.

Some high-angle shear zones occur within the Sparagmite Group; their interpretation is difficult, but they are probably associated with the imbrication zone.

The massive nature of the rocks makes structural analysis difficult. The Sparagmite Group has behaved in a different manner than the overlying rocks in view of its tectonic position.

The Sparagmite Group is separated from the overlying Psammite Group by the Gjeitaa thrust, along which shearing has occurred; this thrust separates sparagmites (probably Eo-Cambrian) from the overlying eugeosynclinal succession (Cambro-Ordovician).

## Petrography

There are four common lithologies in the Sparagmite Group:

1. Feldspathic Quartzites (Sparagmites)
2. Quartzites and micaceous quartzites
3. Semi-pelitic schists
4. Phacoidal quartzite (pseudo-conglomerate)

Detailed descriptions of the lithologies were made by Banham (1962) and a little additional information is given here in this summary.

1. The feldspathic quartzites are assemblages of quartz and K feldspar with smaller amounts of plagioclase, muscovite, biotite and epidote. A mica foliation is sometimes present.
2. The quartzites and micaceous quartzites are assemblages of quartz, muscovite, K feldspar and biotite with small amounts of garnet and plagioclase. A muscovite foliation is always present.
3. The semi-pelitic schists are essentially assemblages of muscovite and varying amounts of quartz, with smaller amounts of biotite, garnet and chlorite.
4. The phacoidal quartzites consist of phacoids of blue and white quartz and quartzite in a micaceous-chloritic matrix. The phacoids have a strong preferred orientation parallel to the axis of maximum elongation.

## Chemistry

Two analyses of rocks from the Sparagmite Group are presented in Table 2. One is a highly feldspathic quartzite; the other is slightly feldspathic. An analysis of sparagmite from Barth (1949) is tabulated for comparison.

Specimen 108 is very high in  $\text{Al}_2\text{O}_3$  and  $\text{K}_2\text{O}$  and rather poor in  $\text{SiO}_2$ . This is due to the high modal K feldspar. Specimen

110 is nearer to Barth's sparagmite; it is a micaceous, somewhat feldspathic quartzite.

The chemical variation within the Sparagmite Group is probably very great and a large number of analyses will be required before any generalisations can be made concerning the chemical composition of this group.

#### Metamorphic Facies

The following common assemblages of the Sparagmite Group:

Quartz-muscovite-K feldspar-garnet-epidote.

Quartz-K feldspar-biotite-muscovite-epidote, are typical of the highest subfacies of the greenschist facies (quartz-albite-epidote-almandine subfacies). There is some retrogressive metamorphism, as indicated by the presence of chlorite.

#### Petrogenesis

The Sparagmite Group probably represents arkosic sediments derived from weathering of dominantly granitic rocks, the rocks were probably derived from mechanical weathering of an upland area of Pre-Cambrian granite-gneiss.

The basal thrust has probably moved several times during the Caledonian orogeny. The dominant foliation is probably a B1 structure.

Three periods of metamorphism have occurred, an early dynamic phase, an upper greenschist phase and a lower greenschist phase.

The rocks have been folded four times.

Analyses of Sparagmite Group Rocks

Table 2

Sp. No.	sp. 108	sp. 110	Barth(1949)
SiO <sub>2</sub>	74.1	83.6	80.89
TiO <sub>2</sub>	0.71	0.11	0.40
Al <sub>2</sub> O <sub>3</sub>	12.96	8.08	7.57
Fe <sub>2</sub> O <sub>3</sub>	1.51	—	2.90
FeO	0.92	0.39	1.30
MgO	0.23	0.27	0.04
CaO	tr.	tr.	0.04
Na <sub>2</sub> O	1.57	1.02	0.63
K <sub>2</sub> O	6.92	5.55	4.74
P <sub>2</sub> O <sub>5</sub>	—	0.05	—

## PSAMMITE GROUP

### Lithologies and Field Relations

The Psammite Group marks the local base of the eugeosynclinal succession. Its contact with the Eo-Cambrian Sparagmite Group is the Gjeitaa thrust (see fig. 84 ) and it passes up into the Limestone-pelite Group with no apparent discordance.

The thickness of the psammite group is variable, probably over 200 metres in places and the group increases in thickness from west to east.

The dominant lithologies of the psammite group are flaggy quartzites and psammitic schists. In addition, there are at least two pelitic horizons represented by garnet-mica schist and near the top of the group is a volcanic band, represented by hornblende schist. This latter bed of meta-volcanics passes laterally into garnet-mica-schist, probably representing facies variation, that is to say, a thinning of lavas and incoming of pelitic material.

The psammites resemble the underlying sparagmites but tend to be much poorer in K feldspar and more thinly layered.

Along the Gjeitaa thrust, the quartzites have been sheared out and are represented by thinly-layered micaceous quartzites (see Figs. 85 and 86 ).

### Petrography

The rocks of the psammite group fall into three main groups:

1. Quartzites and micaceous quartzites
2. Garnet-mica-schists
3. Hornblende-schists (Volcanic horizon).

## 1. Quartzites and Micaceous Quartzites

These occur throughout the psammite group; passage into quartz-mica-schist is considered to represent original sedimentary transition to more pelitic rocks.

### Mineral Assemblages

Quartz-muscovite-biotite-epidote

Quartz-muscovite-K feldspar-magnetite

Quartz-muscovite-K feldspar-biotite-saussurite

### Fabric

The texture is crystalloblastic, granoblastic (sutured), sometimes slightly lepidoblastic. The grain size is fine-grained overall (0.5 mm), although muscovite flakes may be up to 3 mm long. A schistose foliation, defined by planar alignment of muscovite flakes is normally present. There may also be some form of orientation (flattening) of quartz grains within this foliation. Finally the foliation may be folded on a micro scale.

Quartz may form up to 90% of the mode; muscovite up to 20%.

### Mineralogy

- (a) Quartz. Most of the grains are granoblastic with sutured margins (see Fig. 9 ). They contain extensive strain shadows, giving up to 25° undulose extinction.
- (b) Muscovite occurs as scattered flakes and small aggregates with a planar alignment. Very slightly pleochroic from colourless to pale yellow.
- (c) Biotite. A few biotite flakes occur associated with the muscovite aggregates; they are strongly pleochroic with X straw yellow Y, Z brown.
- (d) K-Feldspar. A few grains of K feldspar occur in most slides; most of them are normally less than 0.01 mm..
- (e) Epidote. A few small prisms of epidote occur in some slides; most of them are pleochroic in pale greens.



Fig. 9 . Photomicrograph of micaceous quartzite of the psammite group. X.n.  $\times 30$

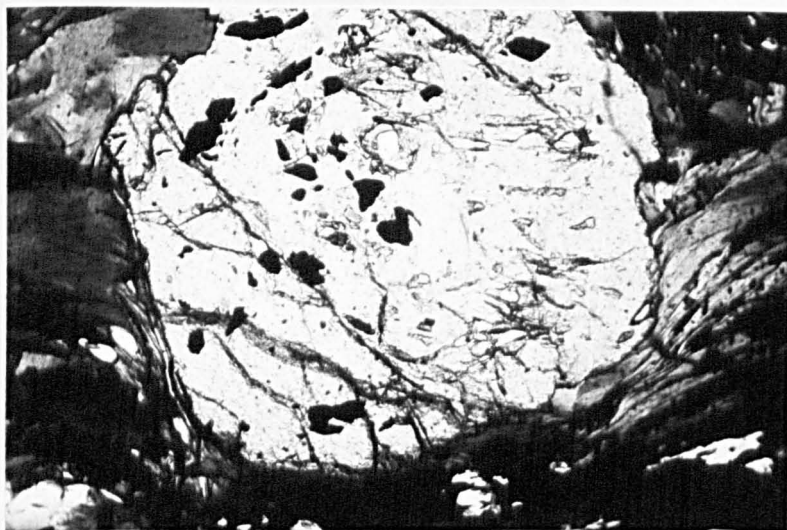


Fig. 10. Photomicrograph of garnet-mica-schist of the psammite group. Note the inclusions within the garnet and replacement by chlorite along cracks.  $\times 30$

(f) Magnetite. A few tiny grains occur.

(g) Saussurite. A few small patches of saussurite occur in some sections; they are taken to be the alteration products of the original plagioclase.

### Garnet-mica-schists

#### Mineral Assemblages

Muscovite-quartz-biotite-garnet

Muscovite-garnet-albite-quartz

Muscovite-biotite-quartz-albite-chlorite.

#### Fabric

The texture is crystalloblastic, lepidoblastic to granoblastic and individual grains may be subidioblastic to xenoblastic in shape. The grain size is variable; some muscovite flakes may be up to 10 mm.; quartz grains are usually less than 0.3 mm. and garnets may be up to 1 cm.. Always developed is a muscovite foliation which is folded on a micro-scale, (see Fig. 10 ). In some cases it is clear that the folds are definitely B3 folds; micas are bent and a strain slip cleavage is associated. Further discussion of the relationship between metamorphism and folding is in Chapter 9 .

#### Mineralogy

(a) Muscovite occurs in folded aggregates. It is slightly pleochroic from colourless to pale yellow and is sometimes associated with a pale yellow-green chlorite.

(b) Quartz occurs in granoblastic (sutured) grains which have extensive strain shadow with up to  $20^{\circ}$  undulose extinction.

(c) Biotite. Scattered flakes of biotite, often altered to chlorite occur in association with the muscovite. Pleochroic X straw yellow, Y, Z deep brown.

(d) Garnet. Large (up to 1 cm.) idioblastic to subidioblastic porphyroblasts occur. Micas are grouped and folded around the



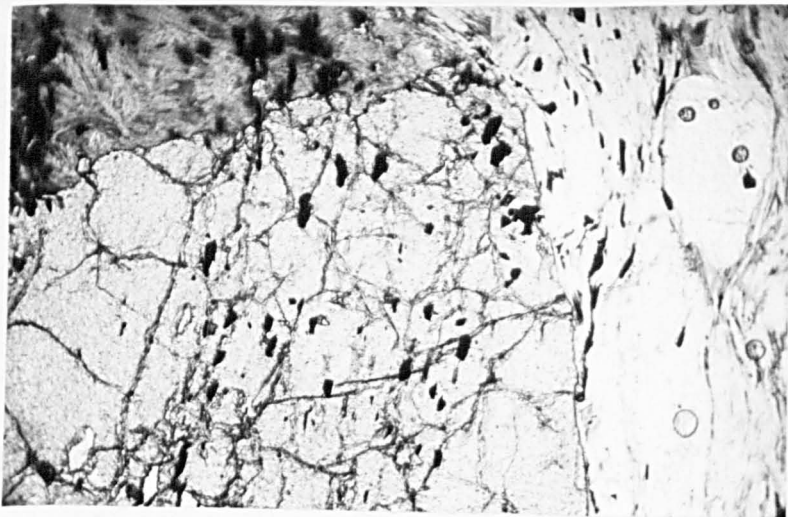


Fig.11 . Photomicrograph of garnet-mica-schist of the psammite group. Note inclusions and replacement of garnet by chlorite.  $\times 30$

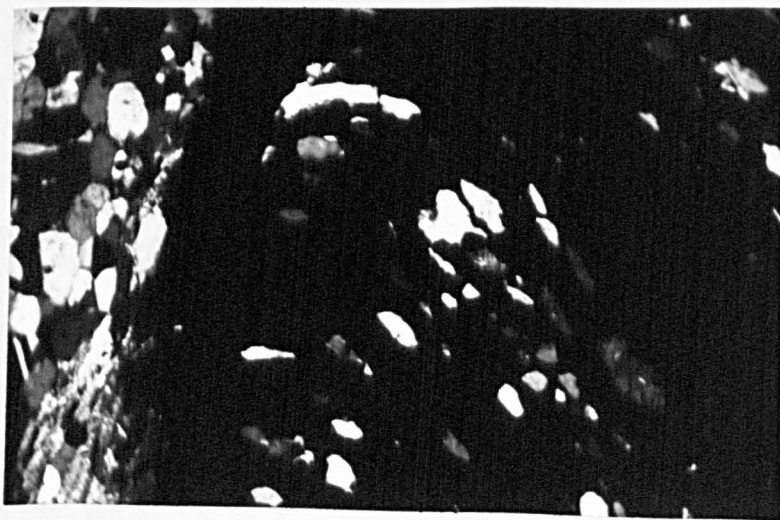


Fig.12 . Photomicrograph of garnet-mica-schist, showing inclusion trail in garnet.  $\times 30$

garnet grains, sometimes bent. The garnet is pink in colour and contains inclusions of magnetite, quartz and epidote. Helicitic textures are common (garnet textures can be seen in figs. 11 and 12). The garnet is probably mainly almandine.

(e) Albite occurs as small cloudy grains, sometimes showing albite twinning.

(f) Chlorite. Yellow-green chlorite occurs replacing biotite and shows anomalous berlin blue interference colours.

(g) Magnetite occurs as small inclusions within the garnets.

#### Meta-volcanic rocks

Occur as hornblende schist-schistose amphibolite.

#### Mineral Assemblages

Hornblende-albite-epidote-ilmenite

Hornblende-albite-biotite-chlorite-ilmenite-leucoxene

Hornblende-albite-epidote-pyrite

Hornblende-albite-epidote-biotite-ilmenite

#### Fabric

The texture is crystalloblastic with subidioblastic to xenoblastic grains. Hornblende tends to produce a nematoblastic texture. The grain size is variable; the hornblendes are up to 4 mm, while the albite is fine-grained with grains less than 0.15 mm. A foliation defined by an alignment of hornblende grains with a and c axes in one plane is present. Micro folding of this foliation frequently by B3 folds is observed. Axial plane strain slip cleavage is sometimes strongly developed and bent hornblende and biotite grains have been recorded. In some cases hornblendes are oriented, producing a linear structure.

#### Mineralogy

Hornblende constitutes up to 70% of the mode; albite up to 30% of the mode.

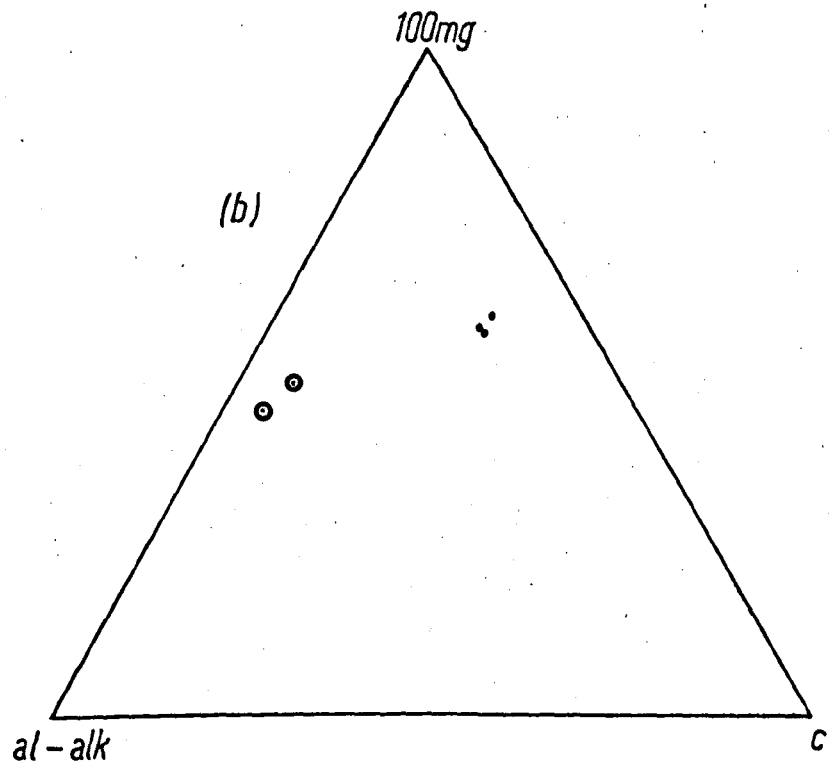
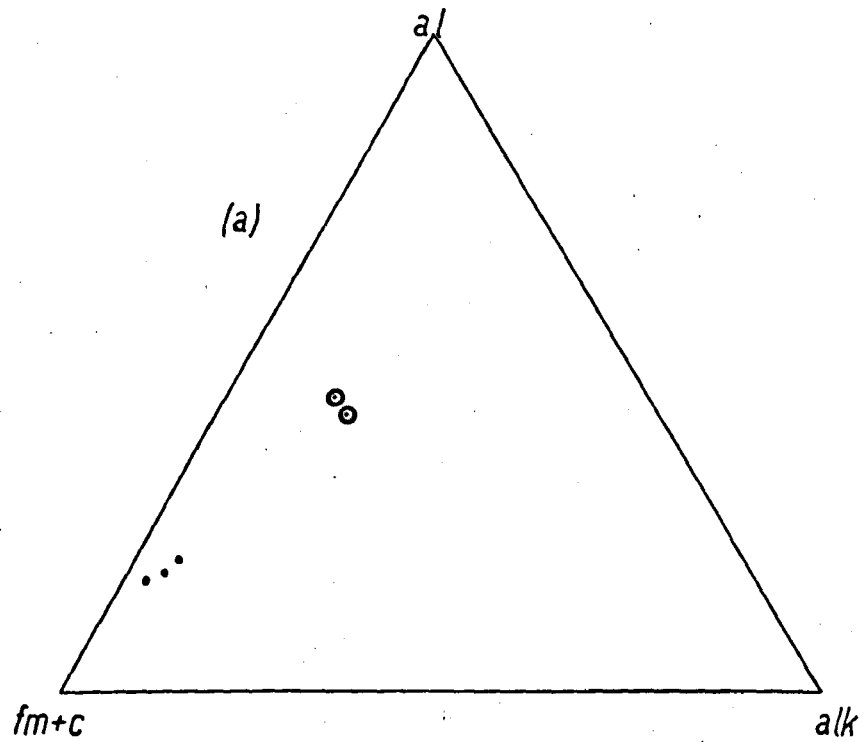
- (a) Hornblende occurs as idioblastic to subidioblastic grains, normally nematoblastic, sometimes poikiloblastic. It occurs as large prisms and smaller grains and is strongly pleochroic, with X pale green, Z deep blue green. The birefringence is moderate. Hornblende is partly replaced by biotite and chlorite. The marked contrast between the strongly oriented, well-shaped large hornblende prisms and the non-oriented small grains suggests two generations of hornblende of the same composition.
- (b) Albite occurs as granoblastic (sutured to lobate) grains less than 0.15 mm, associated with epidote. The cloudy appearance and the inclusions of epidote suggest saussuritisation of original Ca - rich plagioclase.
- (c) Epidote occurs as small rounded grains associated with albite and as inclusions in the hornblende. A few larger (up to 0.6 mm) grains also occur.
- (d) Ilmenite occurs in most sections, partly or completely altered to leucoxene.
- (e) Biotite occurs as small aggregates and scattered flakes associated with and, in some cases, replacing the hornblende. The biotite is itself altered to chlorite in some cases.
- (f) Chlorite. A yellow-green chlorite occurs replacing biotite and, in some cases, hornblende.
- (g) Pyrite. A few grains of iron pyrites occurs in one slide.

### Chemistry

Analyses of two garnet-mica schists and three hornblende schists (meta-volcanics) are tabulated in table 3 . Fig. 13a is a plot of Niggli values  $al/fm + c/alk$  and Fig. 13b is a plot of Niggli values  $100\ mg/al-alk/c$ .

The garnet mica schists are seen to be typical pelites. On the  $100\ mg/al-alk/c$  diagram, they fall in the field of the Littleton and Connemara pelites.

Fig.13 . Niggli Values.



• Garnet Mica Schist

• Amphibolite

The amphibolites are considered in detail in the chapter on Petrochemistry, since they are identical with the volcanic rocks of the Holleindalen Greenstone Group.

On the Niggli diagram 100 mg/c/al-alk, they fall in the central part of the plot of the Karroo dolerites.

### Metamorphic Facies

The common assemblages found in the psammite group:

Quartz-muscovite-biotite-epidote

Quartz-albite-epidote-biotite

Hornblende-albite-epidote

Muscovite-garnet-quartz,

are typical of the higher subfacies of the greenschist facies (quartz-albite-epidote-biotite and quartz-albite-epidote-almandine subfacies).

The presence of chlorite in some rocks may be due to a retrogressive metamorphism in the lowest subfacies of the greenschist facies (quartz-muscovite-albite-chlorite).

### Petrogenesis

The psammite group is part of what is probably a eugeosynclinal succession. Evidence for this is in the form of the alpine-type serpentinites and the presence of volcanic rocks including pillow lavas.

The quartzites of the psammite group may have been deposited in relatively shallow water; transition to pelitic horizons (muscovite-garnet schist) may represent deposition in deeper water. Extrusion of basic lavas occurred towards the top of the succession, probably under marine conditions, although pillow structures have not been recorded from this horizon.

After deposition and burial in the geosynclinal pile, the rocks were overthrust into their present position, metamorphosed in the upper greenschist facies and folded several times. A later

retrograde metamorphism occurred and probably later movement along the Gjeitaa thrust.

The age relations of metamorphism and folding are discussed in chapter 9 .

Table 3 . Analyses of rocks of the psammite group.

The analyses of the three hornblende schists;specimens 76, 77,78 are found in tableA2. (opposite page59).

Garnet-mica-schists

Sp. No.	84	Y
SiO <sub>2</sub>	57.2	59.1
TiO <sub>2</sub>	0.95	0.77
Al <sub>2</sub> O <sub>3</sub>	22.1	19.59
Fe <sub>2</sub> O <sub>3</sub>	1.01	0.61
FeO	8.21	7.91
MnO	0.59	0.31
MgO	2.1	1.93
CaO	0.95	0.88
Na <sub>2</sub> O	1.27	1.01
K <sub>2</sub> O	4.63	6.12
P <sub>2</sub> O <sub>5</sub>	0.15	0.15
al	45	42
fm	38	36
alk	14	18
c	3	4
mg	0.28	0.28

## LOWER LIMESTONE-PELITE GROUP

### Lithologies and Field Relations

The limestone-pelite group consists of pelitic mica-schists and blue marbles. The pelitic schists occur at the base and top of the succession and are rather variable; in so far as they may be fine-grained graphitic mica schists or quartzose mica schists, grading into micaceous quartzites. The limestone, when fresh, is blue coloured and completely recrystallised to a muscovite-calcite rock, with a few rounded quartz grains in it. Veins of quartz and calcite, often highly contorted, are abundant.

The limestone-pelite group is very thin in the west of the area, where the succession is:

30 metres of graphitic mica schist

50 metres of impure limestone

26 metres of quartzose mica schist with a little graphite.

It thickens eastwards and the proportion of limestone increases. At Gjeitaabreen, the following succession was recorded:

Graphitic mica schist

33 metres of limestone

23 metres of graphitic mica schist

40 metres of limestone

10 metres of mica schist

In the extreme east of the area, the limestone is 170 metres thick and the pelitic material at the base is absent.

The limestone-pelite group has very many minor folds and the veins of calcite and quartz are also highly contorted. Many of these folds are polyclinal cylindrical structures, rather irregular in shape, with axial planes inconstant in attitude and with individual bands varying in thickness in an erratic manner. This type of fold is



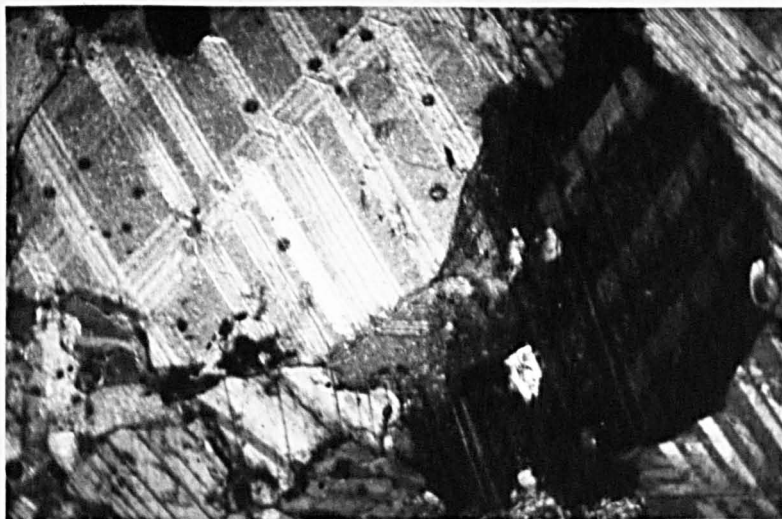


Fig.14 . Photomicrograph of marble of the lower limestone-pelite group, showing twin lamellae. X.n.  $\times 30$

termed irregular by Fleuty (1964). The nature of the folding and the thickening and thinning of the limestone outcrop suggests that the limestone may have behaved in a plastic manner during folding.

### Petrography

1. Meta-limestone (marble) see Fig. 14 .

### Mineral Assemblages

Calcite-muscovite-quartz-epidote

Calcite-quartz-muscovite-magnetite

Fabric see Fig. 14 .

The texture of the rock is crystalloblastic, granoblastic and most of the grains are either subidioblastic or xenoblastic. In general the rock is medium grained with calcite grains up to 1 mm and a weakly defined muscovite foliation is present.

### Mineralogy

Calcite forms up to 80% of the rock; muscovite up to 10%; quartz up to 10%.

(a) Calcite occurs as pale brown subidioblastic grains. It has a complex of internal planes, for in addition to the normal  $10\bar{1}1$  cleavage, it also shows normal twinning on 0001 and well developed multiple strain twinning on  $01\bar{1}2$  (see Fig. 14 ).

(b) Muscovite occurs as small, colourless, tabular flakes scattered through the slide. It shows a small degree of planar alignment.

(c) Quartz occurs as granoblastic grains, generally sutured but sometimes lobate, in which strain shadows are slight. Epidote and magnetite occur in some slides.

### Pelitic schists

### Mineral Assemblages

Muscovite-quartz-graphite-magnetite

Muscovite-biotite-quartz-epidote-graphite-garnet

### Fabric

The texture is crystalloblastic, lepidoblastic to

granoblastic. Most grains are xenoblastic, sometimes subidioblastic. The grain size is variable; quartz grains are usually small (0.05 to 0.1 mm), whereas muscovite flakes may be as large as 5 mm. A muscovite foliation is usually present and in some sections is folded on a micro-scale.

### Mineralogy

Muscovite forms up to 65% of the mode; quartz up to 40%.

- (a) Muscovite occurs in colourless, sheaf-like aggregates, often banded; minor folded in many sections.
- (b) Quartz occurs as small (0.05 mm) grains usually granoblastic (sutured) and with strain shadows.
- (c) Biotite occurs as straw yellow to brown flakes in association with the muscovite.
- (d) Graphite occurs as irregular dark opaque patches.
- (e) Epidote occurs as a few rounded pale green grains.
- (f) Magnetite occurs as scattered irregular grains.
- (g) Garnet occurs as occasional pink grains. They are subidioblastic, generally less than 1 mm.

### Metamorphic facies

The assemblages of this group:

Quartz-muscovite-biotite-epidote-garnet

Calcite-muscovite-quartz-epidote

probably belong to the highest subfacies of the greenschist facies (quartz-albite-epidote-almandine subfacies). No positive evidence of retrograde metamorphism has been obtained.

### Petrogenesis

The limestone-pelite group was deposited in water of unknown depth, under varying conditions; the presence of anaerobic conditions is indicated by the abundance of graphite in some of the

pelitic rocks. The sequence of deposition was pelite/limestone/pelite; this may have been due to a change in the depth of water. There is some facies variation along the strike, resulting in varying proportions of limestone and pelite. During the deposition of the group, some sand grains were introduced as shown by quartz grains within the limestone and by the quartzose mica schists.

The limestone-pelite group probably represents clastic limestones and silty mudstones.

After deposition, the rocks were buried beneath later deposits, thrust into their present position, metamorphosed in the upper greenschist facies and repeatedly folded. Prior to folding, veins of calcite and quartz were introduced. The folding was of a plastic nature and the limestone may have behaved diapirically.

## THE GREENSTONE GROUP

### Part I

#### Lithologies and Field Relations

The Greenstones Group is so named because it contains rocks of definite and probable volcanic origin as well as pelitic schists and quartzites. Evidence of igneous origin is seen in the presence of pillow structures and relict gabbroic textures which can be demonstrated in several places.

The Greenstone Group overlies, probably conformably, the Limestone-pelite Group and underlies the Phyllite Group. Due to its position below the Phyllite Group, the Greenstone Group tends to occupy anticlinal cores, e.g. in the Holleindalen anticline.

In the area mapped there are two main outcrops of the Greenstone Group - the northern outcrop where the Greenstone Group conformably overlies the Limestone-pelite Group and the southern outcrop in the Holleindalen anticline. The work of Banham (1962) to the west of the present area shows that the two outcrops are the same horizon repeated by folding. The Greenstone Group of the Holleindalen anticline disappears below ground level to the east due to the easterly plunge of the major B 2 fold.

In the northern outcrop, the volcanic rocks thin eastwards and psammitic and pelitic sediments become the dominant lithologies. This is due to facies variation from which it has been suggested (see Chapter II) that a delta was depositing sand in the Gjeitaa-Runninge area.

The detailed stratigraphy of the two outcrops is different. This is due partly to original facies difference and

partly to increase in thickness of the northern outcrop by folding about gentle B 2 fold axes.

The thickness of the succession is variable up to a maximum of at least 500 metres. In some areas, especially near Gjeitaabreen the apparent thickness is increased by repetition of beds by B 2 folding.

Lithologically the Greenstone Group shows considerable variation from fine-grained muscovite-chlorite schists to coarse grained amphibolites (meta-gabbros).

#### Northern Outcrop

The Greenstone Group thickens eastwards from N. Tverra to Gjeitaabreen, partly due to the incoming of sparagmite ribs and partly due to repetition of beds by folding.

In the west, in the Tverra cliffs, the succession comprises fine-grained muscovite-chlorite-schists (10 metres), then fine to medium grained hornblende schists with some coarse horizons (100 metres), followed by fine-grained muscovite and muscovite-chlorite-schists (30 metres). A slide occurs near the top of the Greenstones in the Tverra cliffs, and can be traced eastwards to Gjeitaabreen, where it appears to die out.

At Gjeitaabreen to the east, the succession consists of muscovite-chlorite-schists at the base, followed by alternating bands of hornblende-schist and feldspathic quartzite in which lithological repetition is partly due to folding. The thickness is variable up to 450 metres. Above the hornblende schists/quartzites there occurs 30 metres of muscovite schists passing up into the Upper Phyllite Group.

At Kjerringhoe, volcanic rocks are virtually absent and the succession consists of phyllites and feldspathic quartzites

(up to 400 metres). Further east, the Group is mainly represented by phyllites although exposure on the plateau is poor.

Small irregular bodies of coarse-grained meta-gabbroic rocks occur within the Greenstone Group between N. Tverra and Gjeitaabreen. The field relations are rather obscure; the meta-gabbroic rocks may represent small sill-shaped bodies, or may represent pipes which could have been feeders for the lavas.

### Holleindalen Anticline

The succession in the Holleindalen anticline is about 300 metres of muscovite-chlorite-schist, followed by up to 50 metres of hornblende-schist, followed by 50 metres of quartzites.

The muscovite-chlorite-schist is similar to the muscovite-chlorite schist of the northern outcrop. It tends to have more chlorite in the mode and frequently contains quartz veins.

The meta-volcanic rocks of the Holleindalen area consist of dark hornblende-schists very similar to the northern outcrop. Pillow lavas occur at one horizon, meta-gabbros and bands of a feldspar-hornblende rock are also found. The feldspathic hornblende schist may represent a more acid lava than the amphibolites or it may be an intrusive rock of trondjhemitic affinities.

The quartzites are fine even-grained rocks with up to 15% of mica in the mode. Small amounts of feldspar have been recorded in some rocks.

### Petrography

The rock types can be grouped as follows:

1. Hornblende-schist-schistose amphibolite
2. Meta-gabbro-massive amphibolite
3. Muscovite-chlorite-schist
4. Feldspathic quartzite

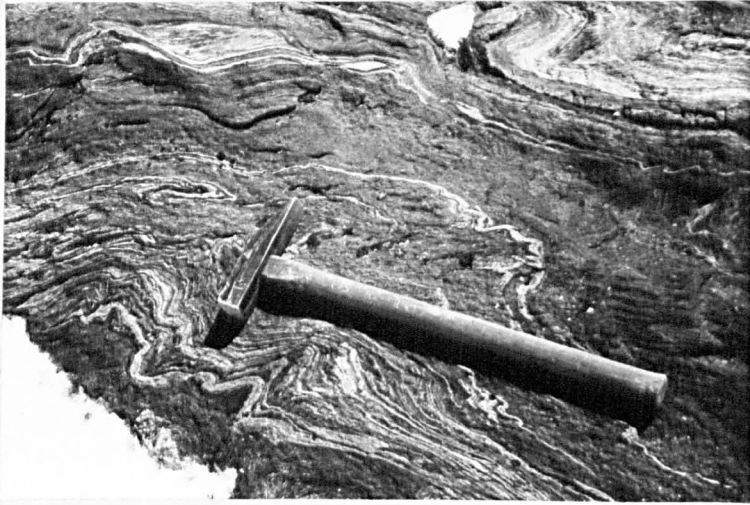


Fig.15. Schistose amphibolite, folded by B2 and B4 folds.

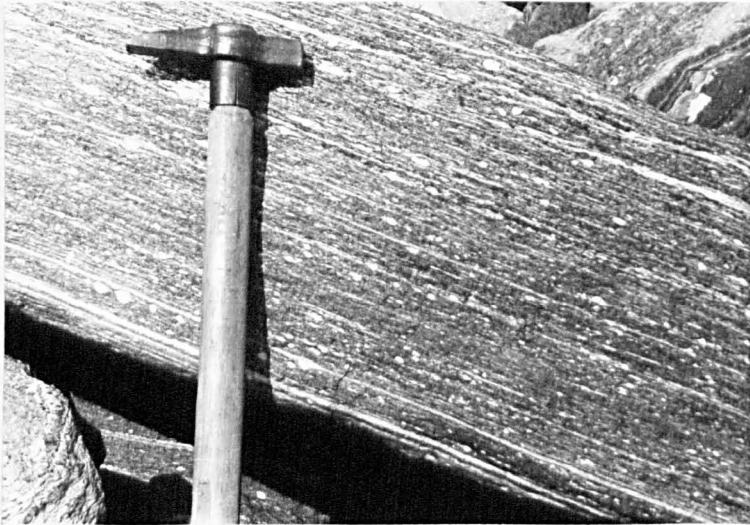


Fig.16. Augen schist; amphibolite at Gjeitaabreen.



5. Epidote quartzite
6. Graphite- mica-schist
7. Feldspathic schist.

#### Hornblende-schist (see fig. 15 )

The hornblende-schists consist of assemblages of hornblende-biotite-albite-chlorite-epidote-almandine-pyrite-ilmenite (leucoxene). The texture tends to be nematoblastic; a foliation is defined by orientation of hornblende prisms with a, c axes in one plane. Some of the albite grains show albite twinning.

In the field these rocks are dark medium-grained hornblende-schists sometimes fairly massive, sometimes almost fissile.

#### Massive Amphibolites (Meta-gabbros)

These occur in small irregular somewhat rounded bodies; they show gabbroic textures and are coarse grained. In thin section they consist of assemblages of hornblende-albite-almandine-epidote. A very poorly developed foliation is present in some rocks.

#### Muscovite-chlorite schist

These rocks have a well defined schistosity with strong alignment of muscovite and chlorite flakes. They consist of assemblages of muscovite-chlorite-quartz with occasional albite.

#### Feldspathic quartzite

The feldspathic quartzites ribs in the volcanic group are rather similar to the Sparagmite Group rock. They consist of assemblages of quartz-K-feldspar (usually microcline)-muscovite-epidote. The K-feldspar in the mode is variable, sometimes it is the major constituent. Some specimens show a cataclastic texture.

### Epidote quartzite

This occurs near Gjeitaabreen. It is a fine-grained quartzite with about 30% epidote in the mode.

### Phyllite

The phyllite is the lateral equivalent of the volcanics to the west. The petrography is identical to the phyllite group.

### Feldspathic schist

This lithology occurs principally in the Holleindalen anticline. It contains flattened feldspar augen in a schistose matrix. Its origin is problematic.

The detailed petrography of the special rock types of the Greenstone Group is now given.

### Massive Amphibolite (meta-gabbro)

#### Mineral Assemblages

Hornblende-albite-epidote-ilmenite (leucoxene)

Hornblende-albite-actinolite-chlorite-epidote-biotite (ilmenite, sphene, leucoxene)

Hornblende-albite-biotite-chlorite-epidote-(ilmenite, leucoxene)

Hornblende-albite-garnet-chlorite-epidote-(ilmenite, leucoxene)  
quartz

Hornblende-albite-garnet-chlorite-epidote-biotite-(rutile-sphene-leucoxene)

Hornblende-albite-chlorite-epidote-biotite-quartz.

### Fabric (see fig. A1A)

Crystalloblastic, heteroblastic, subidioblastic usually but varies from idioblastic to xenoblastic. Sub-nematoblastic to granoblastic. Relict igneous textures (gabbroic) are seen. The grain size is variable. Hornblendes up to 8 mm have been noted; albite is normally fine-grained.

Little evidence of foliation or lineation was seen in the sections cut, weak structures are seen best in the hand specimen. The hornblendes have a more or less random orientation - interpreted as a relict gabbroic textures with some flattening. With increase of biotite in the mode, a foliation tends to develop.

### Mineralogy

(a) Hornblende constitutes up to 60% of the mode.

Subidioblastic to idiomorphic grains up to 8 mm have been recorded. Some hornblende is seen to be replaced by biotite and possibly by epidote. Amphibole grains having a core of blue-green hornblende and a rim of pale-green actinolite have been found. The optic properties of the hornblende are as follows:

Prismatic, tabular form with strong pleochroism, X-green, Y-green, Z deep blue-green; extinction oblique  $Z \wedge c$   $22^\circ$ ; moderate birefringence; biaxial negative; 2V moderate. The hornblende is probably an iron-rich hastingsite (see mineralogy section for analyses, etc.).

(b) Albite constitutes up to 35% of the mode.

Xenoblastic, granoblastic (sutured to lobate) grains, generally fine-grained, occasionally up to 2 mm. The albite is replacing the original plagioclase. It is intimately associated with epidote. Albite twinning is seen in many sections but it frequently occurs untwinned.

(c) Epidote constitutes up to 10% of the mode.

It occurs as small rounded grains associated with the albite produced by the saussuritization of original plagioclase. It occurs as larger prisms (up to 1 mm) associated with the hornblende. In some instances the epidote occurs as inclusions within the hornblende, in others it replaces the hornblende.

(d) Actinolite constitutes up to 15% of the mode in some cases, but is found only in a few sections.

It occurs as rims around hornblende cores and as a few prisms of a pale green colour and slight pleochroism.

(e) Biotite constitutes up to 15% of the mode.

It occurs as subidioblastic aggregates replacing hornblende and as individual grains; the grains commonly show parallel alignment. It shows strong pleochroism X = straw yellow, Y, Z = deep brown.

(f) Chlorite constitutes up to 30% of the mode in some cases.

It is xenoblastic; pleochroic from colourless to pale green; with relief fair; birefringence weak - often shows anomalous Berlin blues; parallel extinction. It occurs as crystals of tabular habit or as radiating fibres. Flakes of chlorite are bent in some cases. It occurs replacing hornblende?

(g) Garnet constitutes up to 10% of the mode.

It occurs as small (up to 0.7 mm) idioblastic, grains. It contains inclusions of quartz, magnetite and epidote. The pink colour and isotropic nature indicate a high proportion of the almandine molecule.

(h) Quartz, small amount in the mode.

A few granoblastic (sutured) grains are found in a few sections.

(i) Ilmenite

Irregular patches of ilmenite, commonly heavily altered to leucoxene are found associated with hornblende.

(j) Sphene

A few idioblastic grains of sphene are found, but generally the sphene is completely replaced by leucoxene.

(k) Rutile

A few isolated grains of rutile have been recorded.

Hb-schist (schistose amphibolite)Mineral Assemblages

Hornblende-albite-epidote-chlorite-leucoxene

Hornblende-albite-biotite-epidote-chlorite-quartz

Hornblende-albite-epidote-pyrite

Hornblende-albite-biotite-epidote-ilmenite

Fabric

The texture is crystalloblastic, subidioblastic to xenoblastic; nematoblastic to granoblastic.

The grain size is variable; hornblendes up to 4 mm occur; albite is generally very fine-grained. A foliation is defined by the alignment of hornblendes with a, c axes in the same plane.

Biotites and chlorites are aligned in the same plane.

Mineralogy(a) Hornblende constitutes up to 60% of the rock

The form is prismatic tabular usually subidioblastic. Optic properties are identical with the hornblendes of the massive amphibolites. Inclusions of epidote and quartz are abundant in many cases.

(b) Albite constitutes up to 40% of the rock

It is fine-grained, granoblastic (sutured to lobate), xenoblastic; intimately associated with epidote - produced by saussuritization of the original Ca rich plagioclase. The composition as determined by the maximum symmetrical extinction angle to 010 on the universal stage is An 5. Albite grains are frequently very clear, usually untwinned, but albite with simple twinning is seen.

(c) Epidote constitutes up to 20% of the rock

There are two distinct occurrences: first, as small



Fig.17. Photomicrograph of amphibolite; meta-pillow lava. Note alteration and broken grains.  $\times 30$

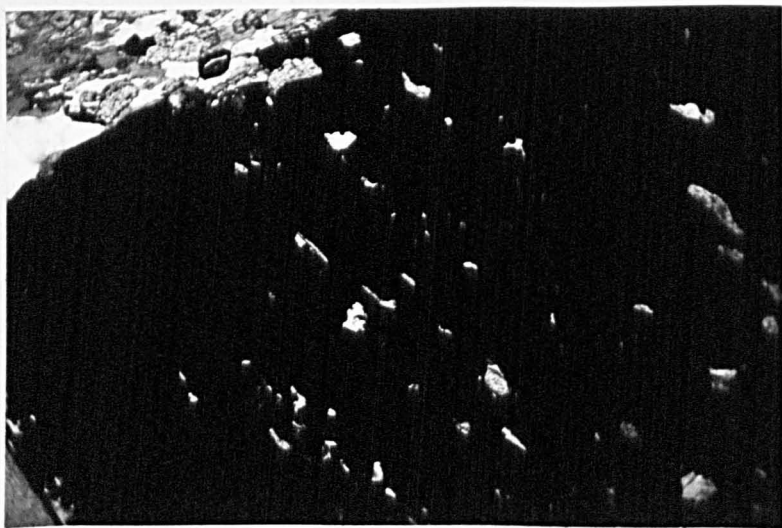


Fig.18. Photomicrograph of pyrite in amphibolite. Note inclusions and pressure shadow.  $\times 30$

rounded grains associated with the albite, second, as large idiomorphic prisms associated with hornblende. It is slightly pleochroic in pale greens.

(d) Biotite constitutes up to 15% of the mode

It occurs as individual flakes and small aggregates of subidioblastic grains, strongly pleochroic with X = straw yellow, Y, Z = deep brown. It is replaced partially by chlorite.

(e) Chlorite

A few flakes of chlorite occur, usually intimately associated with the biotite. They are slightly pleochroic from colourless to pale green, show anomalous Berlin blue interference colours, weak birefringence and moderate relief.

(f) Ilmenite (+ leucoxene)

Irregular patches of ilmenite are found; often extensively altered to leucoxene.

(g) Pyrites

Subidioblastic grains of iron pyrites are found in some sections, these have inclusion patterns (see fig.18 )

Amphibolite (meta-pillow lava)

Mineral Assemblages

Hornblende-albite-biotite-chlorite-ilmenite-sphene-leucoxene.

Hornblende-actinolite-albite-chlorite-epidote-quartz.

Fabric (see Fig. 17 )

The texture is crystalloblastic, subidioblastic to xenoblastic; subnematoblastic to granoblastic. It shows evidence of breaking up grains. The grain size is variable; hornblendes up to 3 mm occur, but the grains are frequently fragmented. The saussuritised feldspar is usually fine-grained. A poorly defined foliation is present, with some alignment of biotite and chlorite and to

some extent hornblende. Shear planes are present - possibly induced by some original mud around pillows. Mica is sometimes aligned parallel to these shear planes.

### Mineralogy

- (a) Hornblende constitutes up to 50% of the rock

The grains are subidioblastic, pleochroic in greens and are extensively broken up and altered to chlorite and biotite.

- (b) Saussurite constitutes about 40% of the rock

Original plagioclase is now saussuritized and replaced by an aggregate of small grains of albite, epidote, actinolite, chlorite, clinozoisite?

- (c) Actinolite

A pale green amphibole is present as small subidioblastic grains in some slides.

- (d) Chlorite constitutes up to 20% of the rock

It occurs replacing amphibole and in the shear zones, both as aggregates and individual grains. It is slightly pleochroic from colourless to pale green.

- (e) Epidote

Occurs as tiny grains in the saussurite and as large subidioblastic prisms.

- (f) Biotite

It occurs as flaky aggregates, often in shear zones. It is pleochroic, X = straw yellow, Y, Z = brown.

- (g) Quartz

A few granoblastic (sutured) grains of quartz occur. They show some strain shadow.

- (h) Ilmenite-sphene-leucoxene

These three minerals are quite abundant in some sections; the sphene shows some corona structure in some cases.



## Muscovite-chlorite schist

### Mineral Assemblages

Muscovite-chlorite-quartz-calcite-magnetite-apatite

### Fabric

The texture is crystalloblastic, xenoblastic to subidioblastic; granoblastic to lepidoblastic.

The grain size is variable. Muscovite flakes up to 4 mm. long can be seen but the rock is essentially fine grained. A muscovite foliation is always present. Some flattening of quartz grains within this foliation has occurred. Minor folding of this foliation is seen.

### Mineralogy

(a) Muscovite constitutes up to 50% of the mode

It occurs in folded aggregates intimately associated with the chlorite.

(b) Chlorite constitutes up to 20% of the mode

It occurs as small aggregates associated with the muscovite. It is pleochroic from colourless to pale greens; has low birefringence; frequently has a radial growth.

(c) Quartz constitutes up to 50% of the mode

It exhibits granoblastic (sutured) grains; variable grain size; extensive strain shadow.

(d) Calcite about 5% of the mode.

It occurs as xenoblastic grains; twinning and rhombohedral cleavage are poorly developed; the colour is pale grey.

(e) Magnetite

It occurs as coating around quartz boundaries.

(f) Apatite

A few rounded grains of apatite occur.

### Quartzites

Many variations of quartzites are found; in

addition to pure quartzites, feldspathic and epidote rich quartzites occur. In view of their identical occurrence they are grouped together.

#### Mineral Assemblages

Quartz-K-feldspar-muscovite

Quartz-K-feldspar-muscovite-epidote-ilmenite

Quartz-epidote-magnetite

Quartz-epidote-albite-muscovite.

#### Fabric

The texture is crystalloblastic, granoblastic (sutured), xenoblastic. The grain size is usually fine grained (less than 0.5 mm) although feldspar may be up to 1 mm. A streaky foliation is present in the more micaceous rocks. Minor folding of this foliation is seen occasionally.

#### Mineralogy

Quartz constitutes up to 90% of the mode

It shows granoblastic (sutured) grains often equidimensional and extensive strain shadows.

(b) K feldspar constitutes up to 20% of the mode

Irregular broken grains often show perthitic textures, although microcline twinning is sometimes seen.

(c) Muscovite constitutes up to 15% of the mode

Thin flattened individuals and scattered aggregates show planar alignment. Slight pleochroism from colourless to pale yellow-green.

(d) Epidote constitutes up to 35% of the mode

Green rounded grains of epidote are found in most sections, while in one rock epidote is a major constituent.

(e) Albite

Irregular, mostly untwinned grains of albite are seen in some slides.

(f) Ilmenite-magnetite

Small grains of ore-mineral occur, some is definitely ilmenite with alteration to leucoxene on its surface.

Feldspathic-schist (augen schist)

This lithology is found interbedded with meta-basalts in the Holleindalen anticline.

Mineral Assemblages

K-felspar-plagioclase-biotite-muscovite-chlorite-epidote-apatite

K-feldspar-biotite-chlorite-muscovite-apatite-rutile-ilmenite (leucoxene).

Fabric (see Fig.19)

The texture is crystalloblastic, cataclastic, granoblastic, xenoblastic, heteroblastic.

The grain size is variable; large feldspars up to 3 mm. occur in a fine-grained matrix (less than 0.5 mm) (see fig.19 ). The matrix has a foliation and the augen are flattened within this foliation. The rock is phyllonitic with augen of broken feldspars separated by streaky micas. Kink bands occur.

Mineralogy(a) K felspar

Occurs as 'augen' composed of large irregular broken grains surrounded by a fine grained groundmass, somewhat altered. Perthitic textures are seen as well as microcline twinning. Complex inclusion patterns occur in some cases (see fig.19 ). It is likely that some of the fine grained matrix is also K feldspar.

(b) Biotite

Occurs in aggregates of small flakes. It is pleochroic, X = straw yellow, Y, Z = browns.

(c) Plagioclase

A few rounded grains of albite are seen occasionally twinned. Much of the fine grained groundmass is probably albite, but this is not determinable.



Fig.19 . Photomicrograph of feldspathic augen schist.  
Note inclusions and cataclastic texture. X.n  $\times 30$

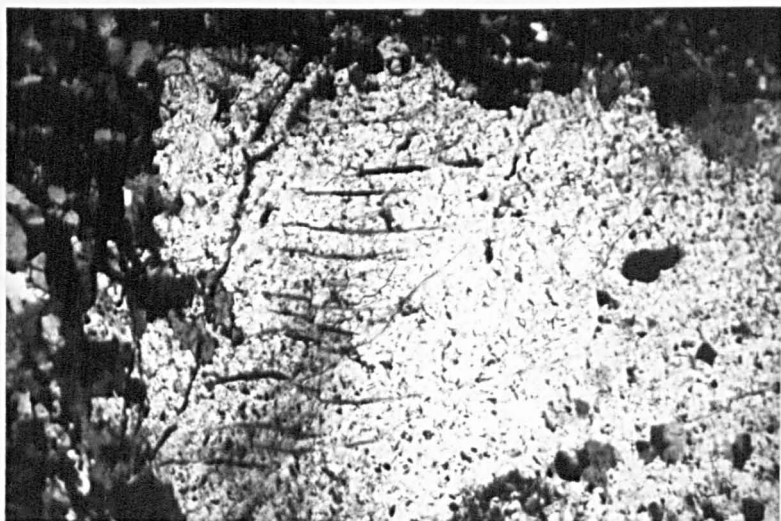


Fig.20 . Photomicrograph of feldspathic augen schist.  
Note inclusions and kink band. X.n  $\times 30$

(d) Muscovite

Aggregates of small flakes occur, often associated with biotite.

(e) Chlorite

Flakey aggregates of small flakes occur sometimes with radial growth. They are pale-green coloured, slightly pleochroic; with low birefringence and frequently anomalous interference colours.

(f) Epidote

Occurs as small rounded grains and a few larger prisms. High relief and high birefringence. This indicates a high Fe content.

(g) Apatite

Occurs as rounded grains in inclusions in the felspar and as scattered grains associated with chlorites and with leucoxene.

(h) Rutile

Stubby aggregates of rutile occur as inclusions within the feldspar.

(i) Ilmenite

A few idioblastic grains of ilmenite remain, but the majority have been completely altered to leucoxene.

Chemistry

Detailed petrochemistry of the amphibolites (meta-volcanics) is found in the next chapter; and it is perhaps sufficient to say here that the composition is similar to basalts and that they show a variation trend similar to the Karroo trend. It is demonstrated that apart from their oxidation state, there is no statistical difference between amphibolites which can be shown to be of igneous origin on field and petrographic evidence and the fine

*Fig.21 Niggli Values For Muscovite-Chlorite Schist.*

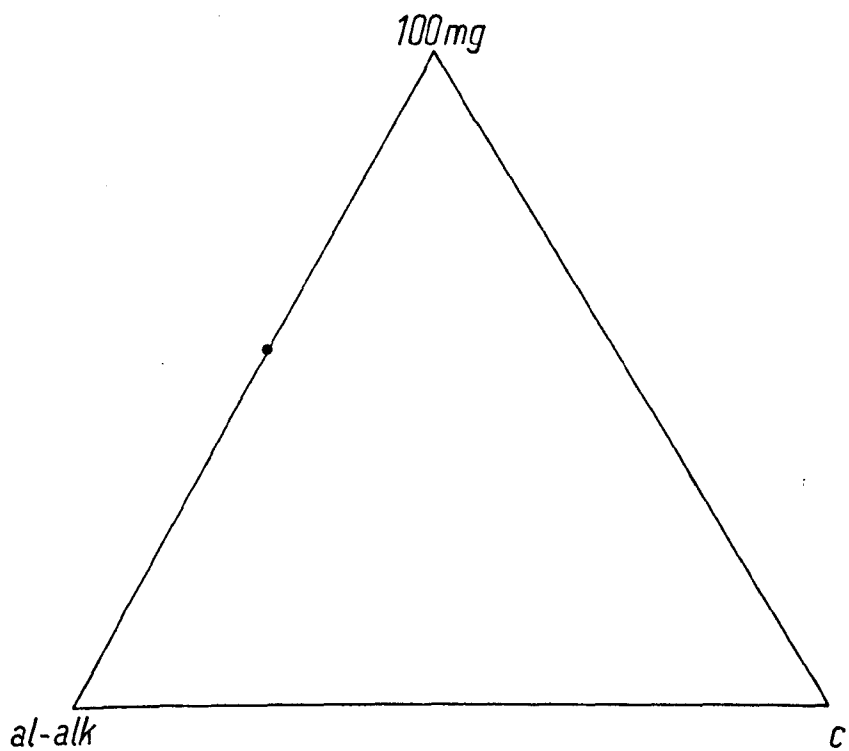
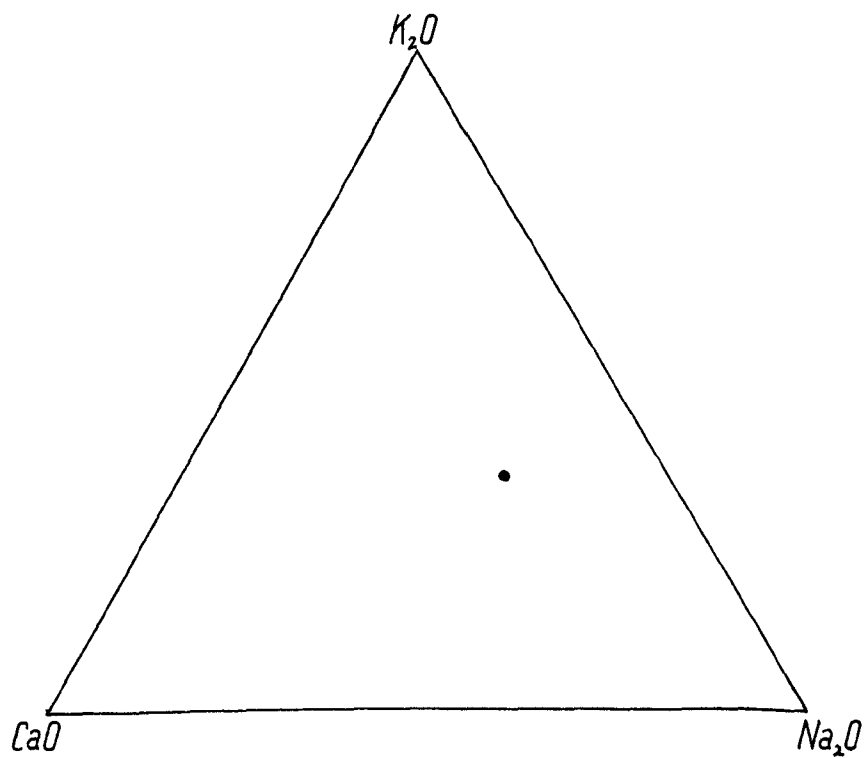


*Fig.22 Augen Schist.*



grained amphibolites which give no hint to their origin.

It is, therefore, extremely likely that all these amphibole-albite rocks are derived from igneous rocks; the schistose amphibolites mainly from lavas and the coarse-grained rocks from bosses and thin sills of the same cycle and kindred as the extrusives.

#### Feldspar-augan schist

These rocks are something of a problem. An analysis is shown in table ( 4 ). They are intermediate rocks rich in  $K_2O$  and  $Na_2O$ , and may be metasomatic.

#### Muscovite-chlorite schists

Analyses of muscovite-chlorite-schists are given in table ( 4 ). They represent altered argillaceous rocks. On the Niggli 100 mg, (al-alk), c plot they fall in the pelite field of the Connemarra and Littleton pelites.

#### Metamorphic Facies

In the Greenstone Group disequilibrium assemblages are quite common; many rocks show evidence of at least two facies. For example, there are actinolite rims around hornblende cores and in some cases assemblages of three generations are present. At present little can be said about the relationships of these assemblages, but this is considered further in the chapter on metamorphic history.

#### Petrogenesis

The Greenstone Group was probably deposited under marine conditions. The muscovite-chlorite-schists represent pelitic sediments into which some arenaceous material was added. After the deposition of the muscovite-chlorite schists extrusion of basic lavas and deposition of sandstones occurred contemporaneously. It is likely that a delta was depositing sand in the Gjeitaa-Kjerringhoe

area, while a volcano was pouring out lavas to the west. Thin basic sills were intruded at the same time as the lavas were being poured out. After cessation of volcanicity quartz-sandstones were deposited, to be covered in turn by the shales of the upper phyllite group.

Deformation followed during the first stage of which alpine-type serpentinites were intruded and the rocks were overthrust into their present position. This earliest, i.e. B1, folding produced a strong axial plane cleavage which later recrystallised and became the dominant planar structure.

During later folding (B2-B4) the present outcrop pattern of the Greenstone Group was attained and a further Strain-slip cleavage developed in fine-grained rocks, particularly as an axial plane cleavage to B3 folds.



Table 4 . Analyses of rocks of the greenstone group.

	Augen schist	Muscovite-chlorite schist.
SiO <sub>2</sub>	59.4	59.9
TiO <sub>2</sub>	1.08	1.30
Al <sub>2</sub> O <sub>3</sub>	17.79	17.28
Fe <sub>2</sub> O <sub>3</sub>	1.58	6.26
FeO	2.1	5.31
MnO	--	--
MgO	1.49	3.10
CaO	3.64	--
Na <sub>2</sub> O	6.75	2.60
K <sub>2</sub> O	5.95	4.10
P <sub>2</sub> O <sub>5</sub>	0.48	0.23
al	36	38
fm	17	52
c	13	--
alk	34	10
mg		0.33

## THE GREENSTONE GROUP

### Part II

#### "Petrochemistry of the amphibolites"

This section is a joint paper written with Dr. R. B. Elliott and submitted to Norsk Geologisk Tidsskrift; it will be published in N. G. T. Vol. 46, part 3, 1966.

### THE PETROCHEMISTRY OF THE AMPHIBOLITES OF THE HOLLEINDALEN GREENSTONE GROUP, JOTUNHEIMEN, NORWAY

R. B. Elliott      and      D. R. Cowan

---

#### ABSTRACT

The amphibolites belong to the quartz-albite-epidote-almandine subfacies of the greenschist facies. Some are massive and show relict igneous textures, while others are schistose. Twenty-seven new analyses indicate trends of variation of chemical composition similar to those of the Karroo dolerites, from which it is concluded that the amphibolites are of igneous origin. The oxidation state of the schistose amphibolites is significantly higher than that of the massive amphibolites. If this difference was induced during metamorphism, it was probably due to differences in the dynamic element of metamorphism; if it is inherited, then it is most probable that the schistose amphibolites were once mainly basic lavas and that the massive amphibolites were largely basic intrusives.

## INTRODUCTION

Between Lom and Fortun at the head of Sognefjord is a long, relatively narrow strip of metamorphic rocks of upper greenschist facies, sandwiched between the Basal Gneiss complex (Bunn-gneiss) on the north-west and the overthrust Jotunheimen masses of plutonic rocks to the south-east. The strip has long been known to contain quartzites, garnet-mica schists, phyllites and marbles (Landmark, 1948); recent mapping north of Høydalen has shown, in addition, a green-schist horizon composed of a variety of chlorite-schists and amphibolites. The assemblage resembles that of the Cambro-Silurian eugeosynclinal facies described by Strand (1951) for the Vaga and Sel map areas, and suggests that the Trondheim facies extends much further to the south-west than had previously been supposed.

In the area between Hestbrepiggen and Høydalen, the Basal complex is overlain by a series of thrust slices of metasedimentary and metavolcanic rocks. The lowest slice consists of a few hundred metres of quartzites and interleaved mica-schists, and is of miogeosynclinal facies. The overlying slice consists of a variety of metasedimentary rocks, including one limestone and contains the thick (200 m) Holleindalen Greenstone Group (Banham & Elliott, 1965). The upper slice consists of contorted grey phyllites of unknown thickness, many of which contain graphite. Considerably further to the south and east, and in ground which has so far only been reconnoitered, is at least one higher sheet containing limestones and a feldspathic quartzite, which may turn out to be the Valdres Sparagmite.

Greenstones occur at two stratigraphic horizons both in the middle thrust sheet. The first horizon is thin and low down, while the second, at the top of the sheet constitutes the main Holleindalen Greenstones.

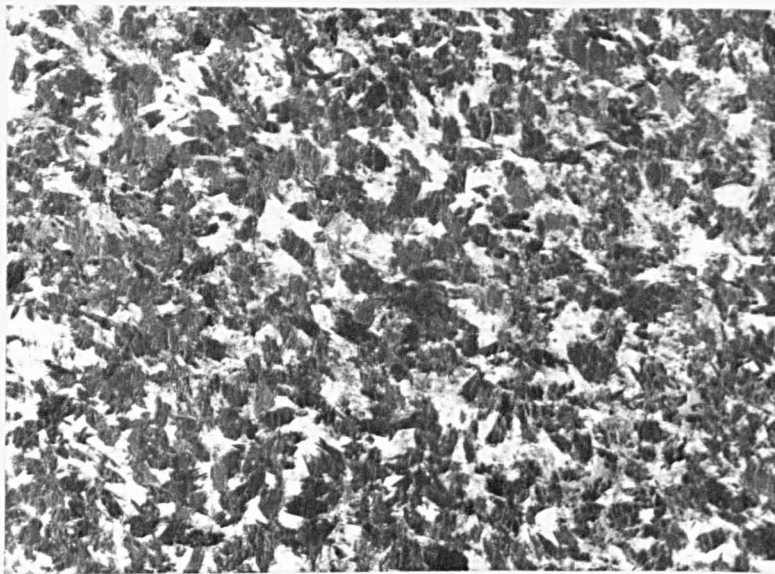


Fig.A . Polished specimen of meta-gabbro.

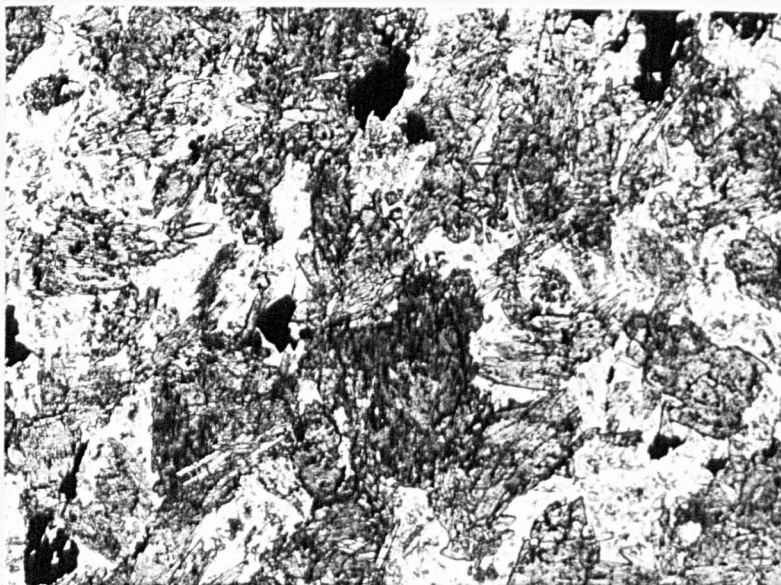


Fig.A1A. Photomicrograph of massive amphibolite  
x 30

Petrographically, the two horizons cannot be distinguished and they occur together in easterly plunging tight folds, from Vardhøe, about 1 Km. north of Høydalseter, they stretch and thin eastwards to Kjerringhøe and are particularly well-exposed in the cliffs immediately north of Høydalen Turistasjon and in Holleindalen.

#### Petrology of the Amphibolites

The amphibolites consists of assemblages of hornblende, albite and epidote, with varying amounts of almandine, biotite, quartz, actinolite, chlorite and calcite along with accessory ilmenite, magnetite, sphene and pyrite. They clearly belong to the quartz-albite-epidote-almandine subfacies of the greenschist facies, i. e. the albite-epidote amphibolite facies of Eskola. Texturally, they are not uniform and two main types can be distinguished: (a) massive amphibolites consisting largely of hornblende and albite, and (b) highly schistose rocks with the biotite and chlorite more conspicuous on foliation surfaces. The massive amphibolites show igneous features in the form of pillow structures and relict igneous textures. The pillows, which occur at only one exposure, are somewhat flattened but are nevertheless clear whilst the relict igneous texture consists of a random orientation of feldspar and hornblende, and the clustering of the ferromagnesian grains (Fig. 1A).

The highly schistose amphibolites show no palimpsest structures; they are completely crystalloblastic and somewhat fine in grain, with a strong preferred orientation of linear and platy minerals (Fig. 1B). Their origin cannot be determined by an examination of a hand specimen, but their persistent association with the massive amphibolites and their occasional passage into the massive type provides strong field evidence for a volcanic origin.

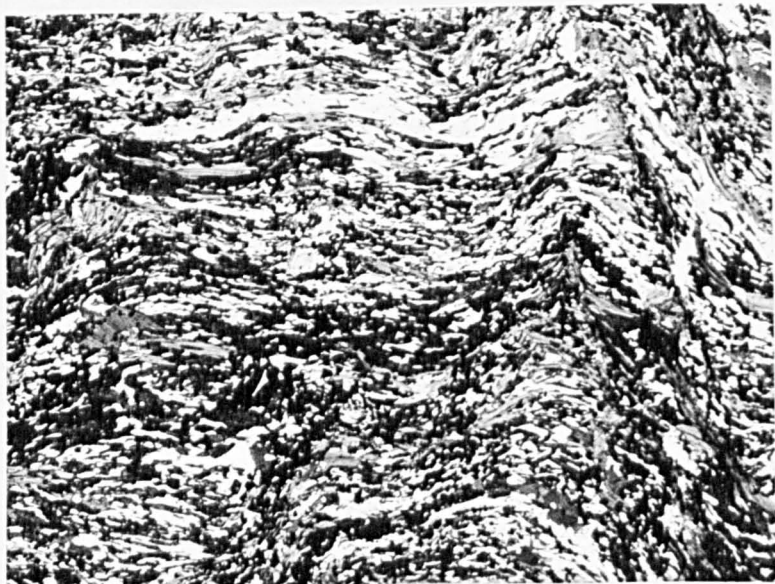


Fig.A1B. Photomicrograph of schistose amphibolite.  
x 30

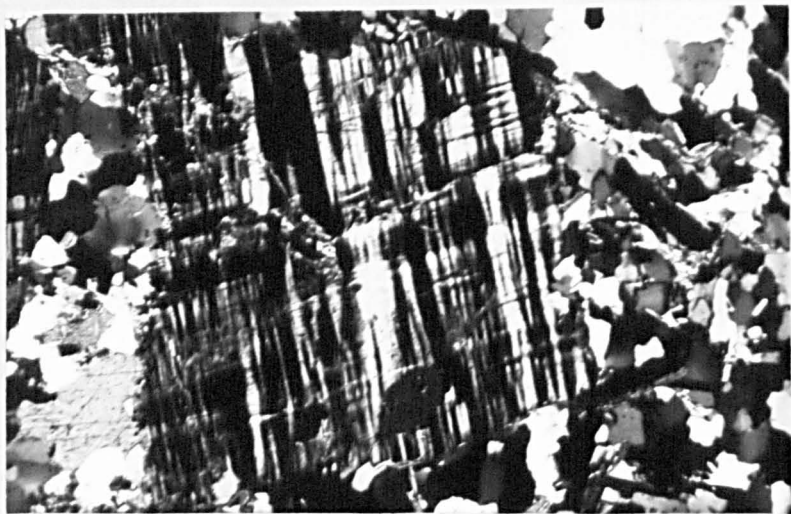


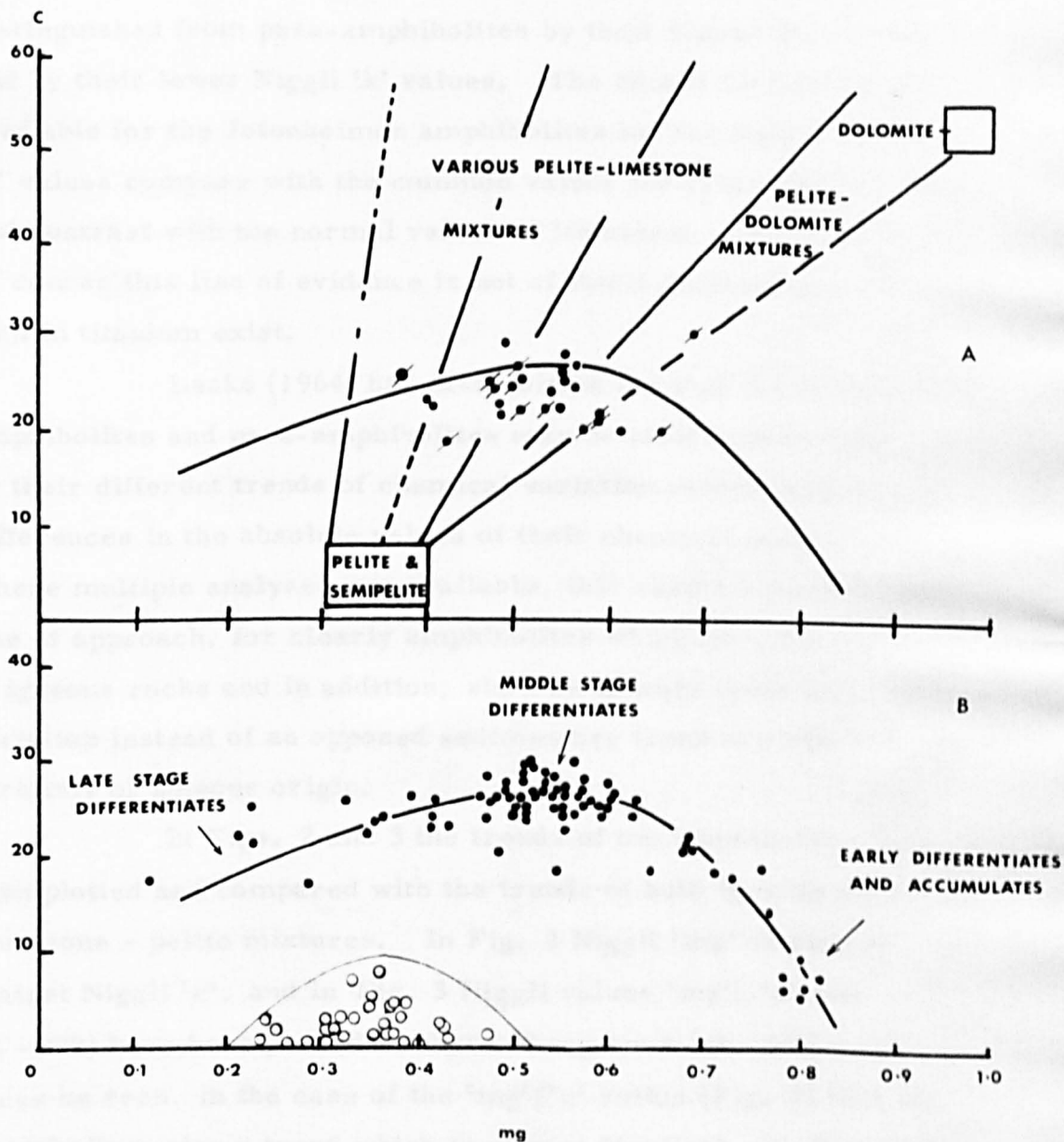
Fig.23. Photomicrograph of feldspathic  
quartzite.  
x 30

### Chemistry of the Amphibolites

The major elements of twenty-seven amphibolites have been determined by a variety of analytical methods and are given in Tables 1 and 2. It would have been of great advantage to have been able to analyse for minor elements, too, in particular for Ni and Cr (see Leake, 1964). Unfortunately, this has not been possible.

Of the major elements  $\text{SiO}_2$ ,  $\text{Al}_2\text{O}_3$ , total iron as  $\text{Fe}_2\text{O}_3$ ,  $\text{TiO}_2$ ,  $\text{MnO}$ , and  $\text{P}_2\text{O}_5$  were determined colorimetrically, by the methods of Shapiro and Brannock (1956) and using a Hilger and Watts 'Uvispek'.  $\text{Na}_2\text{O}$  and  $\text{K}_2\text{O}$  were determined on a Unicam S. P. 900 flame photometer.  $\text{CaO}$  was determined by both E. D. T. A. titration and on the flame photometer, while  $\text{MgO}$  was determined on the flame photometer and by atomic absorption on the Hilger and Watt's Uvispek with atomic absorption attachment.  $\text{FeO}$  was determined by the volumetric method of Wilson (1955).

Table 1 shows the chemical compositions of the massive amphibolites and Table 2 those of the schistose amphibolites. The two groups of analyses are very similar and it is not possible to distinguish between them by inspection. Their average compositions are shown in Table 3, along with their norms from which it can be seen that the average massive rock has some normative olivine and that the average schistose rock is oversaturated. However, both compositions are tholeiitic (Yoder and Tilley, 1962) and the differences in the norms are, undoubtedly, largely connected with the differences in their  $\text{FeO}/\text{Fe}_2\text{O}_3$  ratios. This does not, by itself prove that the amphibolites are of igneous origin because, theoretically, pelite - limestone mixtures can have the same composition as basic igneous rocks. Leake (1963) has presented evidence to show that orthoamphibolites may often be



Amphibolites. Fig 2.



distinguished from para-amphibolites by their higher Ni, Cr and Ti and by their lower Niggli 'k' values. The Ni and Cr figures are not available for the Jotunheimen amphibolites but the high Ti and low 'k' values compare with the common values for ortho-amphibolites and contrast with the normal values of limestone - pelite mixtures. Of course this line of evidence is not of itself conclusive; sediments rich in titanium exist.

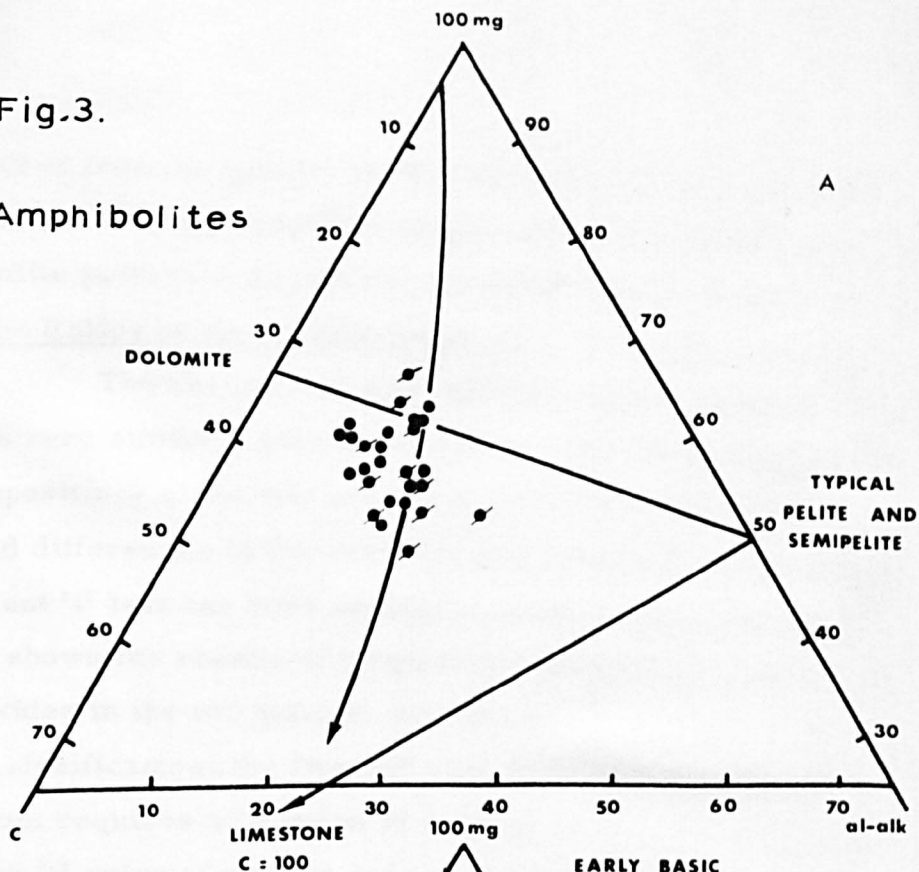
Leake (1964) has also pointed out that the ortho-amphibolites and para-amphibolites may be most readily distinguished by their different trends of chemical variation rather than by the differences in the absolute values of their chemical components. Where multiple analyses are available, this seems a most fruitful line of approach, for clearly amphibolites which have the composition of igneous rocks and in addition, show an igneous trend of chemical variation instead of an opposed sedimentary trend are almost certainly of igneous origin.

In Figs. 2 and 3 the trends of the amphibolites have been plotted and compared with the trends of both igneous rocks and limestone - pelite mixtures. In Fig. 2 Niggli 'mg' is plotted against Niggli 'c', and in Fig. 3 Niggli values 'mg', 'c' and  $(al - alk)$  have been plotted so that  $100\ mg + c + (al - alk) = 100$ . It can be seen, in the case of the 'mg'/'c' ratios (Fig. 2) that the amphibolites give a trend which is almost identical with that of the Karroo dolerites (c.f. Leake, 1964) and which is almost at right angles to that given by a mixture of limestone and pelite. Similarly the  $100\ mg + c + (al - alk) = 100$  diagram (Fig. 3) shows that the amphibolites again follow the Karroo trend and are transcurrent to the trends of mixtures of sediments.

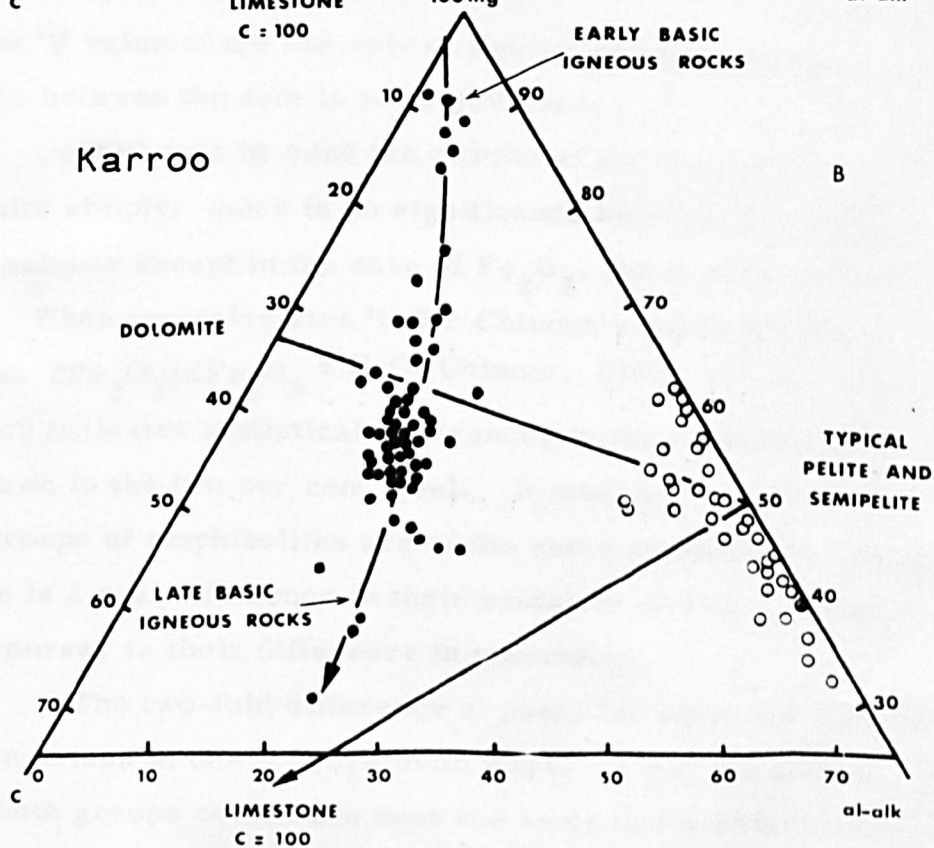
It is concluded, from the information given in Figs. 2 and 3, that the amphibolites are ortho-amphibolites and that they

Fig.3.

# Amphibolites



# Karoo



are derived from an igneous differentiation series. Also, the norms of the average schistose amphibolite and the average massive amphibolite point to a tholeiite or an olivine tholeiite parentage.

#### Oxidation Ratios of the Amphibolites

The analyses of massive and schistose amphibolites, although very similar, are not identical. To test the theory that the compositions of the two groups are identical and that the observed differences in the analyses are produced by sampling, the student 't' test has been applied to each of the oxides in turn. Table 4 shows the results of these tests and gives the mean values of the oxides in the two groups, as well as the value for 't'. To achieve significance at the five per cent level with twenty six degrees of freedom requires a 't' value of 2.06 or more. In other words, where the 't' value of the two sets of figures is below 2.06 the difference between the sets is not significant.

With this in mind the results of the tests can be stated quite simply; there is no significance between the two sets of analyses except in the case of  $\text{Fe}_2\text{O}_3$ , the 't' value of which is 2.45. When one calculates 't' for Chinner's oxidation ratio, i.e.  $\text{mols. } 2\text{Fe}_2\text{O}_3 / 2\text{Fe}_2\text{O}_3 + \text{FeO}$  (Chinner, 1960), the value is 2.59 which indicates statistical differences in the oxidation state almost down to the two per cent level. It must be concluded that the two groups of amphibolites are of the same composition except that there is a real difference in their oxidation states. Added to this, of course, is their difference in texture.

The two-fold difference of oxidation state and texture could have arisen in one of three main ways. First the parent rocks of both groups could have been the same and a difference in metamorphic conditions could have given rise to the two types of amphibolite. Second, the parent rocks could have been similar in

chemistry, including oxidation state, but different in texture. By virtue of the difference in texture they could have reacted differently to uniform metamorphic conditions and in so doing could have achieved different metamorphic textures and oxidation states. Third, the parent rocks could have been different in both oxidation states and textures and could have handed on these differences to their metamorphic successors.

The first possibility is considered unlikely. The association of massive and schistose amphibolites is an intimate one and equally intimate and complex variations in metamorphic conditions would have to be postulated. In addition, these variations would have to be confined to the greenstones for other horizons do not show comparable phenomena.

The second possibility envisages that the oxidation accompanies metamorphism. On this subject, Eugster (1959) has stated that "Higher degrees of metamorphism do not seem to produce any trends in the stage of oxidation of mineral assemblages", and that "Extensive oxidation in nature is usually connected with large volumes of water which are derived from an environment near the surface". Similarly, Chinner (1960) argued that, during metamorphism, of the pelitic gneisses of Glen Clova, Scotland, they behaved as a system closed to oxygen, and he quoted formidable authority in favour of this view as a general truth. Although one sees no evidence of the action of 'large volumes of water' in the metamorphism of the Holleindalen amphibolites, it is difficult to eliminate, finally, the possibility that the more advanced dynamic metamorphism of the schistose amphibolites has produced the higher oxidation state, especially when one considers that the oxidation of ferrous minerals may be accompanied simply by prolonged grinding in the laboratory (Hillebrand, 1908).

However, the acceptance of the idea of metamorphic oxidation necessitates also the acceptance of the view that strong correlations between the oxidation states of the Holleindalen amphibolites and those of certain other rocks are coincidental and insignificant.

The third possibility merits close attention. Many of the amphibolites have a relatively coarse igneous texture and are, almost without doubt, derived from basic intrusions. If we accept this as the general parentage of the majority of the low-oxidation massive amphibolites, then the logical possibilities for the high oxidation schistose amphibolites are, (a) basic extrusions, (b) basic tuffs, or (c) weathered basic rocks.

Two pieces of field evidence suggest that the last possibility is not a likely one. In the first place, the two groups of amphibolites are rather sharply divided on textural grounds and gradations between the slightly foliated massive variety and the strongly foliated schistose varieties are rare. In the second place, passages from a massive to a schistose texture across the strike have not been observed, and such passages as do occur, take place rather abruptly along the strike. In general when fresh and weathered igneous rocks occur together in a sheet, passage from one to the other across the strike is common and is frequently gradational.

At the same time, certain chemical evidence would seem to eliminate both basic tuffs and altered basic rocks as the possible parents. The average percentages of  $\text{Fe}_2\text{O}_3$  and the average oxidation ratios of the Holleindalen Greenstones and of basaltic tuffs (from Washington's tables) are as follows:

	$\text{Fe}_2\text{O}_3$	Oxidation Ratio
Massive amphibolite	2.17	16.8
Schistose amphibolite	3.39	26.6

Basic tuffs

6.70

68.2

From these values it is clear that the schistose amphibolites have not inherited the oxidation characteristics of basic tuffs. Nor, from more meagre data, have they the oxidation condition of weathered basic rocks. This process of elimination, which is in the nature of negative evidence, points to basic extrusions as the likely parent of the hornblende schists. On the positive side, the order of difference of oxidation states, between schistose and massive amphibolites, is strikingly similar to that between basic extrusive and intrusive rocks of the same petrographic province as, for example, in the Karroo, in Spitzbergen and in New Jersey (Table 5).

If it is held that the differences in oxidation ratios are inherited it is logical to conclude, from the data in Table 5, that the schistose amphibolites were, probably, originally basic lavas and that they have acquired a directive texture more readily than the associated basic intrusions because of their finer grain size and consequent greater ease of recrystallisation.

This statement is a generalisation based upon statistical evidence, and it is not meant to imply that all of the schistose amphibolites were lavas and that no intrusions have become schistose. Indeed, it would be a very remarkable coincidence if the metamorphic conditions were such that complete textural separation between original intrusions and extrusions was achieved during recrystallisation. This has certainly not happened here, for whilst most of the massive amphibolites are rather coarse and gabbroic at least one is fine-grained and has a pillow structure. It is almost certainly a lava. Moreover, it has the highest oxidation ratio of all the rocks of the massive group and has moved a good deal on the inter-pillow surfaces.

To this extent it is atypical. It is also possible that one or two of the schist amphibolites were originally intrusions. For example, amphibolite No. 314 has a strong nema-schistosity but is very homogeneous and unfoliated. With its low oxidation ratio of 8.9 it could have been a thin sill of fine grain-size which reacted in the same way as lavas, of equivalent texture, to the dynamic element of metamorphism.

In spite of these exceptions the statistical separation is still believed significant. The writers' conception is that the finer-grained basic igneous rocks have become schistose and the majority of those finer grained rocks were lavas.

### CONCLUSIONS

- (1) The two groups of amphibolites have similar compositions.
- (2) The massive amphibolites are of igneous origin on both textural and field evidence so that the schistose amphibolites are likely to be of igneous origin also.
- (3) The variation trends of both groups of amphibolites match the Karroo dolerite trends and are inconsistent with the trends of sediments especially with respect to 'k',  $\text{TiO}_2$  and the ratio mg/c.
- (4) On the basis of oxidation ratios, the schistose and massive amphibolites are considered to represent extrusive and intrusive basic rocks respectively, always provided that the oxidation ratios are inherited.
- (5) The amphibolites are derived from tholeiites.

### Acknowledgments

The authors would like to acknowledge generous financial help from D.S.I.R. and from the Department of Geology at Nottingham University in furthering both their field and laboratory studies. They also have pleasure in recording their gratitude to Dr. A.J. Rowell for his uncompromising advocacy of the statistical approach to the problems

of geology and for first stimulating, and then prompting, their calculations.

### REFERENCES

- Banham, P.H. & Elliott, R.B., Geology of the Hestrepiggan area.  
Preliminary account. Norsk Geol. Tidssk., 45, 189-198.
- Chinner, G.A., 1960. Pelitic gneisses with varying ferrous/ferric ratios from Glen Glova, Angus, Scotland. J. Pet., 1, 178-217.
- Eugster, H.P., 1959. Reduction and oxidation in metamorphism in Researches in Geochemistry, 397-426. New York: Wiley.
- Hillebrand, W.F., 1908. The influence of fine-grinding on the water and ferrous-iron content of minerals and rocks. J. Am. Chem. Soc. 30, 1120-1131.
- Landmark, K., 1948. Geologiske undersøkelser Luster-Boverdalen. Univers. i Bergen Årbok, 1-57.
- Leake, B.E., 1963. Origin of amphibolites from north-west Adirondacks, New York. Geol. Soc. Amer. Bull., 74, 1193-1202.
- Leake, B.E., 1964. The chemical distinction between ortho- and para-amphibolites. J. Pet., 5, 238-54.
- Nockolds, S.R., 1954. Average chemical compositions of some igneous rocks. Bull. Geol. Soc. Amer. 65, 1007-32.
- Shapiro, L. & Brannock, W.W., 1956. Rapid analyses of silicate rocks. U.S. Geol. Surv. Bull., 1036-C.
- Strand, T., 1951. The Sel and Vaga map areas - geology and petrology of a part of the Caledonides of central Southern Norway. Norg. Geol. Unders. 178.
- Turner, F.J. & Verhoogen, J., 1960. Igneous and metamorphic petrology. 2nd edn. New York. Wiley.



Washington, H.S., 1916. Chemical analyses of igneous rocks.

U.S. Geol. Surv., Prof. paper 14 (revised and enlarged).

Wilson, A.D., 1955. The determination of ferrous iron in rocks.

Bull. Geol. Surv. Gt. Britain. 9, 56-8.

Yoder, H.S. & Tilley, C.E., 1962. Origin of basalt magmas: an experimental study of natural and synthetic rock systems. J. Pet., 3, 342-532.

Footnote to Table 4 (contributed by Dr. A. J. Rowell)

The 't' tests in the above table were made with the usual assumptions of the method; that the populations being compared were normally distributed and had equal variance. Two of the 't' tests suggested significant differences at or below the 5% level. To confirm that these were real differences (at the given probability level) and not spurious results caused by a failure of the assumptions, the data on which the tests were based were themselves examined.

Comparing the observed distributions of the ferric oxide percentages with those expected from a normal distribution with the same mean and variance, the Kolmogorov-Smirnov statistic showed that with both the schistose and massive rocks, the data did not depart significantly from normality (P. 05). Moreover, an F test of the two variances revealed that these were not significantly different at the 5% level and consequently a 't' test was a suitable method of comparing the two populations.

Although a similar test for normality with the Kolmogorov-Smirnov statistic confirmed that the oxidation ratio data of the two samples was also distributed normally (P. 05), an F test indicated that the variances were not equal (P. 05). Consequently the data in Table is to some extent unreliable.

That there is, none the less, a significant difference in the oxidation ratios of the schistose and massive rocks was confirmed by the Fisher-Behrens test for comparing the means with unequal variances but the significance level was 5% and not 2%, as in Table 4.

Table 1 massive amphibolites

	4	7	12	13	14	15	17	18	21	22	80	100	309
SiO <sub>2</sub>	47.90	44.90	45.70	44.10	51.50	47.20	48.75	45.00	51.65	47.40	44.0	42.42	46.51
TiO <sub>2</sub>	2.69	1.76	2.23	2.56	1.02	4.50	2.40	2.7	3.08	1.76	2.15	2.20	3.01
Al <sub>2</sub> O <sub>3</sub>	15.63	14.52	12.57	13.12	12.25	15.34	13.72	12.99	13.68	15.22	17.21	16.13	14.85
Fe <sub>2</sub> O <sub>3</sub>	3.10	1.90	1.52	3.64	3.25	0.16	1.18	2.95	1.56	2.67	1.65	1.76	2.91
FeO	7.99	3.66	10.25	10.88	8.80	12.15	10.61	11.36	8.83	8.53	8.80	9.17	9.40
MnO	0.15	0.11	0.10	0.00	0.15	0.16	0.13	0.18	0.16	0.18	0.05	0.06	0.11
MgO	7.50	7.90	8.30	7.30	8.60	6.93	7.90	7.35	5.63	7.65	7.65	7.50	10.49
CaO	9.95	11.38	12.46	10.40	9.90	10.19	9.56	9.68	10.98	9.40	10.90	0.68	3.50
Na <sub>2</sub> O	1.80	3.30	3.45	3.80	1.90	1.10	2.75	3.60	1.80	3.60	2.30	3.23	2.41
K <sub>2</sub> O	0.11	0.90	0.70	0.80	0.50	0.50	0.55	0.50	0.50	1.00	0.10	0.95	0.13
CO <sub>2</sub>	0.10	0.23	0.27	0.39	0.00	0.01	0.43	0.33	0.63	0.26	0.24	0.20	0.26
SO <sub>2</sub>	0.70	0.21	0.06										
H <sub>2</sub> O	2.10	2.11	2.03	2.01	2.53	2.21	1.96	2.01	1.80	2.38	2.81	2.05	0.53
Total	99.71	99.03	99.74	99.89	100.40	100.45	99.94	99.77	99.84	100.00	99.16	100.35	99.98
Oxidation Ratio	25.89	16.50	11.78	23.14	24.95	1.17	9.10	18.95	13.72	21.98	14.44	14.73	21.79
Niggli values													
al	22	18	16	17	17	21	19	17	21	20	23	21	19
fm	48	45	47	50	53	49	50	51	44	47	45	49	56
c	26	28	29	24	25	26	24	23	30	23	26	21	20
alk	4	9	8	9	5	3	7	8	5	9	6	8	5
Si	114	97	97	96	120	112	113	103	132	108	100	107	101
k	0.03	0.14	0.11	0.13	0.14	0.22	0.12	0.08	0.15	0.16	0.02	0.16	0.025
mg	0.56	0.57	0.56	0.48	0.57	0.50	0.54	0.48	0.49	0.55	0.56	0.59	0.61
qz	-2	-39	-35	-40	0	0	-15	-29	+12	-28	-24	-25	-19

Localities (with Norwegian grid references) for rocks in Table 1

4	Hb-ab-epid-bi amphibolite:	Holleindalen, 535:397	Analyst	D.R. Cowan
7	Hb-ab-epid-bi-chl amphibolite:	Holleindalen, 538:394	Analyst	D.R. Cowan
12	Hb-ab-epid amphibolite:	Upper N. Tverra, 535:433	Analyst	D.R. Cowan
13	Hb-ab-epid-alman amphibolite:	Upper N. Tverra, 535:433	Analyst	D.R. Cowan
14	Hb-ab-epid-alman amphibolite:	Upper N. Tverra, 535:433	Analyst	D.R. Cowan
15	Hb-ab-epid-alman-chl-amphibolite:	Nr. Gjeitaabreein, 536:433	Analyst	D.R. Cowan
17	Hb-ab-epid-bi-chl amphibolite:	Nr. Gjeitaabreein, 536:433	Analyst	D.R. Cowan
18	Hb-ab-epid-alman amphibolite:	Upper N. Tverra, 535:433	Analyst	D.R. Cowan
21	Hb-ab-epid-alman amphibolite:	Upper N. Tverra, 535:432	Analyst	D.R. Cowan
22	Hb-ab-epid-chl amphibolite:	Upper N. Tverra, 536:431	Analyst	D.R. Cowan
80	Hb-ab-epid-chl amphibolite:	Nr. Gjeitaabreein, 543:438	Analyst	D.R. Cowan
100	Hb-ab-epid-alman-bi amphibolite:	Upper N. Tverra, 535:433	Analyst	D.J. Mather
309	Hb-ab-epid-calcite amphibolite:	Høydaalen, 477:357	Analyst	D.J. Mather

Table 2. Chemical analyses of schistose amphibolites

	25	27	76	77	78	79	90	91	105	308	313	314	353	382
SiO <sub>2</sub>	48.20	48.50	47.13	46.40	49.35	56.45	46.60	47.80	47.73	47.50	48.01	47.52	49.60	48.10
TiO <sub>2</sub>	2.60	1.86	1.73	1.33	2.78	1.09	2.97	2.75	1.62	2.20	2.02	2.20	tr.	1.80
Al <sub>2</sub> O <sub>3</sub>	15.12	15.35	14.42	13.83	13.76	14.63	16.37	15.11	13.61	14.19	14.13	14.36	17.80	16.10
Fe <sub>2</sub> O <sub>3</sub>	2.35	2.05	2.05	3.78	5.21	4.95	2.76	2.56	3.03	2.82	1.03	6.02	5.69	1.90
FeO	3.74	3.22	3.05	10.39	9.25	5.70	8.14	9.07	4.33	7.61	11.41	5.56	5.40	10.40
MnO	0.11	0.08	0.09	0.11	0.06	0.07	0.11	0.10	0.08	0.20	0.11	0.13	0.10	0.12
MgO	6.01	6.97	7.21	3.91	5.18	7.13	3.75	7.29	10.32	10.00	9.50	9.70	4.73	6.37
CaO	10.59	8.93	10.53	10.59	6.66	0.19	9.62	9.20	13.99	8.50	8.50	8.50	10.8	10.8
Na <sub>2</sub> O	3.25	2.82	2.57	2.62	2.74	2.20	3.35	2.39	1.30	3.30	2.13	3.10	2.40	2.60
K <sub>2</sub> O	0.23	0.76	0.33	0.48	0.53	0.21	0.55	0.40	0.54	0.90	0.43	0.40	0.30	0.50
P <sub>2</sub> O <sub>5</sub>	0.30	0.21	0.07	0.29	0.29	0.09	0.32	0.25	0.13	0.50	0.40	0.40	0.02	0.23
CO <sub>2</sub>	2.41	2.33	1.90	2.10	1.90	1.81	2.51	1.90	2.33	2.50	1.23	2.20	3.55	tr.
H <sub>2</sub> O														
Total	99.96	100.48	99.60	100.55	99.68	100.02	98.51	99.72	100.86	100.29	100.23	100.15	99.89	100.15
Oxidation Ratio	18.81	16.67	18.28	24.67	33.64	43.87	22.74	18.77	41.65	25.08	7.85	49.60	44.45	14.13
<b>Niggli values</b>														
al	21	23	19	18	20	23	26	21	17	19	19	20	28	22
fm	44	47	49	52	49	46	38	50	48	53	56	52	45	46
c	27	23	25	25	23	25	27	23	32	20	20	21	18	25
alk	8	8	7	6	8	6	9	6	3	8	5	8	8	7
Si	116	115	105	101	124	159	119	112	102	106	108	110	134	113
k	0.04	0.15	0.07	0.11	0.12	0.05	0.10	0.09	0.22	0.16	0.13	0.07	0.19	0.11
mg	0.50	0.53	0.53	0.51	0.41	0.48	0.37	0.51	0.69	0.64	0.58	0.59	0.42	0.48
qs	-16	-17	-23	-23	-8	+35	-17	-12	-10	-26	-12	-22	+2	-15

Localities (with Norwegian grid references) for rocks in Table 2

25	Hb-ab-epid-schist	N. W. of N. Tverra, 528:423	Analyst	D. R. Cowan
27	Hb-ab-epid-bi-schist	N. W. of N. Tverra, 528:423	Analyst	D. J. Mather
76	Hb-ab-epid-schist	Nr. Gjeitaabreein, 540:433	Analyst	D. J. Mather
77	Hb-ab-epid-schist	Nr. Gjeitaabreein, 539:443	Analyst	D. J. Mather
78	Hb-ab-epid-schist	Nr. Gjeitaabreein, 538:443	Analyst	D. J. Mather
79	Hb-ab-qtz-epid-schist	Nr. Gjeitaabreein, 538:443	Analyst	D. J. Mather
90	Hb-ab-epid-schist	Nr. Gjeitaabreein, 548:447	Analyst	D. R. Cowan
91	Hb-ab-epid-chl-schist	Nr. Gjeitaabreein, 547:446	Analyst	D. J. Mather
105	Hb-ab-epid-bi-schist	Nr. Gjeitaabreein, 540:443	Analyst	D. J. Mather
308	Hb-ab-epid-bi-chl-schist	Høydaalen, 477:375	Analyst	D. J. Mather
313	Hb-ab-epid-schist	Høyjelet, 473:382	Analyst	D. J. Mather
314	Hb-ab-bi-epid-chl-schist	Høyjelet, 477:383	Analyst	D. J. Mather
353	Hb-ab-epid-bi-chl-cal site schist	Høydaalen, 480:373	Analyst	M. Dowlman
382	Hb-ab-epid-bi-schist	Høyjelet, 473:383	Analyst	M. Dowlman

**Table 3****Average analyses of massive and schistose amphibolites**

	massive amphibolite	schistose amphibolite
SiO <sub>2</sub>	47.21	48.50 (47.89*)
TiO <sub>2</sub>	2.41	2.05
Al <sub>2</sub> O <sub>3</sub>	14.40	15.00
Fe <sub>2</sub> O <sub>3</sub>	2.17	3.39
FeO	9.65	8.44
MnO	0.12	0.11
MgO	7.82	7.12
CaO	10.20	9.44
Na <sub>2</sub> O	2.77	2.65
K <sub>2</sub> O	0.56	0.51
P <sub>2</sub> O <sub>5</sub>	0.22	0.29
CO <sub>2</sub>	0.38	} 2.52
H <sub>2</sub> O	2.03	
Total	99.94	100.02
q <del>z</del>	—	0.54
or	3.34	2.78
ab	23.58	22.53
an	25.02	27.52
di	19.69	14.19
hy	5.74	20.43
ol	12.11	—
mt	3.25	4.87
il	4.56	3.95
ap	0.50	0.67

\* This omits one abnormal SiO<sub>2</sub> figure of 56.45

Table 4 Significance levels of the chemical constituents of schistose and massive amphibolites

	Massive Amphibolites		Schistose Amphibolites		t value	Significance Level
	Mean	Standard deviation	Mean	Standard deviation		
SiO <sub>2</sub>	47.21	2.351	48.50	2.454	1.39	20%
SiO <sub>2</sub>	47.21	2.351	47.89*	1.121	0.94	40%
TiO <sub>2</sub>	2.41	0.826	2.05	0.833	1.11	30%
Al <sub>2</sub> O <sub>3</sub>	14.40	1.493	15.00	1.313	1.09	30%
Fe <sub>2</sub> O <sub>3</sub>	2.17	0.997	3.39	1.554	2.45	5%
FeO	9.65	1.273	8.44	2.083	1.84	10%
Total Iron	11.823	1.334	11.829	1.480	0.01	≈ 100
MnO	0.12	0.040	0.105	0.034	1.165	30%
MgO	7.82	1.106	7.12	2.048	1.12	30%
CaO	10.20	1.158	9.44	1.757	1.34	20%
Na <sub>2</sub> O	2.77	0.900	2.65	0.554	6.43	70%
K <sub>2</sub> O	0.56	0.310	0.51	0.202	0.48	70%
P <sub>2</sub> O <sub>5</sub>	0.22	0.136	0.29	0.210	1.05	40%
Oxidation Ratio	16.78	7.035	+26.58	13.11	2.59	2%

\* This omits one abnormal SiO<sub>2</sub> figure of 56.45

+ N.B. The mean of the oxidation ratios is not identical to the oxidation ratio of the average rock. See Table 5,

however the difference is small.

Table 5

Oxidation Ratios, i. e., mols  $\frac{2\text{Fe}_2\text{O}_3}{2\text{Fe}_2\text{O}_3 + \text{FeO}}$ , of associated  
intrusive and extrusive basic igneous rocks in various provinces.

	$\text{Fe}_2\text{O}_3$	FeO	Oxidation Ratio
Average Palisades dolerite	1.6	8.7	14.2
Average Watchung basalt	3.4	8.6	26.1
Average Spitzbergen intrusions	3.4	10.3	22.7
Average Spitzbergen extrusions	4.8	10.1	30.0
Average Karroo basic intrusives	1.2	9.3	11.0
Average Karroo basic extrusives	2.7	7.9	23.6
Average of above intrusives	2.1	9.4	16.5
Average of above extrusives	3.6	8.9	26.8
Massive Holleindalen amphibolites	2.17	9.65	16.8
Schistose Holleindalen amphibolites	3.39	8.44	26.6

Thrust rock-anorthosite

A white epidote-albite rock is sporadically developed on the west side of Holleindalen, especially around Blaaho. It consists of extremely tightly folded epidote bands in an albite matrix (see Fig. 24). It is located along the axial planes of B2 folds and appears to be due to thrusting parallel to the axial planes of B2 folds.

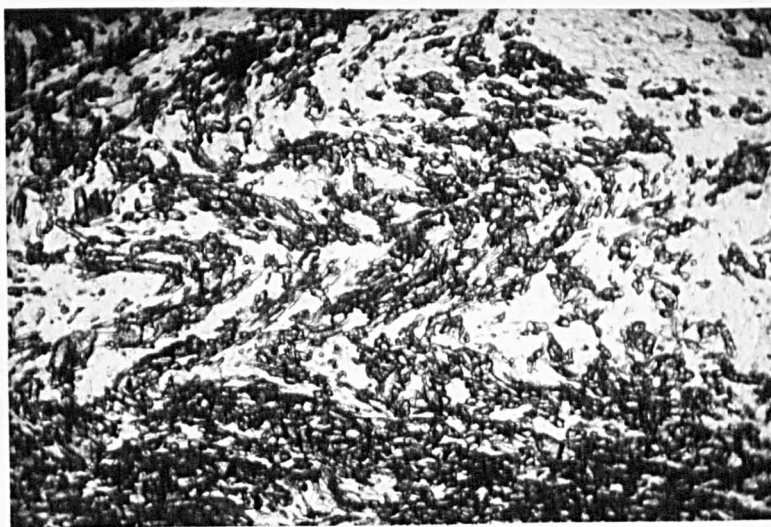


Fig.24 .



## THE UPPER PELITE GROUP

### Lithologies and Field Relations

The upper pelite group is a monotonous succession of graphitic mica-schists with variable quartz-mica-schist horizons and some impersistent quartzite. In view of its stratigraphic position, it tends to outcrop in synclinal areas and it has a wide outcrop in the centre of the area mapped. These phyllites become the dominant rock to the east, around Runninge, where the greenstone group has disappeared.

Small-scale facies variation is quite marked, the quartzite ribs are very impersistent and persist for only a few metres as a rule.

The thickness of the upper pelite group is exaggerated by folding, but must be at least 400 metres.

### Petrography

#### 1. Graphite-mica-schist

These have a brown weathered appearance in many specimens, frequently covered by yellow sulphur deposits. When fresh, the rock has a black, lustrous phyllitic appearance and it fractures along curved mica foliation planes. Pyrite grains are found in some specimens of fresh phyllite and quartz veins are abundant.

### Mineral assemblages

Muscovite-quartz-biotite-graphite-epidote-(sulphur)

Graphite-muscovite-biotite-pyrite

Graphite-muscovite-chlorite-pyrite.

### Fabric (see Fig. 25 )

The texture is crystalloblastic, lepidoblastic to granoblastic. Most grains are xenoblastic. The rock is normally fine-grained but micas may be up to 3 mm. long. A schistose



Fig.25. Photomicrograph of graphitic mica-schist.  
Note B3 micro-folds. X 30

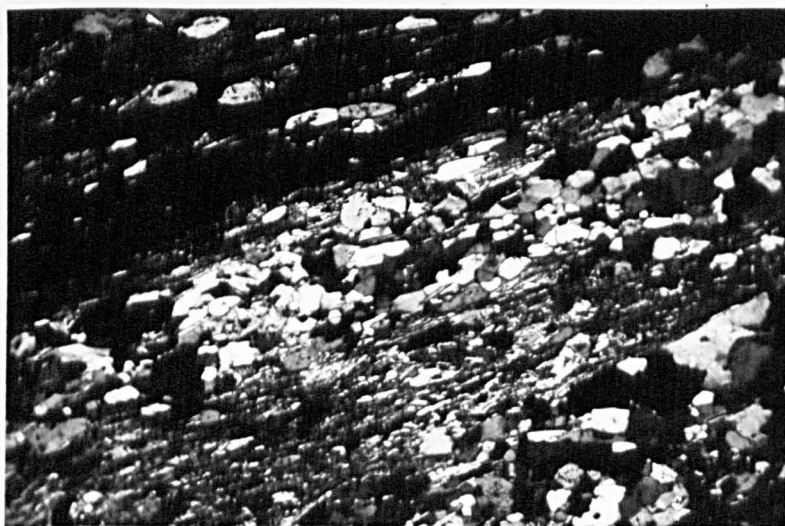


Fig.26. Photomicrograph of quartz-mica-schist.  
Note micaceous and quartz-rich bands. X.n X 30

foliation defined by alignment of micas is present and there is a film of graphite on the surface of the micas. Minor folding of the foliation is clearly visible in thin section; the folds are usually B3 folds, with well developed axial plane strain-slip cleavage.

### Mineralogy

Muscovite constitutes up to 60% of the rock; quartz up to 30% biotite up to 15%.

(a) Muscovite occurs as flattened individuals and abundant folded aggregates. In some cases, the cleavage of the micas can be seen to be bent by minor folds. It is slightly pleochroic from colourless to pale yellow.

(b) Quartz occurs as granoblastic (sutured to lobate) grains showing some strain shadow. Chlorite has grown along grain boundaries in some cases.

(c) Biotite occurs as tabular flakes associated with muscovite and it is strongly pleochroic. It is partially replaced by chlorite.

(d) Graphite occurs as a thin film on mica and chlorite flakes. An analysed specimen gave a residue of 4.2% C. Epidote, pyrite and chlorite are accessory minerals.

### 2. Quartz-mica schist

This is a widespread lithology and frequently contains quartz veins. When fresh it is grey coloured, but it weathers brown.

#### Mineral assemblages

Quartz-muscovite-biotite-chlorite-epidote

Quartz-K feldspar-calcite-biotite-muscovite-apatite

Quartz-muscovite-biotite-calcite-epidote-graphite

Fabric see Fig.26 for a photomicrograph of this rock

The texture is crystalloblastic, granoblastic to sub-

lepidoblastic. Most grains are xenoblastic. The grain size is rather variable; calcite grains are up to 2 mm; quartz grains usually about 0.75 mm; muscovite flakes are up to 2 mm long. A foliation defined by alignment of micas and to some extent form orientation of quartz grains is present. Minor folding of this foliation is seen in thin section.

### Mineralogy

Quartz grains form up to 65% of the rock; muscovite forms up to 20% of the rock; biotite up to 15% of the rock.

- (a) Quartz occurs as granoblastic (sutured to lobate) grains with strain shadows.
- (b) Muscovite occurs as aggregates and scattered flakes, often in intimate association with biotite.
- (c) Biotite occurs as aggregates of small pleochroic tabular flakes; some replacement by chlorite.
- (d) K feldspar occurs as irregular, altered grains up to 2 mm. Perthitic textures are seen.
- (e) Calcite occurs as grains up to 2 mm; strain twinning is developed. Chlorite, epidote, apatite, graphite and ilmenite-leucoxene are accessory minerals.

### 3. Quartzites and micaceous quartzites (see Fig. 27)

Quartzites occur as thin ribs throughout the upper pelite group and are impersistent along the strike. They consist of assemblages of quartz, muscovite, biotite, plagioclase, calcite, epidote and magnetite and their detailed petrography is identical with the quartzites of the upper pelite-limestone group, described in the next chapter.

### Metamorphic facies

The dominant assemblages of the upper pelite group:



Fig.27 . Photomicrograph of micaceous quartzite  
with a quartz vein. X.n  $\times 30$



Fig.28 . " Conglomerate" Hoydalsvatn outflow.

Quartz-muscovite-biotite-epidote

Muscovite-graphite-biotite-chlorite-epidote

Quartz-muscovite-biotite-calcite-epidote

are typical of the intermediate subfacies of the greenschist facies (quartz-albite-epidote-biotite subfacies). Retrograde metamorphism in the lowest subfacies of the greenschist facies (quartz-albite-epidote-chlorite subfacies) is shown by the replacement of biotite by chlorite.

### Petrogenesis

The rocks were probably deposited in a reducing environment as is indicated by the presence of iron pyrites and graphite. The quartz-mica-schists were formed by simultaneous deposition of sand grains and clay minerals.

After deposition and burial, the upper pelite group has been thrust, metamorphosed and folded during the Caledonian orogeny. The main metamorphism was in the intermediate subfacies of the greenschist facies. Later retrograde metamorphism occurred in the lowest subfacies of the greenschist facies. The group has suffered polyphase folding and a complex succession of introduction of quartz veins.

The relationship of metamorphism to folding is discussed in chapter 9 .



Fig.29 .

Contorted meta-  
limestone with quartz  
and calcite veins.

Fig.30 . Folded meta-limestone, showing typical  
weathering pattern.



## UPPER LIMESTONE-PELITE GROUP

### Lithologies and Field Relations

The upper limestone-pelite group is rather a variable assemblage. In the west of the area, it consists of marble with bands of quartz-mica schist, phyllite and micaceous quartzite; in the east, it becomes dominantly pelitic and consists of mainly phyllites with quartz-mica schists and a thin band of marble.

In addition, a phacoidal quartzite occurs at the base of the succession and another occurs at a slightly higher level.

The marble thins rapidly from west to east from about 800 metres to 5 metres.

The top of the succession consists of psammitic schists and quartzites. Facies variation within the group can best be seen on the geological map.

The true thickness of the group is exaggerated by folding, but even allowing for this, the group must be at least 1600 metres thick.

The upper limestone-pelite group outcrops only in the south of the supracrustal area. It is probable that it once outcropped to the north, but has since been removed by erosion.

The following lithologies have been recognised:

1. Marble (impure meta-limestone)
2. Graphite-mica-schist
3. Quartz-mica-schist
4. Quartzites and micaceous quartzite
5. Feldspathic quartzite
6. Phacoidal quartzite



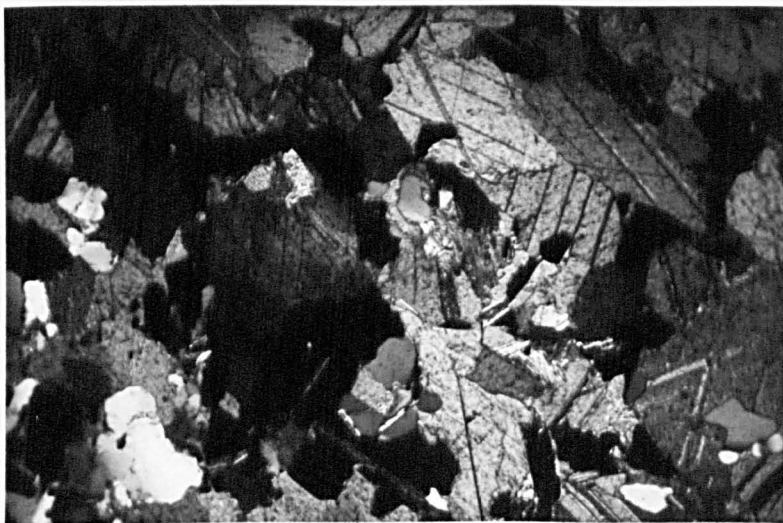


Fig.31 . Photomicrograph of meta-limestone.  
X.n. x 30

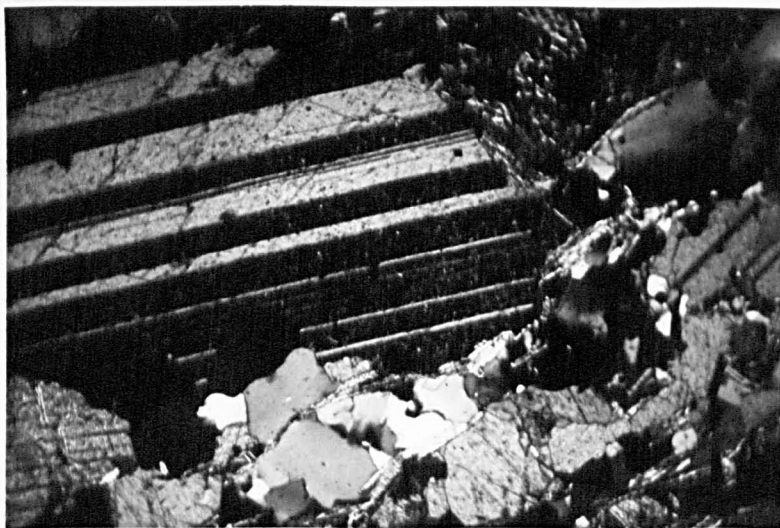


Fig.32 . Photomicrograph of meta-limestone.  
Xn x 30

## Petrography

The graphite-mica-schist (2) and quartz-mica-schist (3) are identical with those of the preceding upper pelite group and will not be described again. Fig.36 shows the field occurrence of quartz-mica-schist and fig.33 is a photomicrograph of this rock.

### 1. Impure meta-limestone or marble

The limestone varies from a fairly pure blue limestone, consisting of calcite and muscovite to a sandy limestone with up to 40% quartz. Contorted veins of quartz and calcite of several generations are common (see Fig.30 ).

## Mineral Assemblages

Calcite-quartz-muscovite-magnetite

Calcite-muscovite-quartz-epidote-pyrite.

## Fabric (see Fig.31 )

The texture is crystalloblastic, granoblastic; most grains are subidioblastic. Normally the limestone is fine-grained to medium grained. A weak muscovite foliation is present in some cases and minor folding of this foliation and the quartz veins is seen in thin section.

Figs. 31 and 32 are photomicrographs of this rock.

## Mineralogy

Calcite constitutes up to 80% of the mode; quartz up to 40%; muscovite up to 15%.

(a) Calcite occurs as pale brown, subidioblastic, often equidimensional grains. Strain twinning is developed on  $01\bar{1}2$  and  $10\bar{1}1$  (see Fig.32 ).

(b) Quartz occurs as granoblastic (sutured to lobate) grains with some strain shadow.

(c) Muscovite occurs as thin, flattened individuals and small aggregates. It is slightly pleochroic from colourless to pale yellow. Magnetite, epidote and pyrite occur as accessory minerals.

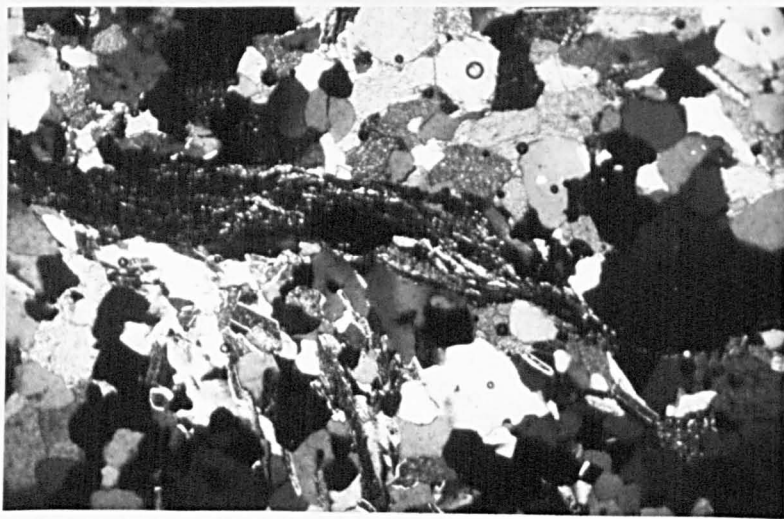


Fig. 33. Photomicrograph of quartz-mica-schist.  
X.n x 30



Fig. 34. Photomicrograph of feldspathic quartzite.  
X.n. x 30

#### 4. Quartzites and micaceous quartzites

Quartzites and micaceous quartzites occur at several horizons in the upper limestone-pelite group, especially near the base and top of the group. Fig.36 shows the quartzite at the top of the group.

##### Mineral Assemblages

Quartz-muscovite-biotite-plagioclase-(calcite-magnetite).

Quartz-muscovite-biotite-chlorite-magnetite

Quartz-muscovite-biotite-chlorite-epidote-clinzoisite

Accessories include magnetite, zircon, sphene, ilmenite and leucoxene.

Fabric (see Fig. 27 )

The texture is crystalloblastic, granoblastic (sutured) and most grains are xenoblastic. The rocks are normally fine-grained, but micas may be up to 2 mm. long. A muscovite foliation is usually present, its intensity depending on the mode of muscovite and quartz grains may show some form of orientation within this foliation. The more micaceous rocks can be seen to be micro-folded.

##### Mineralogy

Quartz constitutes up to 90% of the rock; muscovite up to 15%; biotite up to 7%.

(a) Quartz occurs as granoblastic (sutured) grains, showing strain shadows (up to 30° undulose extinction)

(b) Muscovite occurs as thin, flattened individuals and small aggregates. It is slightly pleochroic from colourless to pale-yellow-green.

(c) Biotite occurs as thin flattened individuals associated with the muscovite. It is strongly pleochroic with X = straw yellow, Y, Z = brown.

(d) Chlorite occurs replacing biotite in some sections

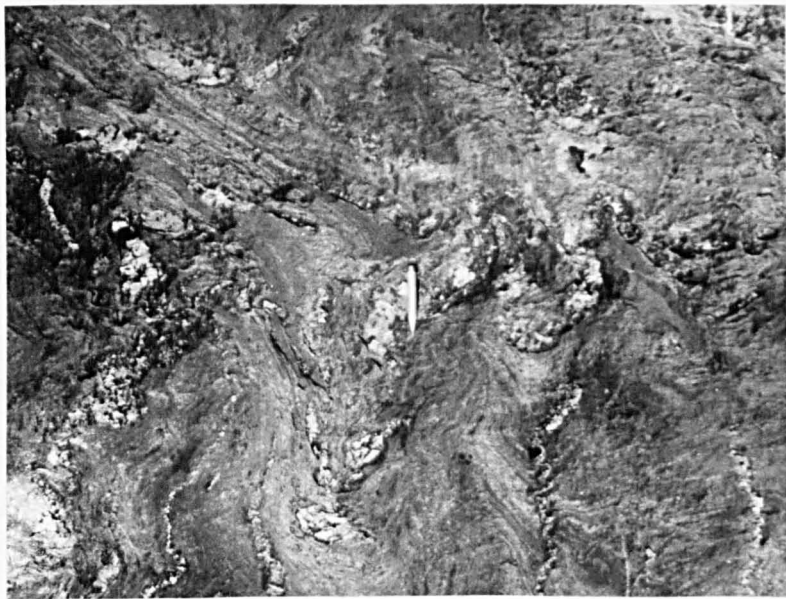


Fig.35. Quartz-mica-schist with quartz veins, showing B2 and B3 folds.

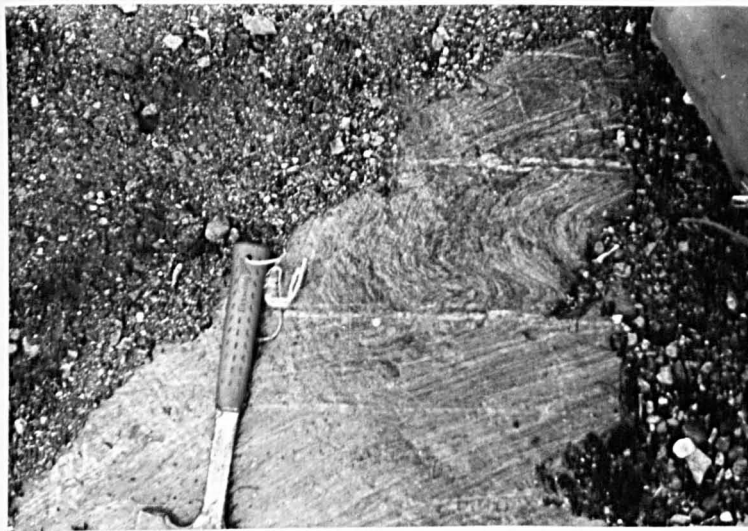


Fig.36. Feldspathic quartzite showing B2 folds and S2 fracture cleavage infilled with quartz.

- (e) Plagioclase occurs as rather altered, irregular-shaped grains, sometimes with albite twinning.
- (f) K feldspar occurs as rounded grains.
- (g) Calcite occurs as irregular shaped brown grains, showing strain twinning.
- (h) Epidote occurs as small green rounded grains
- (i) Clinozoisite occurs as a few elongated crystals showing berlin blue interference colours. Extinction is variable, mainly parallel. Sphene, zircon and ilmenite-magnetite occur as accessory minerals.

#### Feldspathic Quartzite

Thin bands of feldspathic quartzite occur within the limestone outcrop and immediately above and below the limestone. It is variable in both grain size and composition. Fig.34 is a photomicrograph of this rock.

#### Mineral Assemblages

Quartz-K feldspar-plagioclase-calcite-biotite-chlorite-sericite-epidote.  
Quartz-K feldspar-biotite-muscovite.

#### Fabric (see Fig.34 )

The texture is partly crystalloblastic, but is largely cataclastic in some specimens. Grains are granoblastic, usually xenoblastic. The grain size is variable; microclines up to 4 mm occur; quartz is usually fine grained. Little evidence of planar or linear structures is seen.

#### Mineralogy

Quartz constitutes up to 60% of the rock; K feldspar up to 30%; calcite up to 20%; biotite up to 10%.

- (a) Quartz occurs as granoblastic (sutured) grains, showing variable amounts of strain shadow (up to  $30^{\circ}$  undulose extinction). It is probable that several generations of quartz crystallisation are present.
- (b) K feldspar occurs as grains of variable size (0.5 up to 4 mm).



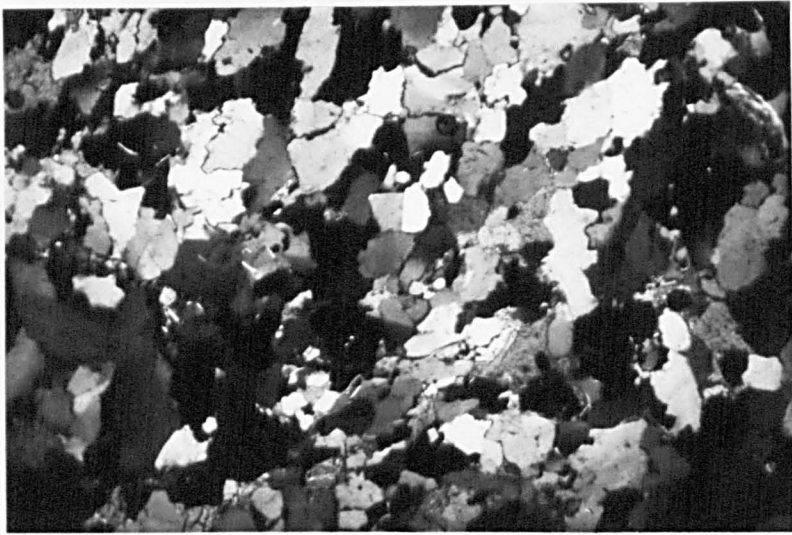


Fig.37. Photomicrograph of phacoidal quartzite  
from Hoydalsvatn outflow. X.n x 30

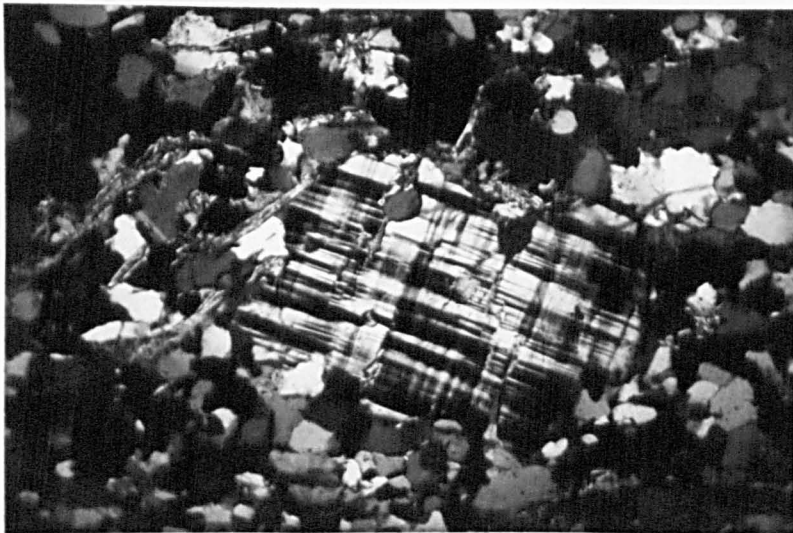


Fig.38. Photomicrograph of Phacoidal quartzite  
from Hoydalsvatn outflow; microcline rich phacoid.  
X.n x 30

Twinning on the microcline law and perthitic intergrowths are common. The larger grains show clear lamellar intergrowths. Extensive sericitisation is found in places.

- (c) Plagioclase occurs as a few altered, subidioblastic grains usually showing albite twinning.
- (d) Calcite occurs in irregular, xenoblastic patches in some sections, frequently associated with plagioclase.
- (e) Biotite occurs as individual flakes showing strong pleochroism.
- (f) Chlorite occurs as pale green, slightly pleochroic flakes, in association with biotite.
- (g) Sericite occurs as tiny flakes, replacing microcline. Muscovite, epidote and magnetite are accessory minerals.

#### Phacoidal Quartzite

A "conglomeratic" rock occurs at the base of the group and has a maximum thickness at the outflow of Hoydalsvatn and thins out eastwards. A second lens of "conglomerate" occurs north of Gjeithoe, but dies out when traced east and west.

The origin of this rock is problematical and it is considered in detail in the structural section. It seems probable that it is partly a true sedimentary conglomerate and in part of tectonic origin.

Fig.28 shows the field occurrence of this rock.

#### Mineral Assemblages

The phacoids consist mainly of quartzite with a few limestone phacoids; in a micaceous-chloritic matrix. Quartz-biotite-muscovite-calcite-chlorite-plagioclase-K feldspar.

Fabric Fig.37 is a photomicrograph of this rock

The phacoids have a granoblastic (sutured) texture and the matrix is usually sub-lepidoblastic. The phacoids are very variable in size and individual quartz grains within the phacoids are up to 1 mm. The quartz grains of the matrix are up to 0.2 mm and



the micas are up to 1 mm long.

A mica foliation is present in the matrix and the phacoids have a strong preferred orientation within the foliation, parallel to B1 fold axes.

Folding of both foliation and phacoids by B2 and B3 folds is common (see Fig.150 ); often a strain slip cleavage is developed and S2 is quite strong in places.

### Mineralogy

#### (a) Quartz

The pebbles consist of large (1 mm), granoblastic (sutured) grains with extensive strain shadows. Quartz grains in the matrix are usually less than 0.2 mm.

(b) Biotite occurs in small, flattened, tabular flakes, sometimes cross-cutting the foliation.

(c) Muscovite occurs as slightly pleochroic, flattened individuals.

(d) K feldspar occurs as a few large altered grains of microcline.

(e) Plagioclase. Occasional sections of plagioclase, showing albite twinning have been recorded.

(f) Calcite occurs as small brown interstitial patches between quartz grains.

(g) Chlorite occurs as flakes within the matrix.

### Metamorphic facies

The typical assemblages of the upper-pelite group: ,  
Calcite-quartz-muscovite  
Quartz-muscovite-biotite, etc.  
probably belong to the intermediate subfacies of the greenschist facies. Retrograde metamorphism in the lowest subfacies of the greenschist facies is shown by the replacement of biotite by chlorite.

### Petrogenesis

Little can be said concerning deposition of these rocks.

The limestone is probably clastic and the pelitic rocks were deposited under anaerobic conditions. The lateral passage from limestone to pelite may represent increase in depth of water.

If the phacoidal quartzite is partly sedimentary, it may represent a shore line feature.

The group has been thrust, metamorphosed and folded during the Caledonian orogeny. The main metamorphism was in the intermediate subfacies of the greenschist facies and later retrograde metamorphism occurred in the lowest subfacies.

The group has suffered polyphase folding and several periods of injection of quartz and calcite veins.



Fig.39 . Feldspathic quartzite ,folded by B2 folds and with S2 axial plane cleavage ,infilled with quartz.



Fig.40 . Feldspathic quartzite, showing fracture cleavage infilled with quartz.

## THE FELDSPATHIC QUARTZITE GROUP

---

### Lithologies and Field Relations

The feldspathic quartzite group occurs between the top of the upper limestone-pelite group and the base of the upper Jotun nappe. The contact between the feldspathic quartzites and the underlying rocks may be an unconformity; This is suggested by some evidence of cross-cutting lithological boundaries, but the evidence is inconclusive. No evidence of any movement along this contact has yet been found.

In a narrow zone below the upper Jotun nappe, the feldspathic quartzites have recrystallised to a very hard, flaggy quartzite; in a few outcrops, there is evidence of feldspathisation.

The dominant lithology is a somewhat feldspathic grey quartzite which may become green in colour towards the top of the succession. In addition, pure quartzites and micaceous quartzites are quite common.

The upper part of the succession is more feldspathic than the lower part.

A typical exposure of feldspathic quartzite is shown in Fig.40 .

In view of its stratigraphic position, this horizon was correlated with the Valdres Sparagmite by Landmark (1948). The present writer considers the evidence to be inconclusive. The succession is not very much like the typical Valdres sparagmite of the south-Jotunheimen, nor is it like the Lom area to the east. However, the feldspathic quartzites do contain coarse perthitic feldspars of the type common in the rocks of the Bergen-Jotun kindred.

The rocks frequently show two planar structures (see Fig.39 ) ; S2 fracture cleavage, infilled with quartz is common in

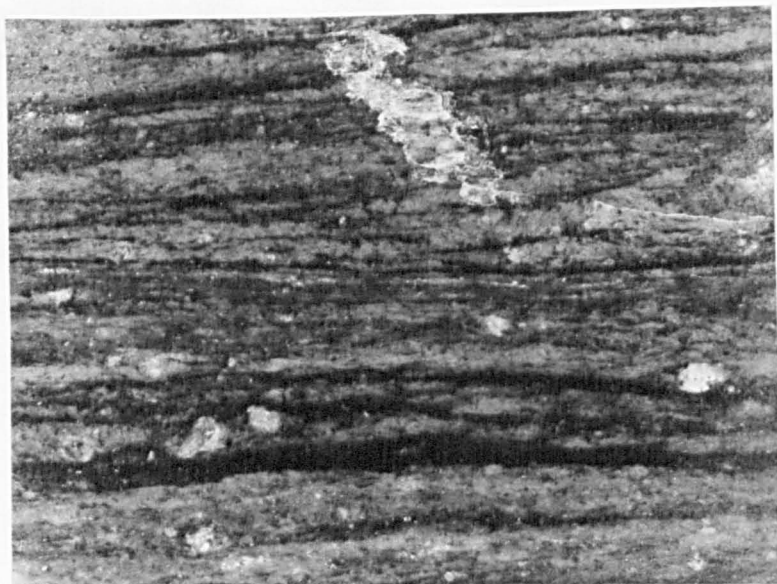


Fig.41 .Polished specimen of feldspathic quartzite showing texture. Note clastic grains.



Fig.42.Feldspathic quartzite with B4 kink-band.  
X.n. x 30.

rocks of this group. Several linear structures may be present.

The feldspathic quartzite group has a maximum thickness of about 600 metres.

### Petrography

#### Feldspathic quartzite

#### Mineral Assemblages

Quartz-K feldspar-muscovite-ilmenite

Quartz-K feldspar-albite

Fabric (see Fig. 41 for overall fabric)

Figs. 42, 43 and 23 are photomicrographs of this rock. The texture is crystalloblastic, granoblastic (sutured) and most grains are xenoblastic. Quartz is usually fine-grained (less than 0.5 mm) and K feldspar may be up to 2 mm. A muscovite foliation is present in the more micaceous rocks and this foliation is folded by micro-folds, sometimes with axial plane strain-slip cleavage.

#### Mineralogy

- (a) Quartz occurs as granoblastic (sutured) grains with strain shadows and small inclusions of magnetite. It forms a large part of the groundmass and also a few larger clastic grains.
- (b) K feldspar-microcline occurs as small grains associated with quartz and albite in the groundmass and as large irregular clastic grains. Microcline twinning and coarse perthitic textures are common (see Fig. 23 and Fig. 43 ).
- (c) Muscovite occurs as small flaky aggregates; it is slightly pleochroic from pale green to colourless.
- (d) Albite occurs as small granoblastic (lobate) grains in the groundmass.
- (e) Ilmenite occurs as scattered, irregular grains, frequently altered to leucoxene.

#### Metamorphic facies

The mineral assemblages of the feldspathic quartzite group are stable over a wide P, T field. The absence of chlorite,

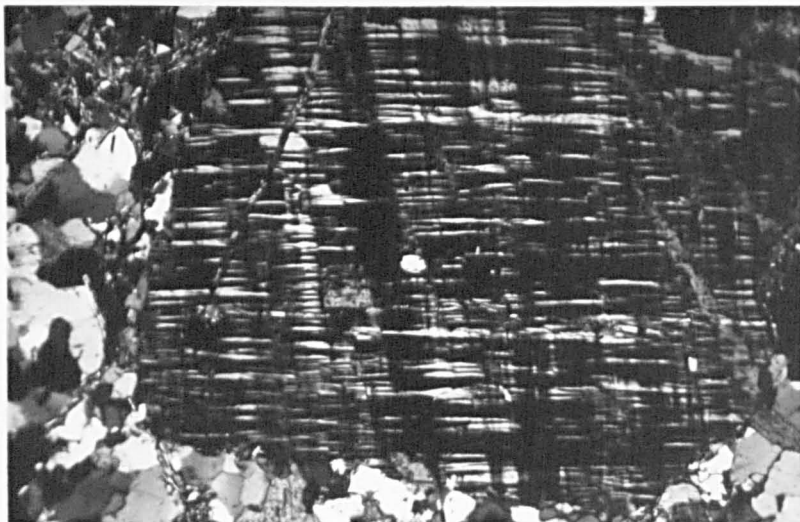


Fig.43. Photomicrograph of feldspathic quartzite,  
showing perthitic K feldspar.  
X.n. x 30

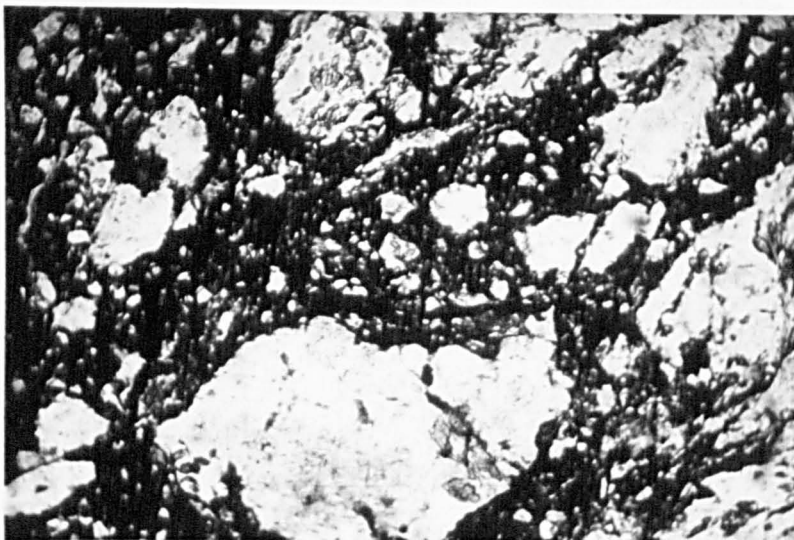


Fig.44. Photomicrograph of cataclastite from  
the base of the upper Jotun nappe.  
X.n. x 30

biotite, almandine makes it impossible to define the metamorphic facies of this group.

### Petrogenesis

The conditions of deposition of this group are not clear. The rocks probably represent dirty, arkosic sandstones.

No fossils have been found in the area mapped, so that the group can not be dated accurately and the correlation with the Valdres Group can not be proved.

The Valdres group is considered to be a "molasse" type synorogenic deposit. Strand considers it contemporaneous with the Jotun nappes and considers the material to be derived from the erosion of the lower Jotun nappe.

The feldspathic quartzite group has suffered polyphase folding.



## THE UPPER JOTUN NAPPE

### Lithologies and Field Relations

The upper Jotun nappe is the highest tectonic unit within the area mapped and its junction with the underlying feldspathic quartzite group is marked by the spectacular development of 150 metres of mylonites, cataclastites and phyllonites. Such thicknesses of crushed rocks are not produced by small scale movements and we are seeing here one of the great thrusts of North-Western Europe.

The lowest part of the upper Jotun nappe consists of a layer of rocks of approximately granitic composition. This layer consists of acid and intermediate acid rocks, most of which have lost their original igneous texture and have acquired a strong cataclastic texture from the movement of the nappe. Hornblende and biotite granites occur and most rocks contain a perthitic microcline feldspar and a plagioclase in the albite/oligoclase range. Most rocks show the effects of metamorphism; the feldspars are somewhat turbid and the ferromagnesian minerals are altered to chlorite. In one section, chlorite pseudomorphous after pyroxene is seen, suggesting that the rocks may have been originally in the pyroxene granulite facies.

The thickness of this granitic layer or sheet is approximately 300 metres.

The thrust at the base of the upper Jotun nappe is well marked in a few places where a fine-grained phyllonite overlies a hard flaggy quartzite; in other outcrops, however, sheared granite overlies sheared feldspathic quartzite and the actual contact is difficult to locate.

A photomicrograph of a cataclastite is shown in Fig. 44 .

The recognition of cataclastites, mylonites and phyllonites within the zone of mylonitisation is something of a problem. Obviously



Fig.45 . Photomicrograph of mylonitised granite  
from the base of the upper Jotun nappe.

X.n. x30.

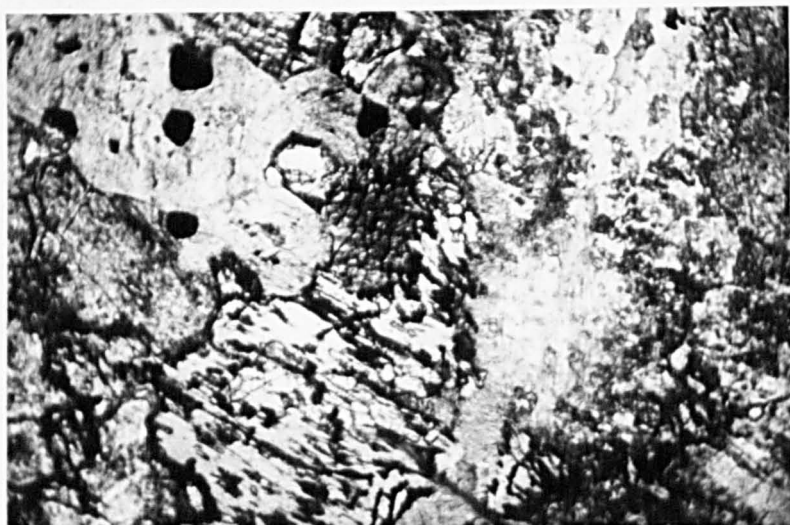


Fig.46 .Photomicrograph of altered meta-gabbro  
from the upper Jotun nappe.

x 30.

cataclastic and crystalloblastic processes must have either operated more or less at the same time or perhaps alternated locally due to fluctuations in some physical condition, for example, pore water pressure. In modern terminology, one would say that evidence of both direct and indirect componential movements can be seen in the same outcrop.

Above the granitic sheet is a thin sheet of meta-gabbro, which is about 200 metres thick and usually shows a metamorphic foliation. In some cases, an ophitic igneous texture is preserved, but even here a weak foliation is apparent. Fig.46 is a photomicrograph of this rock. The gabbro can easily be distinguished from rocks of the gneiss sequence above by hand specimen examination only. The layer is fairly uniform in composition; a few rather basic bodies were noted and a few pegmatite veins were recorded.

The history of the gabbro layer is complex and the following sequence of events is suggested from an examination of several micro-sections:

1. Primary crystallisation of clino-pyroxene-ortho-pyroxene-labradorite-ore mineral. A deep brown hornblende crystallised at a late stage producing a poikilitic texture.
2. Metamorphism occurred in the upper greenschist facies; a blue-green hornblende replaced pyroxene in places; the brown hornblende appeared to be stable. Alteration of plagioclase occurred and biotite may have formed.
3. Metamorphism in the lower greenschist facies, with alteration of remaining ortho-pyroxene to green chlorite and clino-pyroxene to tremolite. At the same time, small fractures were formed.

The basic differentiated bodies were originally assemblages of olivine-ortho-pyroxene-clino-pyroxene-labradorite and had a poikilitic texture. Later metamorphism caused the alteration of olivine to



Fig 47 . Pyroxene-gneiss of the upper Jotun nappe.



Fig 48 . folded layered ultramafic of the upper Jotun nappe.

serpentine along cracks, alteration of feldspar to a cloudy aggregate and growth of phlogopite. The shape of these bodies is uncertain, but they are very small; the largest being 2.3 metres in extent.

The assemblage olivine-labradorite in the differentiated bodies is of interest, since in the gneiss sequence above, this assemblage is unstable, the following reaction occurring:

olivine + labradorite  $\rightarrow$  ortho-pyroxene + clino-pyroxene + spinel.

This is the usual reaction in the granulite facies; hence the olivine-labradorite must be a relict igneous assemblage. The pegmatites are assemblages of biotite-feldspar.

The upper margin of the gabbro layer is obscured by moraine and permanent snow and the lower margin is poorly exposed and difficult to interpret; it could be a thrust, but it may be an igneous contact.

North-south vertical shear zones are common within the gabbro layer; these have a strong foliation and lineation and are assemblages of hornblende-chlorite-epidote. They can be seen to post-date the brown hornblende of the gabbro; they may be the same age as the shears seen in section in the gabbro.

#### Pyroxene-gneiss sequence

The upper part of the succession consists of well foliated two-pyroxene gneisses (granulites), with layers of pyroxenite and peridotite. Many of the gneisses possess a foliation and a lineation.

The gneisses are fairly uniform (see Fig.47); a few outcrops show layering but this is exceptional; this layering is due to variation in the ratio of pyroxene/feldspar. Fig50 is a photomicrograph of pyroxene gneiss.

The ultramafic layers are often differentiated, with layers of pyroxenite separated by thin layers of feldspar-rich rock



Fig49 . Layered ultramafic of the upper Jotun nappe.

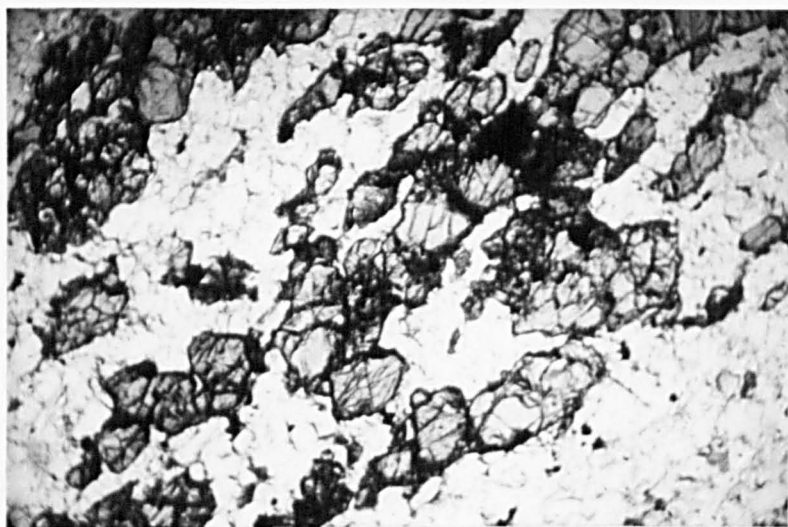


Fig50 . Photomicrograph of pyroxene gneiss of the upper Jotun nappe.

x 30

(see Figs.48 and 49 ). In addition in the thick ultramafic layers, some layering of ferromagnesian minerals is shown by a variation in the ratio of olivine/pyroxene.

No rocks have been observed containing a stable olivine-feldspar assemblage. It seems probable that the following reaction occurs:

olivine + anorthite = ortho-pyroxene + clino-pyroxene + spinel.

A few pegmatite veins occur and these are assemblages of hornblende-biotite-feldspar.

Cataclastic fabrics are common in both the gneisses and the ultramafics (see Figs.51,52 ).

#### Metamorphic facies

##### Granitic layer

There is a little evidence to show that these rocks originally contained ortho-pyroxene suggesting granulite facies. The present mineralogy is in the lower greenschist facies, chlorite being abundant.

##### Gabbro layer

The metamorphic history of the gabbro layer is complex. The igneous suite is a pyroxene gabbro which has differentiated to give olivine rich rocks and some pegmatites. The formation of brown hornblende in the gabbro was probably a late-stage igneous phenomenon. The first metamorphism of the gabbro was in the upper greenschist facies or lower amphibolite facies and pyroxene was partly replaced by green hornblende. The second metamorphism was in the lowest greenschist facies as shown by the abundance of chlorite.

##### Pyroxene gneiss-ultramafic complex

The assemblages of this group are typical of the pyroxene granulite facies. No definite evidence of retrograde metamorphism has been obtained.





Fig.51 . Photomicrograph of sheared ultramafic of the upper Jotun nappe. Note cataclastic texture.

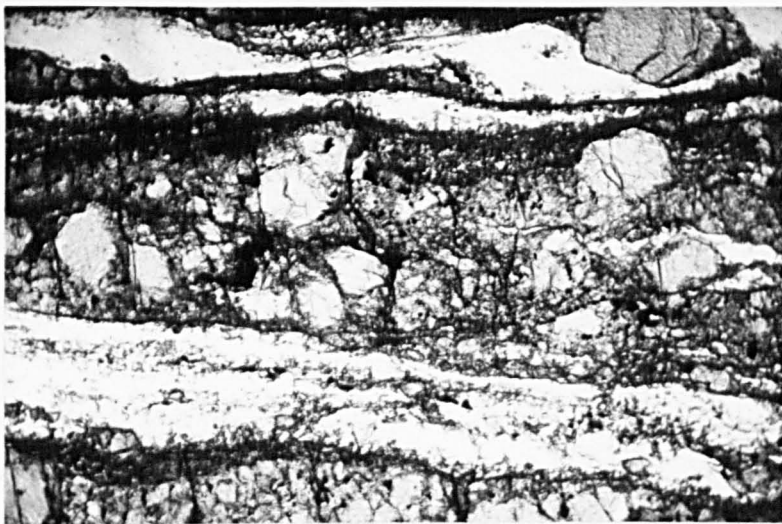


Fig.52. Photomicrograph of sheared ultramafic of the upper Jotun nappe. Note strong cataclastic texture.

x 30.



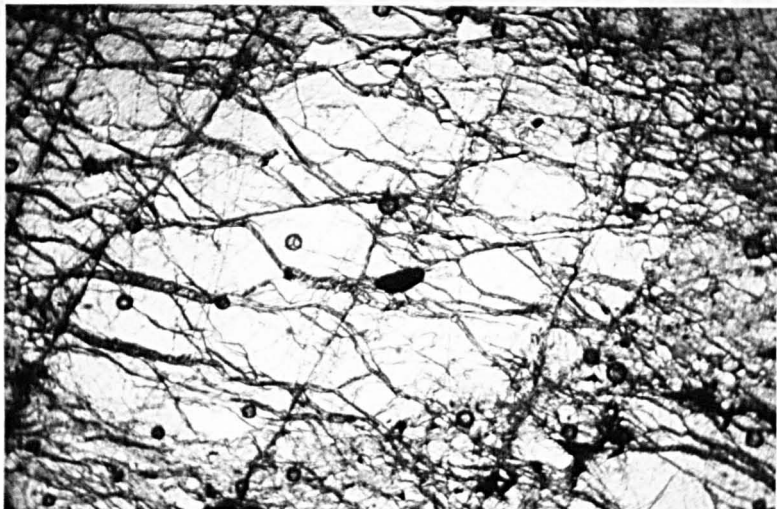


Fig.53 . Photomicrograph of ultramafic of the upper Jotun nappe. Note breaking up of grains of olivine.

### Petrogenesis

This is far from complete, but a tentative scheme is as follows:

#### 1. Pre-Cambrian

Crystallisation of an igneous complex comprising (a) A granitic layer (b) A gabbro layer (c) Differentiated intermediate-ultramafic layer.

The rocks were metamorphosed in the pyroxene-granulite facies and a foliation and often a lineation were induced. The complex was then folded.

#### 2. Age uncertain

Retrograde metamorphism of the lower part of the succession in the upper greenschist or lower amphibolite facies. This may be Pre-Cambrian or Caledonian.

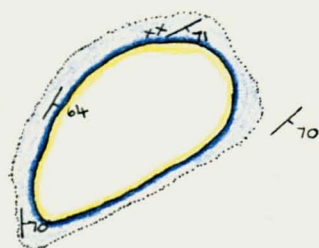
#### 3. Caledonian

Cataclastic deformation of the complex during emplacement in its present position. Mylonitisation of the base (granite layer) occurred at this time and the N.-S. vertical shear zones in the gabbro layer may be part of this deformation.

Later metamorphism in the lowest greenschist facies occurred.

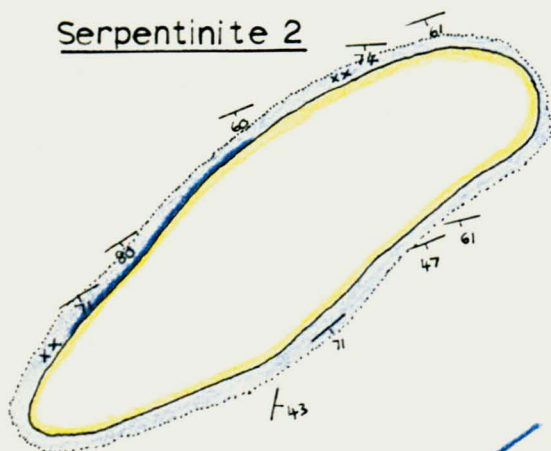
# Fig 54 Form of Serpentinite Bodies

## Serpentinite 1



scale 1:10,000

## Serpentinite 2



796

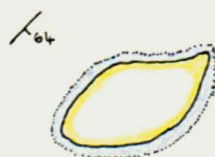
chlorite magnetite rock

## Serpentinite 3



ultra basic aureole —  
chlorite, magnetite,  
biotite some hornblende.

## Serpentinite 4



abundant talc-magnesite

xx

tourmaline present

## DUNITE-SERPENTINITES AND RELATED ROCKS

### General Introduction

Small intrusive bodies of dunite-serpentinite occur in the greenstone group and at the base of the upper phyllite group. They are particularly abundant on Holleindalen, where four large bodies (up to 800 metres long) occur as well as several smaller bodies (around 10 metres).

In the north of the area, several small bodies of talc-magnesite have been found intrusive into the greenstone group; these bodies are only a few metres long.

The ultra-basic bodies are all elongated parallel to the regional strike and have steeply inclined contacts. In section the bodies seem to be parallel to the axial planes of the major B2 folds.

The bodies are typical "alpine-type" serpentinites unrelated to any other igneous rocks in the area. Their location mainly within the volcanic group is probably due to tectonic control and it is considered likely that the bodies moved up into the crests of anticlines during B2 folding.

In most cases, the contact between ultrabasic and country rock is a thrust plane, generally marked by a zone of talc.

The serpentinization of the bodies is fairly uniform; unrelated to the margins of the bodies or to joint planes. "Auto-brecciation" phenomena are quite widespread, providing abundant evidence for movement in a fairly solid state.

The degree of alteration to talc depends on the size of the body; the small bodies are completely altered to talc-magnesite-actinolite assemblages; whereas the larger bodies have rims of talc followed by talc-magnesite and then a core of dunite-serpentinite. Magnetite is abundant in the talc rock.

In the contact zones the country rocks, which here consist



Fig.55 . General view of Holleindalen, showing serpentinites 1 and 3 ; Storhoe is in the far distance.



Fig.56 . Photomicrograph of serpentinite, showing fibro-lamellar intergrowth of antigorite flakes.

of muscovite-chlorite-schist and quartz-mica schist, have been altered to chlorite-magnetite rocks over a distance of up to 60 metres. Within a few metres of the contact, the country rocks have become altered to pure chlorite-magnetite rocks with occasional development of tourmaline, apatite, hornblende, garnet and phlogopite.

The large bodies have steep cross-cutting joints containing fibres of chrysotile asbestos, with the fibres aligned at right angles to the joints. •

The chrysotile veins are probably the latest phase in the evolution of the ultra-basic bodies.

#### Occurrence

The detailed occurrences of individual bodies are considered separately as follows and reference should be made to the accompanying lithological map and the diagrams (fig.54 ).

#### Serpentine 1

This is the eastern-most ultrabasic in the area mapped. The body is lensoid with elongation parallel to the regional strike. The contact with the country rock can be seen to dip steeply to the south and is probably a thrust plane (see fig.55 ).

The body is almost completely serpentinised; mesh structures in the serpentine show it was derived from olivine; in some cases olivine and a little orthopyroxene are seen in thin section. Auto-brecciation is extensively developed within the serpentinite and the body is strongly jointed (see fig.60 ).

The country rocks, hereabouts, mica-schists, have been altered to chlorite-bearing schists over a distance of up to 60 metres. Within a few metres of the contact the country rock has become completely altered to a chlorite-magnetite rock. On the southern contact the country rock has become altered to a phlogopite-sphene-



Fig.57 .

Serpentinite 5  
Contact relations.



Fig.58.

Serpentinite 5.  
Close-up of Fig.57 .

apatite assemblage.

The outer rim of the serpentinite has been altered to an outer zone of talc and an inner zone of talc-magnesite.

Joints containing chrysotile cross fibres have been recorded.

### Serpentine 2

This is the largest ultra-basic body found in the area mapped. The body is about 800 metres long and is lensoid in shape, elongated parallel to the strike. The contact with the country rocks is rarely seen but where visible is steeply dipping to the south.

The body is almost completely serpentinitised but a few patches of partly serpentinitised dunite have been found. Auto-brecciation is common and both steep and gently inclined joints are abundant.

The country rocks have been chloritised over a distance of up to 40 metres. Near the contact, the country rock has been altered to a chlorite-rich rock in which magnetite is quite abundant; tourmaline and apatite have been recorded from several localities.

The serpentinite has a rim of talc rock up to a maximum of about 50 metres. Magnesite is found within the inner zone of talc rock and within the serpentinite.

Many of the joints contain cross-fibre chrysotile asbestos and probably some actinolite. The chrysotile formation is later than the development of talc; the chrysotile fibres are frequently bent.

### Serpentine 3

This small body is lensoid in shape and elongated parallel to the regional strike; it is about 100 metres long (see fig.55 ).


The contact with the country rock is obscured but in the few localities where it is observed, it dips steeply to the south.



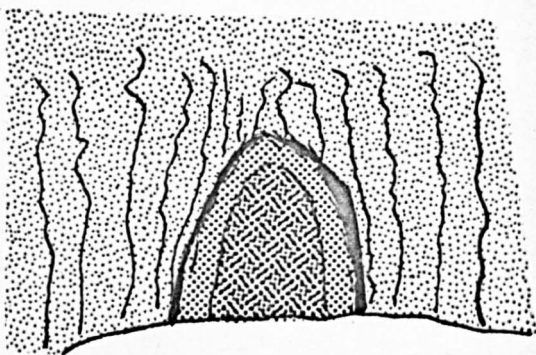


*Fig.59 Profile of Serpentine 5  
seen in cliff section*

*Serpentinite* 

*Talc zone* 

*Contact rock* 

*Country rock* 

The body is completely serpentinised and auto-brecciation structures are quite common (see fig.61 ). High angle joints are abundant.

The ultra-basic has an outer rim of talc, an inner zone of talc with magnesite and a core of serpentinite. The contact with the country rock is probably a thrust plane.

The country rocks have been chloritised to some extent around the ultrabasic, while near the contact occurs a zone of chlorite-magnetite rock.

A few joints containing cross-fibre chrysotile have been recorded. Slickensides have been noted.

#### Serpentine 4

This body has not been studied in detail. It is elongate, lensoid in shape and about 200 metres long. Its contact with the country rock dips steeply to the south. The original minerals have been completely serpentinised: autobrecciation has been noted; a rim of talc rock is present and the country rock has been chloritised to some extent over a distance of about 20 metres.

High angle joints containing chrysotile asbestos are abundant; it can be shown that they are later than the time of talc formation.

#### Serpentine 5

This small body (20 metres long) is lensoid and elongated parallel to the strike. A vertical section showing contact relations is seen in a rather inaccessible cliff section; the profile is shown in fig.59 . The ultra-basic body has been completely serpentinised and has a wide rim of talc rock. The contact alteration is unusual; a section is shown in figs.57 and 58 .

#### Small talc-magnesite bodies

Several small talc-magnesite bodies occur in the area mapped, both in the northern outcrop and Holleindalen.



Fig.60. Auto-brecciation in serpentinite.  
Serpentinite 1.



Fig.61 . Auto-brecciation in serpentinite.  
Serpentinite 3.

They are small elongate lenses, parallel to the strike. They are essentially two mineral rocks with only occasional nodules of radiating actinolite. A little chloritisation of the country rocks has occurred around them.

### Structure

The massive nature of the ultra-basic bodies is strikingly contrasted with the foliated and strongly minor folded country rocks, consisting mainly of mica-schists and greenstones.

As can be seen from the maps, the strike of the country rocks tends to swing round parallel to the margin of the ultra-basic (see especially Serpentine 1).

No folding of massive serpentinite has been observed, but the talc rock zone near the contact has been folded by B3 folds. The ultra-basic bodies tend to occur in anticlinal crests and are parallel to the axial planes of B2 folds. Most contacts appear to be thrust planes.

It seems likely that the ultra-basic bodies rose up the axial planes of B2 folds into the crests of anticlines, during folding.

The swing of the foliation around the ultra-basic bodies could be due either to pushing apart of the country rocks by the upward movement of the ultra-basics or to the influence of rigid ultra-basic bodies on the stresses producing the foliation. It would appear from scanty evidence that the foliation is pre-chloritisation of country rock by the ultra-basic, so that the deflection of strike is probably due to the upward movement of the ultra-basic bodies.

### Petrography

The ultra-basic rocks can be considered as two petrographic types:

1. Serpentinites
2. Talc and talc-magnesite rocks



Fig.62 . Photomicrograph of serpentinite.  
Antigorite-magnesite.

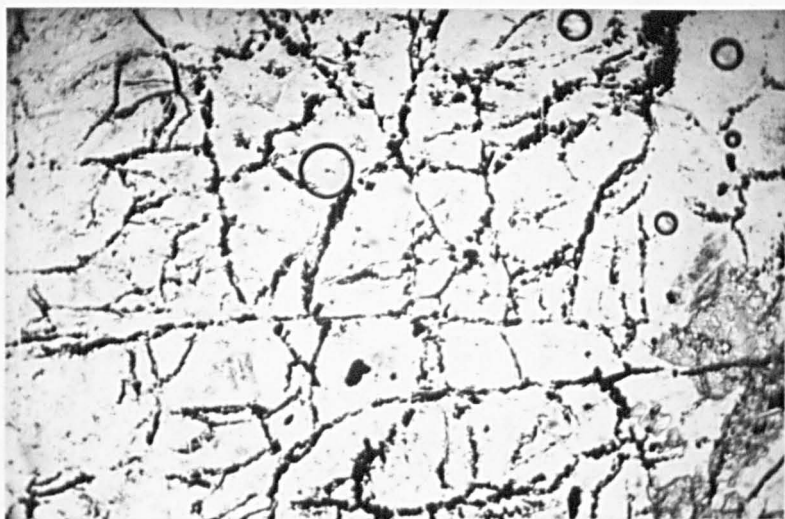


Fig.63 . Photomicrograph of serpentinite.  
Magnetite grains outline relict olivine  
structure.

## 1. Serpentinites

The dunite-serpentinites are rather variable, from slightly serpentinised dunite to completely serpentinised dunite with patches of magnesite; most rocks, however, are completely serpentinised. In hand specimen the rocks are fine grained dark rocks when fresh, weathering red or yellow-brown. Magnetite is a common accessory.

### Mineral Assemblages

Serpentine-magnesite-magnetite

Serpentine-olivine-orthopyroxene-magnetite

Serpentine-magnetite

Serpentine-magnesite (talc-magnetite).

### Fabric

The texture is rather variable; the slightly altered dunite tends to be cataclastic, with rounded olivines. This is in accord with the fact that auto-brecciation is observed in the hand specimen. Olivines with well-developed 100 cleavage have bent cleavage traces and extinction lamellae (see fig.64 ). The normal serpentinite tends to have flaky antigorites, possibly developed under stress, arranged either in sheaf-like bundles or in fibro-lamellar intergrowths (see figs 56 and 62). Occasional bastite structures are found; cross-fibre chrysotile veinlets are found in some specimens; mesh structures are found infrequently. Granules of secondary iron ore outline the boundaries of the original olivine crystals (see fig.63). The talc tends to have a planar alignment.

The grain size is variable. The serpentine tends to be very fine grained but flakes of antigorite up to 1 mm. also occur. Magnesite grains up to 3 mm. have been found; the olivine grains are up to 3 mm.; talc is usually fine-grained.

Many rocks have a slight foliation, probably due to flattening and movement along shear planes, but the massive



Fig.64. Photomicrograph of dunite.  
Olivine showing cleavage and lamellae.

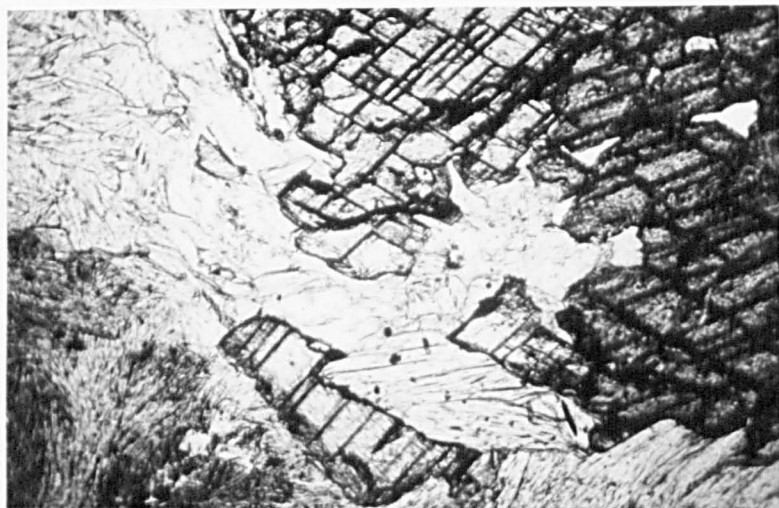


Fig.65. Photomicrograph of Talc-magnesite rock.

serpentinites are un-foliated.

### Mineralogy

(a) Serpentine constitutes up to 90% of the rock

Usually colourless or very pale green. Occurs in aggregates of fibro-lamellar structure or in sheaf-like bundles (see fig.62 ).

Occasional mesh structures seen. Infrequent bastite structures.

Granules of secondary iron ore outline the boundaries of the original olivine crystals (see fig.63 ).

The serpentine is mainly antigorite. The birefringence is weak; maximum interference colours are pale yellow of first order. Parallel extinction and length slow. Several occurrences of cross-fibres chrysotile.

(b) Magnesite constitutes up to 20% of the rock

Occurs replacing serpentine minerals. Usually irregular shapeless grains, but occasionally idiomorphic rhombohedral grains. It has a brown colour, rhombohedral cleavage and high birefringence.

(c) Olivine constitutes up to 30% of the rock

It occurs in anhedral with flattened polygonal outlines, up to 3 mm. long. It has the following properties: colourless; cleavage seen in some sections (100 cleavage planes); irregular fractures; biaxial positive, 2V high ( $84^{\circ}$ ). Extinction lamellae are found and cleavage traces are bent. It is dominantly forsterite; with  $+2V = 84^{\circ}$ , composition is  $For_{95}$ .

(d) Ortho-pyroxene constitutes up to 10% of the rock

Occurs in prismatic crystals up to 1.5 mm. Perfect cleavage.

Extinction parallel (oblique in one case). Birefringence low.

(e) Talc

Occurs in fine fibrous and tabular aggregates. Perfect cleavage (001). Relief fair, birefringence very strong. Some alignment of talc flakes in most specimens.

(f) Magnetite

The ore mineral is dominantly magnetite but it contains some  $TiO_2$ .



It occurs as

1. primary magnetite, in the form of subidioblastic grains with corroded edges, broken up by antigorite flakes
- and 2. very small granules of secondary iron ore which outline boundaries of original olivine crystals (fig.63 ).

### Talc rocks

Within the talc rock zone, pure talc rocks and talc-magnesite rocks occur. Usually the outer margin of the ultra-basic intrusion is in two parts; an outer zone of talc with possibly a little magnesite and an inner talc-magnesite zone in which the % of magnesite can be quite high. Petrographically they can be grouped together.

### Mineral Assemblages

Talc-magnesite-serpentine

Talc-magnetite

Talc-magnesite-serpentine-magnetite

Talc-magnesite-chlorite-magnetite

Magnesite-chlorite-biotite-talc-quartz-magnetite.

### Fabric

The texture is crystalloblastic, xenoblastic to subidioblastic and granoblastic to lepidoblastic.

The grain size is variable, often coarse grained and magnesite grains up to 2 cm are found (see fig.65 ). Talc flakes may be up to 2 cm long but are more frequently fine-grained. A foliation, defined by planar alignment of talc flakes, is often present. Some rocks possess a lineation-a rodding of magnesite. In many cases talc flakes appear to bend around magnesite grains.

### Mineralogy (see fig. 65 )

(a) Talc constitutes up to 90% of the rock

It occurs in thin platy aggregates and fibrous aggregates, occasionally

as radiating fibres and veins. It has perfect 001 cleavage, moderate relief and high birefringence. Flakes and fibres are sometimes bent.

(b) Magnesite constitutes up to 80% of the rock. It is colourless or light brown. It occurs as large grains, up to 2 cm, which are usually subidioblastic, sometimes idioblastic. The grains have fairly high relief, high birefringence and show rhombohedral cleavage. Strain twinning is developed.

(c) Serpentine constitutes up to 20% of the rock

It occurs in small irregular patches. It has a flaky habit and is fine grained. It is probably antigorite.

(d) Chlorite

A few flakes of pale green chlorite are seen in a few sections of magnesite rich rock. It has a tabular habit and is pleochroic in pale greens. The birefringence is low. The chlorite occurs in association with biotite.

(e) Biotite

A few flakes of biotite occur between magnesite grains in more massive magnesite rocks. Tabular habit. Pleochroic X-straw yellow, Y, Z brown.

(f) Quartz

Granoblastic (sutured) grains of quartz occur in some slides. In some cases they are later veins.

(g) Magnetite

Idioblastic grains of magnetite common (up to 2 mm).

Finer grained material (0.05 mm) is scattered through many slides.

#### Contact Rocks

Three types of contact alteration are found:

1. chlorite rocks - the usual contact rock,
2. phlogopite-sphene-apatite rock, of limited occurrence,
- and 3. hornblende-garnet rock, which is also of limited occurrence.

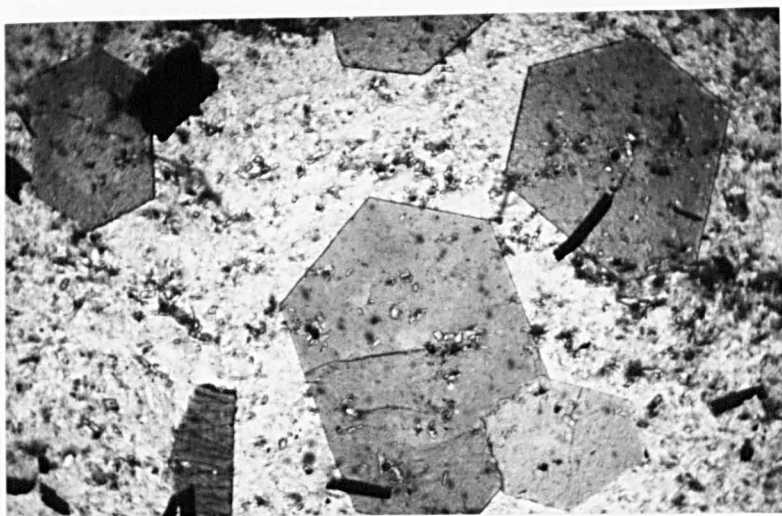


Fig.66 . Photomicrograph of ultra-basic contact.  
Tourmaline-chlorite-magnetite rock.

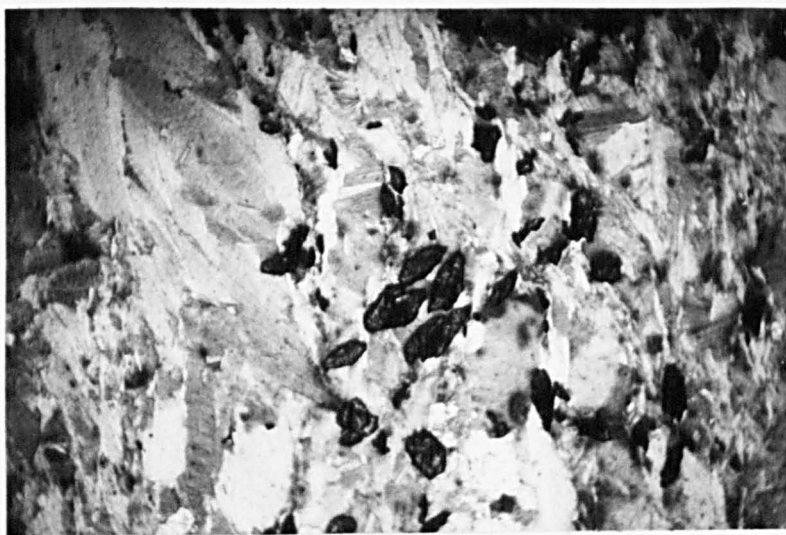


Fig.67 . Photomicrograph of ultra-basic contact.  
Phlogopite-sphene-apatite rock.

# 1. Chlorite rocks (see figs.66 and 68)

## Mineral Assemblages

Chlorite-tourmaline-epidote-serpentine

Chlorite-apatite-serpentine-magnetite

Chlorite-apatite-magnetite

Chlorite-talc-magnetite.

## Fabric

The texture is crystalloblastic, xenoblastic. The grain size is variable, although chlorite is usually fine-grained; talc flakes may be up to 3 mm long. A planar alignment of chlorite and talc is seen in some slides; but chlorite frequently has a radial growth. Strain-slip cleavage is found (see fig.68 ).

## Mineralogy

(a) Chlorite constitutes up to 85% of the rock.

It is xenoblastic and it occurs in aggregates of radiating fibres and in small grains. It is pleochroic in pale greens and its birefringence is low.

(b) Tourmaline constitutes up to 25% of the rock.

It occurs as prismatic crystals with 6 sided cross sections, which are strongly pleochroic from brown to green and which may show zoning (see Fig.66 ).

(c) Epidote

A few grains of pale green epidote occur; they have high relief and high birefringence.

(d) Serpentine constitutes up to 10% of the mode.

Patches of fibro-lamellar serpentine (antigorite?) are found in some slides. They are colourless with low relief and weak birefringence.

(e) Apatite constitutes up to 10% of the mode.

It occurs as colourless rounded grains, often in aggregates.

(f) Talc constitutes up to 20% of the mode.

It occurs in fine fibrous and tabular aggregates; tabular flakes may be

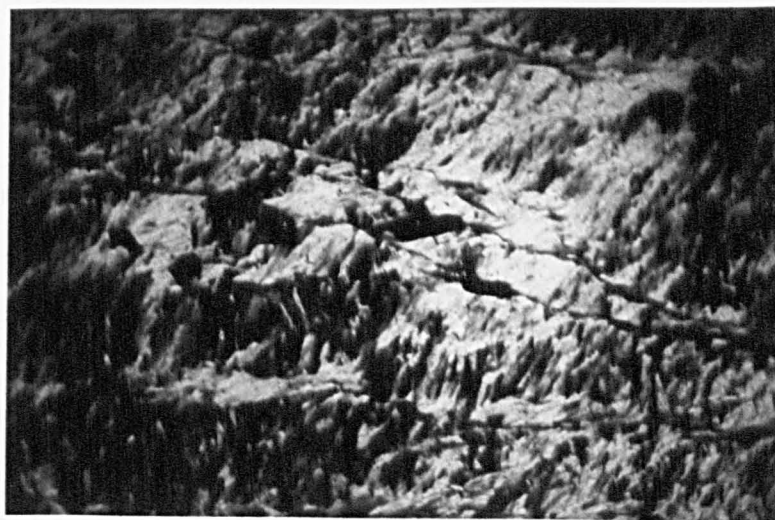


Fig.68. Photomicrograph of ultra-basic contact.  
Chlorite-magnetite rock, showing strain-slip cleavage.

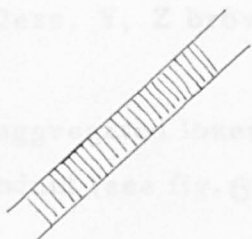


Fig.69. Form of chrysotile occurrence.

up to 3 mm long. A planar alignment of flakes is common.

(g) Magnetite

Idioblastic grains of magnetite (up to 1 mm) are usually quite abundant.

Smaller grains (0.01 mm) are usually scattered through the rock.

2. Phlogopite-sphene-apatite rock (occurs in serpentine 1)

Mineral assemblage

Phlogopite-sphene-apatite

Fabric

The texture is crystalloblastic, subidioblastic, lepidoblastic. The rock is medium grained and possesses a mica foliation.

Mineralogy

(a) Phlogopite constitutes 65% of the rock.

It occurs in aggregates of small, pale flakes, which show pleochroism with X colourless, Y, Z brown.

(b) Sphene

Scattered or aggregated lozenge shaped grains of dark brown sphene are quite abundant (see fig. 67 ).

(c) Apatite

Patches of small rounded apatite grains are abundant.

Fig. 67 is a photomicrograph of this rock.

3. Hornblende-garnet rock

Mineral Assemblage

Hornblende-biotite-epidote-garnet-albite-chlorite-quartz-apatite.

Fabric

The texture is subidioblastic to xenoblastic; sub-nematoblastic to granoblastic. The grain size is variable from fine to coarse grained; hornblendes are up to 1 cm long, the albite is very fine grained. A schistosity defined by alignment of hornblendes with a, c axes in the same plane is present.

## Mineralogy

(a) Hornblende constitutes up to 40% of the mode.

It occurs as subidioblastic to idioblastic grains, with prismatic habit and showing pleochroism with X green, Z deep blue green.

(b) Biotite constitutes up to 10% of the mode.

Some of the flakes are at right angles to alignment of the hornblendes.

(c) Epidote constitutes up to 10% of the rock.

Rounded grains of epidote are scattered through the slide; they have high relief and high birefringence.

(d) Garnet

Pink, idioblastic to subidioblastic grains occur, with inclusions of quartz and epidote, and chlorite along cracks. Hornblendes frequently bend around garnets.

(e) Chlorite

This occurs either

1. Intimately associated with biotite in flaky aggregates,
- or 2. In cracks within the garnet.

Its birefringence is low and it sometimes shows anomalous Berlin blue interference colours.

(f) Albite constitutes up to 35% of the rock

It occurs as granoblastic (sutured) grains, generally untwinned, but a little albite twinning is normally seen.

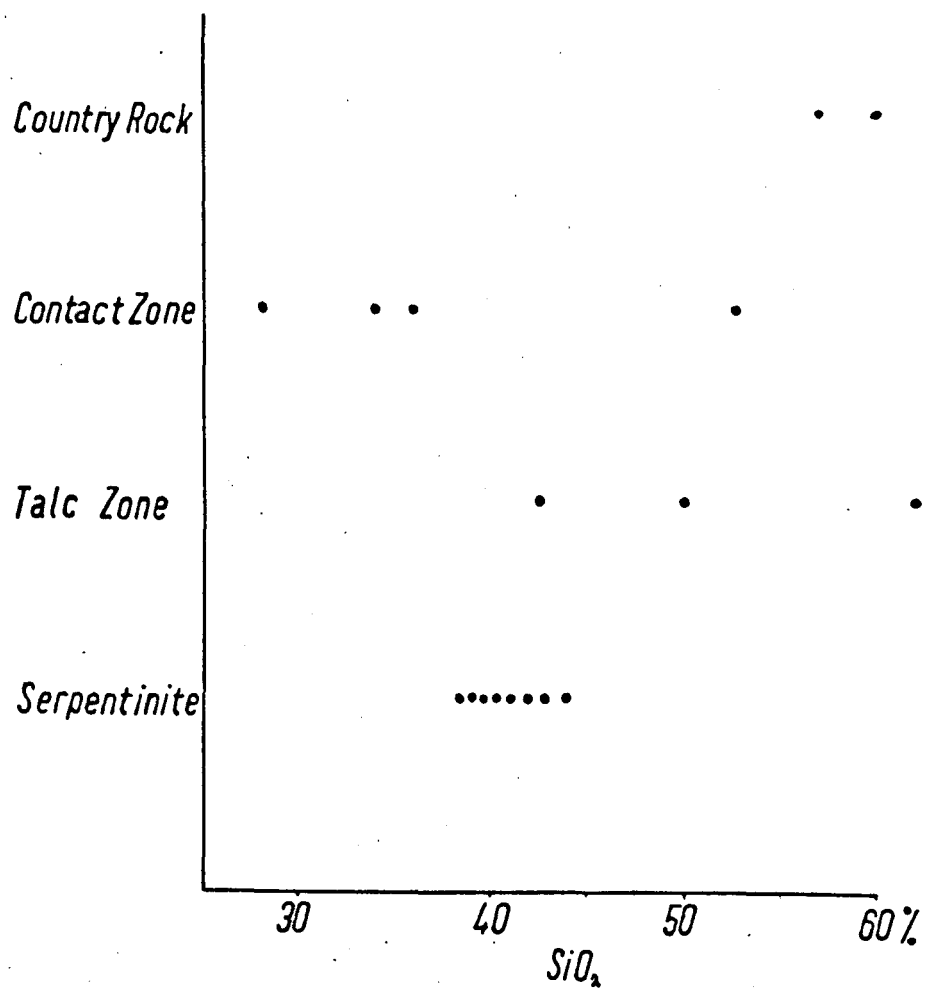
Quartz, apatite and magnetite grains also occur.

The minerals of the contact aureole appear to have grown parallel to a pre-existing schistosity, but there are some cross-cutting relationships.

## Vein Minerals

Cross-fibre chrysotile asbestos and some actinolite occur in high angle joints and occasionally in low angle joints, where they show sharp contacts with the serpentinites.

Fig 70 Silica Variation





The chrysotile differs from normal chrysotile asbestos in being rather harsh and splintery, with a wood-like texture.

The width of the joints filled with fibres is variable; about 20 cm is a maximum. Some of the chrysotile is fibrous, but some is more platy - flaky in habit.

This harsh form of chrysotile has been named "metaxite" by Foslie (1931). In all the veins investigated chrysotile was the sole mineral.

Chrysotile is also found on joint faces; here it is more fibrous in habit.

Other vein minerals are of limited occurrence. A few veins containing actinolite and some containing talc have been recorded.

The veins containing talc or actinolite appear to have formed before the asbestos veins.

### Chemistry

Twenty analyses of ultra-basic rocks, their contacts and minerals have been carried out and the results are presented in Table 5 .

### Dunite-serpentinites

The analyses of dunite-serpentinites are very similar. The following important features should be noted:

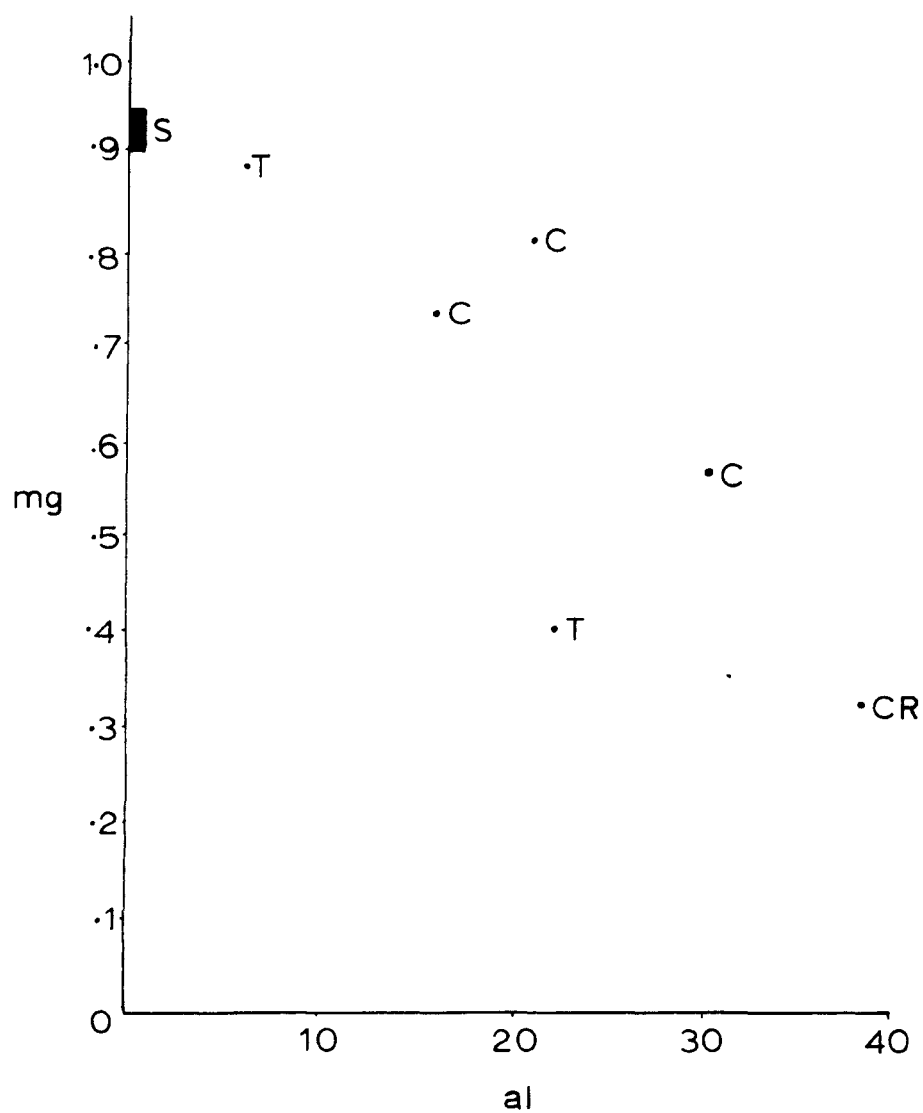
1. MgO/FeO is very high
2. CaO is almost absent.

The composition of the dunite-serpentinites fits very well with almost pure dunitic composition, i. e. the original ultrabasic rock was composed dominantly of olivine crystals with only a little pyroxene.

### Talc rocks

Talc-magnesite rocks, talc-serpentine rocks and pure talc rocks have been analysed. It can be seen that the talc rocks and talc magnesite rocks are significantly higher in SiO<sub>2</sub>, Al<sub>2</sub>O<sub>3</sub>, CaO and lower in MgO than the serpentinites.

Fig Niggli Values for Ultra Basics.  
71 mg against al.



S = Serpentinite

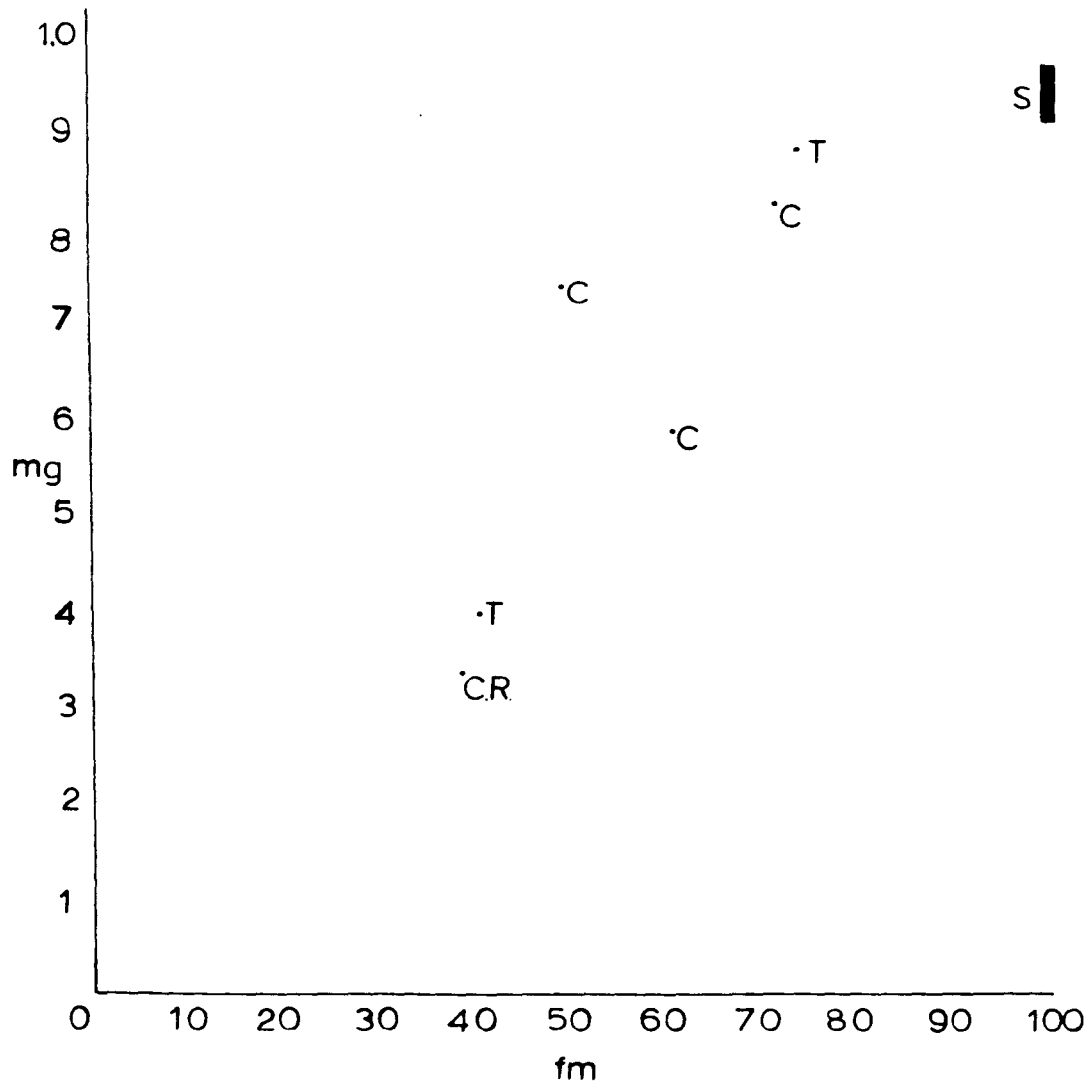
T = Talc-Magnesite

C = Contact

CR = Country Rock

Fig Niggli values for ultra-basics

71 mg against fm.



S Serpentinite

T Talc magnesite

C Contact

CR Country rock

The composition of the rocks of the talc zone is variable depending on the mineral modes, especially on the modal proportion of magnesite.

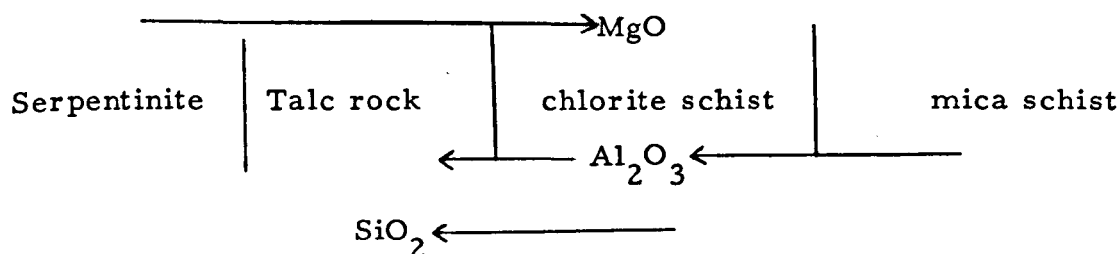
### Contact Rocks

Several analyses of chlorite contact aureole rocks have been carried out. These are compared with the normal country rock in Table 5. From these results it can be seen that the chlorite country rocks are deficient in  $\text{SiO}_2$  and have greater amounts of MgO than the normal country rocks. The chlorite rock is very under-saturated with respect to silica.

### Reactions within the contact zone

From a study of field, petrographic and chemical evidence it is apparent that the alteration of serpentinite to talc rock and the alteration of country rock to chlorite schist are complementary reactions.

The mechanism is probably as illustrated below:

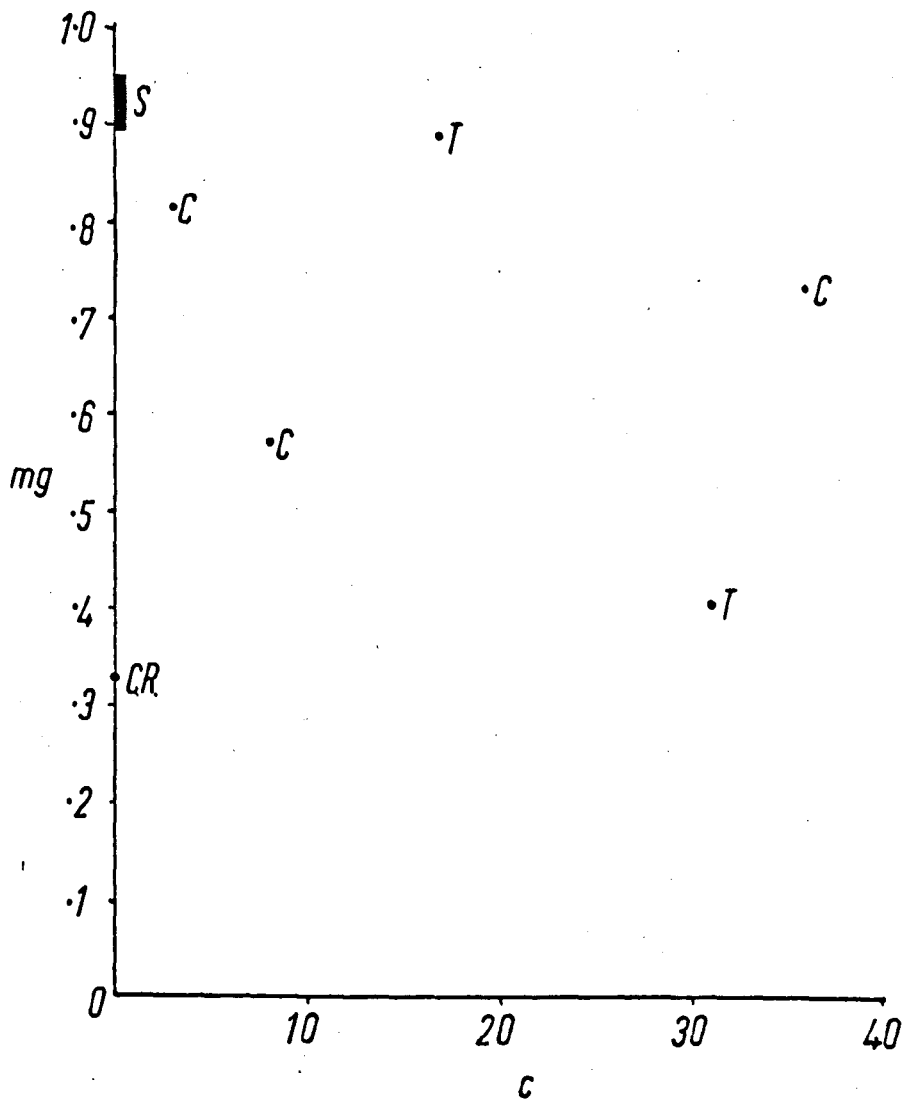


$\text{MgO}$  has moved from the ultrabasic into the contact rock;  $\text{SiO}_2$  and  $\text{Al}_2\text{O}_3$  have migrated from the country rock into the ultrabasic to produce talc.

At the same time there has been movement of volatiles from the country rock into the contact zone ( $\text{B}$ ,  $\text{P}_2\text{O}_5$ ,  $\text{Cl}_2$ ,  $\text{F}_2$ ) to form the specialised minerals of the contact zone such as tourmaline, apatite and hornblende.

These reactions are low grade, metamorphic and metasomatic changes in the greenschist facies. They probably occurred during the main period of metamorphism (syn B2), just after the intrusion of the

Fig( ) Niggli Values For Ultra Basics  
71 mg against c



*T* - Talc Magnesite

*C* - Contact

*S* - Serpentinite

*CR* - Country Rock

**Table 5 . Analyses of dunite-serpentinites and related rocks**

Sp. No.	54	55	56	57
SiO <sub>2</sub>	38.53	38.13	41.07	39.62
TiO <sub>2</sub>	--	0.07	--	0.02
Al <sub>2</sub> O <sub>3</sub>	0.19	0.26	0.04	--
Fe <sub>2</sub> O <sub>3</sub>	4.55	3.30	4.21	4.54
FeO	2.93	3.79	3.78	3.59
MnO	0.06	0.10	0.02	0.10
MgO	42.5	43.5	40.2	40.2
CaO	--	--	--	--
Na <sub>2</sub> O	0.09	0.02	0.01	0.01
K <sub>2</sub> O	0.12	0.06	tr.	tr.
P <sub>2</sub> O <sub>5</sub>	0.03	0.01	0.01	0.01
al	--	--	--	--
fm	99	99	99	99
c	--	--	--	--
mg	0.91	0.92	0.91	0.90

Table 5 . (continued)

Sp. No.	58	59	60	61
SiO <sub>2</sub>	44.4	39.93	39.53	41.29
TiO <sub>2</sub>	--	0.01	0.14	0.03
Al <sub>2</sub> O <sub>3</sub>	0.19	0.26	0.04	--
Fe <sub>2</sub> O <sub>3</sub>	1.58	4.02	2.95	3.76
FeO	3.97	3.66	3.54	3.76
MnO	0.10	0.04	0.05	0.08
MgO	42.78	40.2	41.8	41.8
CaO	--	--	--	--
Na <sub>2</sub> O	0.01	0.02	0.07	0.01
K <sub>2</sub> O	0.01	0.03	0.01	--
P <sub>2</sub> O <sub>5</sub>	--	--	--	--
fm	99	99	99	99
mg	0.93	0.91	0.92	0.91

Table 5 . (continued)

Sp. No.	70	45 (Talc-magnesite)	51(Talc magnesite)
SiO <sub>2</sub>	42.58	50.14	43.43
TiO <sub>2</sub>	--	4.0	tr.
Al <sub>2</sub> O <sub>3</sub>	--	12.53	4.69
Fe <sub>2</sub> O <sub>3</sub>	3.29	1.57	0.25
FeO	2.21	9.14	4.14
MnO	0.04	0.18	0.15
MgO	43.6	4.05	21.0
CaO	--	10.16	7.26
Na <sub>2</sub> O	0.02	1.5	0.79
K <sub>2</sub> O	--	0.73	0.42
al	--	22	6
fm	99	42	75
c	--	31	17
mg	0.94	0.4	0.89



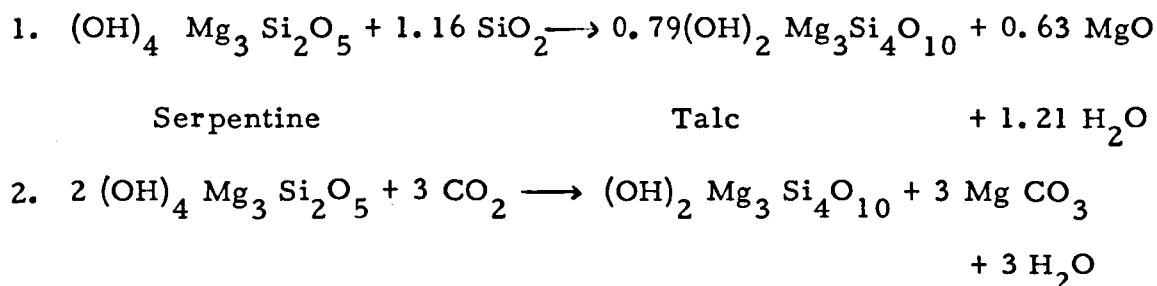
Table 5 . (continued) Contact rocks

Sp. No.	42	68	71	chrysotile
SiO <sub>2</sub>	28.3	36.2	53.05	41.81
TiO <sub>2</sub>	1.98	1.0	2.8	--
Al <sub>2</sub> O <sub>3</sub>	12.35	20.95	23.38	0.10
Fe <sub>2</sub> O <sub>3</sub>	0.69	2.1	0.12	0.54
FeO	6.50	7.88	13.44	0.32
MnO	--	0.22	0.83	--
MgO	10.52	23.75	10.5	42.31
CaO	15.49	1.75	3.44	--
Na <sub>2</sub> O	1.6	0.8	0.6	0.01
K <sub>2</sub> O	6.21	0.4	0.7	0.01
P <sub>2</sub> O <sub>5</sub>	5.01	tr	tr	--
H <sub>2</sub> O	n.d.	n.d.	n.d.	14.1
al	16	21	30	
fm	47	74	60	
c	36	3	8	
mg	0.73	0.81	0.57	

ultrabasic bodies. The metasomatism and formation of talc rock definitely postdate the serpentinization.

Fig. 71 shows a Niggli plot of al/mg; mg/c; mg/fm, etc. for the rocks involved in the reaction.

The reactions can probably be represented as follows:



It seems likely that both the above reactions occur in the contact zone described. Reaction (1) explains the outermost ultrabasic rim, generally of pure talc, which forms by addition of  $\text{SiO}_2$  from the country rocks; at the same time MgO and water migrate in-to the country rock to form chlorite.

Reaction (2) may occur in the inner part of the talc rim where magnesite is usually abundant. The  $\text{CO}_2$  probably came from the ultrabasic. Discussion of the reactions is found in the petrogenesis.

### Vein Minerals

One analysis of chrysotile has been carried out and this is shown in Fig. 5. The analysis is a typical chrysotile serpentine.

### Other Mineral Analyses

Analysis of talc and magnesite from the talc rock are presented below (Table 5p181).

### Petrogenesis

"Alpine-type" serpentinites have been the subject of much discussion and controversy for many years. The question of

solid versus liquid intrusives has still not been completely settled.

Hess (1938, 55) believes alpine-serpentinites to be intruded as liquids at low temperatures.

The experimental work of Bowen and Tuttle (1949) on the system  $\text{MgO} - \text{SiO}_2 - \text{H}_2\text{O}$  has indicated that serpentines can only be formed by the action of water on forsterite at temperatures below  $400^\circ\text{C}$  and that serpentine is unstable above  $500^\circ\text{C}$ . Since they found no liquid phase in the system at temperatures up to  $1,000^\circ\text{C}$  and pressures of 15,000 lb/sq. in., Bowen and Tuttle concluded that serpentines cannot be formed by the intrusion at comparatively low temperature of a magma of serpentine composition.

Later work by Wiley (1960) has shown that introduction of CaO into the system  $\text{MgO} - \text{SiO}_2 - \text{H}_2\text{O}$  could bring about a lowering of temperature, but since many 'alpine-type' serpentinites are lacking in CaO, this is not very important.

Other workers (Reitan, etc.) have derived dunites and serpentinites by vague processes of metamorphic differentiation at high metamorphic grade but the present writer considers this most unlikely. Examination of the work of these authors has not produced any evidence incompatible with intrusion of masses of dunite and later metamorphism of ultrabasic and contact. Much of their work is incompatible with elementary considerations of phase rule and the experimental studies.

Literature on the petrogenesis of peridotites and serpentines of the alpine type is most confused but the most widely held views can be summarised as follows (Turner).

Peridotites and serpentinites of alpine type can be distinguished from other ultrabasics by a combination of field, petrographic and chemical evidence.

Emplacement of the ultra-basic bodies has involved

intrusion of highly magnesian "material" along stratigraphically or structurally controlled surfaces of weakness. It is probable that at one stage in their history the ultra-basic bodies consisted largely of crystalline forsterite with subordinate orthopyroxene in most cases. Associated contact metamorphism is of low grade, probably below  $500^{\circ}\text{C}$ . This is incompatible with the intrusion of forsterite magma which can only exist at high temperatures.

The amount of ultra-basic material is incompatible with differentiation and settling of olivines from basaltic magma as suggested by Bowen since in many cases the ultrabasic is associated with only a small amount of basic material.

Hess's theory of derivation of ultra-basic bodies from the peridotite of the mantle during the early stages of a geosyncline seems the most likely to the present writer; although the writer would consider the material as a "mush" of olivine crystals rather than a liquid magma as Hess suggested. After the removal of the peridotite masses from the mantle during the first (and greatest) deformation of the orogen the ultra-basic would be squeezed upwards by sideways pressure and in some cases may have moved upwards again during a later period of deformation. They are, therefore, found outside their own environment.

The source of water for serpentinization is another problem. Hess and Benson consider the water to come from within serpentinite; the serpentinization is an automorphic reaction - "The ultrabasic stews in its own juice" (Benson).

Bowen thought that the serpentinisation was due to intrusion of peridotite into wet country rocks.

The general uniform nature of serpentinization unrelated to the margins of the bodies or to fractures within the ultrabasic bodies - is in agreement with the theory of Benson and Hess. However,

in some cases, marginal serpentization has been recorded (Benson, Taliaferro). The problem of the mechanism of serpentization is still not solved.

The alteration of serpentine to talcose-rock - that is to say, steatization, is another not fully understood process. Most authors (e.g. Hess) consider steatization to be a hydrothermal alteration.

Turner (1938) has shown that steatization can arise by silicification, carbonation or addition of CaO. In some cases the solutions causing steatization have apparently been derived from within the ultrabasic body itself. In other cases the source of the solutions can be traced to an adjacent intrusion (granite, etc. - Hess).

Actinolite-chlorite assemblages are believed to be intermediate stages in the development of talc rocks.

The present work would suggest another mechanism of steatization; metasomatic reaction between ultrabasic and country rock during post-intrusion metamorphism in the greenschist facies.

It is probable that talcose rocks can arise by several processes independently or associated. A further problem of serpentization is what conditions govern the formation of chrysotile or antigorite? The presence of antigorite in rocks which have been subjected to high stresses may suggest that stress favours the formation of antigorite. Chemical environment has been suggested as another factor (Hess 1952). The problem is not yet solved.

Most authors accept that cross-fibre veins of chrysotile asbestos are late stage, since the field relations are often conclusive.

#### Petrogenesis of the ultra-basic bodies in the Nettoseter Area

The petrogeny of the U/B bodies in the Nettoseter area can be divided into several stages:

1. Intrusion of U/B bodies in first deformation. Serpentinization at the same time.
2. Squeezing up of the U/B bodies along axial planes into crests of anticlines during B2 folding. Metamorphism of ultrabasic and country rock producing chloritization of country rock and formation of talc.
3. Formation of cross-fibre veins of chrysotile asbestos. Possible formation of a few talc and tremolite veins.

#### Stage 1

The ultrabasic bodies were intruded into the Cambro-Ordovician succession during the first deformation. They may have been intruded at the same time that the rocks of eugeosynclinal succession were being overthrust or slightly earlier.

At the time of intrusion the rocks were dominantly forsterite olivine with subordinate orthopyroxene. Serpentinization occurred at the same time as intrusion; some auto-brecciation of the ultrabasic bodies occurred. The dunites were almost certainly intruded as a mush of olivine crystals with a liquid between the grains. The serpentinization was an autometasomatic reaction; serpentinization is uniform, unrelated to the margins of the bodies. The effect of stress during serpentinization can be seen by the abundance of antigorite.

#### Stage 2

During the major folding in the area (B2) the ultrabasic bodies were squeezed upwards into anticlinal crests, parallel to the axial planes of B2 folds. During the main metamorphism (probably mainly syn B2) the ultrabasic rocks reacted with the country rock. Complex metasomatic exchanges took place between the rims of the ultrabasic bodies and the surrounding country rocks.  $\text{SiO}_2$  and  $\text{Al}_2\text{O}_3$

moved into the ultrabasic from the country rock, MgO and water moved out of the ultrabasic into the country rock.

The outer rim of the ultrabasic was altered to talc by this reaction and at the same time some carbonation occurred producing an inner rim of talc-magnesite.

The country rock was altered to chlorite; volatiles including B, Cl, F diffused into the contact zone producing tourmaline and apatite. The alteration was completed by B3 phase of deformation since talc flakes are deformed by B3 folds.

The intrusion of the ultrabasic bodies caused a swing in the foliation parallel to the margins of the ultrabasics.

### Stage 3

The last stage was the formation of joint fillings of tremolite-actinolite and talc, followed by more widespread development of cross-fibre veinlets of chrysotile asbestos. Some later movements affecting the ultrabasics are shown by the bending of chrysotile flakes. Most of the chrysotile veins are steeply dipping.

Many problems remain, however. The distinction between chrysotile and antigorite is inadequate. Use of the electron microscope is probably the only way.

The abundance of antigorite in the serpentinites is interesting, because several authors (Turner) have suggested that in deformed ultrabasics, antigorite is the stable form.

### Regional Significance

According to the Norwegian literature (Strand, etc.), intrusive serpentines of Caledonian age are found in the lower part of the eugeosynclinal western facies (Trondheim facies). This has been described by Stand from his so-called "Otta" nappe equivalent to the Lower Jotun Nappe.

Up until the time of the study of the Jotunheim by Nottingham workers, the present area was believed to be mio-geosynclinal and was supposed to be composed of mica schists and phyllites.

Work by the present writer has shown the presence of amphibolites with definite igneous textures - gabbroic textures, pillow structures, etc., i. e. the area is of eugeosynclinal aspect.

The presence of these Caledonian serpentinites is further evidence of the correlation with the Trondheim facies.

However, the generally accepted view is that the serpentinites are found in the lower part of the Trondheim facies succession. (Heidal schists - quartz mica schist) and are generally below the Støren (greenstones=metavolcanics) group.

In the present area the serpentinites are found high up in the greenstone group. Two possibilities occur:

1. The U/B's in the present area were intruded below the present level and moved into their present level during B2 folding. In other areas described the U/B's are in their normal position; low down in the psammitic part of the succession.
2. The greenstone group in the present area is not equivalent to the Støren metavolcanic group, but represents an earlier phase of vulcanism, perhaps equivalent to the Heidal schists.



## CHAPTER 4

## STRUCTURE

### Introduction

The geological structure of the Nettoseter area is complex; it forms a part of the Caledonian orogenic belt, which has been subjected to polyphase deformation during the long history of the Caledonian orogeny. In addition, Pre-Cambrian structures are found within the basal gneiss complex and the upper Jotun nappe.

The basal gneiss complex has behaved more or less as a stable block during the Caledonian orogeny and has deformed in a brittle manner, mainly along joint surfaces. It is considered as a separate tectonic unit.

The supracrustal rocks lying between the basal thrust and the upper Jotun nappe can be considered as one tectonic unit, since they show the same sequence of structures. However, the ~~sparagmite~~ group has behaved in a slightly different manner in view of its tectonic position between two thrust planes.

The highest tectonic unit in the area mapped is the upper Jotun nappe. This has a history of Pre-Cambrian deformation and metamorphism and in the lower part, at least, has suffered Caledonian deformation. The detailed structure of the upper Jotun nappe is uncertain.

Several distinct phases of Caledonian deformation have been recognised. These have been designated B1, B2, B3, B4, B5, since the age relationships between them can be worked out using criteria such as folded folds, deformed linear structures and to some extent style and symmetry of the various phases. The time interval between successive phases may not have been very great.

In this section, reference should be made to the geological map and the structural maps. Fig.72 is a tectonic section across the area.

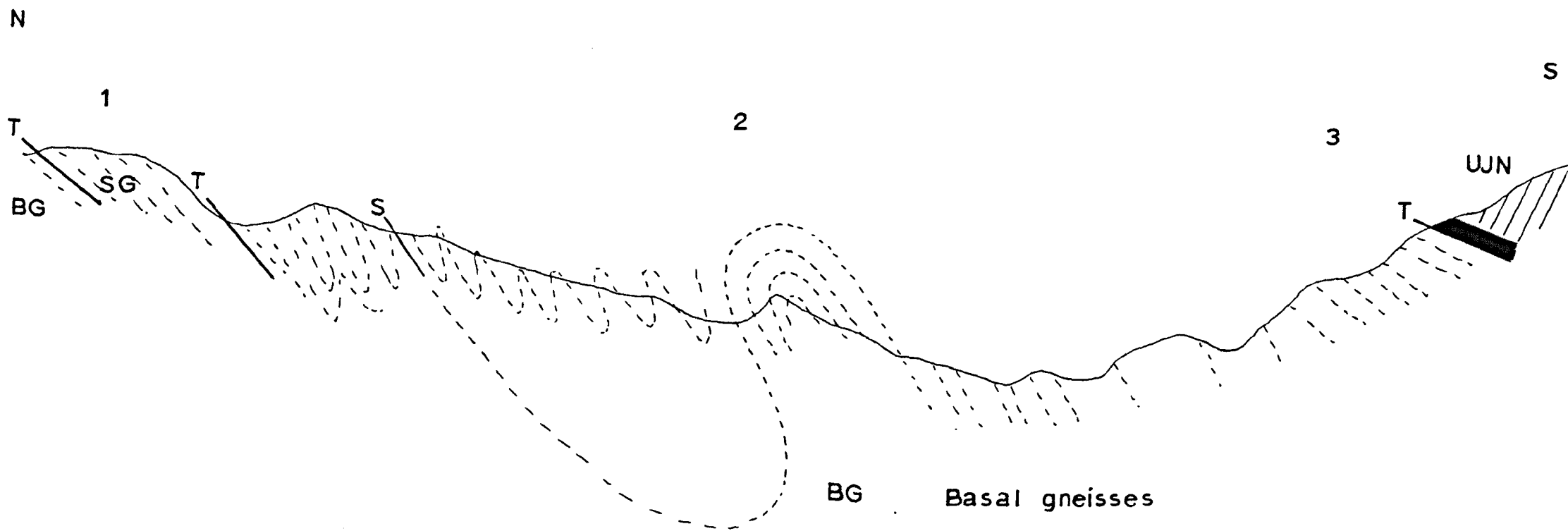


Fig 72 Tectonic Section

BG	Basal gneisses
UJN	Upper Jotun nappe
1SG	Sparagmite group
2	Eugeosynclinal succession
3	Feldspathic quartzites
T	Thrust
S	Slide

In the first part, the style, orientation and symmetry of minor and major structures produced by successive deformations are described and the effect of later folding on earlier structures discussed.

The second part describes the "conglomeratic" structures and suggests an origin for them. This is followed by a chapter on a quantitative study of fold styles.

The total evidence of structural analysis and deformation is considered and a movement picture suggested for each deformation.

Finally, some implications of this work are discussed and the mechanism of folding is discussed with reference to theoretical and experimental studies.

#### Field Methods

Structural analysis was carried out mainly on a scale of 1 : 20,000, although some early work was done on a 1 : 10,000 scale; both corrected A. M. S. series maps and aerial photographs were used.

Measurements on pseudo-conglomerates were made from enlarged oriented photographs.

#### Sequence of structures

Five phases of Caledonian tectonic movement have been distinguished, each with its own suite of minor folds, axial plane cleavage and generally a lineation parallel to fold axes. Only one period of major folding has been recognised.

These fold systems differ considerably in orientation, style and symmetry. In addition, each system can vary within the area, probably due to the reaction of different lithologic units to strain.

The sequence of folding is as follows:

##### 1. Pre-Cambrian

- (a) Folding of the basal gneiss complex.
- (b) Folding of the upper Jotun nappe.

## 2. Caledonian

### (a) First movement phase (B1)

Formation of isoclinal minor folds with a penetrative axial plane cleavage and a lineation parallel to fold axes.

### (b) Second movement phase (B2)

Formation of minor and major folds with a quite well-developed axial plane cleavage and a lineation parallel to fold axes.

### (c) Third movement phase (B3)

Formation of minor kink folds, often with axial plane strain-slip cleavage (S3) and a penetrative lineation parallel to fold axes.

### (d) Fourth movement phase (B4)

Formation of kink bands with evidence of conjugate folding.

### (e) Fifth-movement phase (B5)

Formation of a localised strain-slip cleavage.

The outcrop pattern is controlled essentially by B2 folding, with some warping due to B4 folds. Little is known of the effect of B1 folds on the outcrop pattern.

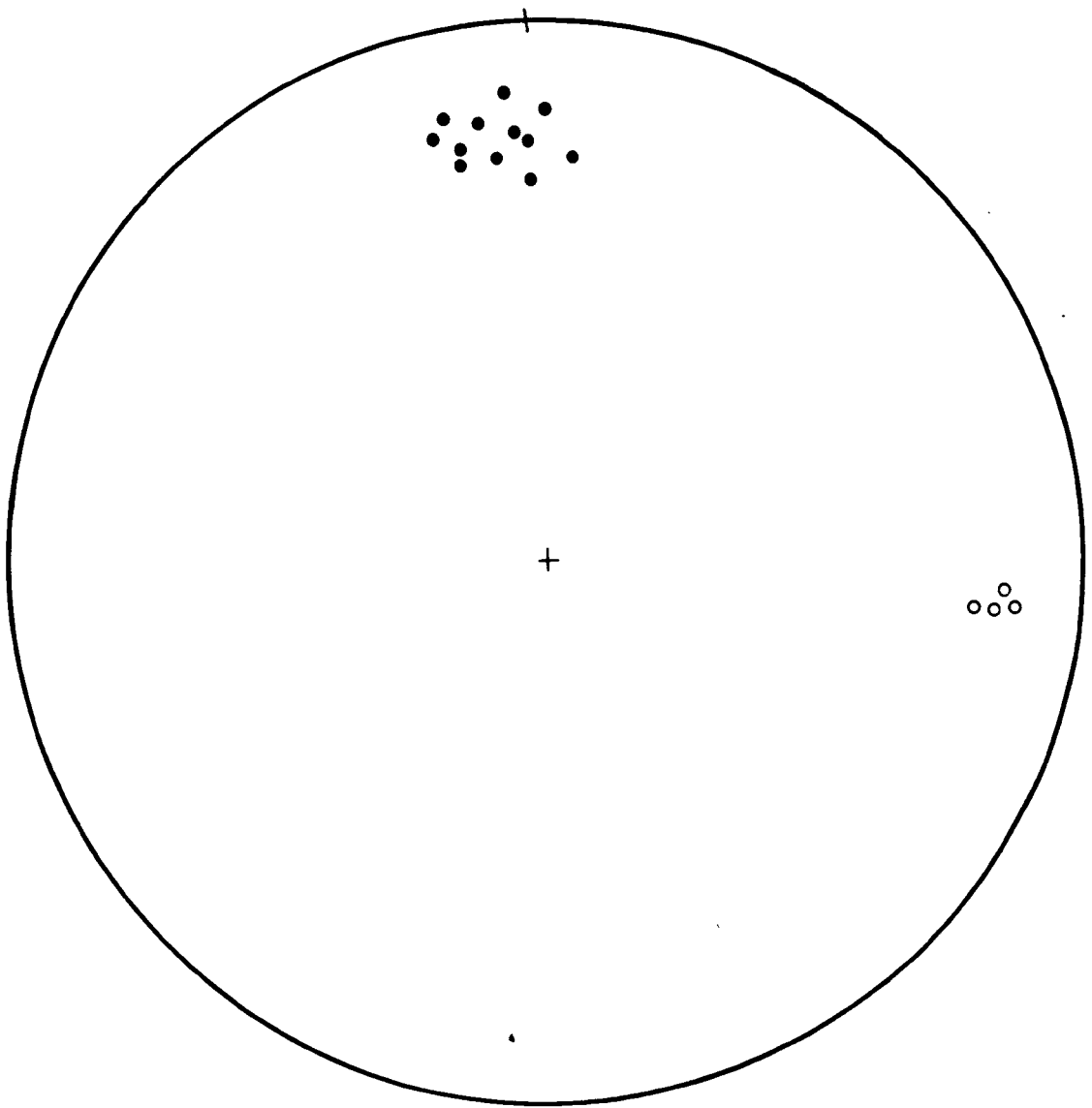


Fig 73

Basal gneisses

foliation •

lineation ◦

## Pre-Cambrian structures

### (a) Basal gneiss complex

The dominant structure of the basal gneiss complex is the biotite foliation of the biotite gneisses and Hestbrepiggan granite. This foliation is defined by planar alignment of biotite flakes and some flattening of other minerals within this plane.

In the small area of Hestbrepiggan granite mapped; away from the contact, the biotite foliation strikes approximately E.-W. and dips steeply to the south. In some cases, a weak lineation lies within the foliation and pitches east at about  $10^{\circ}$ . . . Foliations and lineations are plotted in Fig.73 .

On symmetry arguments, this combination of foliation and lineation would be attributable to an orthorhombic system of pure strain and stress. Unfortunately fabric data is lacking but  $\sigma_1$  is likely to be at right angles to S, so that the foliation could be identified with the AB plane of the strain ellipsoid (Turner and Weiss 1963).

Thus the biotite foliation is likely to have formed by compression from north-south.

Near the basal thrust plane, a foliation defined by planar alignment of muscovite flakes cross-cuts the biotite foliation. This foliation is parallel to the basal thrust plane and to axial planes of B1 folds. It is almost certainly a B1 Caledonian structure and its tectonic significance is discussed later.

### (b) Upper Jotun Nappe

In view of the small number of structures observed, it has not been possible to present a detailed structural pattern. However, it is possible to make a number of observations on the evidence available.

The dominant foliation within the upper Jotun nappe is a strong preferred orientation of feldspar lensoids parallel to mineralogical banding. This foliation strikes approximately  $80^{\circ}$  T

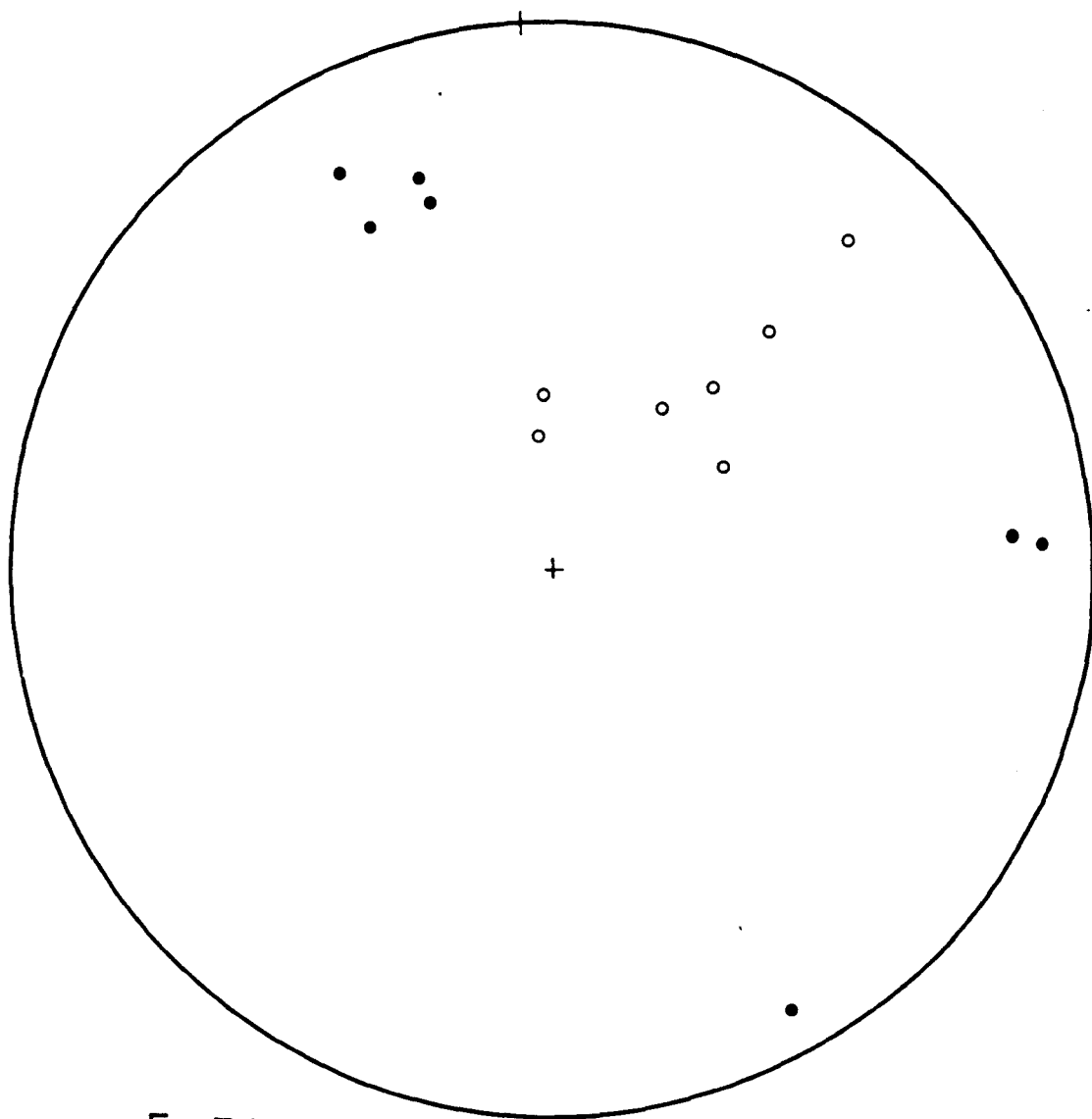


Fig 74

upper jotun nappe

fold axes    ○       poles to axial planes    ●



and dips fairly steeply to the north. A lineation, defined by alignment of pyroxenes lies within this plane, pitching at  $70^{\circ}$  E.

Measurements of seven folds which are definitely Pre-Cambrian structures are plotted in Fig.74 . At least two phases of folding are present. The probable earlier phase has a trend of 36 to 55 and a plunge of 20 to 60; axial planes have a strike of 64 to 79 and dip to the north. The folds are tight similar folds. This is probably one phase of folding, but may represent more than one phase. The later phase has an axial plane striking N.-S. with a steep dip to the west and the folds pitch steeply to the north on the axial plane. One of these folds is illustrated in Fig.48 . An axial plane fracture cleavage is present and these structures are more open than the earlier ones.

Other structures found in the lower part of the upper Jotun nappe are related to the emplacement of the nappe and later Caledonian movements. These include folds, linear structures, joints and joint infillings and are discussed along with the Caledonian movements.

In view of the scarcity of data, little can be said concerning the symmetry of structures in the upper Jotun nappe.

The Pre-Cambrian history of the upper Jotun nappe can be tentatively stated as follows:

1. Formation of foliation and lineation parallel to mineralogical banding.
2. Formation of folds with axial planes striking approximately  $75^{\circ}$  and dipping north. The folds trend approximately north east.
3. Development of folds with a N.S. steep axial plane and a plunge to the north. Formation of axial plane fracture cleavage.

### Caledonian Structures

Caledonian structures are dominant from the basal thrust zone of the basal gneiss complex to about 300 metres above the mylonite zone of the upper Jotun nappe.



Fig.75 . B1 fold N.W. of Høyøyen.



Fig.76 . Sheared out B1 folds at Nettoseter.

The sparagmite group has behaved as a separate unit, as can be seen by the imbrication zone and the drag folds below the Gjeitaa thrust. Accommodation during deformation has occurred along the two thrusts, but within this zone, the rocks have had typical B1, B2, B3 and B4 folds impressed upon them.

#### First movement phase B1

Evidence of B1 deformation is not abundant. B1 folds are found in isolated exposures and no continuous large scale pattern has emerged. However, over much of the area, especially in more pelitic rocks, S1 (axial plane cleavage of B1 folds) is quite prominent.

##### (1) Minor folds (Figs.75 and 76 ) Fig 77

The majority of B1 folds are very acute structures, usually easily distinguished from the more open later folds. Fig.78 is a plot of poles to axial planes of B1 folds.

In micaceous rocks, B1 folds are isoclinal, similar folds, with marked thickening in the hinge regions (see chapter 6 ). They are plane cylindrical folds; isoclinal and similar in style. Frequently they are reclined folds (see Fig.80 ) with the axial plane striking normal to the trend of the axis and with orthorhombic ( $C_{2V}$ ) or monoclinic ( $C_{1h}$ ) symmetry, depending on relative lengths of the limbs.

In the gorge-section, west of Netto seter, B1 minor folds are highly sheared out along axial plane cleavage (see Fig.83 and Fig.76 ); almost complete transposition of bedding by S1 is achieved.

##### (2) Planar surfaces

The first axial plane cleavage (S1) is quite conspicuous over much of the area and in many outcrops forms the dominant foliation. In pelitic rocks, S1 is a slaty cleavage with a lepidoblastic arrangement of tiny micaceous flakes. Throughout the upper pelite and upper limestone-pelite groups, S1 is extremely well displayed.

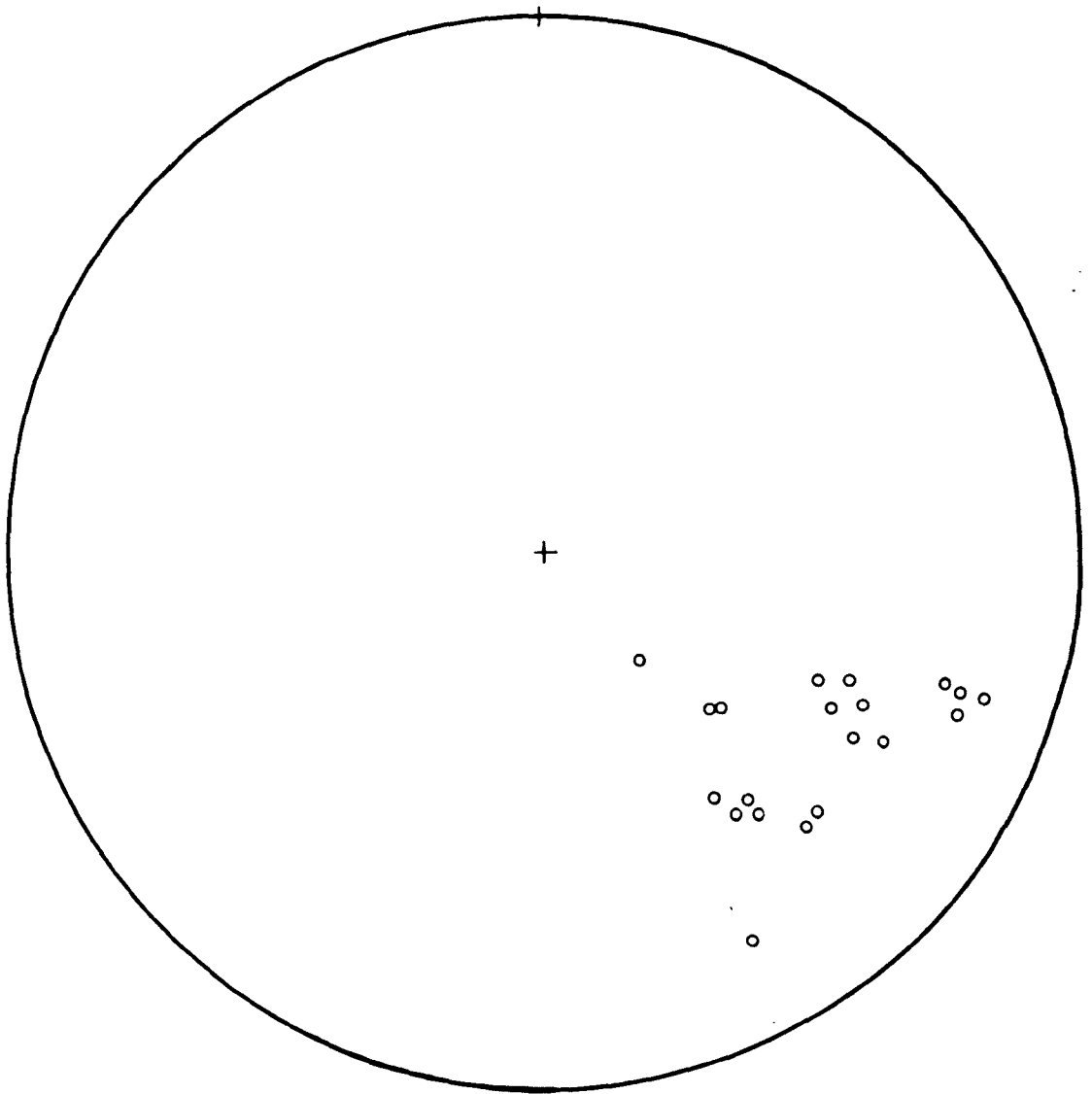


Fig 77

B1 fold axes

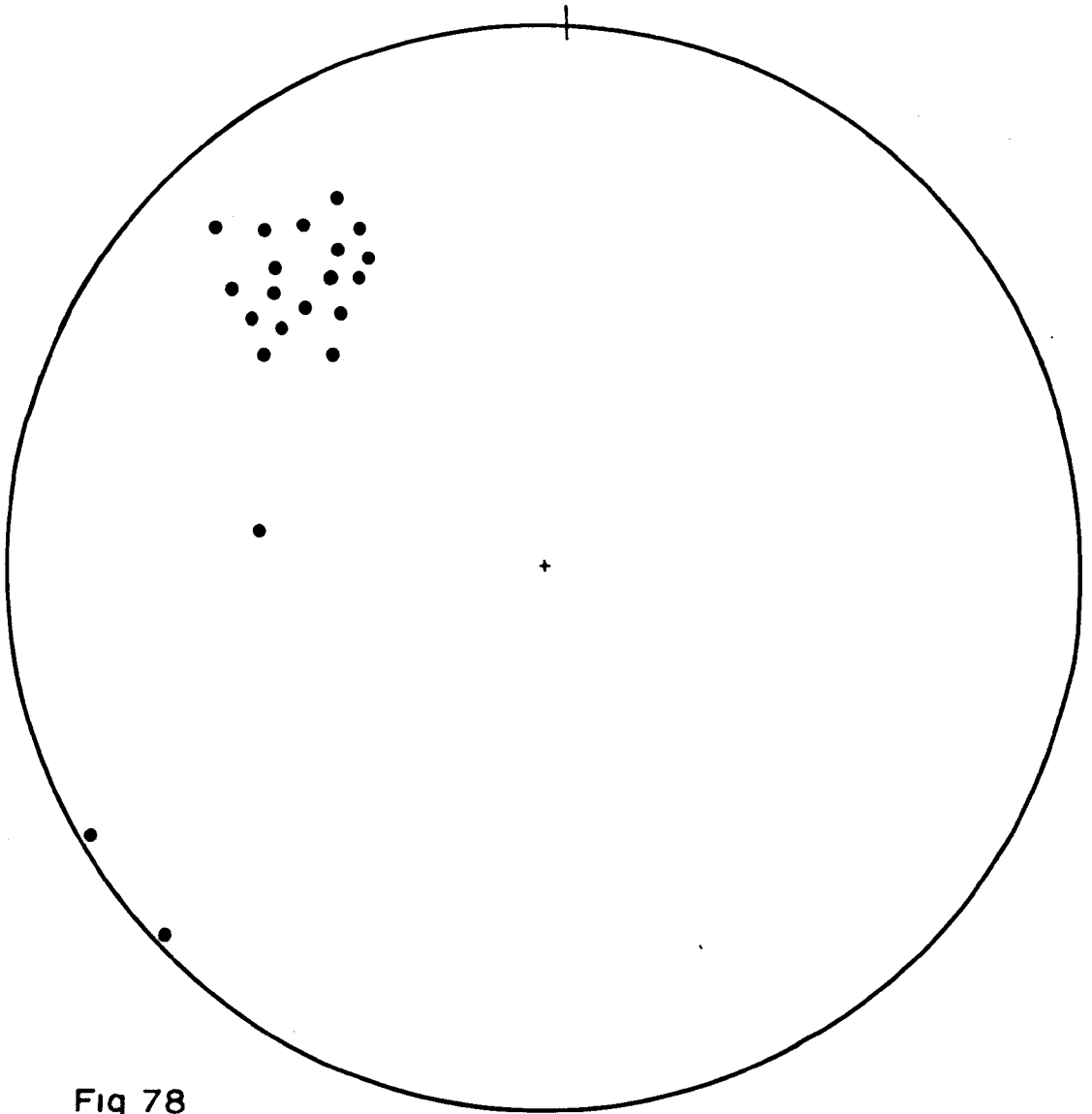


Fig 78

Poles to axial planes of B1 folds

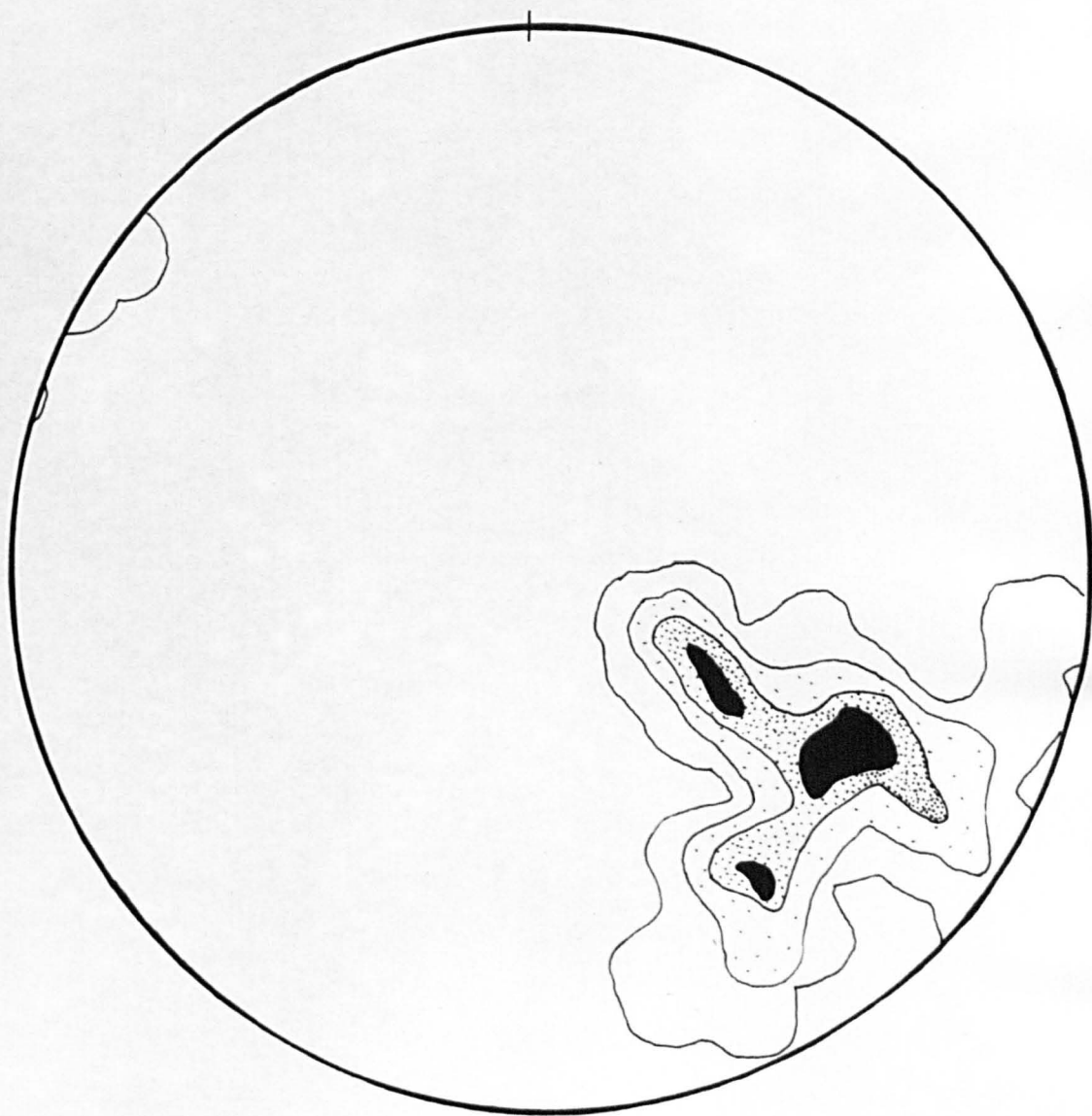
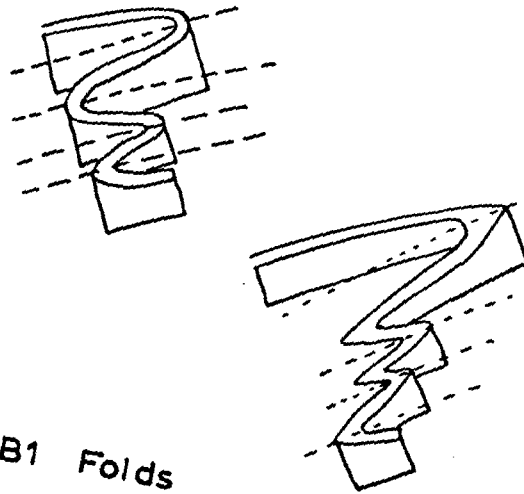


Fig 79

L1

10, 5, 2, 1 %  
contours

Fig 80



B1 Folds

Fig 81



L2 mullion structure

In more competent rocks, S1 consists of close set slip planes, usually occupied by micaceous films which divide the psammite into thin plates. This is well developed around the basal thrust area, where S1 may be the dominant foliation. In many cases, however, a recrystallisation of micas has probably occurred parallel to bedding planes.

### (3) First linear structures

B1 linear structures include the hinges of small B1 folds, intersection of bedding and S1 and the "phacoidal structures" of the pseudo-conglomerates. Fig.82 shows the distribution of L1 and Fig.79 is an equal area plot of these structures.

All the first linear structures, except for a few instances of quartz rodding at Gjeitaabreen, are parallel to B1 fold axes. The Gjeitaabreen rodding (Fig.123) is at right angles to B1 fold axes and is probably a stretching lineation.

### Thrusts, slides, etc.

Two large thrusts of B1 age occur within the area; these are the basal thrust and the Gjeitaa thrust; both are sub-parallel to the axial planes of B1 folds. In addition, in several places, minor structural discontinuities of probable B1 age occur and these are probably slides. These include the structural discontinuity near the top of the greenstone group, seen in the north-Tverra cliffs and again in Holleindalen.

### Basal thrust

The basal thrust strikes approximately N. E. to E. N. E. and dips at moderate angles to the southern hemisphere. Throughout the area mapped, quartzites and feldspathic quartzites have been thrust over onto the basal gneiss complex. The dominant foliation in the sparagmite group and also within the muscovite-chlorite gneisses of the basement is S1 and this can be shown to be parallel to the axial planes of B1 folds and to the thrust planes. A lineation within this



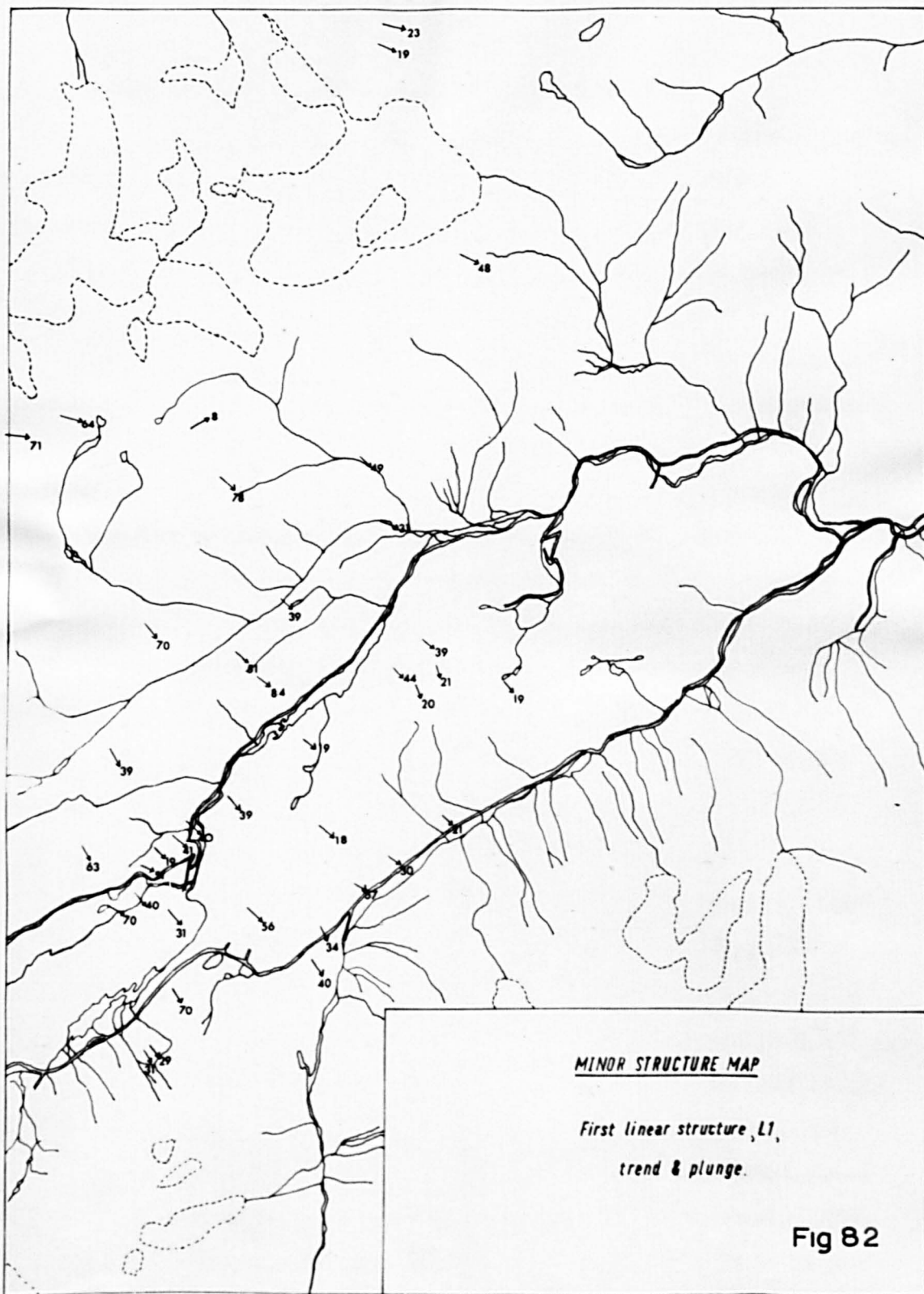


Fig 82



Fig.83 . Sheared out B1 folds at Nettoseter.



Fig.84 . The Gjeitaa thrust exposed in the north-Tverra cliffs. Note the drag folds in the sparagmite group below the thrust.

foliation trends 90 to 110 and is parallel to B1 fold axes.

Within about ten metres of the thrust, S1 is extremely well developed. The quartzites become rather flaggy and the pelitic bands develop a strong foliation parallel to the thrust plane; the basal gneisses have recrystallised as flaggy muscovite-chlorite gneisses with strong development of S1 and L1.

In the west of the area, evidence of an imbrication zone between the basal and Gjeitaa thrusts is found. This is discussed in detail by Banham (1962). To the east, exposure on the permafrost block-field is rather poor and evidence of imbrication is absent.

The tectonic significance of the basal thrust can not be positively stated on the present evidence. It formed at some stage of the B1 deformation and formed parallel to S1, the axial plane of B1 folds.

It is likely that the rigid nature of the basal gneiss complex prevented it from folding and that strain was localised along the lines of differing physical properties which reacted by thrusting. This is considered further in the tectonic synthesis.

### Gjeitaa thrust

The Gjeitaa thrust is approximately parallel to the basal thrust and it is a tectonic discontinuity separating the sparagmite group from the overlying psammite group. The thrust plane is marked by a narrow zone of sheared, flaggy quartzite (see Figs 85 and 86). Drag folds in the sparagmite group below the thrust may have formed either during B1 or during later movements along the Gjeitaa thrust plane.

In the north Tverra - Gjeitaabreen area, an imbrication zone is present between the basal thrust and the Gjeitaa thrust. The Gjeitaa thrust is almost certainly B1 in age. It is not seen to be folded by major B2 folds, due to lack of profile exposure, but variation in its dip is due to B2 folding.

The tectonic significance of the Gjeitaa thrust is uncertain; this problem is discussed in chapter 7. Any conclusions



Fig.85. Exposure of the Gjeitaa thrust in the Tverra cliffs. Note the flaggy nature of the rocks in the thrust zone.

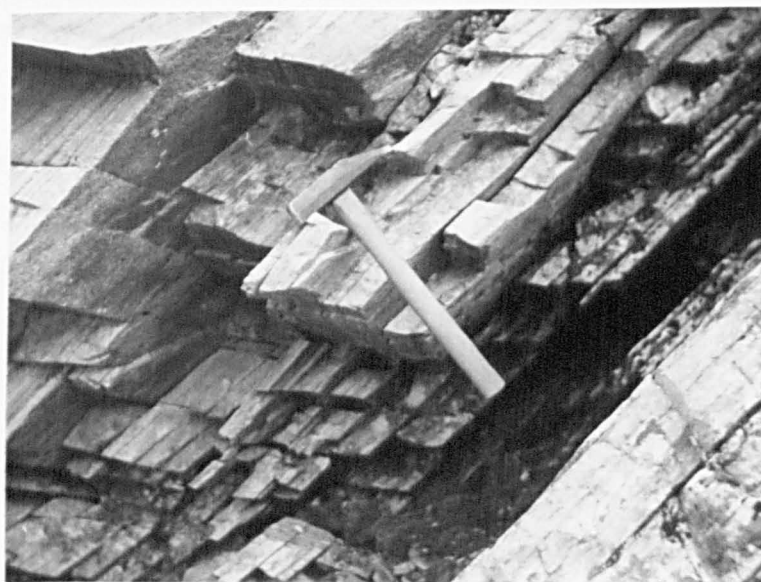


Fig.86. Close up of the Gjeitaa thrust, showing the sheared, flaggy and jointed nature of the quartzites.

must be tentative at this stage. It seems likely that the eugeosynclinal succession was emplaced above the Gjeitaa thrust during the B1 deformation. The sparagmite group may have been the original sole of the eugeosynclinal succession before emplacement, or it may have previously been in situ and suffered deformation during emplacement of the eugeosynclinal succession.

The possibility that the small area mapped is a part of one limb of a large B1 recumbent fold must not be overlooked. The outer limb could either be sheared out or buried beneath the upper Jotun nappe.

### Second movement phase B2

During the second movement phase, the major folds of the area developed, together with a suite of minor folds, an axial plane cleavage and associated linear structures. Deformation at the base of the upper Jotun nappe occurred at this time and evidence is presented suggesting that the upper Jotun nappe was thrust into place at this time.

#### (A) Minor structures

##### (1) Minor folds

B2 minor folds show considerable variation in style, symmetry and orientation throughout the area.

B2 folds vary in style from isoclinal similar folds to open, almost concentric folds. In orientation, the folds have a fairly constant axial plane orientation, striking approximately N. E. - S. W. and dipping fairly steeply to the south. Within this axial plane, the folds pitch at variable angles (0 to 60°) to both north-east and south-west quadrants.

The folds have either orthorhombic or monoclinic symmetry. In the hinges of major B2 folds, the minor folds often have



Fig 87

B2 fold axes

15,10,5,2,1 %

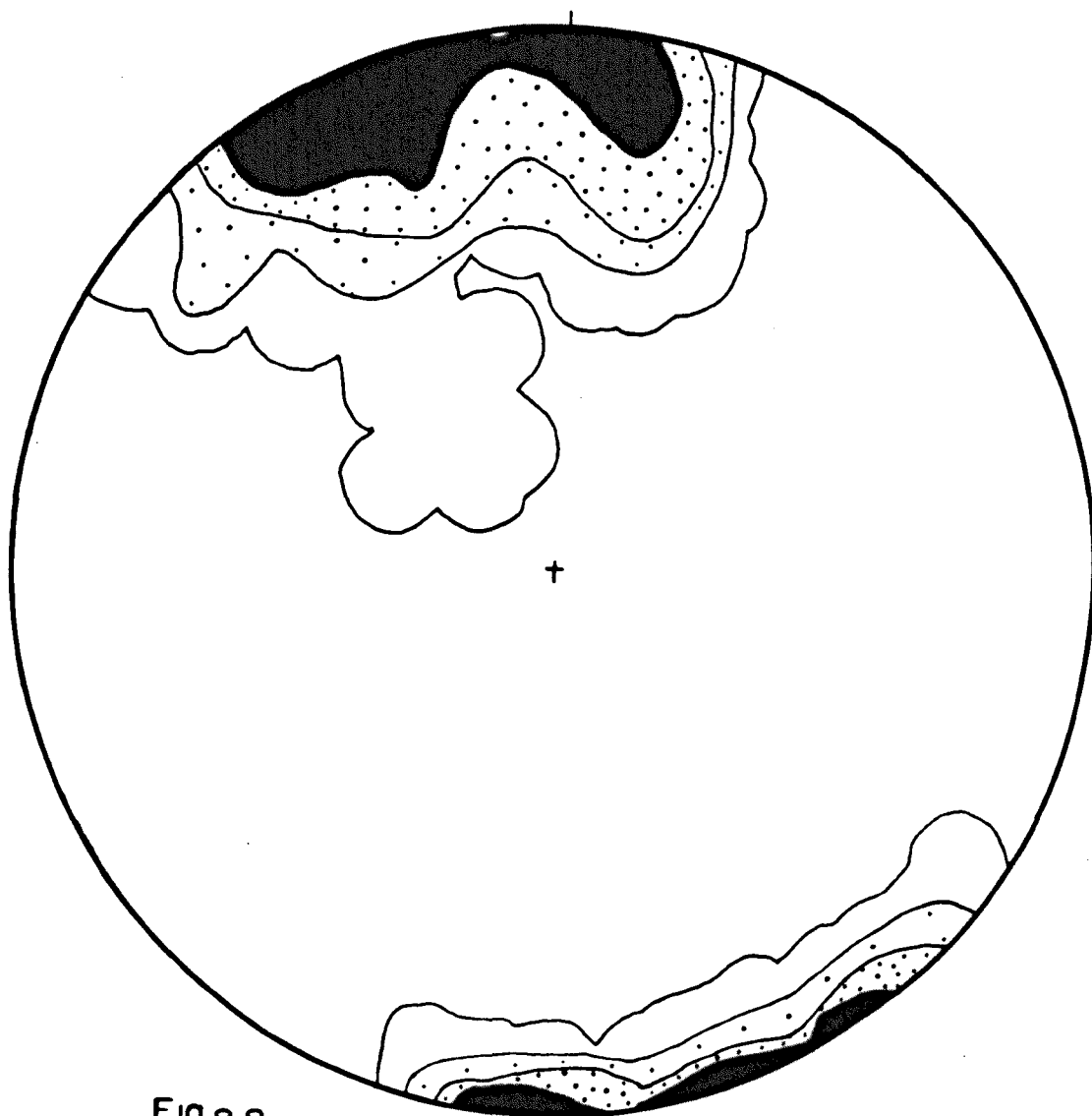


Fig 88

Poles to axial planes of B2 folds

10 , 6 , 3 , 1 %

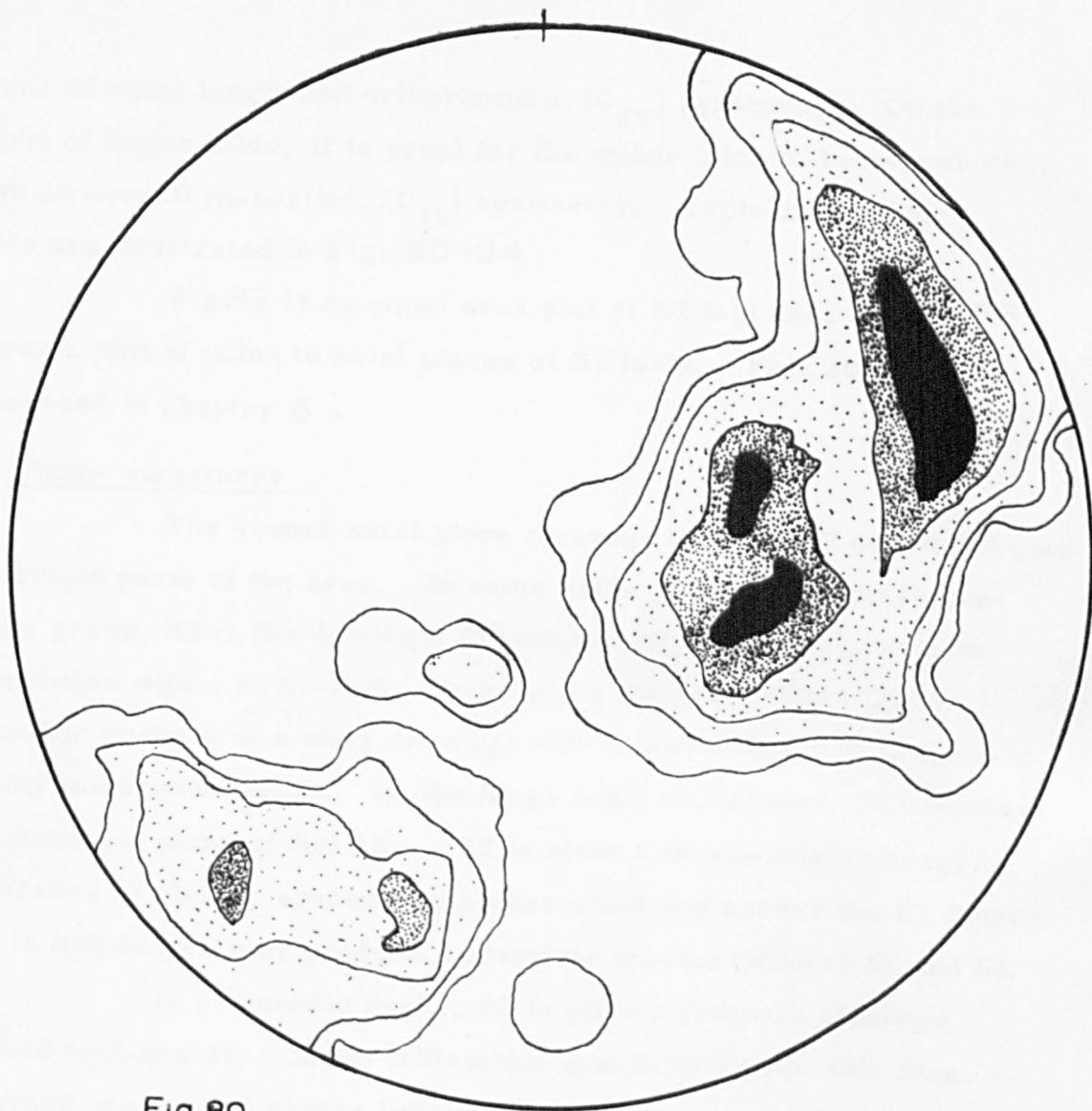


Fig 89

L2

15, 10, 5, 2, 1%



limbs of equal length and orthorhombic ( $C_{2V}$ ) symmetry. On the limbs of major folds, it is usual for the minor folds to be asymmetric with an overall monoclinic ( $C_{1h}$ ) symmetry. Typical B2 minor folds are illustrated in Figs.90-94 .

Fig.87 is an equal area plot of B2 fold axes and Fig.88 shows a plot of poles to axial planes of B2 folds. Fold styles are discussed in chapter 6 .

## (2) Planar structures

The second axial plane cleavage (S2) is well developed only in certain parts of the area. In some parts of the upper limestone-pelite group, S2 is the dominant foliation. S2 is fairly constant in orientation with a N. E. -S. W. strike and a steep dip (see Fig.88 ). In pelitic rocks it is a slaty cleavage with a lepidoblastic arrangement of tiny micaceous flakes. In the large scale fold hinges, S2 becomes the dominant plane of fissility. S2 is often a strain-slip cleavage, consisting of closely spaced slip planes which cut across the B1 fabric and in fold hinges may produce a complete transposition of S1 and S2.

In psammitic rocks, S2 is often a fracture cleavage infilled with quartz. In the feldspathic quartzite group, this fracture cleavage consists of gashes infilled with quartz, suggesting that it formed in a late stage of tension (see Fig.94 ).

## (3) Second linear structures

A suite of second linear structures, parallel to the hinges of B2 folds, was impressed on the rocks by the B2 deformation. They include a parallel ribbing on bedding or S1, produced by the hinges of tiny B2 crumples and also the intersection of S2 with bedding or S1. In the hinges of some B2 folds, a strong rodding of quartz veins is present; these are well developed at Nettoseter. At Kjerringhoe, irregular mullions of the type described by Wilson (1956) are found (see Fig.95 ). These have irregular cross-sections and

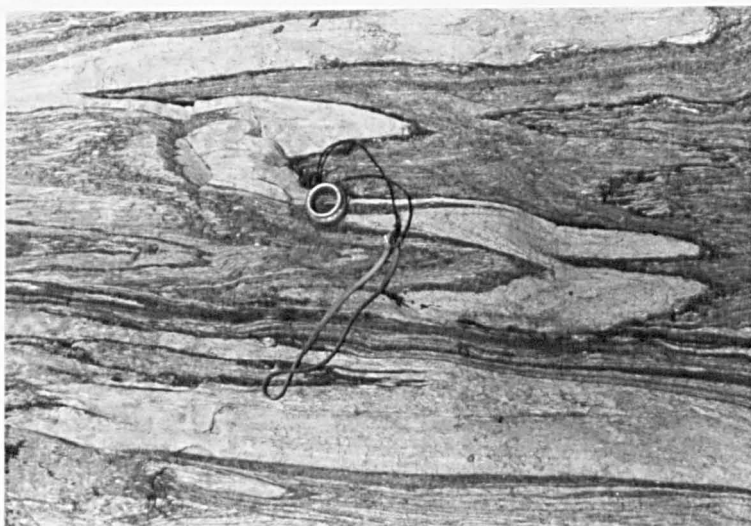


Fig.90 . B2 minor folds in quartzites and mica-  
schists. Note the intense thickening in hinges  
and thinning on limbs.



Fig.91 . B2 minor folds in the closure of  
the Holleindalen anticline.

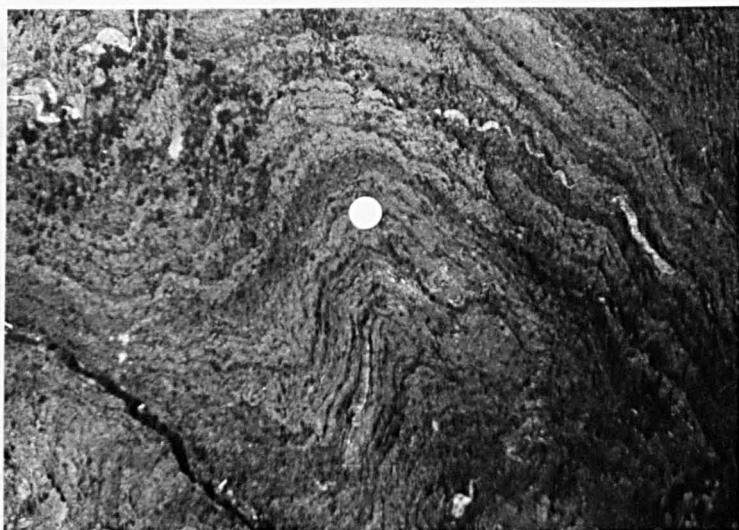


Fig.92 . B2 folds in the Holleindalen anticlinal closure.

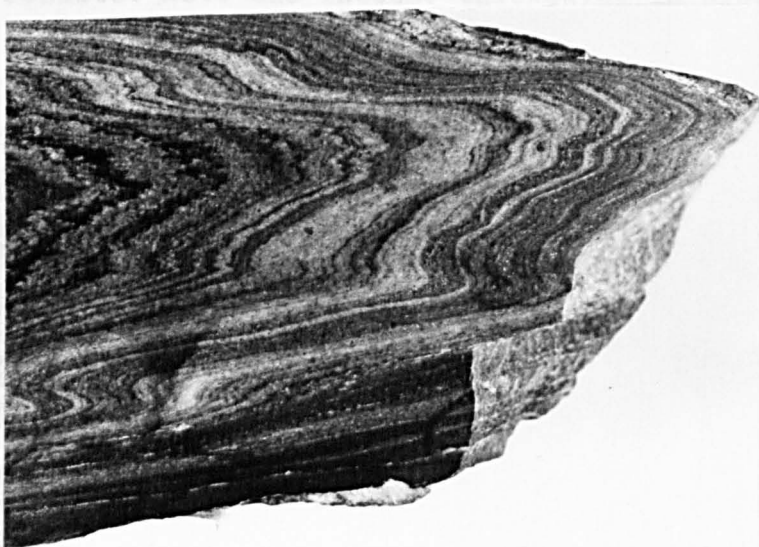


Fig.93 . B2 minor folds above Nettoseter.



Fig.94. B2 minor folds in feldspathic quartzite.  
Note the axial plane cleavage infilled with quartz  
veins.



Fig.95. L2 mullion structures at Kjerringhoe.

split along micaceous films (see Fig.95 ).

### Major folds

#### 1. Gjeitaabreen area

In the north, especially around Gjeitaabreen, the large-scale folds are isoclinal in style and have axial planes striking approximately  $55^{\circ}$  with a steep dip to the south. The folds pitch at low angles to the east on the axial plane.

South of Gjeitaabreen, the wide outcrop of the upper pelite group is a synclinorium with a constant axial trace and with plunges varying from  $0$  to  $50^{\circ}$  . Individual fold closures are difficult to map due to the lack of marker horizons, the shearing out along axial planes and the effect of later folding.

Fig.96 is a plot of fold axes for this area, from Gjeitaabreen south towards Holleindalen. Fig.99 shows the distribution of B2 linear structures across the area.

#### 2. The Holleindalen anticline

This is the largest fold within the area mapped and is responsible for the shape of the southern outcrop of the greenstone group. The fold plunges to the east and closes in Nettoseter.

The plunge of B2 minor folds varies along the axial trace, but is usually about  $60^{\circ}$  . Fig.97 is an equal area plot of B2 fold axes for the Holleindalen anticline; this shows the plunge variation. The minor folds are usually normally plunging structures but in places they are almost reclined folds.

#### 3. Southern area

South of Holleindalen, plunge variation is marked and plunges to eastern and western hemispheres are found. Within the upper limestone-pelite group, only one major fold closure has been found, but this lack of fold closures may be due to a combination of

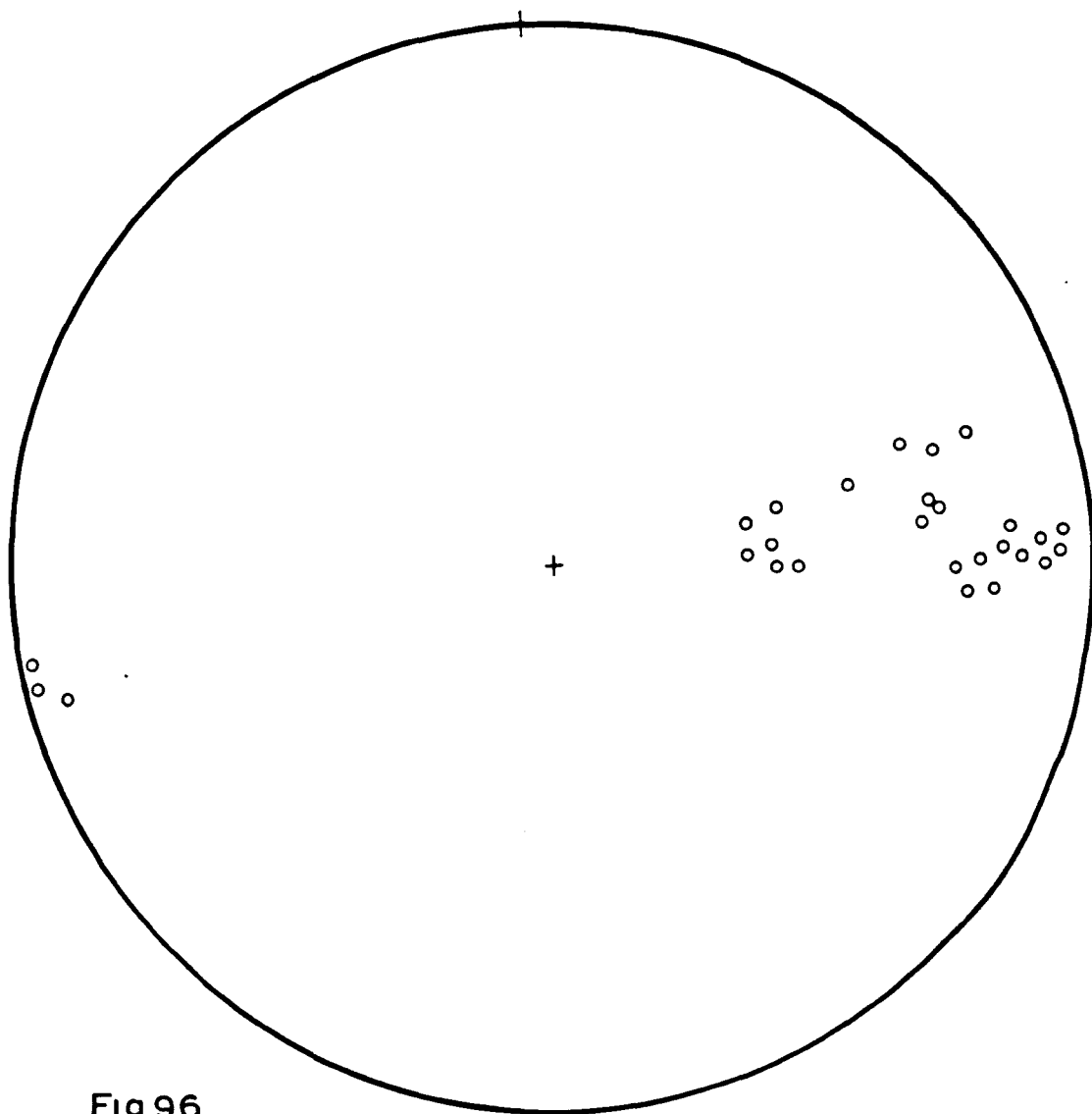


Fig 96

B2 folds, Gjeitaabreen area

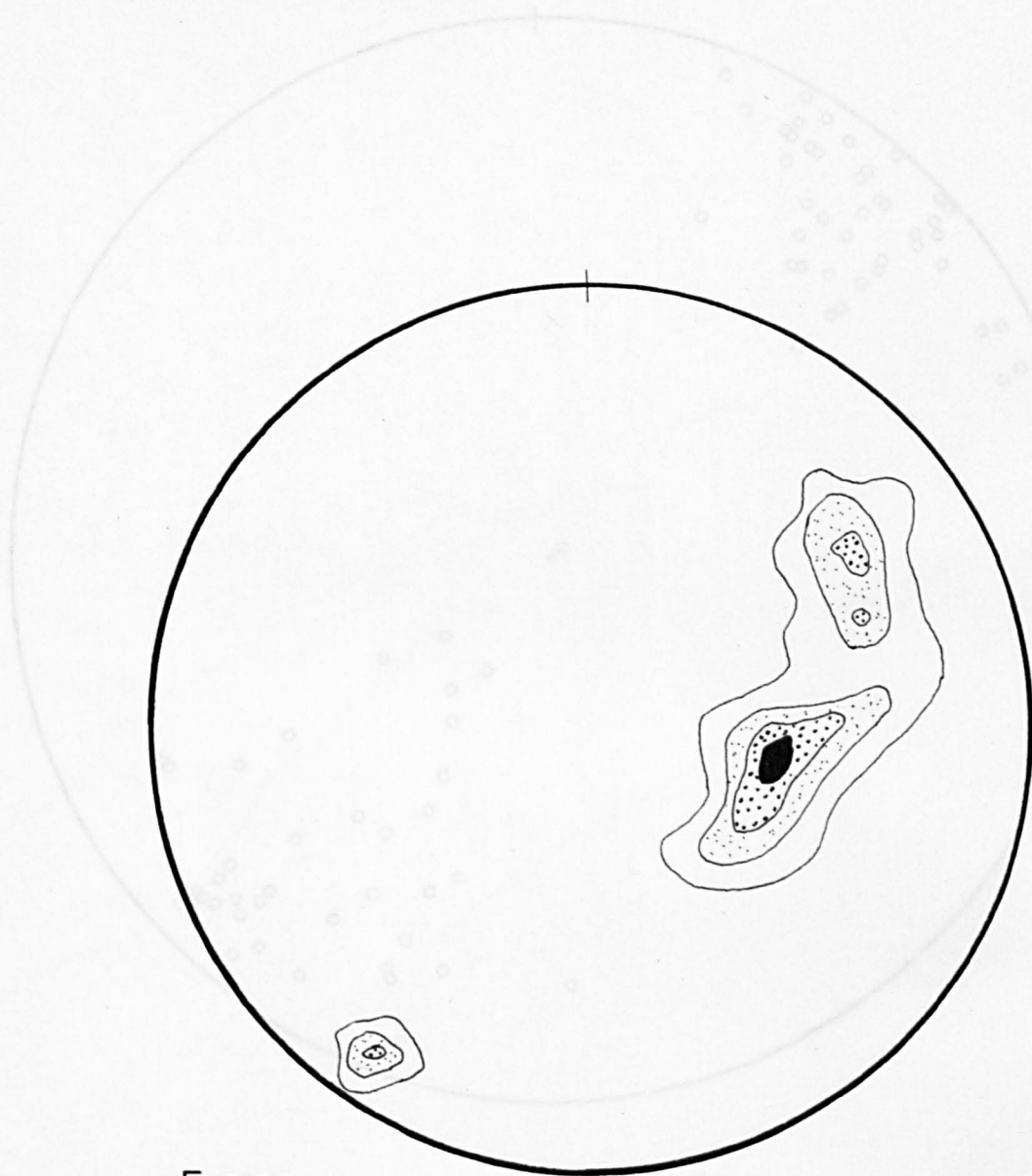
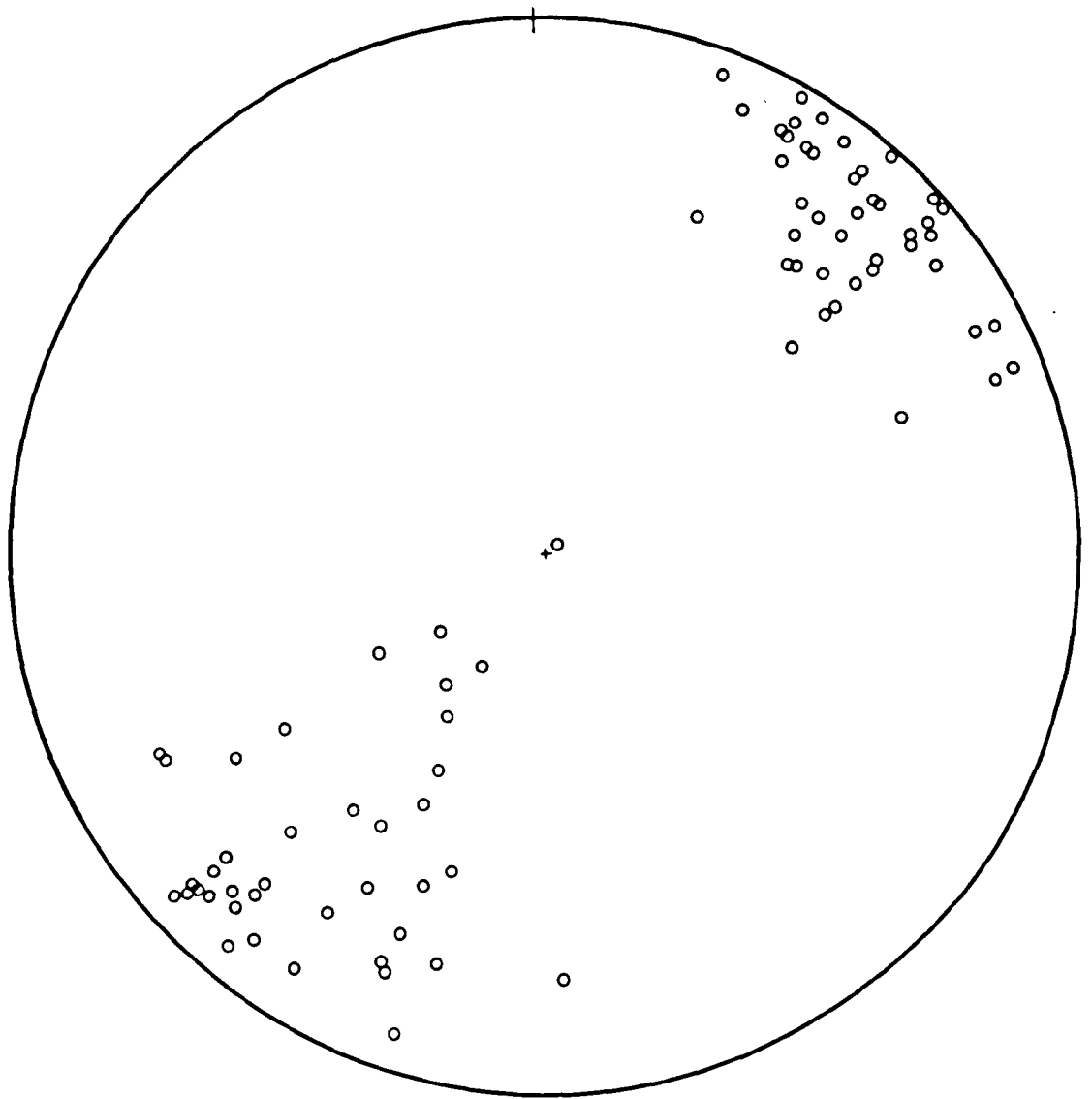


Fig 97

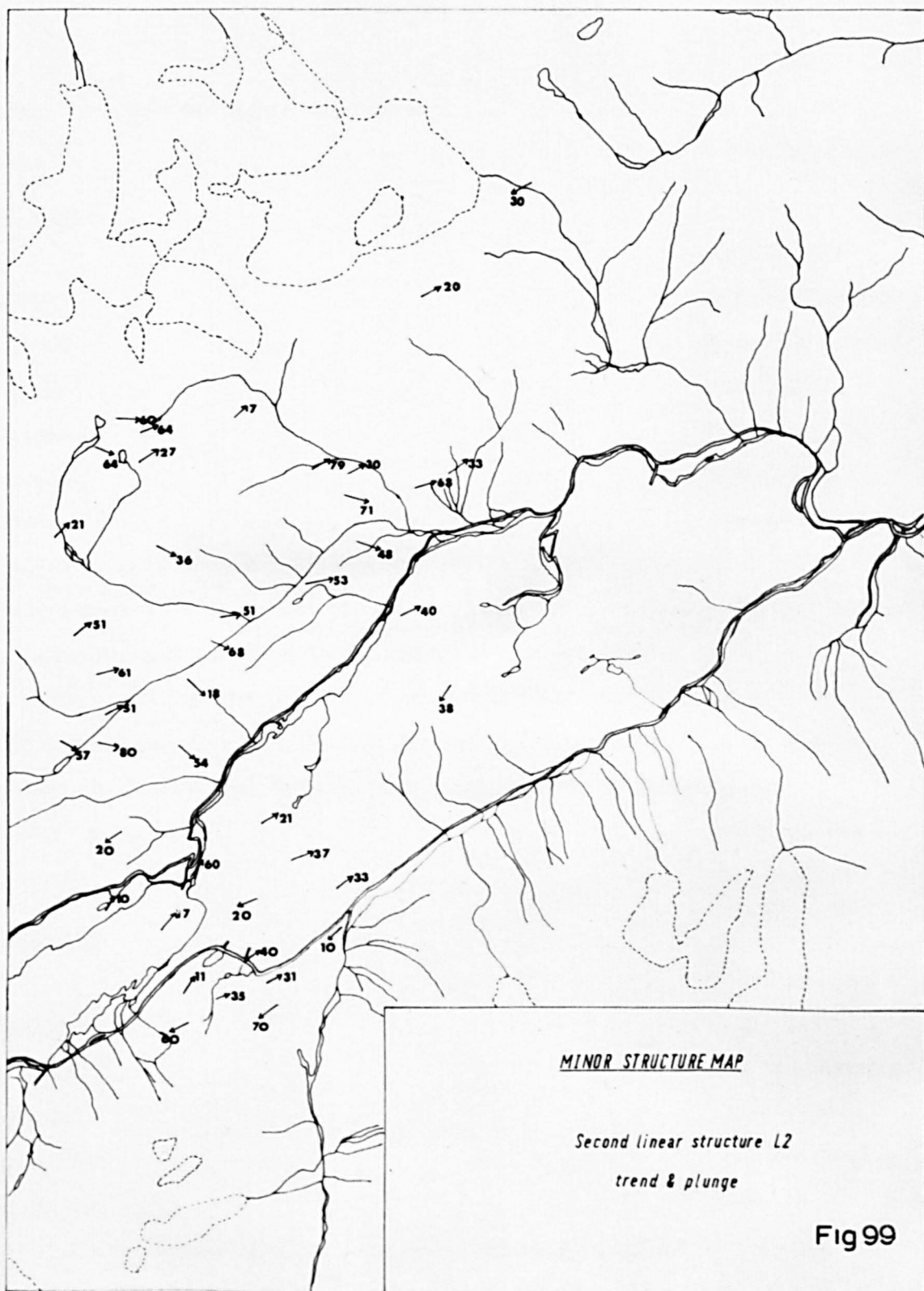
B2 fold axes, Böverdal area  
B2 fold axes, Holleindalen



**Fig 98**

**B2 fold axes, Böverdal area.**





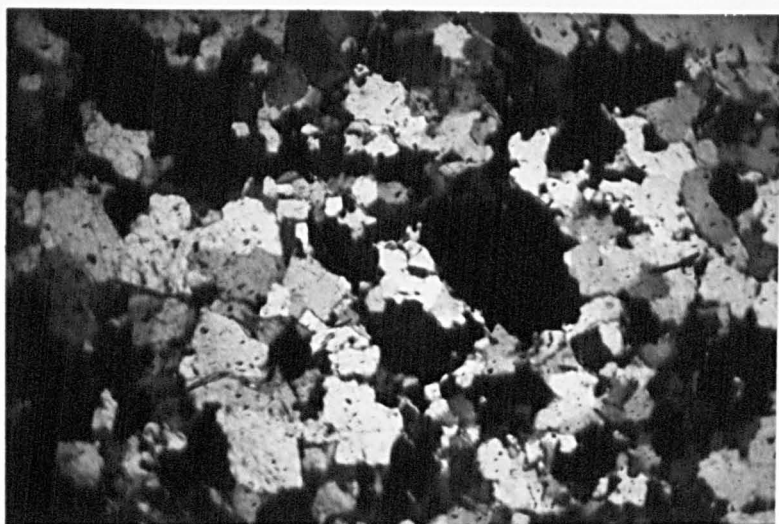


Fig.100. Photomicrograph of mullion; section cut at right angles to elongation.

X.n. x 30

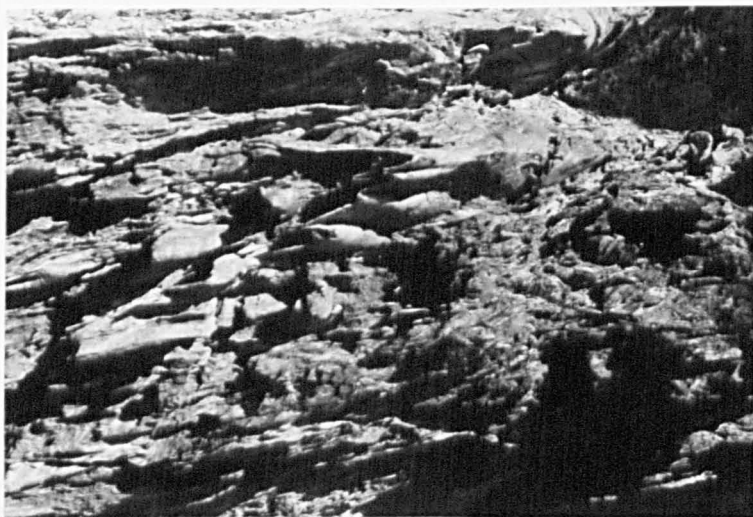


Fig.101. B3 folds in mica-schist with quartz veins. Note relict B2 folds refolded by B3 folds.

facies variation and poor exposure.

Fig.98 is a plot of B2 fold axes from the southern area.

#### Variation in B2 axial plunge

The plunge of the B2 fold system to eastern and western hemispheres shows diversity in both amount and direction (see Figs.96-9). Some of this variation is due to the superposition of the later B3 and B4 folding, but much of it is original and was formed during the B2 movements. In contrast, the axial planes of the major folds and the accompanying S2 cleavage are fairly constant in orientation. This variation in plunge of congruous minor folds and related structures is parallel to undeformed axial planes of the parent folds and must be synchronous with their formation. In addition, considerable plunge variation occurs from north to south across the area.

This complexity is probably attributable to three-dimensional deformation with differential flattening in the ab and ac planes, combined with variation in homogeneity of lithologies. Fig.99 shows a generalised picture of B2 plunge variation over the area, the significance of which is discussed in the tectonic synthesis.

#### Upper Jotun Thrust

The upper Jotun thrust is a major tectonic discontinuity separating pyroxene-granulite rocks of the upper Jotun nappe from the underlying supracrustal rocks. The base is marked by a mylonite zone and the movement picture within this mylonite zone is probably very different from that of either the overlying nappe or the underlying supracrustal rocks. This is probably why there is difficulty in correlating structures from the feldspathic quartzites up into the upper Jotun nappe.

Fig.99 shows the distribution of the minor structures at the base of the nappe and the evidence can be summarised as follows.

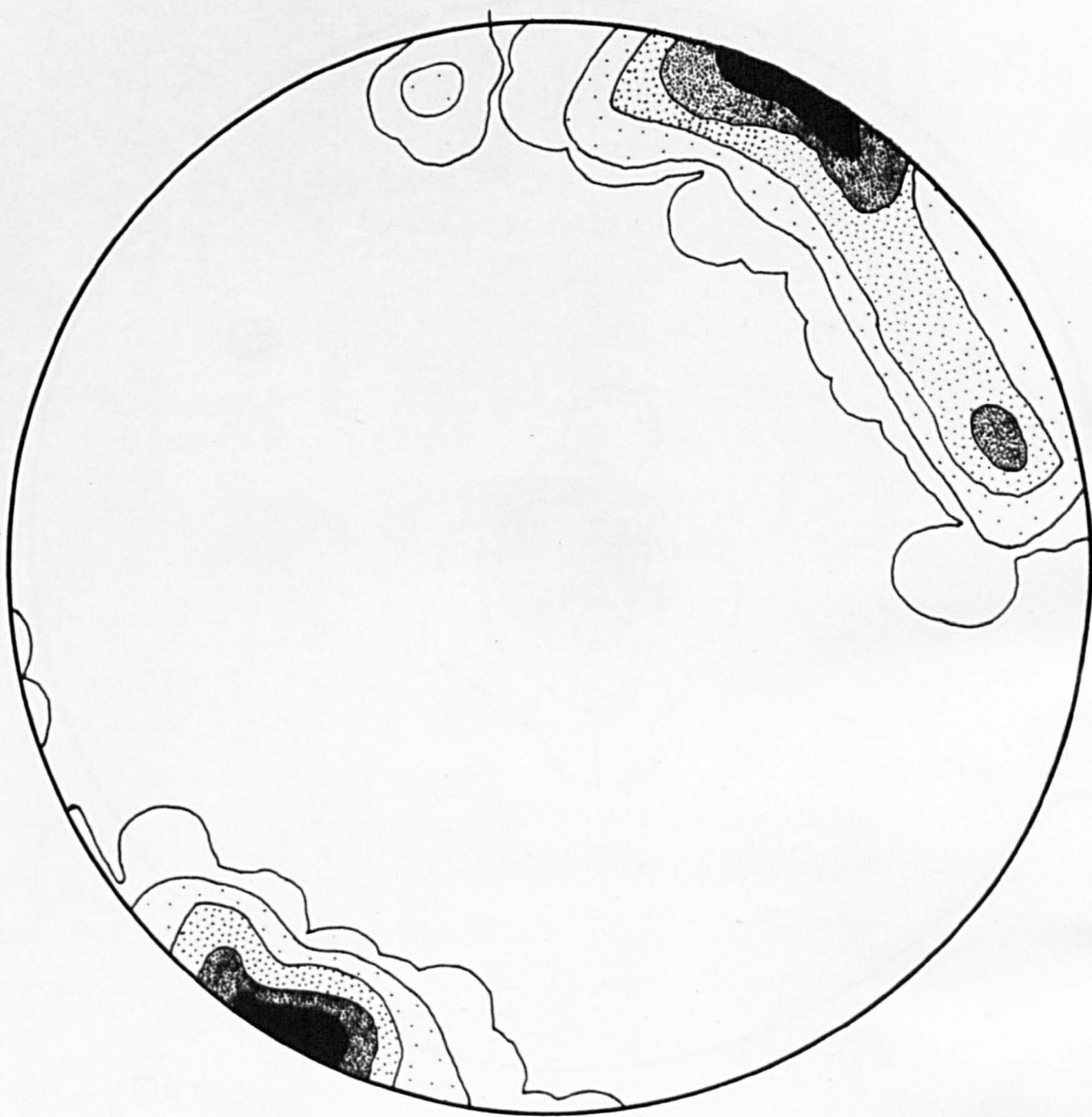


Fig102

B3 fold axes

15 , 10, 5, 2, 1 %

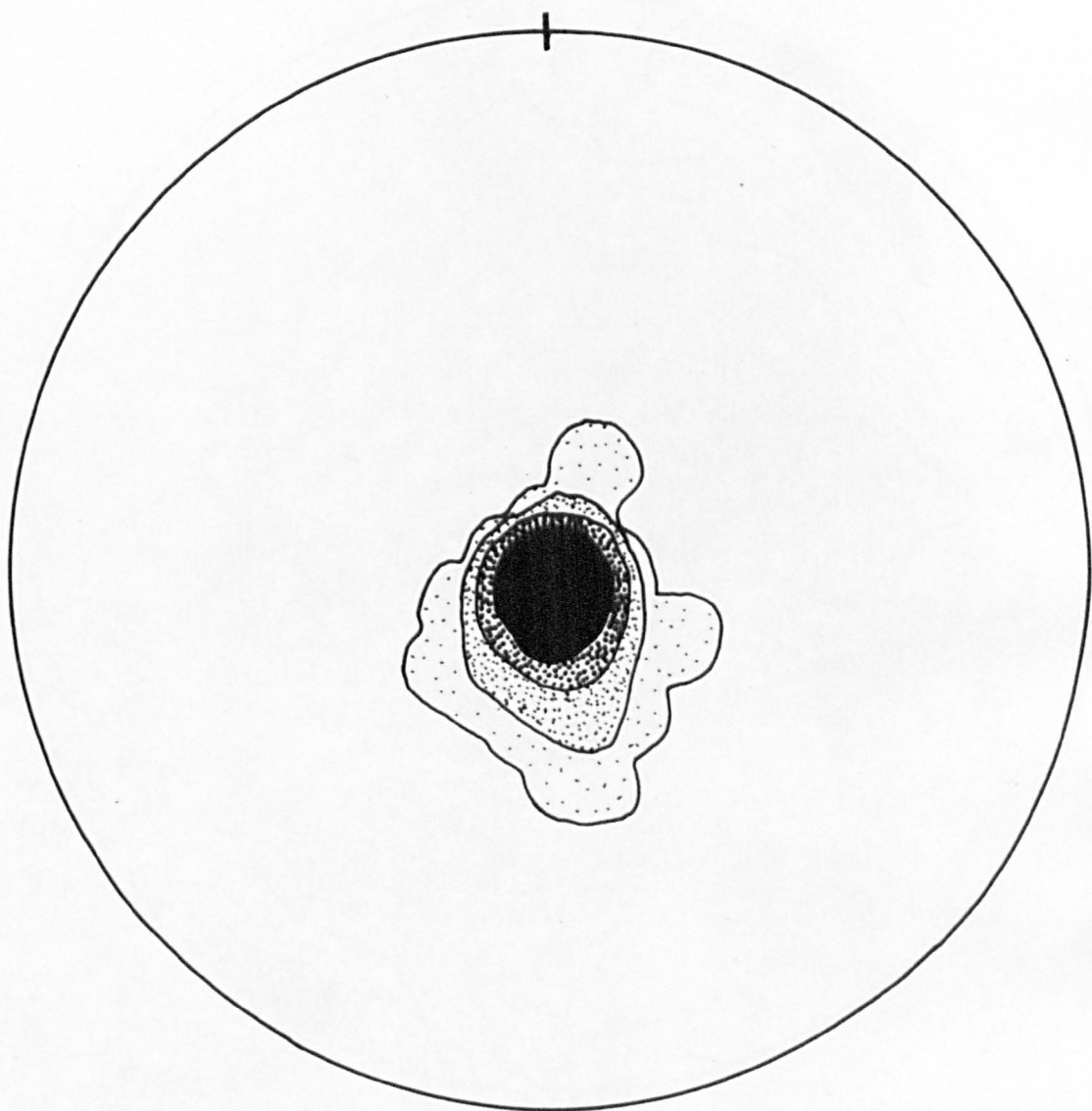


Fig103

Poles to axial planes of B3 folds

10,7,4, 1 %

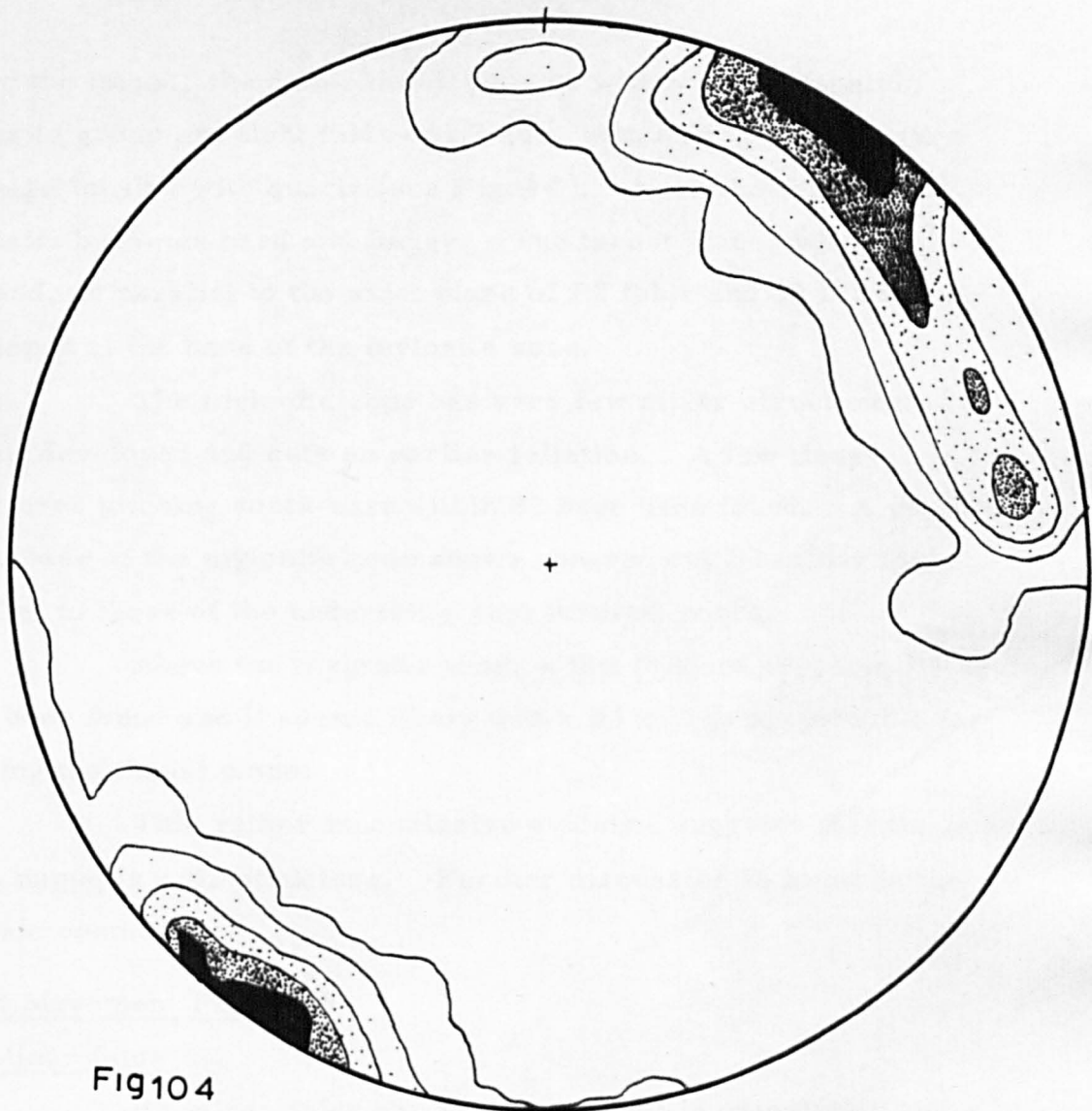


Fig104

L3

15, 10, 5, 2, 1 %

Below the thrust, the dominant structures within the feldspathic quartzite group are tight folds of B2 age, with axial plane fracture cleavage infilled with quartz (see Fig.94). Near the thrust the quartzite becomes hard and flaggy. The thrust plane, where exposed, is parallel to the axial plane of B2 folds and S2 is strongly developed at the base of the mylonite zone.

The mylonite zone has very few minor structures; S2 is well developed and cuts an earlier foliation. A few linear structures pitching south-east within S2 have been found. A phyllonite at the base of the mylonite zone shows sheared out B2 minor folds parallel to those of the underlying supracrustal rocks.

Above the mylonite zone, a few folds of probable B4 age have been found and it seems likely that a B4 fold is responsible for warping the thrust plane.

This rather inconclusive evidence suggests that the upper Jotun nappe is a B2 structure. Further discussion is found in the tectonic synthesis.

### Third Movement Phase B3

#### (1) Minor folds

B3 minor folds are fairly constant in orientation. They generally have flat-lying axial planes and low plunges. Their trend is thus largely controlled by the pre-existing S-surfaces. Fig102 is an equal area plot of B3 minor fold axes and Fig103 is a plot of poles to axial planes of B3 folds. The distributions of plunges of B3 structures is shown in Fig.109 .

In style the B3 folds are of a general flexural type, often kink-folds, but more open structures are found. B3 folds are illustrated in Figs.110—116 .

The symmetry of B3 folds is dependent on the pre-existing structural pattern. On the limbs of major B2 folds, the B3

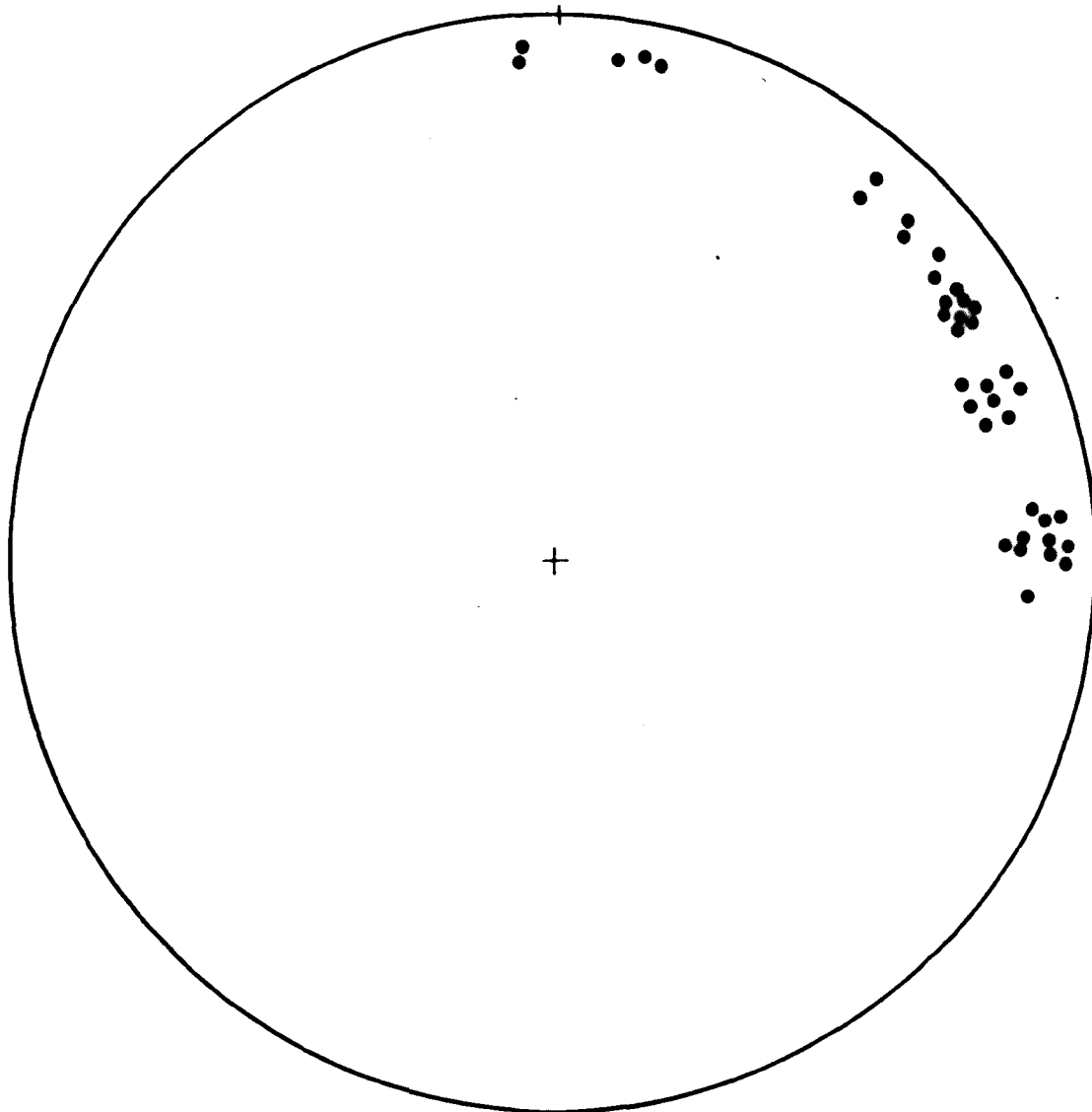


Fig105

B3 fold axes, Holleindalen closure



Fig 106

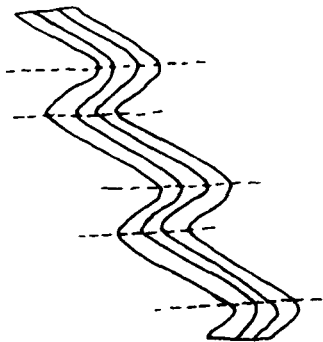


Fig107

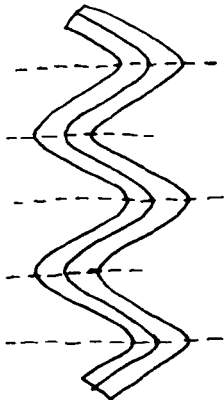
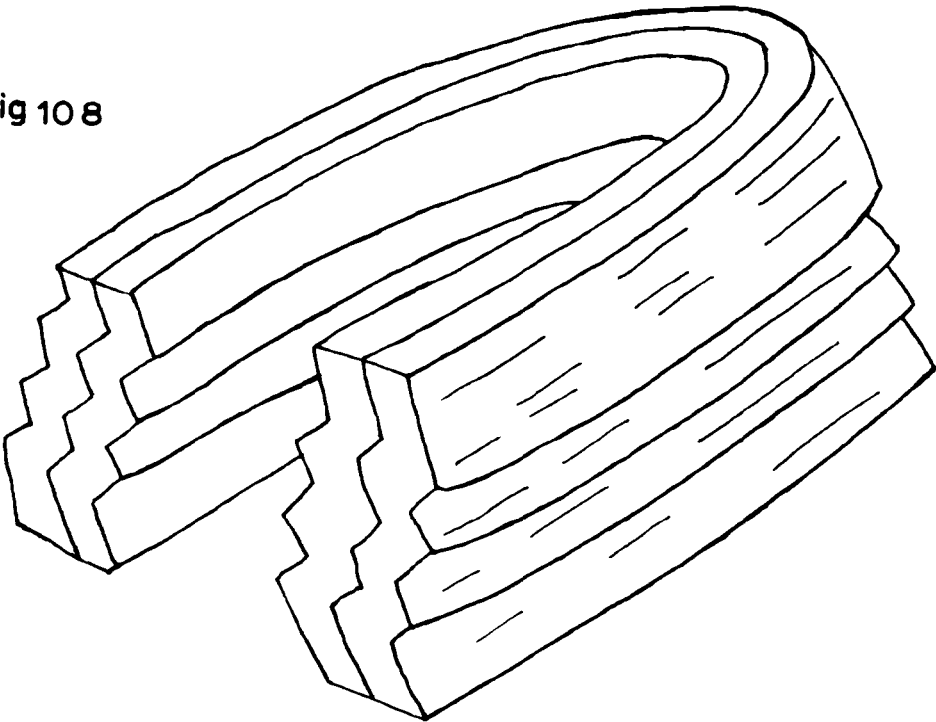
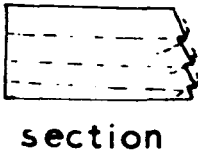
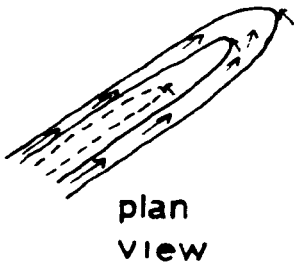


Fig 108



Holleindalen Anticline (diagrammatic)



linear structure

folds have a monoclinic ( $C_{1h}$ ) symmetry (see Fig.106 ). Where the foliation was originally vertical, the minor B3 flexures have orthorhombic ( $C_{2v}$ ) symmetry with limbs of equal length (see Fig.107 ). This may be due to compression acting normal to the axial planes, but this is not the only possible cause.

The axial planes of B3 folds are fairly constant in orientation; variation in trend of the folds is quite marked in places and depends on the geometry of the major B2 folds.

This is clearly seen in the Holleindalen anticline (see Fig.108 ). At the closure of the major anticline, the trend of the B3 folds swings round the closure showing the dependence of B3 on B2. This explains the partial girdle in the plot of B3 fold axes (Fig.105 ). This type of structure can be seen in a single hand specimen and has been verified experimentally using silicone putty.

It is not possible to explain the vergens of B3 folds; the possibility of the existence of major B3 folds must not be excluded.

The orientation of B3 folds must have been due to a near vertical attitude of  $\sigma_1$ ;  $\sigma_2$  and  $\sigma_3$  may have been equal; stress was most likely axial compression.

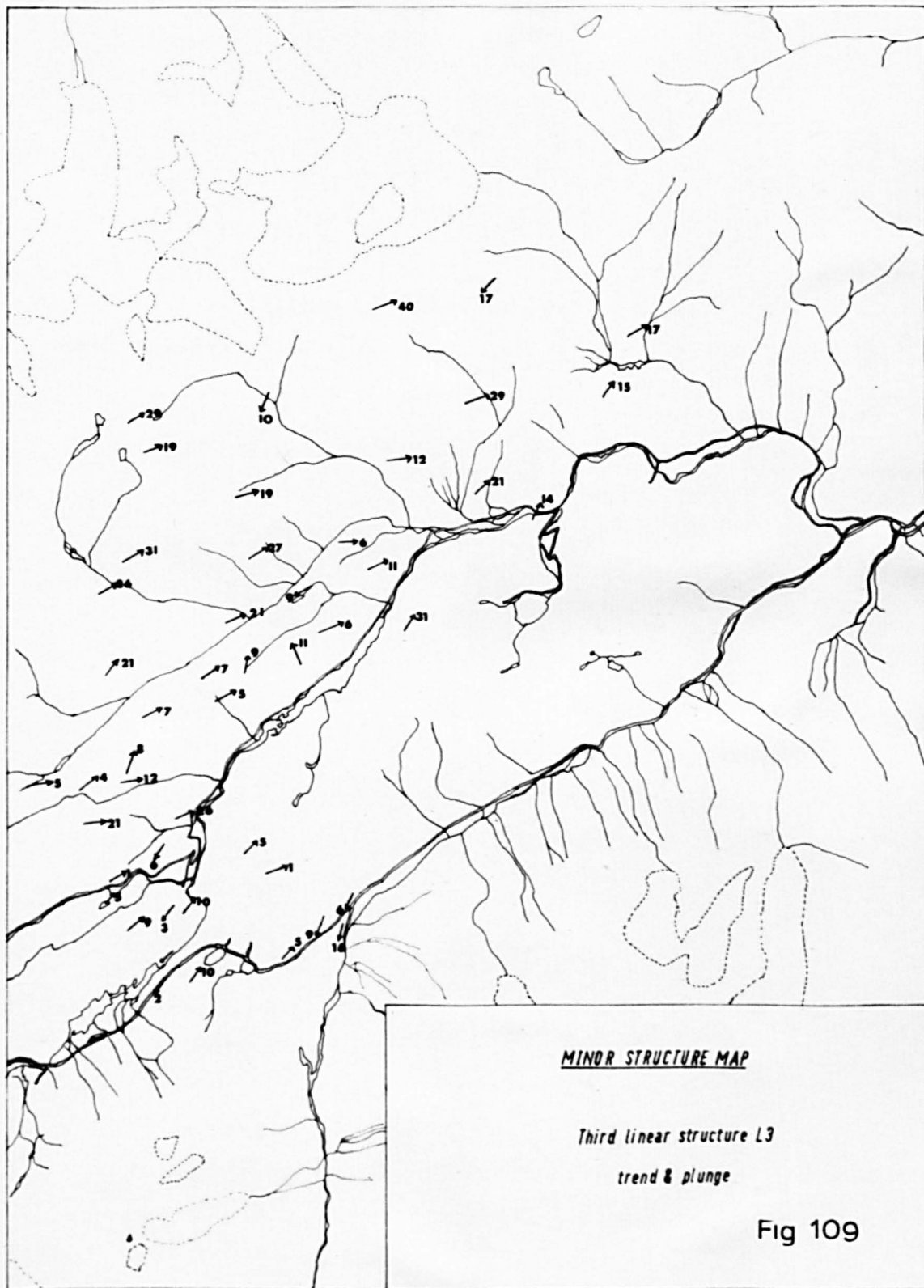
## 2. Third axial plane cleavage S3

In pelitic rocks, a late axial plane strain slip cleavage is often present. This is usually weakly developed, but in some phyllites it forms a penetrative structure.

In some more competent rocks a late stage fracture cleavage may be present. In a few examples quartz veins up to 1 metre thick are found along these axial plane fractures (see Fig.115 ). This is obviously a late stage feature.

## 3. Third linear structure L3

A suite of third linear structures was impressed on the rocks by the B3 deformation. These are always parallel to the hinges of



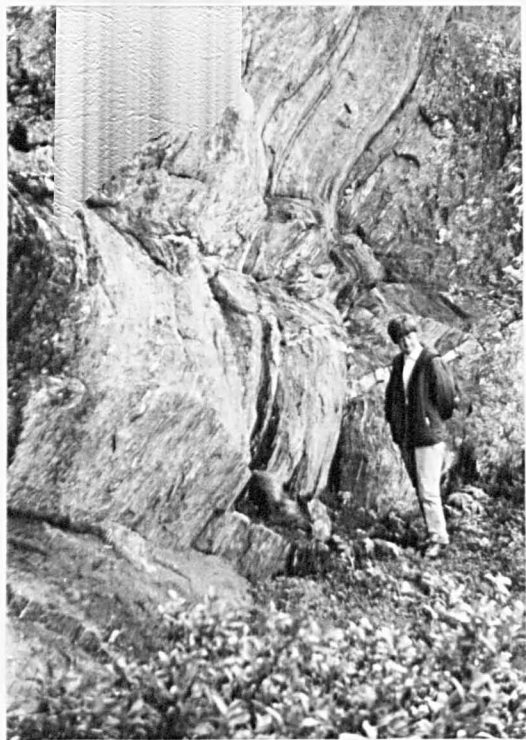


Fig.110.

B3 folds Holleindalen.

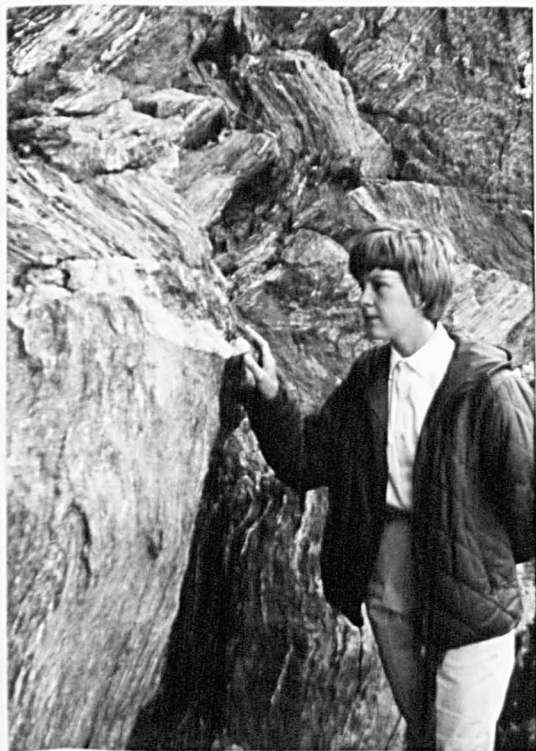


Fig.111.

B3 folds in mica-schist  
on Holleindalen.



Fig.112. B3 fold refolding B2 fold, Holleindalen.



Fig.113.

B3 folds in thinly  
banded quartzites.  
Axial plane cleavage  
infilled with quartz  
and some B1 boudinage  
seen.

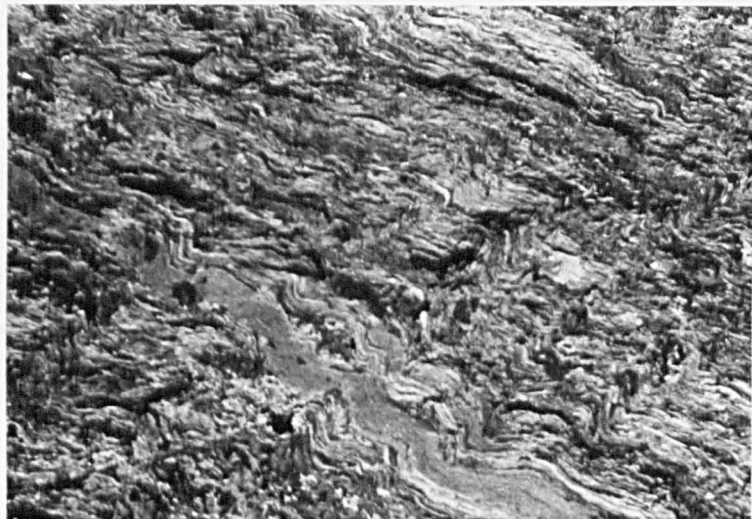


Fig.114. B3 folds in quartz-mica-schist,  
Holleindalen.



Fig.115 Quartz vein along axial plane of  
B3 fold. Note that the vein is discordant.

Fig11 6

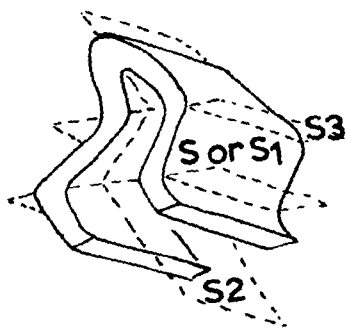
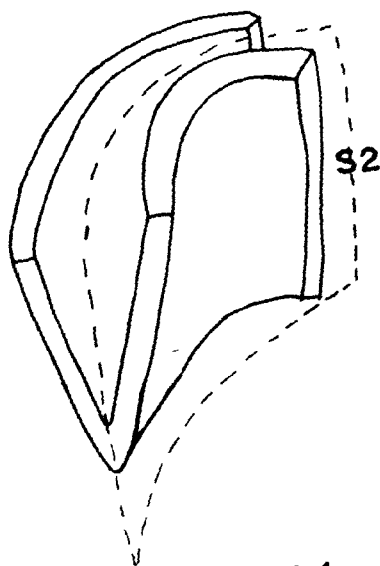


Fig117



B2 refolded by B4

B3 folds and include a parallel ribbing, produced by the hinges of tiny B3 folds, on bedding, S1 or S2 and also the intersection of S3 with bedding, S1 or S2.

#### Fourth movement phase B4

B4 folds are nowhere abundant, but from the isolated examples observed and measured, the following pattern has emerged.

B4 folds are essentially flexure folds (see chapter 6 ); their orientation is rather constant, they have a trend approximately  $180^{\circ}$  and a fairly steep plunge. In the feldspathic quartzite group, especially, they are kink-bands (see Fig.121 ); in the north, from Gjeitaabreen to Kjerringhoe, they are more open warps.

Two conjugate axial planes are developed, which intersect on the fold axis, but in most cases, one or the other axial plane is developed and true conjugate folds are rare. Equal area projection of fold axes and axial planes are shown in Figs.118 and 119 . The conjugate nature of the folding can be seen from the geological map, since kinks in outcrop pattern are obvious between Gjeitaabreen and Kjerringhoe.

These folds probably originated by approximately E.-W. compression.

The symmetry of the B4 folds depends on the attitude of the surface being folded. Where the surface being folded was vertical, the folds have an overall orthorhombic symmetry, but elsewhere have a monoclinic symmetry.

A B4 fold is probably responsible for warping the upper Jotun thrust and causing the upper Jotun nappe to be exposed further north in Leirdalen than would be expected.

#### Fifth movement phase B5

The fifth movement phase is very localised and is



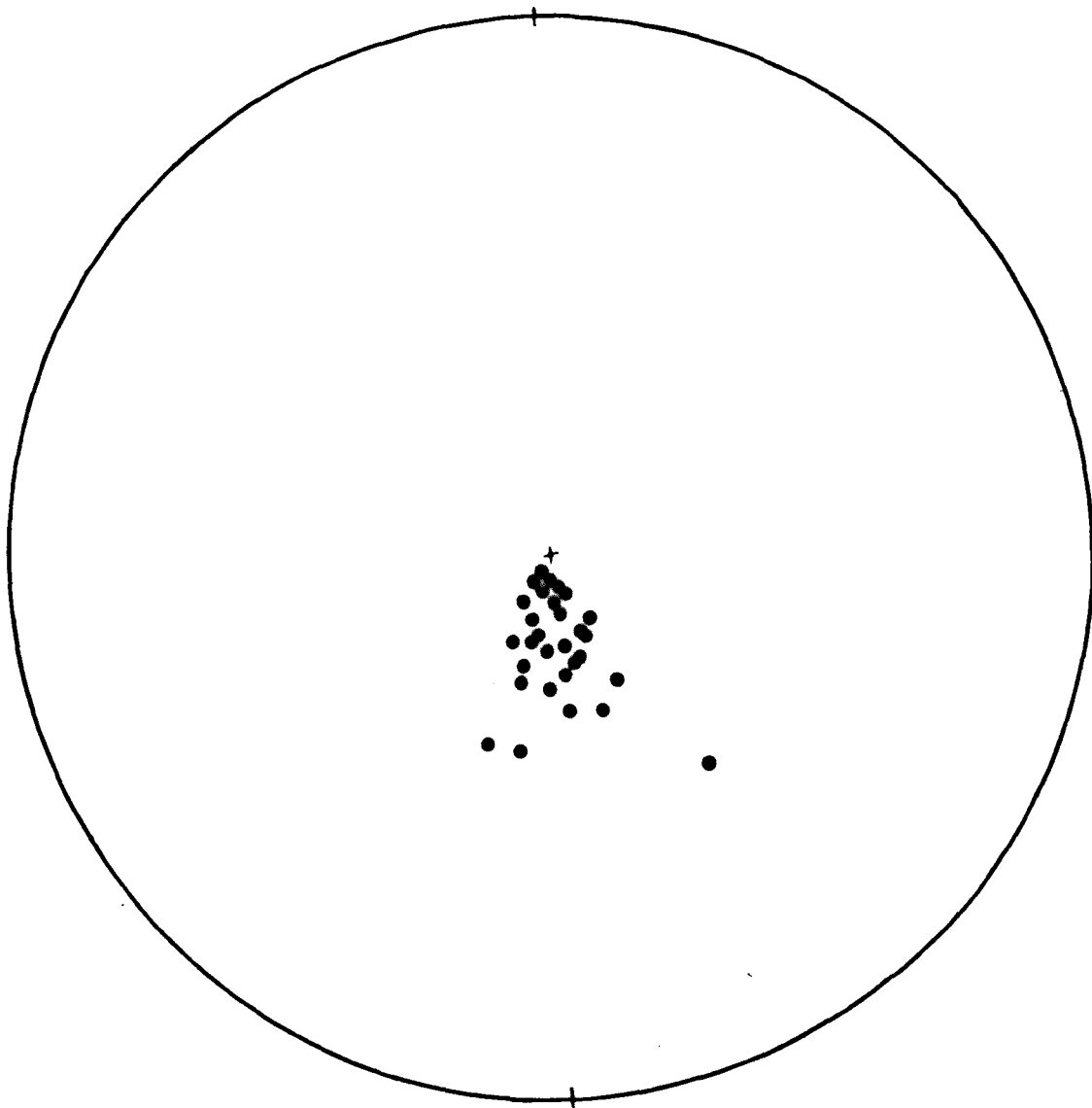


Fig 11 8

B4 fold axes

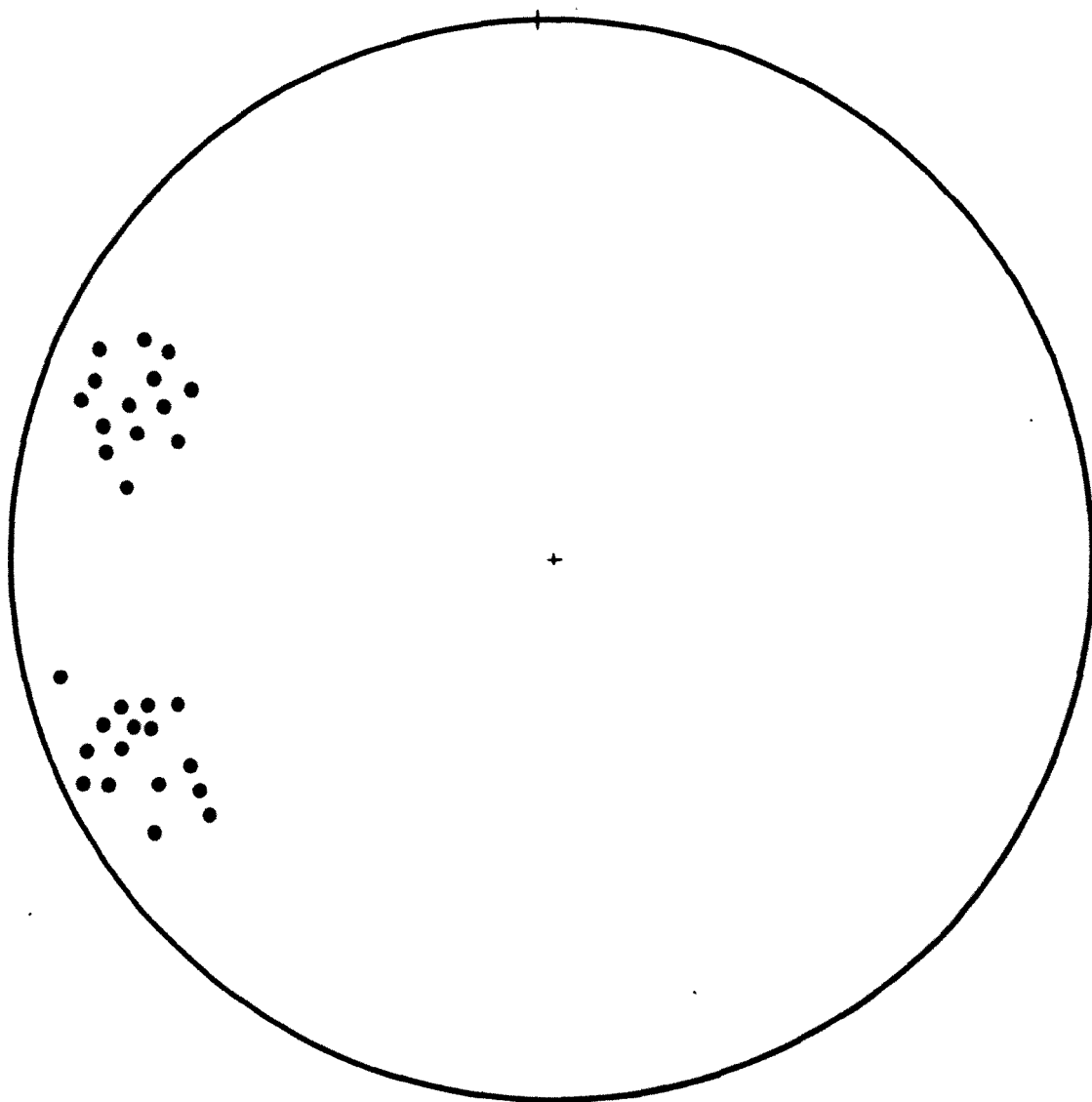


Fig 119

Poles to axial planes of B4 folds

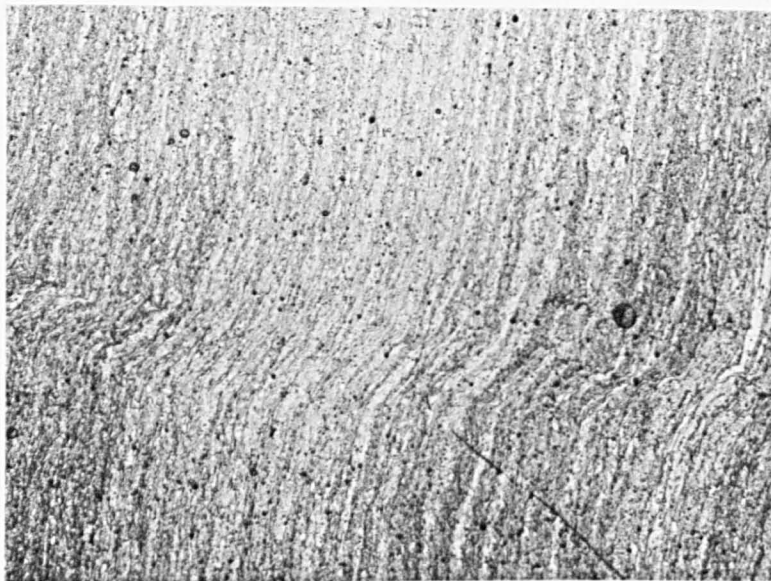


Fig.120. Photomicrograph of B4 kink band,  
Leirdalen.

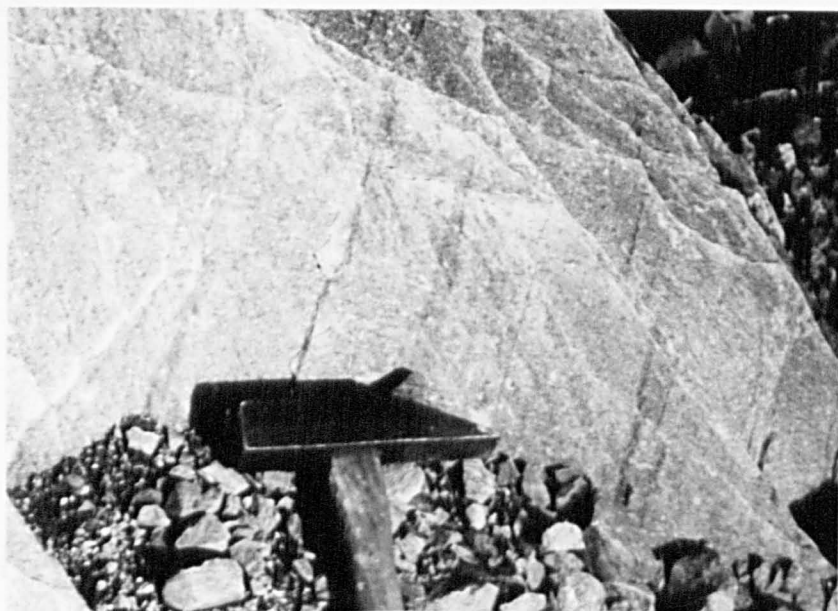


Fig.121. B4 kink-bands in quartzite, leirdalen.

sporadically developed within the feldspathic quartzite group, especially near the base.

The fifth structure is a kink-band with strain slip cleavage; it has a trend approximately N.E. and a sub-horizontal plunge. The axial plane strikes N.E.-S.W. and is vertical.

The fifth structure can be seen to cut across B4 and B3 folds above the Jotunheimen Hotel. A fifth structure is sketched in Fig. 122 .

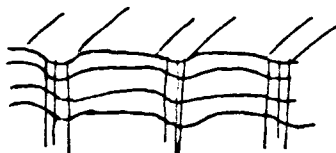




Fig.123. L1 stretching lineation, refolded by B2 fold, Gjeitaabreen. Note L2 and faint trace of B1 lineation parallel to B1 fold axes.

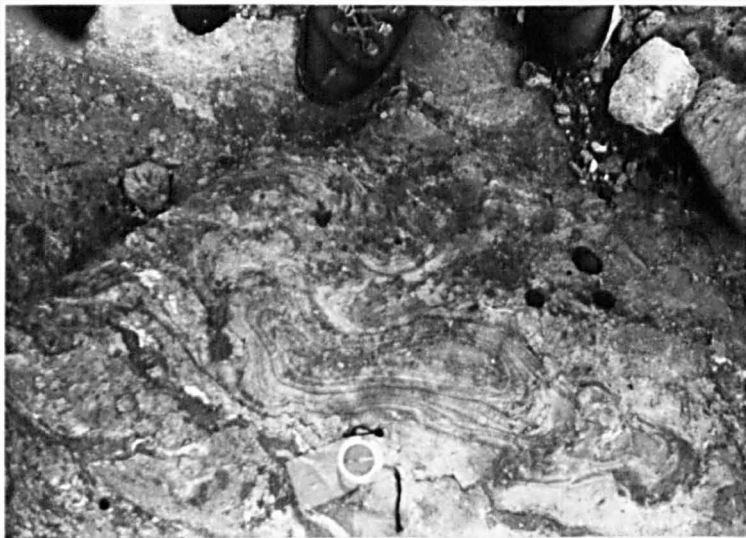


Fig.124. Eye fold at Gjeitaabreen; interference of B2 and B4.

## DEFORMATION OF PRE-EXISTING STRUCTURES BY LATER FOLDS

---

### Deformation of B1 by B2

B1 folds are deformed by B2 folds only at Hoyoyen. Here B1 folds trending  $110^{\circ}$  are refolded about axes trending  $85^{\circ}$ .

Examples of refolding of L1 by B2 folds are quite common. At Hoydalsvatn outflow, L1 phacoids are bent around B2 folds (see Fig.151 ). The deformed L1 structures plot out on a partial great circle.

Evidence of deformation of S1 by B2 folds is common. In many cases, S1 is displaced by an S2 strain-slip cleavage.

Fig.123 shows an L1 "stretching" lineation refolded by a B2 fold at Gjeitaabreen.

### Deformation of B2 by B3

Over much of the area, B2 folds refolded by B3 folds can be seen. Where the plunge of B2 folds is low, refolding of B2 by B3 is often co-axial (see Fig.116). B3 is a flexural-slip folding. B2 folds refolded by B3 folds are illustrated in Figs.35 and 112 .

Examples of B3 folds folding S2 are common and many instances have been recorded (see Fig.35 ).

Cases of B3 folds refolding L2 structures are abundant (see Fig.125 ). In many cases the deformed L2 plots out on a small circle, indicating probable B3 flexure folding (see Fig.126 ). In other cases, the deformed L2 gives neither a great circle nor a small circle projection (Fig.127 ).

### Deformation of B1 by B3

A few cases of deformation of first linear structures by B3 folds have been noted. At hoydalsvatn and Gjeithoe, L1 phacoids are deformed by B3 folds (see Fig.150). B3 folds frequently fold S1.



Fig.125. L2 refolded by B3 fold.

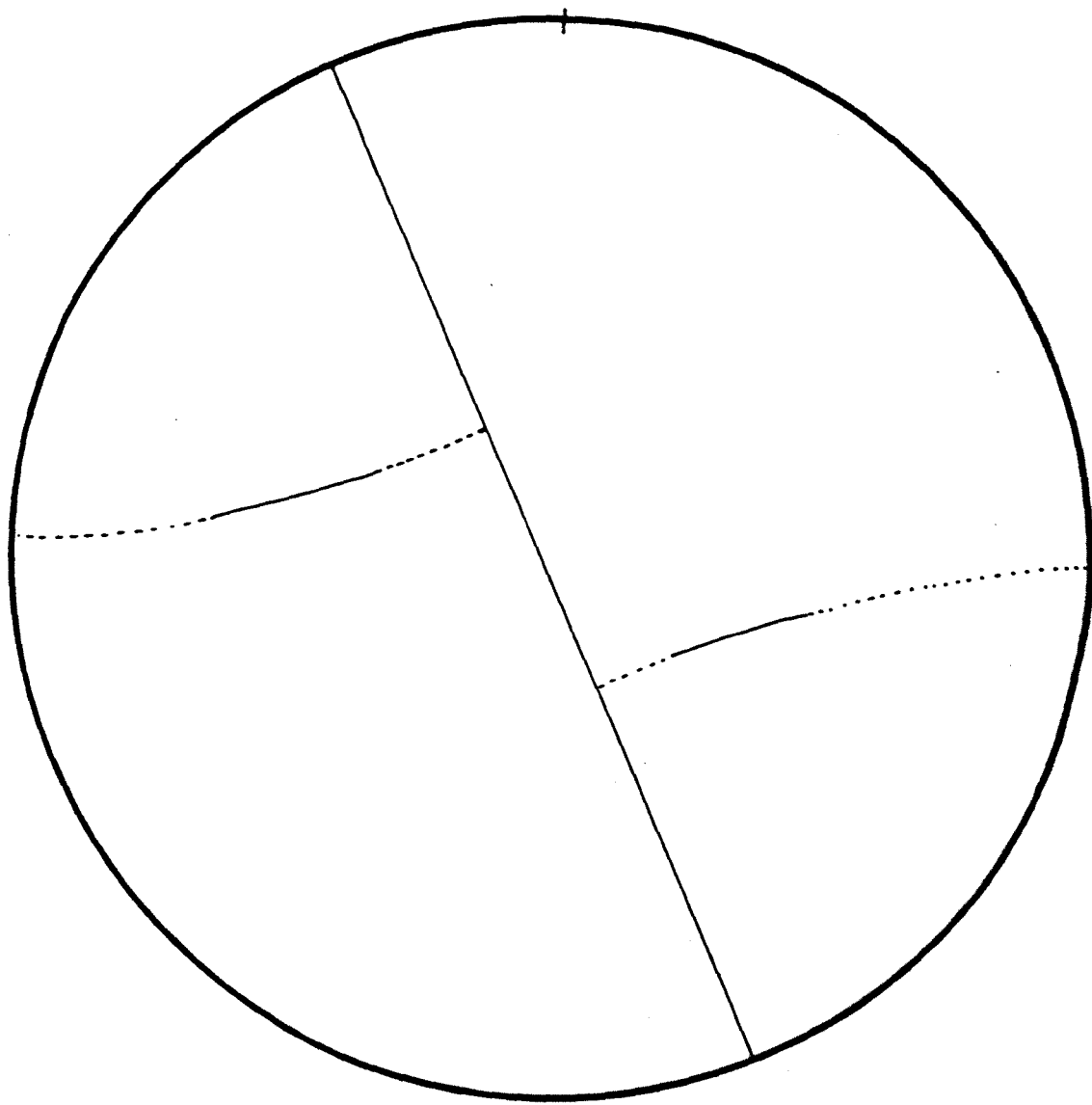


Fig 12 6

L2 refolded by B3 fold



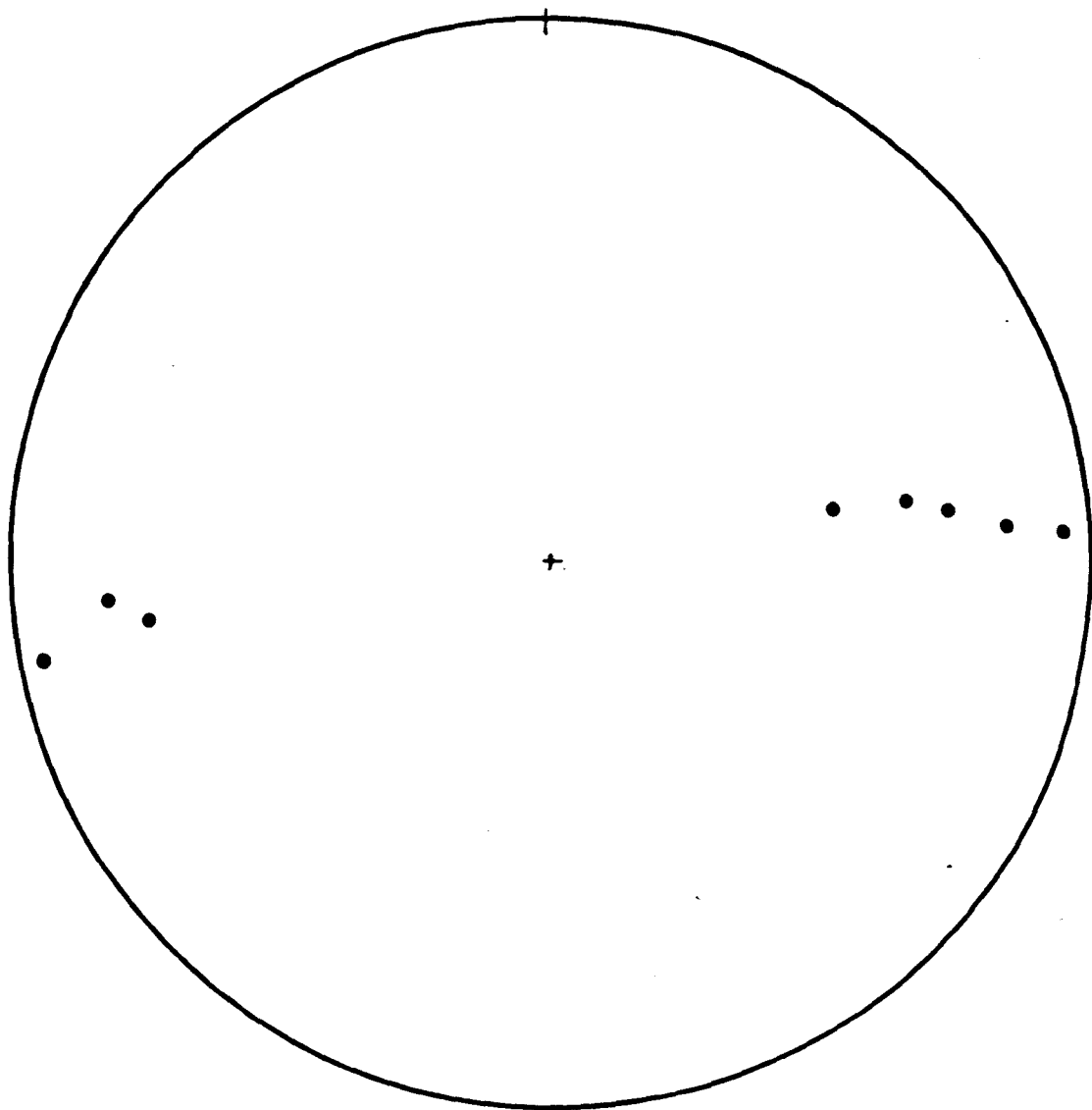


Fig 127

L2 refolded by B3 fold

Deformation of B1, B2, B3, by B4 folds

Little evidence of deformation of earlier structures by B4 folds has been obtained. However, at Høyen and Kjerringhoe, B4 folds which deform both B2 and B3 structures are exposed (see Fig.117 and Fig.124 ).

In the feldspathic quartzite group, B4 kink bands displace B3 folds and flex the S2 axial plane cleavage (see Fig.121 ).

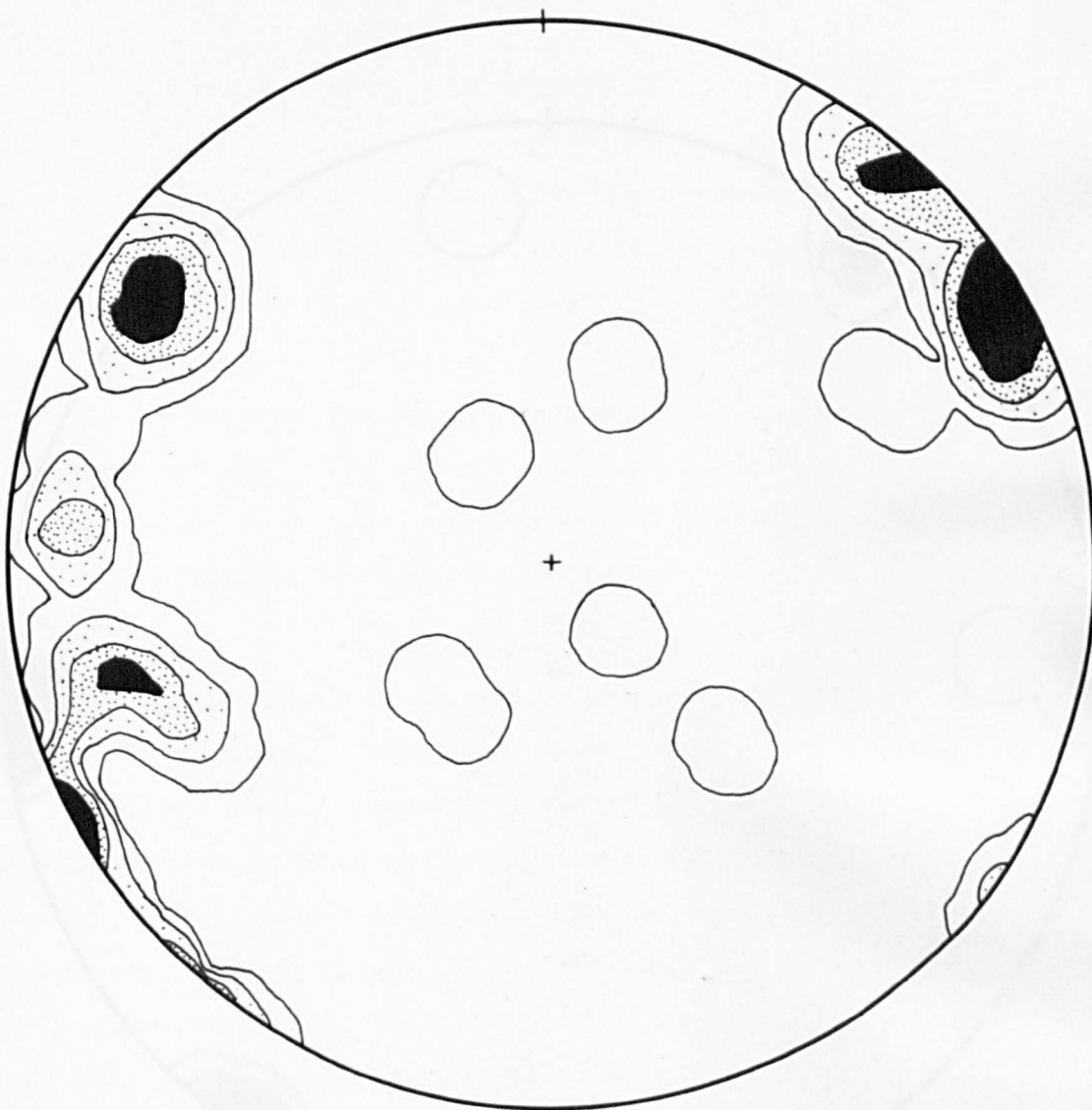


Fig 128

Poles to joints NE area

10,5,2,1%

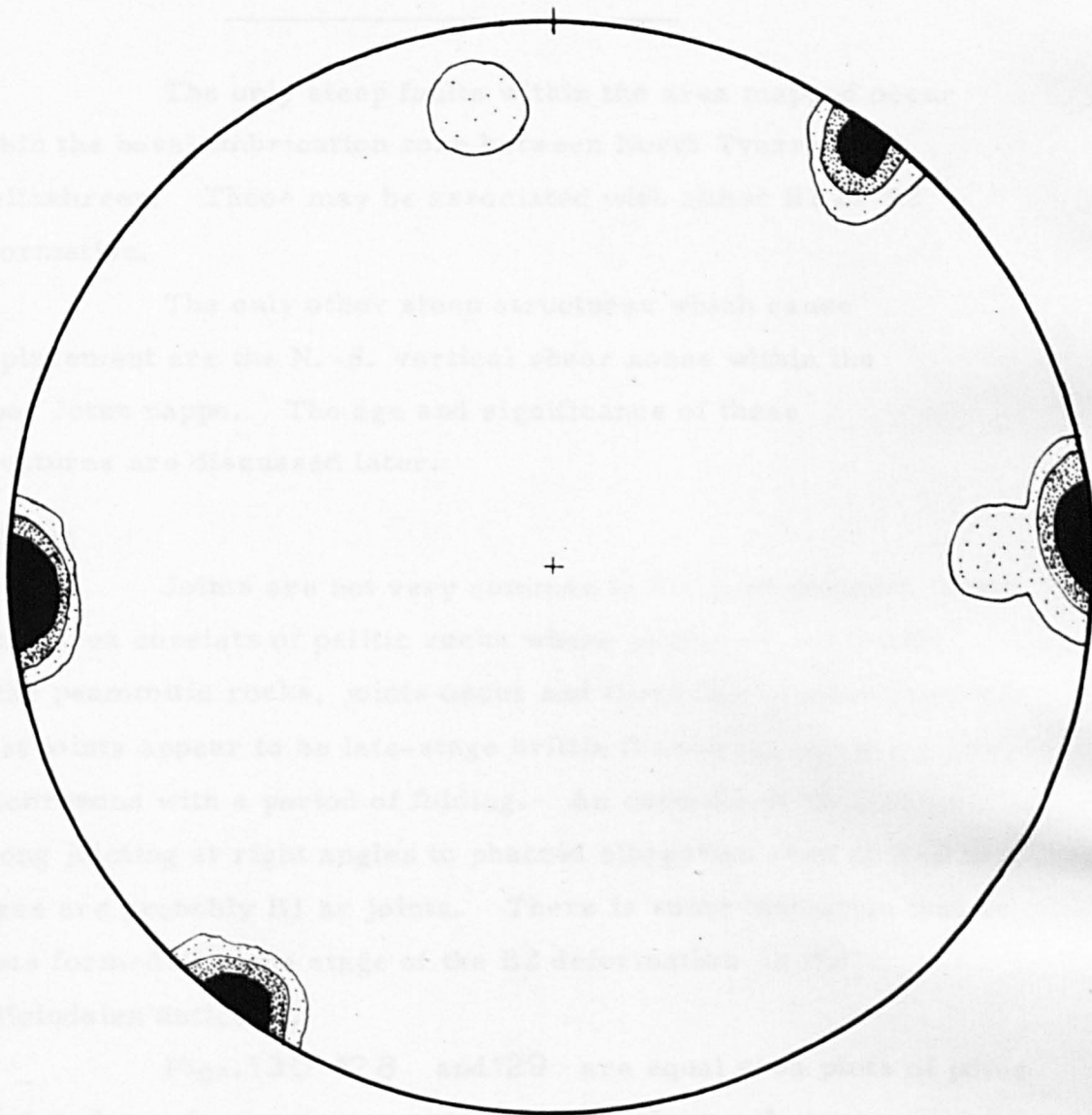


Fig 129

Poles to joint planes

southern area

5,21%

## FAULTING AND JOINTING

The only steep faults within the area mapped occur within the basal imbrication zone between North Tverra and Gjeitaabreen. These may be associated with either B1 or B2 deformation.

The only other steep structures which cause displacement are the N.-S. vertical shear zones within the upper Jotun nappe. The age and significance of these structures are discussed later.

### Jointing

Joints are not very common in the area mapped; much of the area consists of pelitic rocks where joints are not found. In the psammitic rocks, joints occur and these have been measured. Most joints appear to be late-stage brittle fractures, but some are synchronous with a period of folding. An example of this is the strong jointing at right angles to phacoid elongation seen at Hesthoe. These are probably B1 ac joints. There is some indication that ac joints formed at some stage of the B2 deformation in the Holleindalen anticline.

Figs. 130, 128 and 129 are equal area plots of poles to joint planes for western, eastern and southern sub-areas.

From these diagrams it can be seen that several sets of joint planes exist. It is probable that the joints measured belong to the following sets.

40 at 60 west

125 at 80 W.

150 at 80 W.

N-S at 70 W.

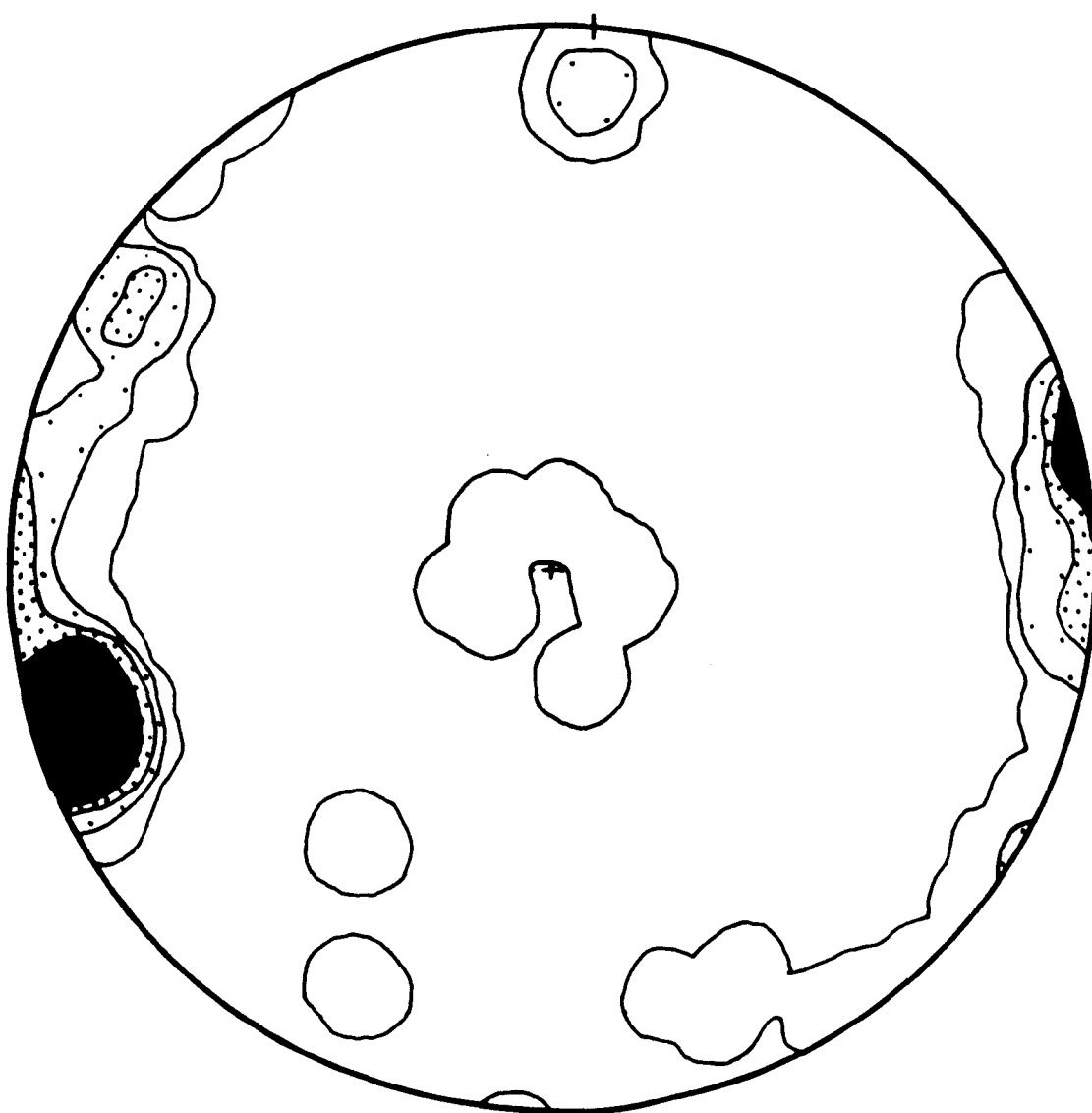
Eastern area

Several low-angle joints

**Fig 130**

**Poles to joints NW area**

**10,5,2,1%**



160	at 80 W.	}	Western area
50	at 70 W.		
E-W	at 70 N.		
low angle joints			
N-S	at vertical		Southern area
125	at 80 (E. or W.)		

This variation in orientation of joint directions may indicate a different stress orientation for the three sub-areas.

Joint mineralisation is not very common; in some cases  $150^{\circ}$  joints are infilled with clinoclre and quartz. In the upper limestone-pelite group, joints are often infilled with quartz and calcite.

## CHAPTER 5.



## THE PHACOIDAL QUARTZITES - CONGLOMERATES OR PSEUDO- CONGLOMERATES?

---

"Intersection of planes, fold axes, rotation and elongation grade into each other and may be hard to distinguish. Strongly elongated pebbles in conglomerate parallel to fold axes should be approached with mistrust. Pseudo-conglomerates look like stretched conglomerates and disrupted and rolled bedding resembles spindle-shaped elongated pebbles. One should question the elongation of pebbles parallel to fold axes if it exceeds all other evidence such as arcuation, elongation of fossils, oolites or amygdules. A pebble stretched more than its matrix or environment is unlikely and should be treated with care." (E. CLOOS 1946).

### Conglomerate deformation

The shape of a deformed pebble is a function of a number of factors as well as the strain component. The factors involved in a statistical treatment of data include:

1. Variation in original shape and orientation relative to stress axes.
2. Volume loss during deformation
3. Effect of repeated deformation
4. Varying pebble composition
5. Inadequacy of measurement.

#### 1. Original pebble shape and orientation

This is an important factor in determining final pebble shape; this problem has been discussed by Flinn (1956), Higgins (1964) and Hossack (1965).

Most undeformed conglomerates have pebbles which may depart markedly from spherical. Pettijohn (1949) states that in modern gravels "relatively homogeneous pebbles have sphericities of 0.71 to 0.75". Prior to deformation, the pebbles may have had either

Fig.131

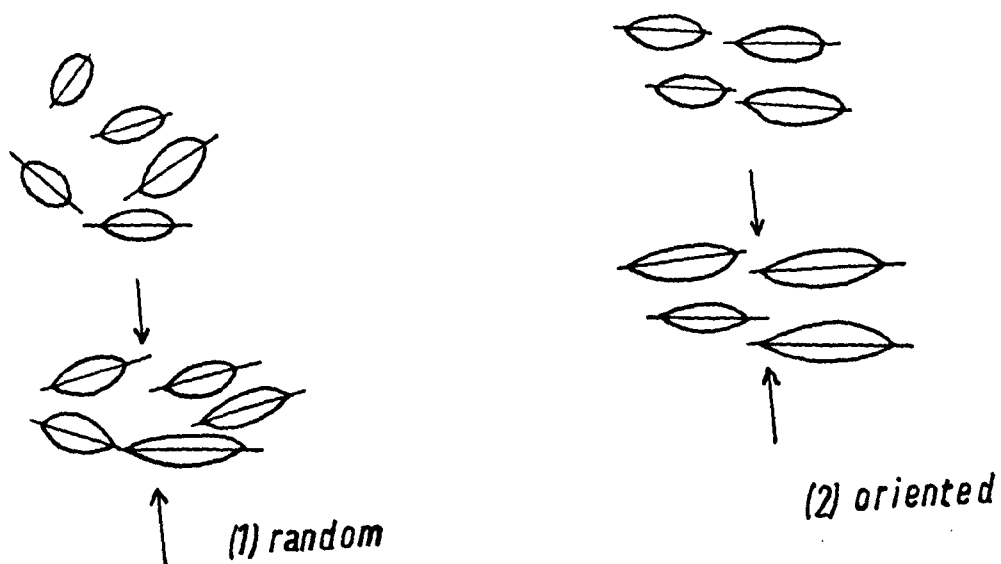
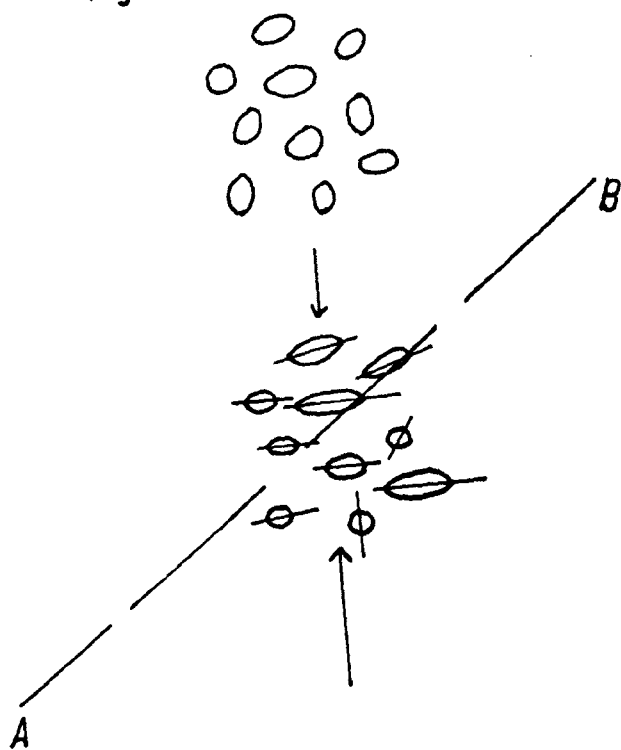


Fig.132



a random orientation or else some preferred orientation. These two cases are shown in Fig. 131. It is obvious that deformation of conglomerates 1 and 2 in Fig. 131 will produce different pebble shapes and orientations, depending on the magnitude and direction of principal stress. This factor is considered in detail later.

## 2. Volume loss during deformation

In order to calculate volume loss it is necessary to have information on undeformed pebbles. Volume loss may have an important effect on pebble shape. Calculations by Ramsay (unpublished data) suggest that volume loss may affect the shape of the final ellipsoid and place it in the flattening field, even though the deformation was not one of flattening.

## 3. Effect of repeated deformation

This is important where a deformed conglomerate has suffered several strains of the same type. The effect of superposition of strains should be apparent from structural analysis. Where a pebble has suffered more than one deformation, it is difficult to evaluate the effect of individual strains. In strain calculations, it is best to measure pebbles where the strain pattern is clear.

## 4. Varying pebble composition

Flinn (1956) and Mehnert (1939) have shown that there is a relationship between pebble composition and shape in a deformed conglomerate. Pebbles of material less competent than quartzite are much more deformed than those of quartzite. In order to compare deformation over an area it is necessary to compare pebbles of the same composition.

## 5. Inadequacy of measurement

In measurements made in the field, only small errors in measurements are involved if the pebbles can be extracted from the matrix. In measurements made on joint faces, etc., other factors such as the difficulty of locating the long axis exactly are involved.

Fig. 133

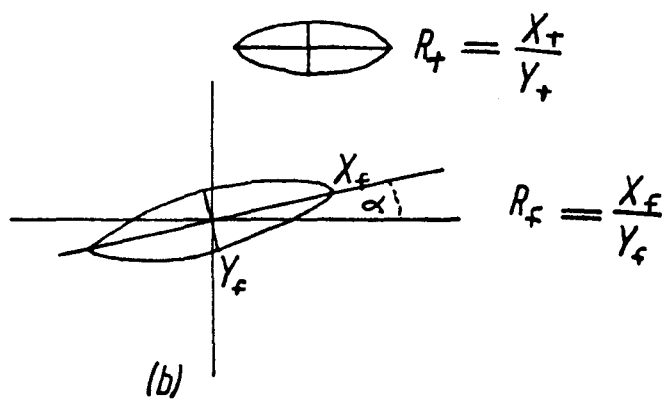
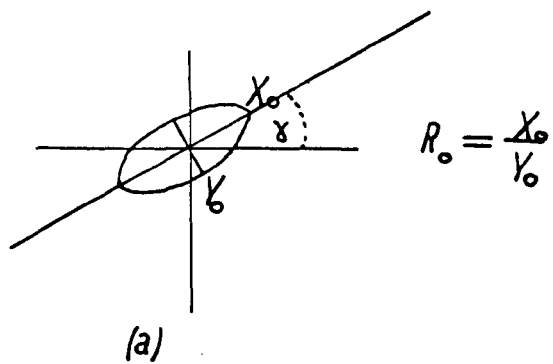
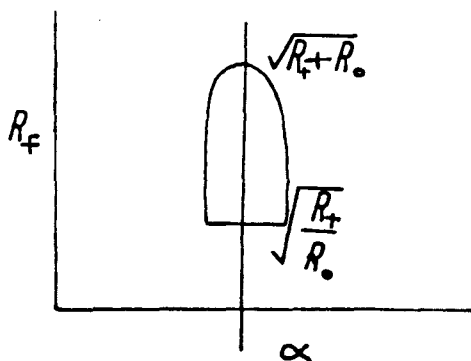


Fig. 134



In measurements made on oriented field photographs, errors due to lens distortion, slight inaccuracy of camera orientation and errors in printing due to paper distortion, etc. are involved. Most of these can be overcome or corrected for.

### Geometric Model

Most of the errors discussed above can either be minimised or calculated and the following geometric model is suggested (after J.G. Ramsay).

### Random orientation

Fig.132 shows the effect of flattening on randomly oriented pebbles. Eliminating errors due to 2, 3, 4, 5 above, the final shape is a combination of sedimentary and tectonic ellipsoids.

Fig.133 (a) shows a cross-section of a pebble prior to deformation, with axial ratio  $R_o = \frac{X_o}{Y_o}$ .

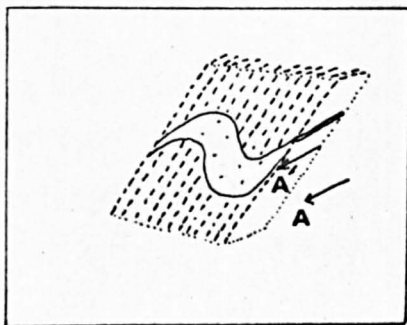
Fig.133 (b) shows the pebble after superposition of a flattening component, represented by a tectonic ellipse with axial ratio  $R_t = \frac{X_t}{Y_t}$ ;

the final ellipse has an axial ratio  $R_f = \frac{X_f}{Y_f}$ .

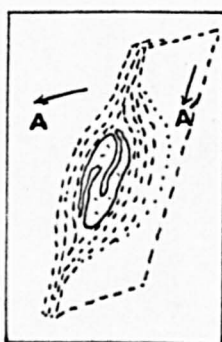
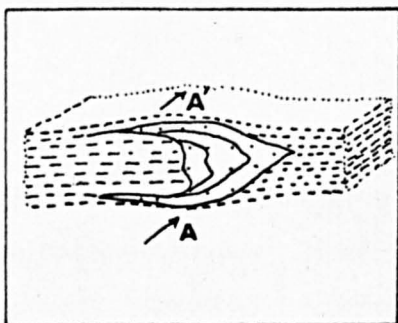
In Fig.132 (b), an arbitrary line AB is drawn and for each pebble the axial ratio and the angle between the long axis and AB is measured. The axial ratio (R) for each pebble is plotted against the angle between long axis and AB as shown in Fig.134. If sufficient data is available, the points define an area from which the functions  $\sqrt{R_t + R_o}$  and  $\sqrt{\frac{R_t}{R_o}}$  can be obtained.

$R_t$  is the axial ratio of the strain ellipsoid.

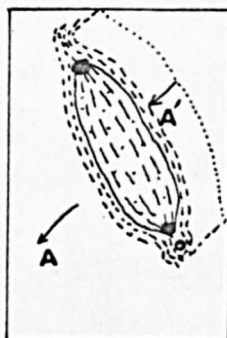
$R_o$  is the sedimentary shape factor.



*relicts of folds*





*contorted  
relict*



*boudin*

*Fig.135(after Rast 1956)*

 *schist*

 *quartzite*

*A* *fold axis*

*A'* *elongation of tectonic inclusions*

This construction can be developed for three-dimensional data (J.G. Ramsay). It is possible to determine the principal axes of the strain ellipsoid from measurements made on any three mutually perpendicular planes.

### Preferred orientation

If the pebbles had a sedimentary alignment, it is not possible to compute a sedimentary shape factor. Information on the original nature can be obtained if undeformed or slightly deformed pebbles are found. If slightly deformed pebbles are found, it may be possible in many cases to estimate minimum strain.

### Tectonic Inclusions

The striking feature of tectonic inclusions, i.e. fold closures, rods, mullions, boudins, etc., is their constant orientation parallel to fold axes.

A tectonic inclusion is defined by Rast (1956) as any isolated body formed by the tectonic disruption of any originally more or less extensive layer.

Rast discusses and illustrates several types of tectonic inclusion (see Fig.135). 1. Relict of a fold. In this type, the schistosity of the surrounding less competent medium is axial planar and the longest dimension of the relict is parallel to the fold axis. Extensive movements on the planes of schistosity and the consequent shearing out of the limbs is responsible for this type. Occasionally portions of the limbs are also preserved as separate relicts.

2. Contorted relicts around which the schistosity of the surrounding matrix is deflected. Such forms have the shape of an eye with the longest dimension roughly at right angles to the axis of contortion and extensive rotation of the contortions is seen. Occasionally some tectonic inclusions are morphologically between types 1 and 2.

3. The third type has a perfect oval or lozenge-shaped cross-section. Elongation is normally parallel to axes of local folds. When the inclusion possesses internal schistosity, such schistosity tends to follow the outline of the inclusions. These are boudins. Two varieties of boudinage exist; barrel shaped and lozenge shaped; the difference between these two types is that in lozenge-shaped varieties, rotation of individual segments (utilising joints as slip surfaces) takes place, whereas in barrel-shaped varieties, this does not occur. In some cases, boudins are oblique to fold axes.

Rast concludes that the essential difference between lozenge and barrel-shaped boudins is due to the composition of the rock units. In lozenge shaped types, the boudins are surrounded by incompetent material. In barrel-shaped types, the boudined layers are only slightly more competent than the surrounding medium. Oblique boudins are explained on geometric properties of the rigid material and its reaction to stress.

Ramsay (1956) concluded that the supposed Moinian basal conglomerate at Glen Strathfarrar, Invernessshire was tectonic in origin. He found that the "conglomeratic" structures occurred in areas of alternating competent/incompetent beds where the beds are folded. In the least disturbed rocks, the competent granulite bands are gently folded and boudinaged. Where the fold movements are more intense, the schistose matrix is drag folded and the psammitic bands are disrupted into elongated pseudo-pebbles. All stages of separation of competent bands into "pebble like" fragments are seen. These fragments are elongated parallel to the prominent linear structures (striping, lineation and minor fold axes) found in the surrounding rocks which can be shown to be parallel to the axes of major folds in the area. Even in intensely folded rocks, the original band-like nature of the original granulite pebbles in a schistose matrix can be traced.



Wilson (1953) described mullion and rodding structures from the Moinian. Mullions are formed from country rock and rodding from quartz veins. Both these structures are elongated parallel to fold axes.

1. Bedding (or fold mullions) These are formed by the parting of the rock along cylindroidal undulations or flexures of bedding. Bedding lamination is parallel with the mullion surfaces. Thin laminae within the mullions are smoothly bent into similar folds and the outer mullion surface is covered by a thin micaceous veneer, which is conformable with the core. The effect of this micaceous skin is to form a discontinuity between mullion and host rock. Fold mullions present every gradation from corrugated bedding planes through crests of drag folds or tight isoclinal folds formed from a continuous bed to the separated, pinched-off crests of small isolated folds.

#### Cleavage mullions

Cleavage mullions are long rock prisms which may be angular, sub-angular or roughly rounded in section. They owe their origin to fracture along intersecting cleavage and bedding planes. These, like other mullions, are covered with a thin micaceous veneer.

#### Irregular mullions

These are long cylindroidal masses of rock of very irregular cross-section. Irregularities vary from fine striations to grooves. The curved surfaces of these mullions may be controlled by contorted bedding, but, on the whole, there is little relationship between external form and bedding lamination.

#### Orientation and symmetry of mullions

Individual mullions show a remarkable constancy along their lengths. They are cylindroidal in form and have monoclinic symmetry with a plane of megascopic symmetry normal to the

direction of plunge; the lengths of the mullions are parallel to the B structural axis.

Cross jointing, often normal to the elongation is well developed.

### Quartz-rodding

There is every gradation between plane or flatly lenticular quartz-veinlets and cylindroidal quartz-rods; both are products of quartz segregation. The clean-cut, undisturbed veins formed at the end of the period of movement; those formed during movements are distorted, folded or rolled to varying degrees and are now seen as rods.

Segregations formed during folding tended to become concentrated in the reduced pressure zones of fold apices. As folding continued, the segregations were rolled by the movement and the quartz masses became detached and became more linear. Composition of the country rocks has controlled the formation of quartz rods; they are best formed in semi-pelitic rocks.

The rods are monoclinic linear structures, elongated normal to the plane of symmetry; parallel to fold axes.

Flinn (1961) discussed the theory of folding during progressive deformation. He suggested that two boudinage directions at right angles should form parallel to the principal directions of strain in the layers. This would explain boudinage both parallel and oblique to fold axes described by Rast (1956).

Paterson (unpublished data) has produced folding and boudinage experimentally in the same specimen. Folding occurred on one side of the specimen and boudinage on the other. The plane of no strain must have been located between them.

Hence it can be seen that tectonic inclusions vary in form and mechanism. However, in most cases these structures form

Fig. 13 6

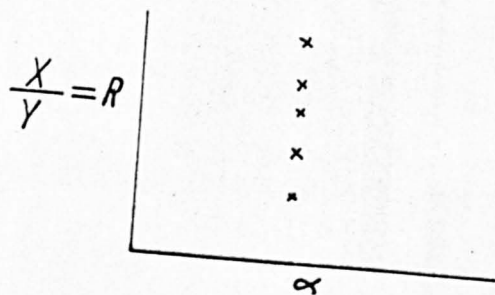


Fig. 137

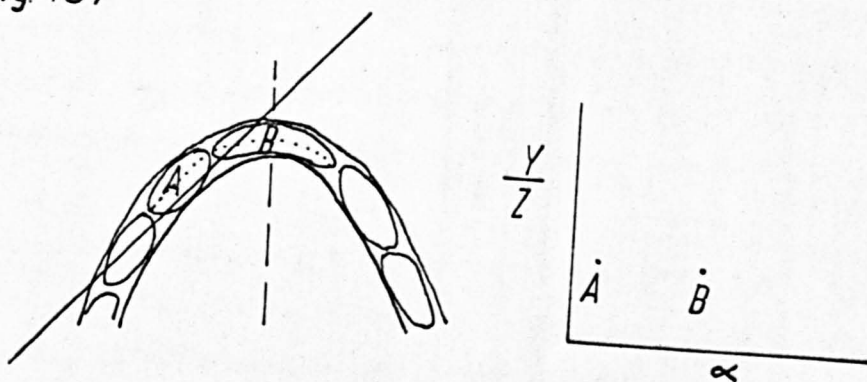
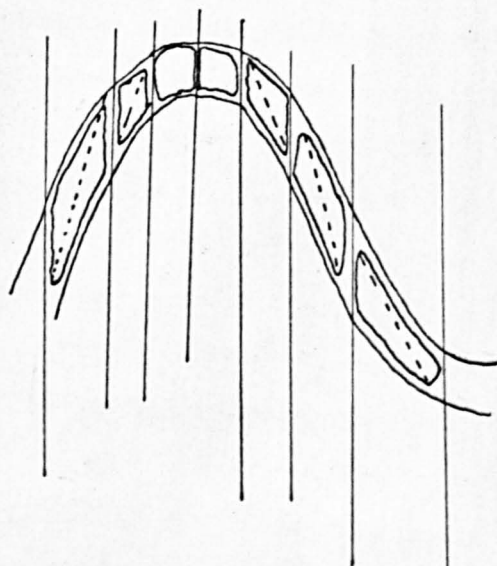


Fig. 13 8



during folding and are parallel to fold axes.

Theoretically a plot of  $\frac{X}{Y}$  for pseudo pebbles should show a constant orientation with varying axial ratio (see Fig.136 ). Note that  $X$  = long axis.

A plot of  $\frac{Y}{Z}$  for pseudo pebbles is less certain. For fold hinge type structures, these should be irregular, but should depend on some fixed relationship to folding. Boudinage would be expected to vary with respect to the hinge of the fold (see Fig.137 ).

$\frac{Y}{Z}$  for mullions would vary depending on the type of structure. Fold mullions would be dependent on the orientation relative to folds. Cleavage mullions would vary according to distance from fold hinges, similar to boudins (see Fig.138 ). Irregular mullions would be variable in ratio and orientation.

On the evidence available, it seems probable that tectonic inclusions resembling conglomerates can be recognised on a combination of variation in shape and orientation of pebbles, relationship to minor structures and overall symmetry of the deformation.

### Present Work

In the present study, three occurrences of phacoidal quartzite in the Høyden area were examined. Two of the occurrences lie near the margins of the mapped area; the third example is a few miles to the west, in the area mapped by R. B. Elliott.

The detailed occurrences of these rocks are compared and contrasted; phacoid shapes and orientations are described and their most likely modes of origin and subsequent deformations are discussed. Petrofabric data is not available at the present time.

The outcrops of the three phacoidal quartzites are:

1. North-west of Høyden



Fig.139. Phacoidal quartzite, Hoyoyen

Fig.140



Fig.141



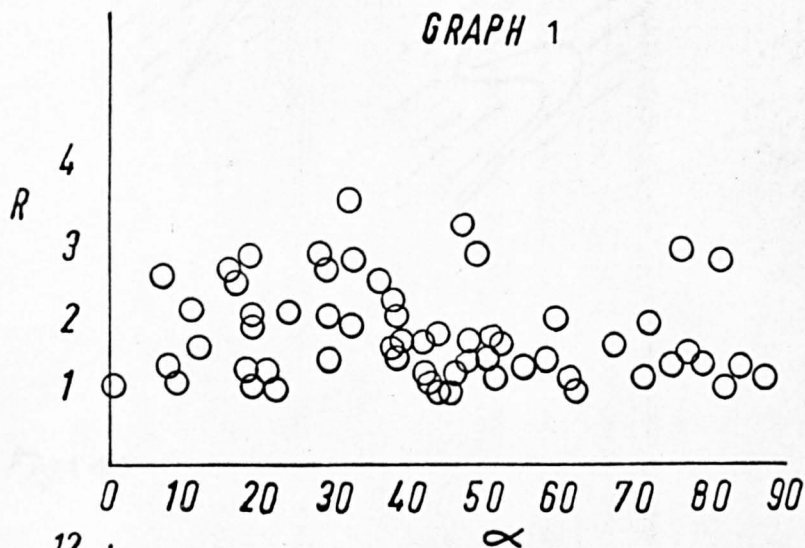
Fig.142



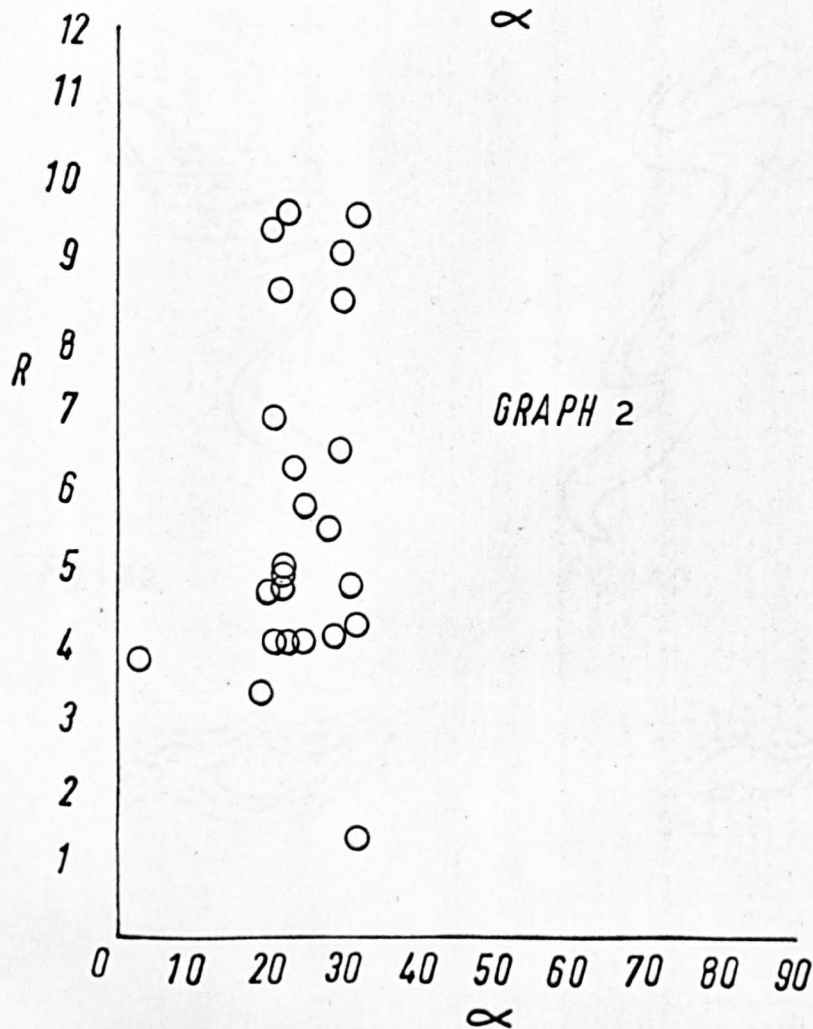
Fig.143



GRAPH 1



GRAPH 2



2. On Hesthoe
3. The east end of Høydalsvatn and north-west of Gjeithoe.

1. North-west Høyøyen

The phacoidal quartzites are found at the base of the sparagmite group, not far above the basal thrust plane. Elongate white quartzite (or quartz) phacoids occur in a blue chloritic quartzite or quartz-mica schist (see Fig.139).

The phacoids consist entirely of white quartz; the matrix is semi-pelitic and consists of quartz, muscovite, chlorite, biotite and magnetite. A well defined foliation is present in the matrix; this foliation is partly axial planar to relict folds within the phacoids and partly deflected around the phacoids.

Relict fold closures are abundant and contorted relicts are found (see Fig.140).

The elongation of the phacoids is parallel to the small-scale folds, and in many cases, the phacoids can be seen to be continuous bands (see Figs. 139 and Fig.141).

Graphs 1 and 2 show the type of data obtained on axial ratios and orientations of the phacoids. It can be seen that the long axes have a strong preferred orientation parallel to fold axes. (Graph 2) These fold axes trend  $110^{\circ}$  and structural analysis has shown that they are B1 folds. Graph 1 for measurements at right angles to long axes of the phacoids shows considerable variation, but this variation is dependant on fold axes (B1)

From the field evidence, it can be stated that the phacoids formed during folding by a combination of:

- (a) Thickening in fold hinges
- (b) Shearing of the limbs
- (c) Rotation of the phacoids.





Fig.144. Phacoidal quartzite, Hesthoe. The photograph is parallel to the long axes of the phacoids. Note strong preferred orientation of long axes.

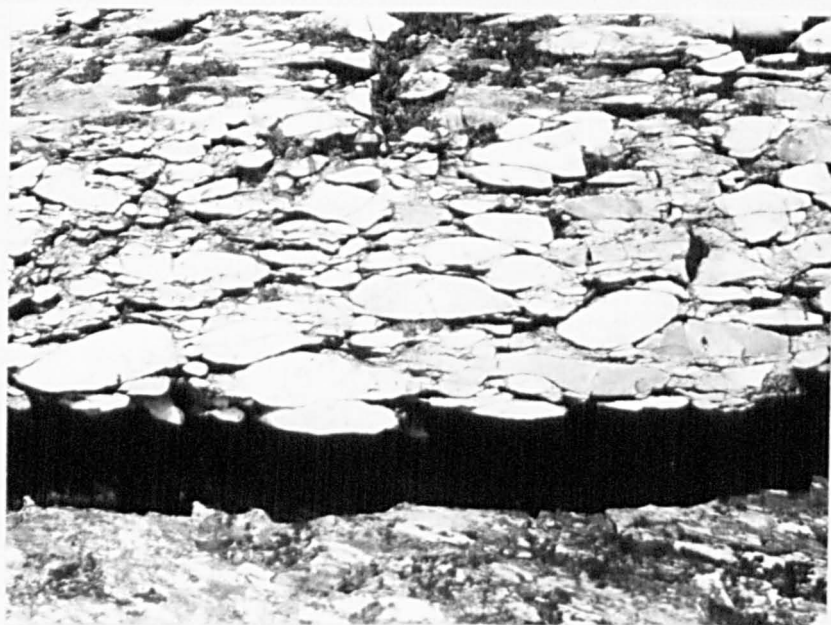


Fig.145. Hesthoe phacoidal quartzite; at right angles to long axes.



Fig.146. Phacoidal quartzite, Hesthoe.

Note thickening in fold hinges.

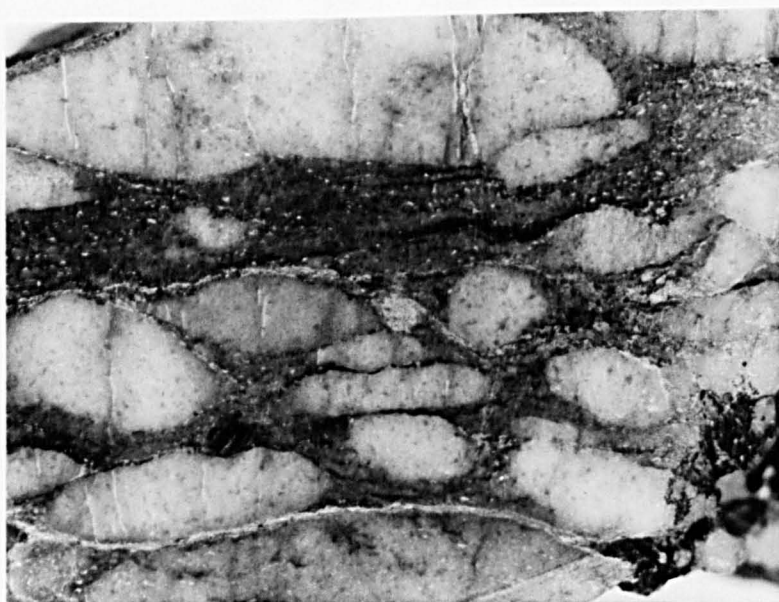


Fig.147. Phacoidal quartzite, Hesthoe.

At right angles to elongation. Note the small folds and the cracks in the phacoids.

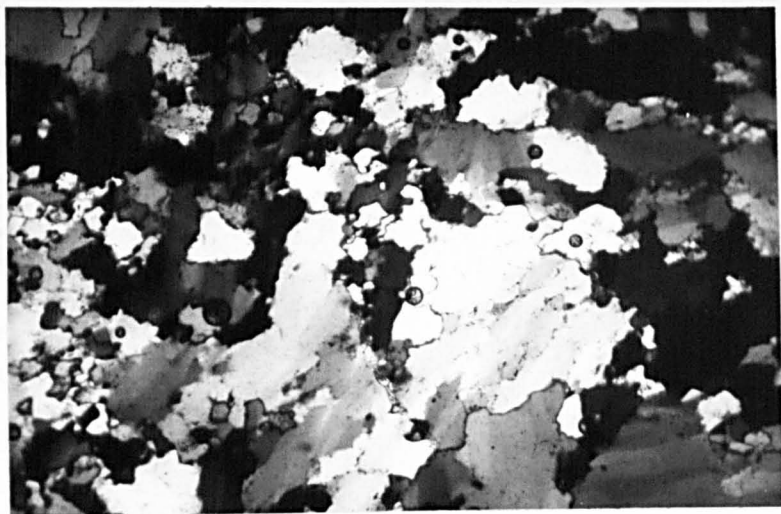


Fig.148. Photomicrograph of Hesthoe phacoidal quartzite.

Evidence of rotation of the phacoids can be seen in several cases, but elsewhere the mechanism can be inferred. The phacoids probably represent quartz veins which segregated during folding and metamorphism.

## 2. Hesthoe

These phacoidal quartzites are found in the lower part of the sparagmite group, in the north of the area mapped. The outcrop is about 100 metres thick and extends about 800 metres. Elongate white quartzite (or quartz) phacoids occur within a schistose matrix (see Fig.147).

The phacoids consist of pure white quartzite (or quartz) and the matrix is semi-pelitic, consisting of quartz-muscovite-biotite. The matrix possesses a well defined foliation; this foliation is mainly deflected around the phacoids and is affected by small folds (see Fig.142).

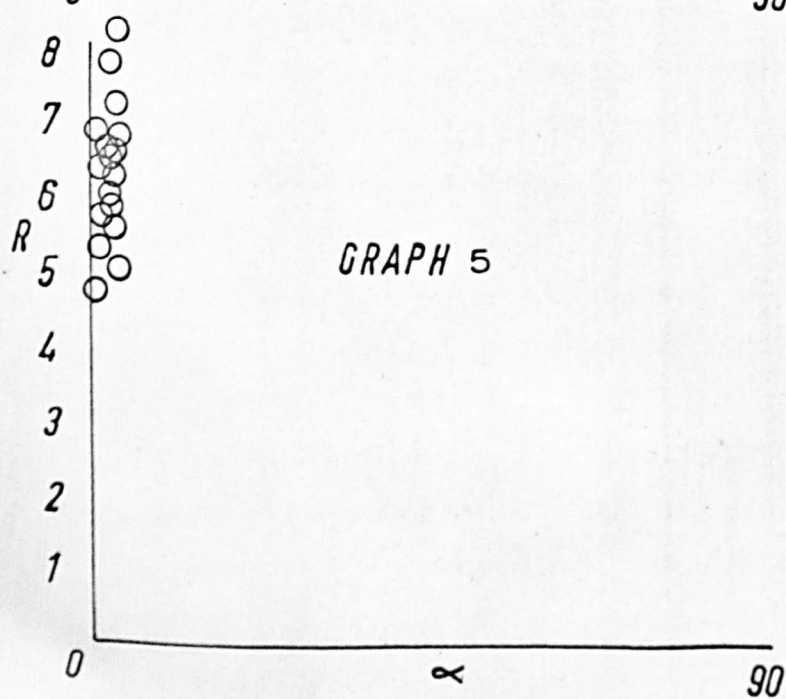
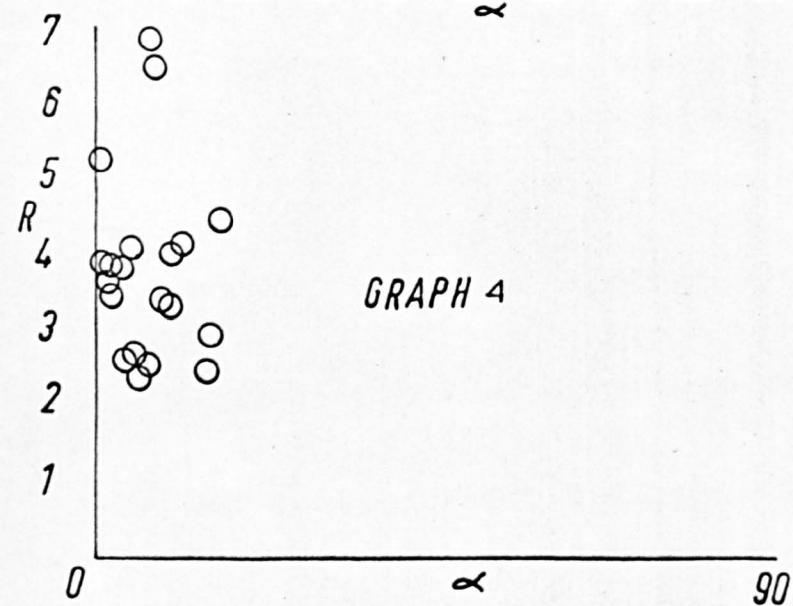
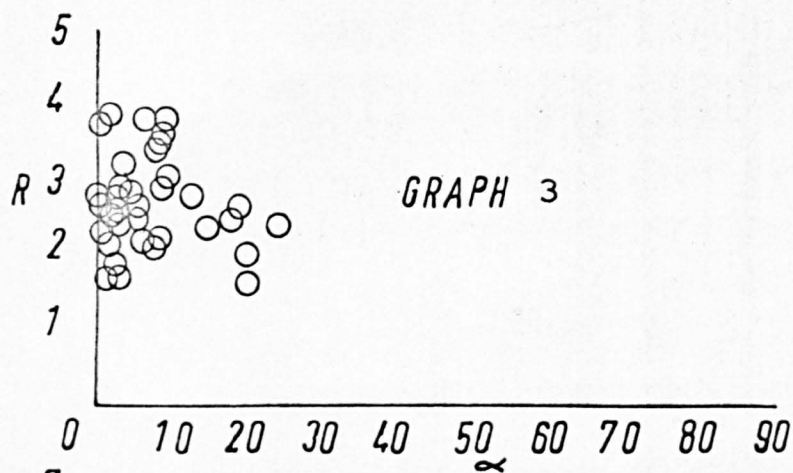
In cross-section, the larger phacoids are lozenge-shaped and possess well marked cracks parallel to the XZ plane (see Fig.147 ). The smaller phacoids are rather contorted and irregular; they are probably partly contorted relict fold closures (see Fig.143 ).

The long axes of the phacoids have a strong preferred orientation; a fine linear structure parallel to this direction is present in both phacoids and matrix.

Critical evidence on the origin of these phacoids can be seen in a few localities where folds are still preserved. Here the formation of the phacoids during folding, by thickening of material in fold hinges and thinning on limbs can be appreciated (see Fig.146 ). In this outcrop (Fig.146) the proportion of pelitic material is high. A strong lineation parallel to fold axes is produced. In many cases the phacoids occur as continuous layers, but where folding is intense, isolated bodies occur.

The type of tectonic inclusion seems to be localised in

HESTHØE



areas where thin quartzite (or quartz) layers occur interbedded among pelitic horizons. Where the quartzite layers are thicker or the proportion of pelitic material less, deformation seems to have proceeded by a type of boudinage structure.

In most cases a strong jointing is observed at right angles to the elongation direction.

The direction of elongation of the phacoids is parallel to fold axes which have been shown to be B1 structures by structural analysis.

Figs.144 and 145 show the form of these phacoids. Data on axial ratios and orientations of the phacoids is shown in graphs 3,4 and 5. Graphs for orientation parallel to the long axes show that the orientation of the long axes is constant, but that axial ratios vary. Graphs at right angles to elongation show that where no fold axes are seen, the orientations of the intermediate and short axes are constant; where B1 folds occur, orientation is variable depending on the folding.

The cracks in the pebbles are late-stage brittle fractures.

The origin of these structures is discussed later, but a tentative interpretation is that they are tectonic inclusions formed by a combination of:

- (a) Boudinage in competent bands
- (b) Thickening of layers in fold hinges, combined with rolling and shearing in rocks where thin competent layers are interbedded with incompetent material.

#### Hoydalsvatn

Two isolated bodies of phacoidal quartzite occur at the base of the upper limestone-pelite group. The lower one has a maximum outcrop at the outflow of Hoydalsvatn and outcrops for 3.5

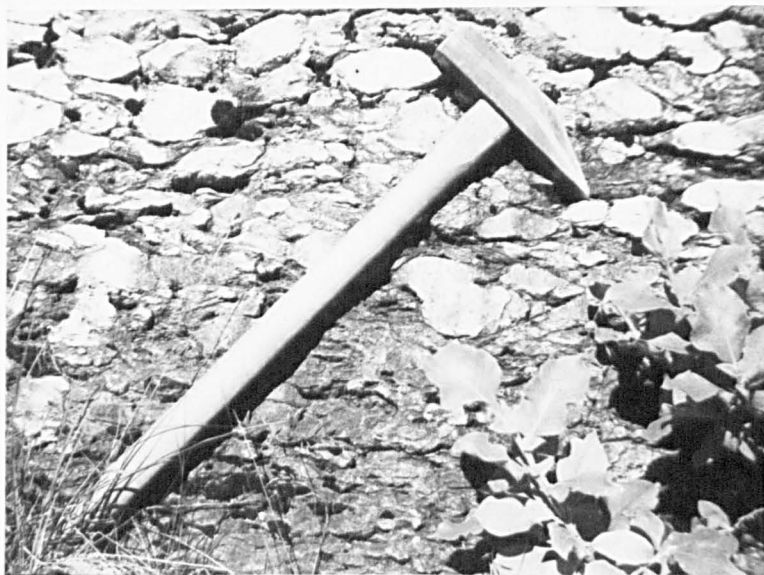


Fig.149. Phacoidal quartzite, Hoydalsvatn; at right angles to long axes.



Fig.150. B2 and B3 folds refolding quartzite phacoids, Hoydalsvatn.



km along the south shore of Hoydalsvatn. To the west, it thins out over 4 km and dies out.

The higher horizon is lensoid in shape and outcrops north-west of Gjeithoe.

These two outcrops are similar in composition and structure. Unfortunately the Gjeithoe outcrop is extensively affected by B2 and B3 folding, so that "pebble" measurement was not attempted.

The Hoydalsvatn outcrop was studied in detail and measurements of dimensions and orientations of quartzite phacoids made where B2 and B3 folds were absent. Within this outcrop, the phacoids exhibit a large number of shapes; large flattened cakes, triaxial rods and lensoid blocks occur. In addition boudinaged limestone blocks are found.

Within the outcrop of the phacoidal quartzite, limestone, quartzite and quartz-mica schist horizons are found.

The phacoids are dominantly white or yellow quartzites, but feldspar-rich (usually microcline) phacoids have recently been found. The matrix is rather variable from pelitic to semi-pelitic.

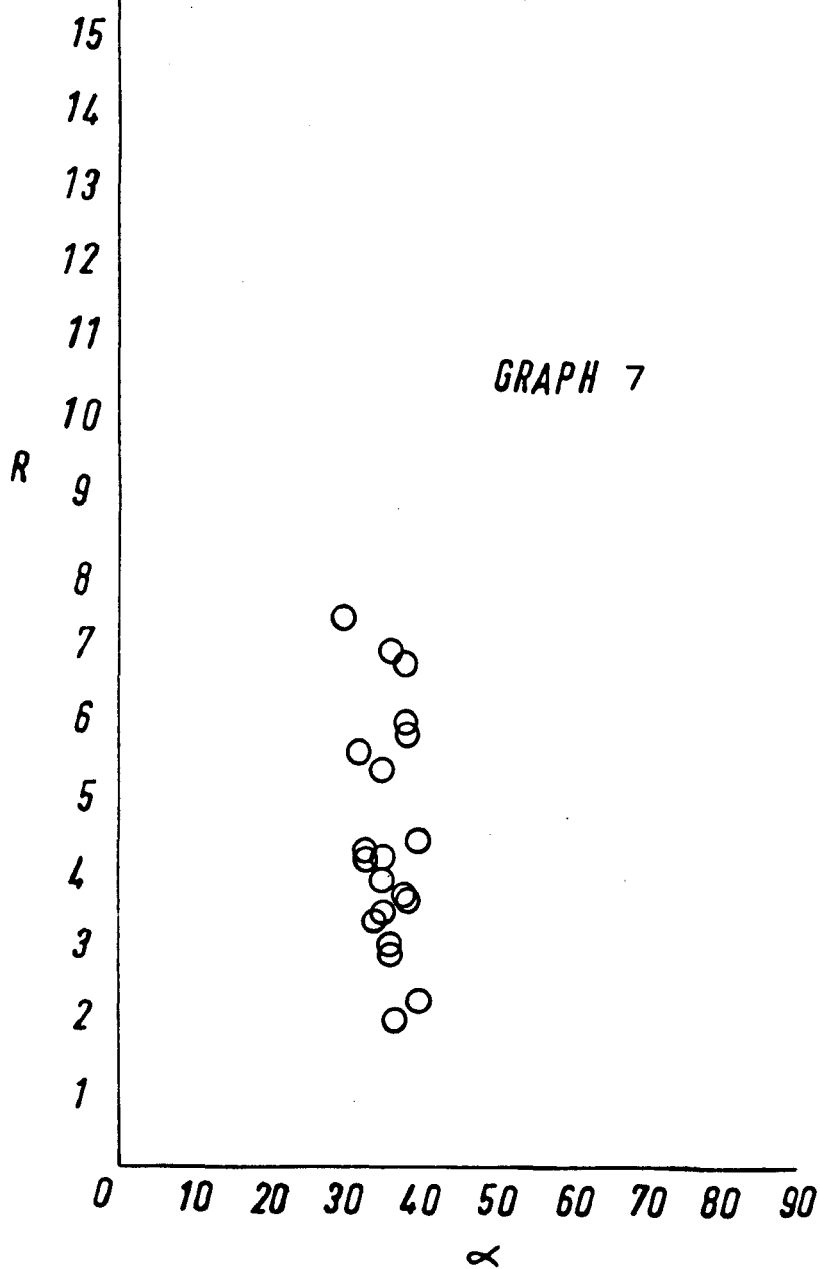
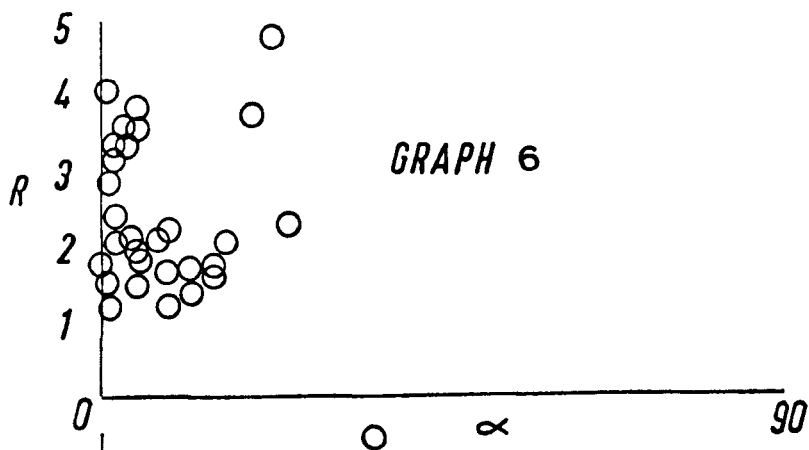
Long axes of the phacoids have a strong preferred orientation within a single outcrop. On a larger scale, these are affected by later folding, but a general trend of around  $140^{\circ}$  is apparent. This is parallel to L1 structures in adjacent pelitic rocks and the phacoids are visibly folded by B2 folds. The phacoids are probably elongated parallel to B1 fold axes, but unfortunately no B1 fold axes have been found within the outcrop.

Considerable variation in shape and size of the phacoids is obvious. Many of the larger blocks are lensoid in shape (see Fig.149 ).

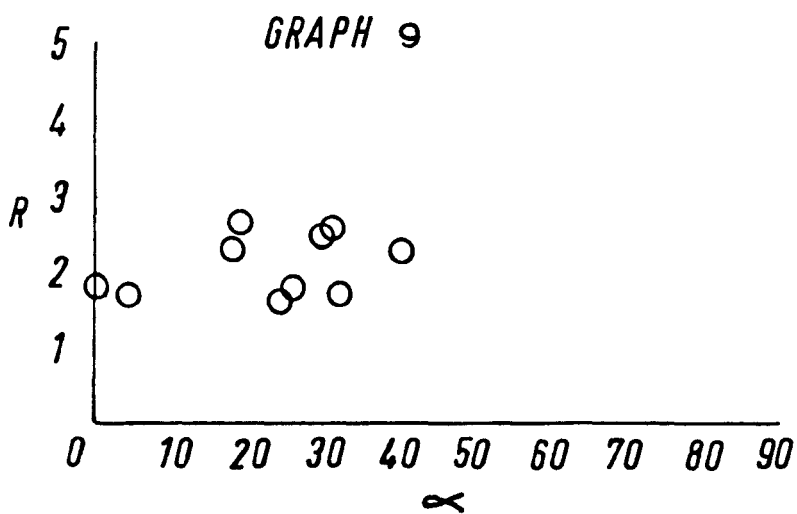
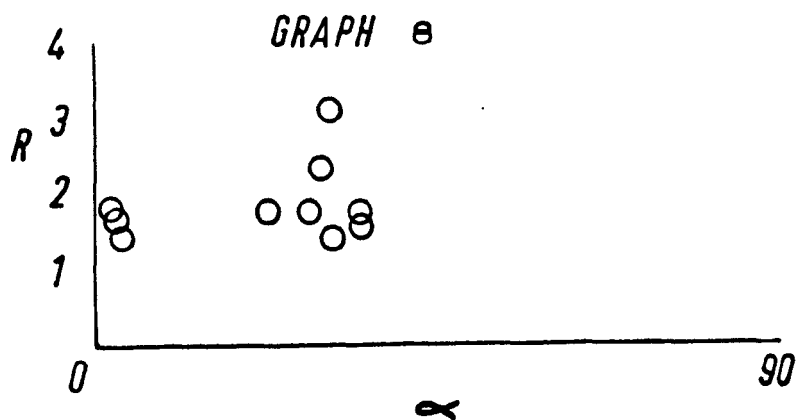
In some cases, boudinage of quartzite layers surrounded by pelitic material can be seen, but elsewhere the rock consists of



HÖYDALSVATN



# HÖYDALSVATN



aggregates of these lensoid phacoids, often separated by pelitic material, but sometimes in contact.

Near Hoydalsvatn outflow, boudinage and breaking up of a limestone band is seen.

The smaller phacoids are irregular in shape; rocks with equi-dimensional cross-sections are found in the same hand specimen as flattened cakes. A few small contorted relicts have been found. In the old stream channel, at Hoydalsvatn outflow, exposure of the phacoidal quartzite is very good and cross-sections are abundant; most of the phacoids are lensoid in cross section.

Graphs 6 and 7 show the data obtained on dimensions and orientations of the phacoids. It can be seen that the long axes of the phacoids are rather constant in orientation, but some variation in intermediate and short axes is apparent. Axial ratios are rather variable and there is no correlation between orientation and amount of elongation of long axes.

South of the bridge at Hoydalsvatn outflow, a sparagmitic conglomerate outcrops. Pebbles of both quartz and K feldspar occur and the pebbles are small in size, ranging up to 2 cm. The pebbles are lensoid in shape and slightly flattened; some pebbles are smooth lensoid shapes, while others have sharp, irregular outlines. They show only moderate percentage elongation; much less than the larger phacoidal quartzites. The matrix is sparagmitic in composition.

Graphs 8 and 9 show variations in dimensions and orientations for these pebbles. There is some variation in orientation of all three axes and axial ratios are fairly constant. This seems to be a true sedimentary conglomerate which is only slightly deformed.

The origin of the main phacoidal quartzite is not certain. The data obtained is not conclusive of a tectonic origin for the entire outcrop. It is obviously tectonic in part, but some of the phacoids may represent deformed pebbles, while others are certainly boudinaged,



Fig.151. Quartzite phacoids refolded by B2 folds, Hoydalsvatn. Note cleavage in schist bands.

rolled or sheared quartzites. All that can be said is that elongation of the phacoids is almost certainly parallel to B1 fold axes and some of the phacoids are formed by some combination of boudinage, rolling, shearing and flattening.

Folding of the phacoids by B2 folds and in some cases B3 folds can be seen (see Fig.150 and Fig.151 ). Gently plunging, rather open B2 folds with steep axial planes contort the phacoids. The fold axes are oblique to the elongation of the phacoids; in the micaceous bands, a strain slip cleavage S2 is developed. B3 folds are seen in some localities (see Fig.151). They produce tight folds of the phacoids.

### Conclusions

#### 1. Outcrop N. W. of Høyøyen

It is concluded that the phacoidal quartzites have a tectonic origin. They are most likely formed from quartz veins which segregated during folding and metamorphism. They are elongated parallel to B1 fold axes and have formed by thickening of the quartz in fold hinges, combined with shearing and rolling.

#### 2. Hesthoe

The phacoidal quartzites at Hesthoe are considered to have a tectonic origin. They are formed by a combination of boudinage in fairly thick competent bands with thickening in fold hinges, rolling and shearing in thin competent bands interbedded with incompetent material. They are parallel to B1 fold axes. They were probably mainly quartzite layers, but some phacoids may represent quartz veins.

#### 3. Hoydalsvatn

Here a true sedimentary conglomerate with an outcrop of a few yards is found; it is only slightly deformed.

The origin of the main phacoidal quartzite is problematical. In part it represents boudinaged, rolled quartzite bands but it may be

composed in part of deformed pebbles. The pattern is complex and no firm conclusions can be drawn except that these structures are B-tectonites (Sander 1912).

It is likely on theoretical grounds that the distinction between pseudo-conglomerate B-tectonites and sedimentary conglomerate B-tectonites would be difficult in detail. In the present area, it seems likely that the two occur together.

The conglomerate/pseudo-conglomerate problem is at present unresolved. "Pebbles" oriented parallel to fold axes should be examined with care. A large number of variables are involved. In some cases it is possible to distinguish pseudo-conglomerates from sedimentary conglomerates, but in some cases, this is not possible.

In true conglomerates, before any strain calculations can be made, a sedimentary shape factor must be calculated. If the pebbles had a sedimentary preferred orientation, only a minimum value for the strain can be estimated.

## CHAPTER 6.

## QUANTITATIVE STUDY OF FOLD STYLES

---

### Introduction

In this chapter, it is proposed to describe the styles of successive phases of folding and discuss them in kinematic terms.

The geometry of ideal similar folds is such that the thickness of individual beds, measured along a line parallel to the axial plane is constant, whereas the thickness measured at right angles to the bedding (or compositional banding) is variable. For parallel or concentric folding, the thickness measured at right angles to the bedding surface will be constant, whereas thickness measured along a line parallel to the axial plane will be variable.

De Sitter (1958) calculated that crustal shortening by flexure folding (other than flexural concertina folding) can never exceed 36% of the original length of the beds and suggested that further shortening could be achieved by "flattening" the previously formed flexure fold.

Ramsay (1962 a) examined natural folds and found that many natural flexural folds have been modified by flattening and show a thickening in the hinge region. However, Ramsay found that thickening of beds in the hinge of folds often occurs early in the deformation and long before the limbs became parallel to the axial plane.

"Flattening" is defined by Ramsay as the process of deformation by which an original rock shape is plastically changed by compression. This compression results in contraction in a direction parallel to that of the principal compressive stress and an expansion at right angles to this in the direction of minimum stress. This is a homogeneous pure plane strain.

Ramsay found that folds of ideal similar shape are



uncommon, but folds of a "general similar shape" are common and suggests that these folds are formed by a mechanism of differential flattening. According to Ramsay, folds of general similar type can be distinguished from modified flexure folds primarily on the basis of measurements parallel to the axial planes. In modified flexural folds, the flattening is uniform.

#### Nettoseter area

##### B1 folds

It has not been possible to find B1 minor folds suitable for measurement, but a few observations can be made concerning the B1 folds seen in the field.

Since B1 folds are isoclinal, it would have been of little use to measure thickness parallel to the axial planes of these folds. Considerable increases in thickness of compositional banding usually occurs towards the hinge and hence the folds can not be pure flexure folds. However, folds which are truly isoclinal would be the end point of a flattening mechanism. Folds which are truly isoclinal cannot have originated solely by a mechanism of axial plane shear, since in the limiting case of shear folding, the limbs could only become sub-isoclinal.

Many B1 folds are isoclinal similar folds with sub-parallel limbs. These could have originated by several mechanisms or by a combination of mechanisms.

##### B2 folds

Major and minor B2 folds in the area mapped show great variation in style from isoclinal to fairly open structures. No major folds were suitable for quantitative study but several minor folds have been measured. Most folds appear to show a combination of similar and concentric styles. The results of measurement on three B2 minor folds are given below.

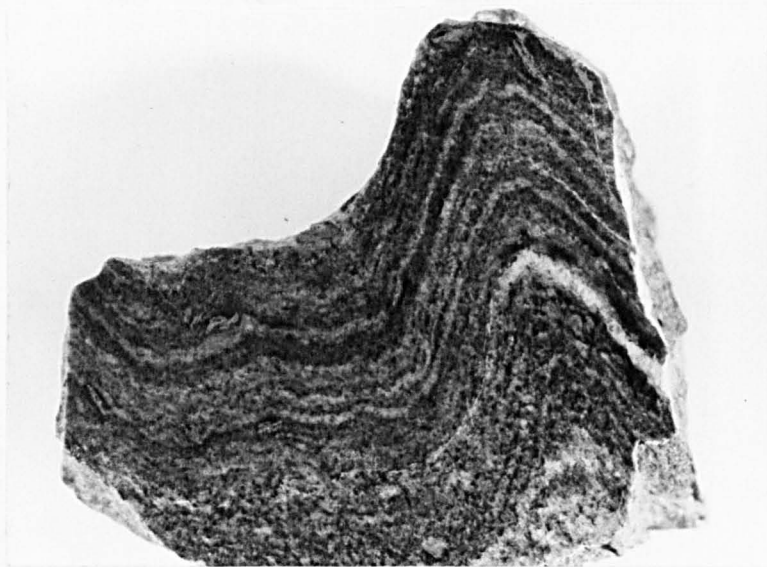


Fig.152. B2 fold in micaceous quartzite.

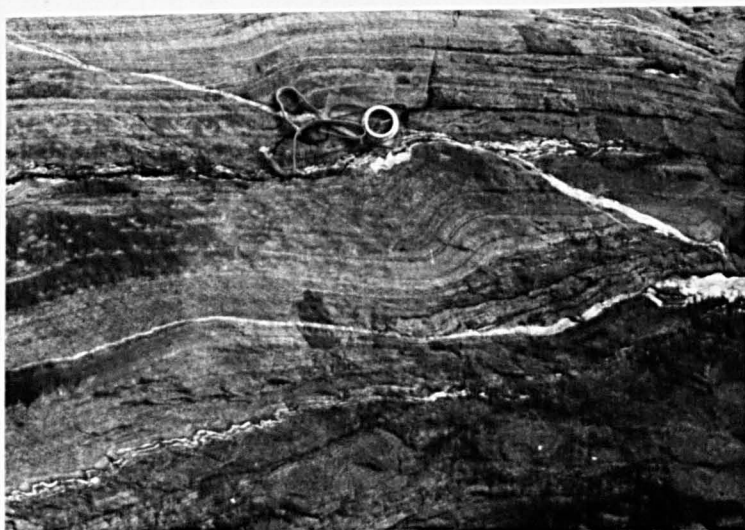


Fig.153. B4 fold in quartzite.

The first example is from a micaceous quartzite and Fig.152 is a photograph of the fold profile. In thin section it is seen that most of the micas are parallel to the compositional banding but some are parallel to the axial plane of the B2 fold. Garnet has overgrown the fabric post-tectonically.

In Fig.154 bands 1 and 2 are two quartzite bands; band 1 is more micaceous than band 2.

Both bands 1 and 2 for measurements at right angles to the compositional banding, show thickening at the hinges and hence the fold has not deformed entirely by flexure.

Measurements parallel to the axial plane are difficult to interpret. Band 2 shows minima at the hinges and maxima on the limbs, suggesting a flexural fold. Band 1 shows a low value around the synformal hinge and a large maximum value at the antiformal hinge, indicating that the band has deformed by shear or flow parallel to the axial plane.

Hence this fold is difficult to classify, since band 1 indicates that the fold is a similar fold and band 2 that it is a modified flexure fold.

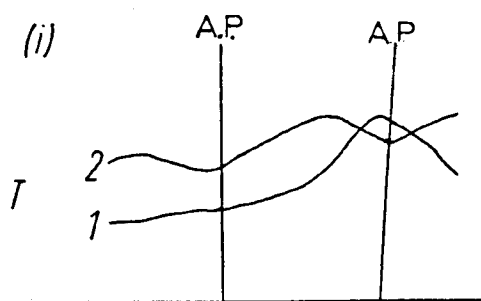
Band 2 gave amounts of flattening varying from 30 to 60%, suggesting that differential flattening has occurred. This suggests that the fold might be a flexure fold modified by differential flattening.

Band 1 gave extremely variable values which would not fit with any flexural slip mechanism.

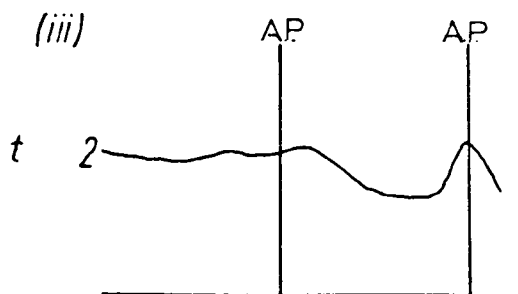
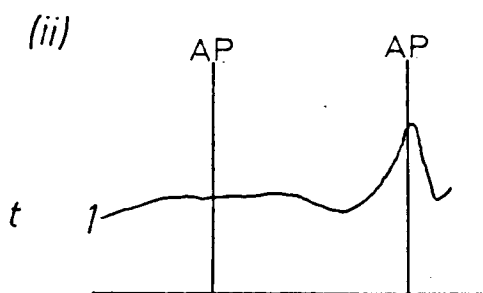
It seems probable that the two bands differ in the amount of flattening and that modified flexural folds may be flattened sufficiently to produce a fold of similar type. It is likely that folding began by flexural-slip along the banding and that band 2 was more competent during deformation.

Fig.154

B2 FOLD



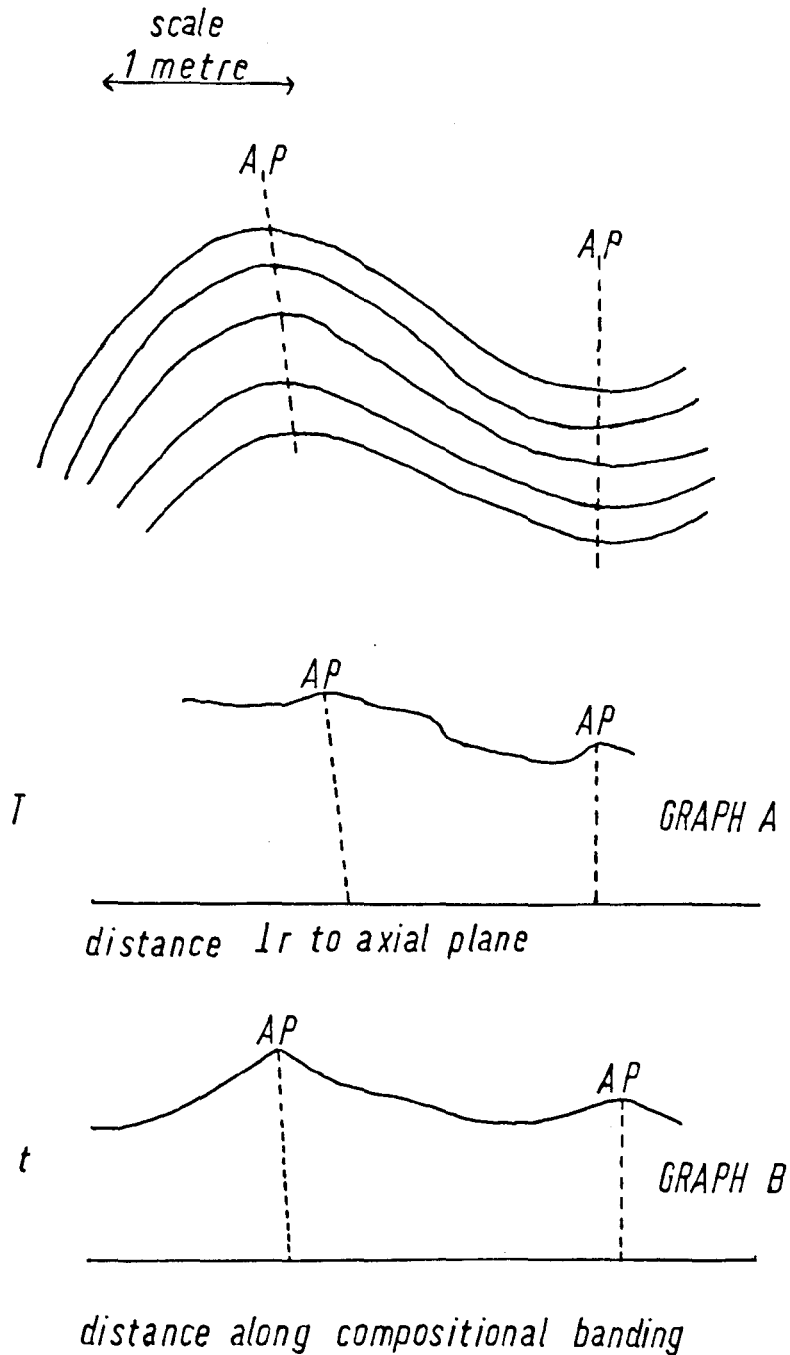
$T$  = Thickness parallel to axial plane.



$t$  = Thickness normal to compositional banding.

B2 FOLD IN MICACEOUS QUARTZITE FROM GJEITAA

Fig.155



*t* - thickness normal to bedding plane.

*T* - thickness parallel to axial plane.

In conclusion the fold is probably a fold of "general similar type" produced by differential flattening of a modified flexure fold.

The second example is a large mesoscopic structure in micaceous quartzite which was measured in the field. In thin section, most of the micas are parallel to the compositional banding of the rock, but some are parallel to the axial plane of the fold.

In Fig.155 , graph A for measurements parallel to the axial plane shows a fairly uniform line, with maxima at the hinge areas indicating that the fold has formed by shear or flow parallel to the axial plane. Graph B for measurements at right angles to compositional banding shows maximum values at the hinges and minimum values on the limbs, consistent with similar folding.

This is the nearest example to a true similar fold of B2 age measured in the area.

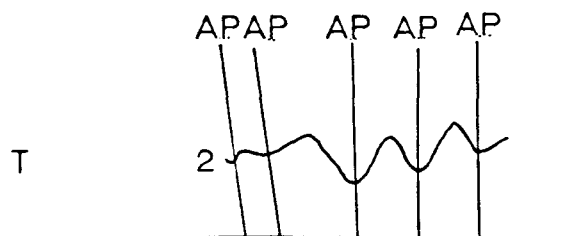
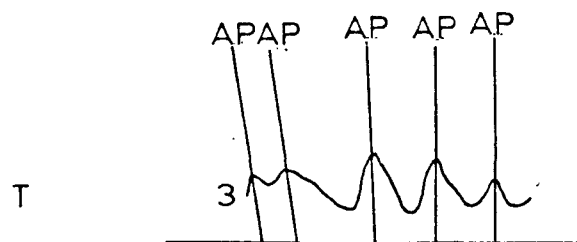
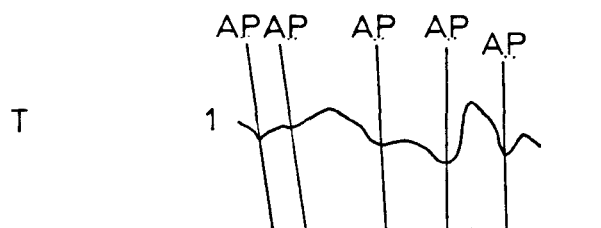
The last example is a B2 minor fold from a semi-pelitic schist with bands of quartzo-feldspathic material. Fig. is a drawing of the folds made from a profile photograph. Two quartz-feldspathic bands and the pelitic band between them have been measured. The folds have non-parallel axial planes and are quite persistent. In Fig.156 and Fig.157 , 1 and 2 are quartzo-feldspathic bands and 3 is the pelitic band.

Graphs 1 and 2 for thickness parallel to the axial plane (Fig.156 ) show considerable variation with minimum values at the hinges and maximum values on the limbs, indicating flexural folding.

Graphs 1 and 2 for measurements at right angles to the compositional banding again shows considerable variation with minimum values on the limbs and maximum values at the hinges,

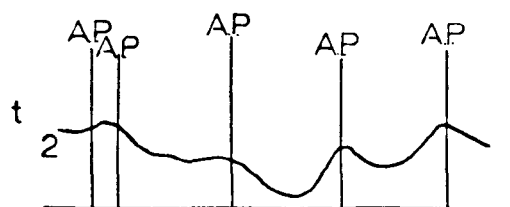
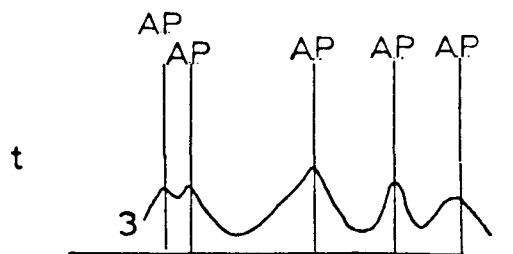
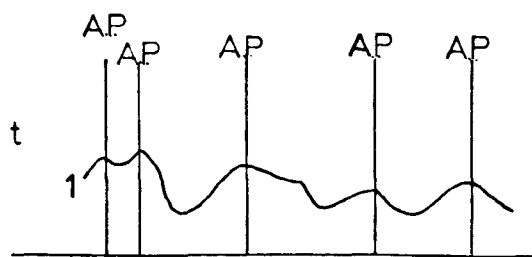
*Fig B2 Fold*

156



$T$  = *Thickness parallel to axial plane.*

*Fig. B2 Fold*  
157



$t$  = thickness normal to compositional banding.



suggesting considerable modification due to flattening.

Graph 3 for the pelitic band measured parallel to the axial planes shows extreme variation with maximum values at the hinges and minimum values on the limbs. This indicates a fold of "general similar type" and shows that although flow has occurred, it was not uniform. Graph 3 for measurements at right angles to compositional banding (Fig.157) shows great variation with maxima at the hinges and minima on the limbs suggesting a fold of similar type.

This fold is obviously composite; bands 1 and 2 indicate that the fold is a modified flexure fold and band 3 suggests a fold of similar type.

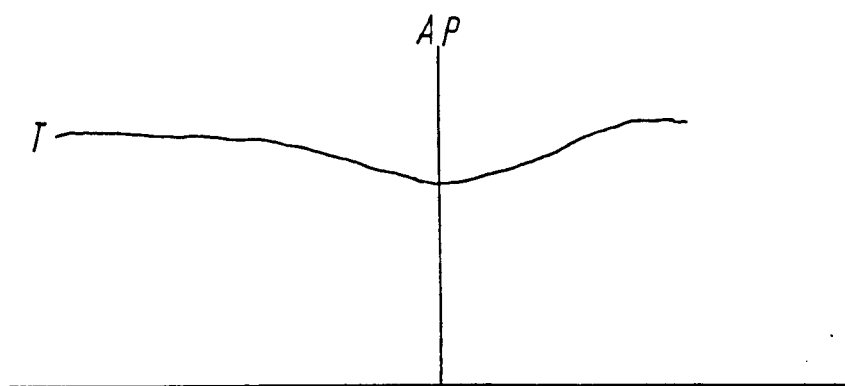
The evidence suggests that the quartzo-feldspathic bands have deformed by a modified flexural mechanism and that the less competent pelitic band has thickened at the hinges in order to accommodate the more flexural folding of the competent bands. Passive flow in the pelitic bands, combined with a small amount of flow in the competent bands allows the fold to persist in the direction of the axial plane. With increasing flow in the competent bands, these folds would closely resemble similar folds and it seems probable that folds of near similar type could be generated by a combination of flexure and flow.

The measurements of B2 folds are from psammitic rocks. In dominantly pelitic rocks, a strong axial plane cleavage S2 is prominent; often a strain-slip cleavage and the earlier foliation may be transposed. These folds are of similar-type, but their generation may well be dependent upon active folding in adjacent, less homogeneous rocks.

Several problems remain; there is a variation in geometry of B2 folds across the area and structural analysis indicates

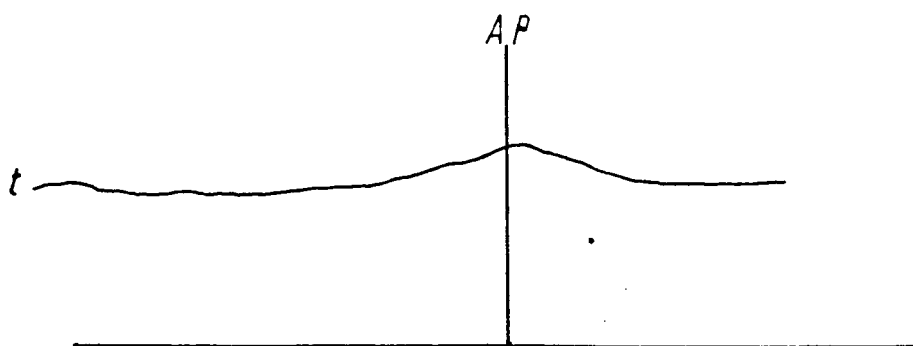
Fig.158

B3 FOLD IN MICACEOUS QUARTZITE



*T = Thickness parallel to axial plane.*

GRAPH A



*t = Thickness normal to compositional banding.*

GRAPH B

**Fig. 159**

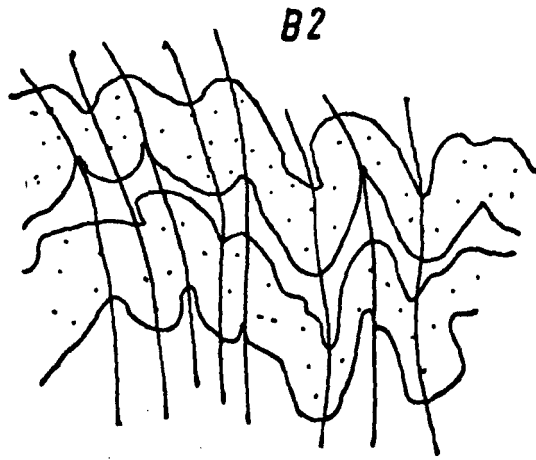
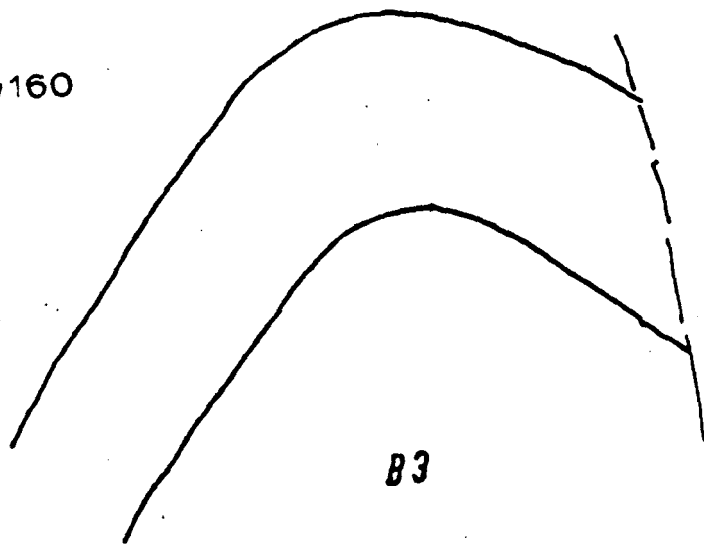


**Fig 160**



that B2 deformation was probably three-dimensional. Differential flattening in ab and ac, combined with variations in homogeneity of lithologies, can obviously produce great variation in fold styles and even orientations.

### B3 folds

B3 folds vary in style from open flexures to penetrative kink folds and range in size from  $\lambda = 50$  metres to micro-folds. They usually have flat axial planes and the geometry varies with the inclination of the pre-B3 foliation; where this is vertical, the B3 folds have a pure orthorhombic symmetry.

In many pelitic horizons, a late strain-slip cleavage (S3) forms parallel to the axial planes of B3 folds. It is probable that initial folding was by flexural slip along compositional layering and in the last stage of movement, movement occurred parallel to the axial plane in the hinge regions. This strain-slip cleavage is parallel to a fracture cleavage in quartzites.

Measurement of a B3 fold in quartzite is described below. Fig.160 is a profile of the fold.

In Fig.158, graph A for measurement parallel to the axial plane is a flat curve with a minimum value at the hinge and maxima on the limbs, indicating that the fold is of a flexural type.

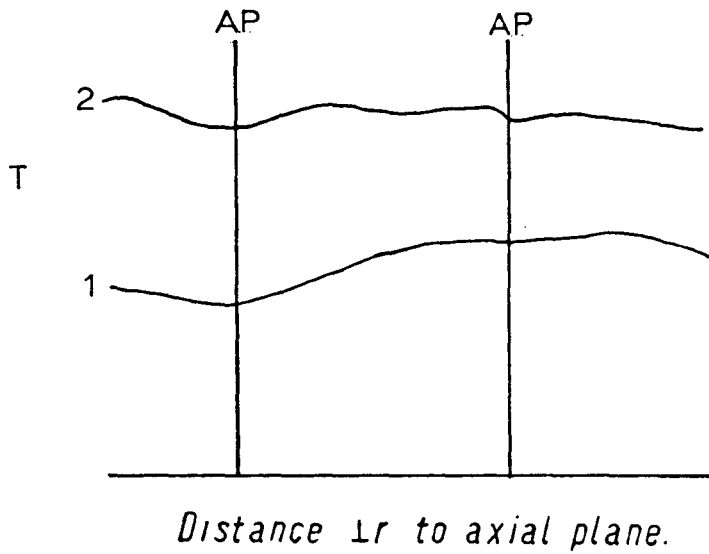
Graph B for measurement at right angles to compositional banding is a fairly uniform line, with a maximum at the hinge indicating a fold of modified flexural type.

Estimation of the flattening gave values of 22-26%. The fold is essentially a flexure fold with slight modification by uniform flattening in the hinge region.

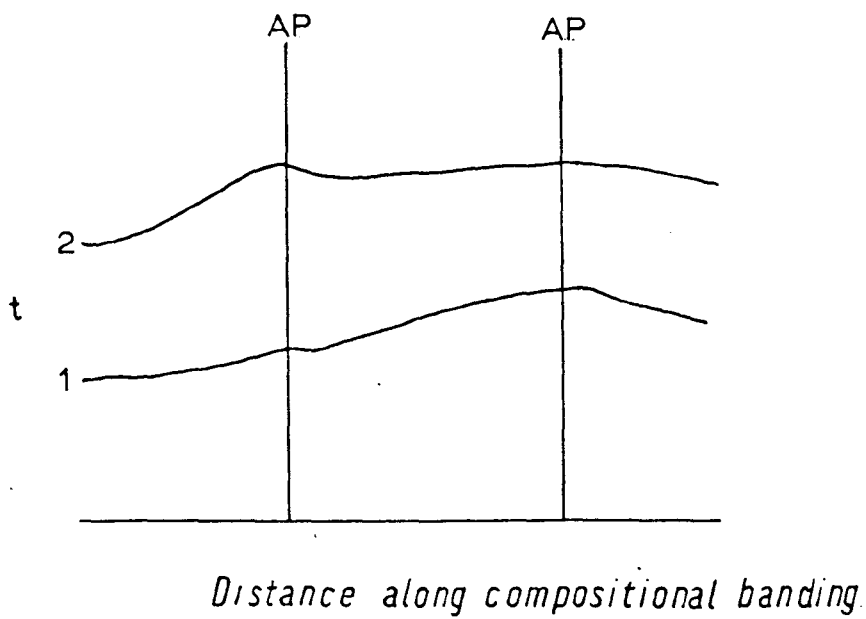
The fold is sheared out parallel to the axial plane, but the fracture has occurred on the limb and not in the antiformal hinge region. The fold may have deformed by a modified flexural

*Fig 161 B4 Fold Measurements.*

*Graph A*



*Graph B*



mechanism up to a limiting value and then responded to further deformation by fracture.

#### B4 folds

Field observations have shown that B4 folds are variable in style. They often consist of conjugate sets of kink-folds, but more open flexures also occur. Kink-bands are a common feature of the fourth-movement phase and these non-penetrative structures undoubtedly formed by a flexure-glide mechanism. However, some B4 folds show thickening in the hinges and hence these folds did not deform by flexure alone.

The results of measurements on a B4 fold are presented below (Fig.161) and Fig.153 is a photograph of the fold profile. The specimen is a micaceous quartzite and the fold is a flexure of small amplitude with a slight late-state fracture cleavage parallel to the axial plane. The amplitude of the fold varies and it dies out in a few metres.

Bands 1 and 2 are two quartzite bands (Fig.161).

Graph B for measurements at right angles to the compositional banding, shows fairly uniform lines with maxima at the hinge zones. Graph A, for measurements parallel to the axial planes, shows slight minima in the hinge zones. The data suggests that the folds are modified flexure folds.

The pelitic band at the base of the fold has thickened below the antiformal crest and axial plane cleavage is developed, showing that the band has deformed by flow or shear.

Measurements on the quartzite bands, together with the impersistence of the fold and its small amplitude suggest that it is a modified flexure fold. Estimation of the flattening gave 26-28% for band 1 and 22-29% for band 2.

It is suggested that B4 folds are primarily flexure folds with some modification due to uniform flattening. In pelitic bands, the mechanism was probably axial plane shear with some flow. It is likely that the pelitic band has behaved passively and that deformation was controlled by the active folding of more competent units.

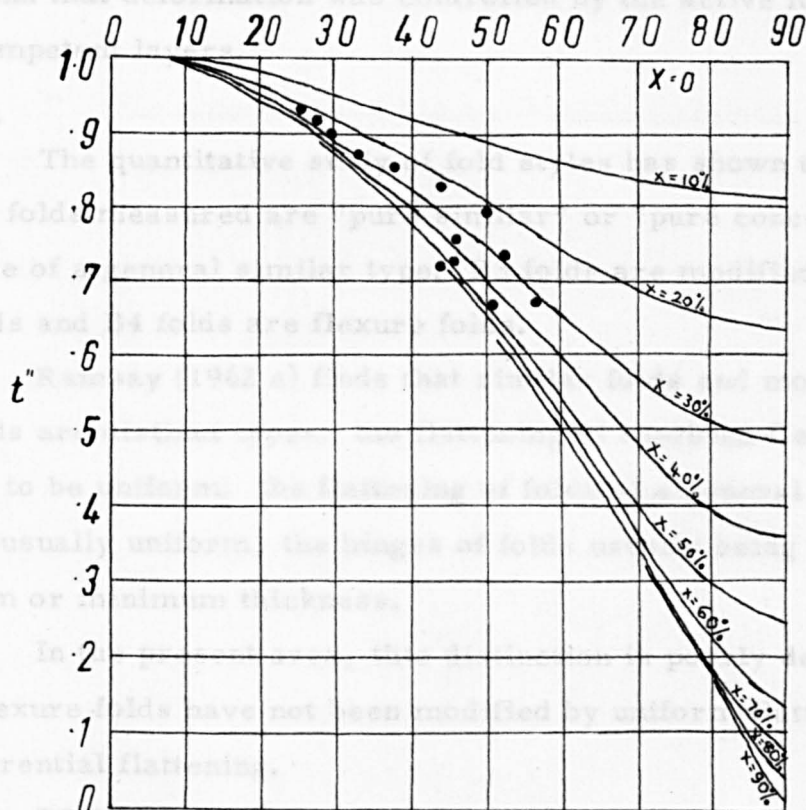


Fig. 162

*Fig. 162*

It is suggested that B4 folds are primarily flexure folds with some modification due to uniform flattening. In pelitic bands, the mechanism was probably axial plane shear with some flow. It is likely that the pelitic band has behaved passively and that deformation was controlled by the active folding of more competent layers.

### Discussion

The quantitative study of fold styles has shown that none of the folds measured are "pure similar" or "pure concentric". B2 folds are of a general similar type; B3 folds are modified flexure folds and B4 folds are flexure folds.

Ramsay (1962 a) finds that similar folds and modified flexure folds are distinct types; the flattening of modified flexure folds tends to be uniform; the flattening of folds of a general similar type is not usually uniform, the hinges of folds usually being zones of maximum or minimum thickness.

In the present area, this distinction is poorly defined. Modified flexure folds have not been modified by uniform flattening, but by differential flattening.

B2 folds may be an extreme case of production of similar type folds from modified flexure folds.

In many cases evidence indicates that both compositional banding and axial planes have behaved actively during some part of the deformation.

It is likely that the folds first formed by slip and flow parallel to layering, controlled by viscosity differences between layers and that axial plane cleavage was imposed after initial folding. Viscosity differences between layers is important in the evolution of these folds. In uniform rocks folding of a passive nature produced similar folds; in rocks containing layers of varying viscosities, concentric and similar folds might form.



During progressive deformation, an active fold may become passive as the fold axis rotates away from a principal direction (Flinn 1962). Folds actively formed as flexural of modified flexural types may later be passively opened or closed and it is probable that such folds would assume a near similar style.

Further discussion of the mechanism of folding is in chapter 8 .

## CHAPTER 7.

## MOVEMENT PICTURE AND TECTONIC SYNTHESIS

A reconstruction of the movement picture of successive deformations, using the data on symmetry of minor folds and fold styles, is attempted and from this data, strain and stress syntheses are discussed.

Unresolved problems include the lack of detailed knowledge of the first deformation; the relationship of thrusting to folding; and the problem of the movement of the upper Jotun nappe. Assumptions required for a stress synthesis are critically examined.

### 1. Movement picture of the first deformation

The scarcity of data on the first deformation and the absence of major structures makes the interpretation insecure. The relationship of the basal and Gjeitaa thrusts to the folding is uncertain. Did thrusting precede folding or did folding produce the thrusting?

The overall symmetry of B1 folding has at least monoclinic symmetry, possibly orthorhombic. Allowing for the effect of B2 folding, the axial planes of B1 folds were probably flat lying and the folds may have been recumbent.

Petrofabric data on these folds is lacking so that nothing is known concerning the symmetry of the total fabric and subfabrics.

The strong axial plane cleavage shows that in the latter part of the deformation, the axial plane must have been active.

The origin of the two thrusts and the imbrication zone is uncertain. What seems clear is that they are part of the B1 deformation and have formed parallel to the axial planes of B1 folds; what is not clear is the timing of thrusting within the B1 deformation.

It is tentatively suggested that the direction of movement was from the west and that the structures were produced by gliding of the supracrustal rocks over the Pre-Cambrian basement. The sparagmite group, forming the sole of the thrust, suffered imbricate thrusting.

## 2. Movement picture of the second deformation

Structural analysis has shown that the second deformation is complex and that deformation was probably three-dimensional. Studies of fold styles indicate that folding was initiated by flexural slip along bedding or S<sub>1</sub>, but the mechanism was replaced by planar slip parallel to the fold axial planes as a means of effecting further deformation.

It is tentatively suggested that the folds formed by compression at right angles to their axial planes and that differential flattening in ab and ac planes, combined with inhomogeneities of lithological groups has produced the complex three-dimensional picture seen on the ground.  $\sigma_1$  probably acted in a N. W. -S. E. direction.

The possibility that B2 deformation was due to the movement of the upper Jotun nappe has already been noted, but the evidence is inconclusive; both formed at the same time, but it is not possible to say that overthrusting of the upper Jotun nappe caused B2 folding. The movement of the upper Jotun nappe is considered later.

## 3. Movement picture of the third deformation

The constancy of orientation of B3 fold axial planes and the dependence of orientation of B3 fold axes on the geometry of B2 major folds have already been noted. The B3 folds are flexure folds with slight modification in the hinges due to uniform flattening.

In B3 folding, the folded S-surfaces were kinematically active until at a late stage when the axial plane behaved in an active manner resulting in a strain slip cleavage.

This dependence on orientation of earlier S-surfaces and the horizontal axial planes suggest a vertical compression. The overall symmetry of B3 folding is orthorhombic. However, the work of Paterson et al (1962 and personal communication) shows that in flexure folding, the axial planes of the folds are not usually at right angles to  $\sigma_1$ , unless deformation is high.

It is suggested in this case that  $\sigma_1$  was at right angles to axial planes and that the folds are gravity structures, produced by a vertical axial compression (symmetry  $D_{\infty h}$ ) and that  $\sigma_2$  and  $\sigma_3$  may have been locally variable.

This vertical compression may have been due to the weight of the upper Jotun nappe which had been thrust over during B2. The time interval between B2 and B3 could represent the period of reduction in pore water pressures at the base of the upper Jotun nappe.

#### Forth movement picture

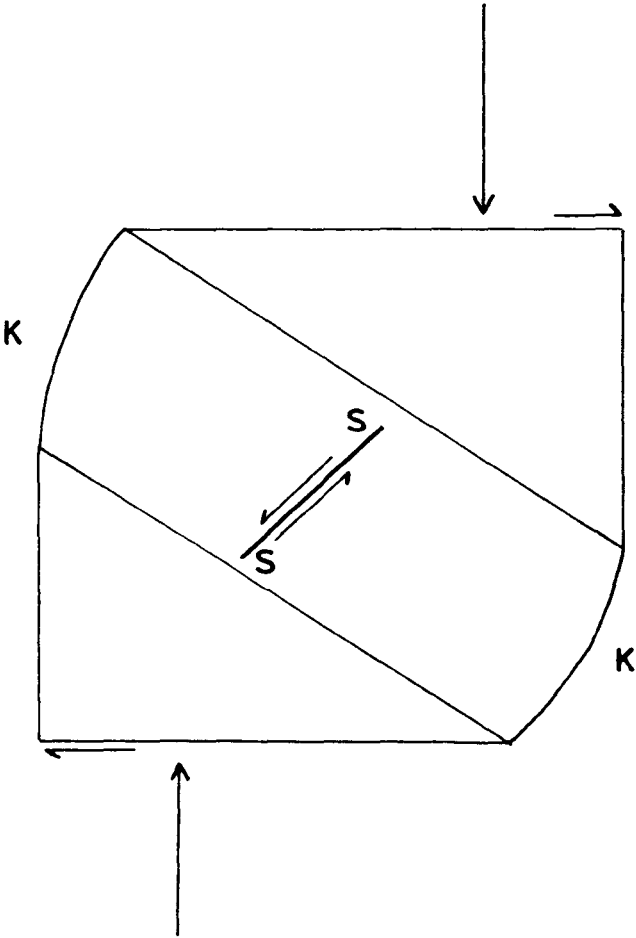
The overall symmetry of B4 folding is probably orthorhombic. These structures can be attributed to a compression from E.-W., assuming that  $\sigma_1$  was parallel to the pre-existing foliation.

#### Thrusting

##### Upper Jotun nappe

The problem of thrusting of a rigid block such as the upper Jotun nappe has been discussed by Hubbert and Rubey (1959). They explained the movement of such large blocks as due to a reduction of frictional drag on the base of the nappe by fluid pore pressure. If fluid pore pressures approaching the pressure due to

Fig 163



after Turner et al. 1956

the weight of the overlying nappe were present in the rocks beneath the nappe, movement could be easily accomplished. High pore water pressures may have been operative beneath the upper Jotun nappe, since impervious crystalline rocks were thrust over either sediments or low grade meta-sediments.

Scott-Smithson (1964) has calculated a minimum thickness of 82 kms for the upper Jotun nappe. The movement of such a thickness of crystalline rocks is difficult to envisage unless friction at the base was low.

The movement picture within the mylonite zone is probably radically different from the displacement of the overlying nappe relative to the underlying supracrustal rocks. This has been compared with eccentric loading in the experimental studies, which have shown that strain tends to be concentrated in a diagonal domain whose opposite boundaries are mutually displaced in the opposite sense to that of gliding within the strained domain. (Turner et al 1956, Turner and Weiss 1963). This is illustrated in Fig.163 . The glide planes which define the movement picture in the diagonal zone K K are oriented transversely with reference to the external boundaries of the large-scale displacement zone.

The mechanics of the movement of the upper Jotun nappe are complex and it is not surprising that there is difficulty in correlating structures from the nappe into the supracrustal rocks.

#### Basal and Gjeitaa thrusts

Movement along the Gjeitaa thrust is effected along a narrow zone of flaggy, sheared, jointed quartzite, whereas movement along the basal thrust is over a wide zone. This might be explained if the Gjeitaa thrust were merely the contact between two rock groups of similar competence and the sparagmite group occupied the sole of the thrust. Most of the movement would be within the basal thrust

area and the Gjeitaa thrust would merely show differential movement between the overlying rocks and the sparagmite group. This would explain the drag folds below the Gjeitaa thrust and the basal imbrication zone. The B1 thrusting may have occurred in several stages.



## CHAPTER 8.

## THEORETICAL

### 1. Fold Description

From an objective point of view, a purely geometric description of folds is necessary before any kinematic interpretation is possible.

Any geometric classification of folds must contain all types; both simple and complex. The features which define a fold are:

1. Its position in space, either relative to arbitrary co-ordinates or relative to other folds
2. The attitude of the fold
3. The style of the fold
4. The symmetry of the fold
5. The size of the fold

Several fold classifications have been proposed, usually in terms of a linear element (fold axis) and a planar element (axial surface). For a discussion of qualitative fold classifications, reference should be made to Turner and Weiss (1963) and Fleuty (1964). The fold classification used in this thesis is a combination of the classifications given in the two references above.

The qualitative description of folds is subjective and there is no agreement on many terms in common usage. A purely objective mathematical description of folds is therefore desirable. The writer has been interested in fold description for some time and has followed up several lines of investigation. Unfortunately these methods are designed for high-speed electronic computers, and the data is still incomplete. A brief outline of some of the methods used is given for completeness.

It is possible to describe folds by a statistical analysis of the  $s$ -surfaces involved. Folds are vectors and require elaborate statistical analysis. Structural data is normally recorded as a

direction and an angle-strike and dip; trend and plunge. This data can be converted to mathematical functions and computed.

If a fold can be represented by an equation its characteristics can be easily specified. For example, if a series of folds have the form  $y = f(x)$ , the domain of a single fold is given by two points of inflexion where  $f'(x) = 0$ ; the crestal point is defined by  $f'(x) = 0$ ,  $f''(x) = -ve$ .

#### Direction Cosine Method (see Loudon 1962)

In the direction cosine statistical analysis of fold profiles, the data is expressed as a variance-covariance matrix and functions such as latent vectors, variance, skewness, and kurtosis are calculated by taking moments about the transformed origin. The latent vectors give the attitude of the fold in space. In the direction of the appropriate axes, tightness is given by the variance, symmetry by skewness and shape by kurtosis.

#### Representation by functions of two variables

In analytical geometry, surfaces in space are represented by functions of two variables, so that between such surfaces and functions of two variables there is a reciprocal relation. This can be achieved by using a rectangular co-ordinate system in space, or preferably by means of contour lines.

#### Trend surface analysis

The final method is a trend surface analysis with irregular control-point spacing. This involves the calculation of a large number of cubic and quartic polynomials using a high-speed electronic computer.

## 2. Mechanism of folding

The mechanism of folding has been discussed by many authors from a theoretical and an experimental point of view. These discussions fall into two groups; the first group consists of attempts to deduce a simple model of folding and in many cases to verify this by simple experiments; this work is rather limited in its application in view of the large number of assumptions required. The second group deals with experimental deformation of rocks in the laboratory and while this is obviously an over-simplification, in many cases a close approach to natural conditions may be obtained.

The theoretical approach attempts to predict the response of material to stress. Between the extreme cases of elastic and viscous behaviours lies a wide field of intermediate behaviours. The study of flow and permanent continuous deformation is termed rheology. In the analysis of mathematical models of ideal materials, differing rheologic states have been assumed by different authors. The application of these studies to natural tectonites is rather limited, since in many cases, they are not even first-order approximations to natural conditions, but they are useful as a guide to a general pattern of behaviour.

In laboratory experiments on strain of rocks, temperature and confining pressure can be varied to correspond to metamorphic conditions. However, two criticisms can be levelled at the experimental conditions; firstly most strains have been accomplished in a short period of time and insufficient data on the rheologic behaviour of rocks under stresses of long duration has been obtained; secondly, in many cases, the applied stress and the resultant strain have a higher symmetry than that frequently recorded in natural tectonites.

With these reservations in mind, some of the interesting and anomalous features of the folding in the Nettoseter area will be

examined in the light of this theoretical and experimental work.

### B2 deformation

The complexity of the B2 fold phase has already been discussed in chapters 4 and 8. This complexity could be caused by a number of factors, acting independently or together.

The rocks of the Nettoseter area were undergoing a greenschist metamorphism during B2 folding; it is likely that during folding, the temperature, pressure, chemical nature and stress system of the rocks all changed.

The work of Ramberg (1962) has shown the dependence of initiation of folding on viscosity contrasts. If, in a rock unit composed of alternating competent/incompetent layers, the separation of competent layers is greater than two wavelengths, each layer will buckle independently. As the separation decreases the layers of competent material will buckle in phase and hence a multilayer will buckle more and thus suffer a smaller amount of uniform compression than a single layer having the same density contrast.

Up to a critical strain, a layer will deform by uniform compression until the stress is adequate to initiate buckling. This depends on the viscosity ratio; the higher the viscosity ratio, the earlier buckling will commence. Ramberg (1963) has shown that variations in fold style from concentric to similar folding are to be expected in areas where the rock units are composed of layers of varying viscosities.

McBirney and Best (1961) found an approximate correlation between the amplitude of folds and 1. the thickness of the more viscous layers and 2. the ratio of the viscosities of the two layers. They also found that at very slow deformation rates the surfaces of separation of the two media are almost passive in their behaviour so that folding is minor or fails to develop.

The properties of a competent bed are not usually constant, but often show lateral variation. The material will deform most where it is weakest; a competent layer is likely to deform most where it is thinnest or least competent. The scale of localisation of folding will depend on the scale over which the physical properties of the rock vary. Under these conditions, it is possible that folding in response to stress in the intermediate stress direction would be more intense locally than folding in response to the maximum stress.

Flinn's (1962) analytical work has shown that neither fold axes nor fold axial planes bear any special relationship to the axes of the deformation ellipsoid. He states that when fold systems are subjected to a later deformation, the resulting structures will be very complicated. According to Flinn, similar folds form by finite homogeneous strain. The initial folding, he generates by appealing to non-planar layering, competency differences between the layers and changes in homogeneous strain from place to place.

From this short discussion it can be seen that viscosity differences between lithologic layers may play an important part in the initiation of folding. Folding in its early stages may be as much dependent on the stratigraphy as on deformation rates.

Subsequent development of a fold phase would be dependent on 1. the role of strain, 2. the viscosity differences between layers, 3. the role of cleavage.

In the Nettoseter area, the variation in style, symmetry and orientation of the B2 fold phase may be partly attributable to viscosity contrasts, dependent on the stratigraphy.

The presence in many cases of a strain-slip axial plane cleavage displacing S1 or bedding shows that the B2 folds have suffered some movement parallel to the axial planes.

The quantitative study of fold-styles (chapter 8 ) has shown that B2 similar-type folds may have been produced by the extreme flattening of modified flexure folds.

It is suggested that the folds deformed, initially by flexure and plastic flow, controlled by viscosity differences between the layers and that the axial plane cleavage was impressed later.

During progressive deformation, the deformation path would be largely dependent on viscosity contrasts. In rocks of near uniform viscosity, passive folding produces folds of near similar type. If there is a sufficient viscosity contrast to allow active folding, the folds formed could be either of concentric or similar type. Flinn(1962) has shown that in progressive deformation, active folds may become passive as the fold axis rotates away from a principal direction. A fold which may have actively formed as a flexural (or modified flexural) fold may be subsequently opened or closed and it is probable that these folds would be of a "general similar type".

The complexity of the B2 fold phase is probably due to a combination of three-dimensional deformation and varying viscosities of the rock units.

In conclusion, fold development is probably in two stages

1. Initial flexural folding producing buckles by active folding.
2. Subsequent deformation by finite homogeneous strain; folding may be active or passive depending on a number of variables.

## CHAPTER 9.



## METAMORPHIC HISTORY

### 1. Metamorphic facies

#### (a) Pre-Cambrian metamorphism

##### (1) Upper Jotun Nappe

In the interior of the upper Jotun nappe, which has suffered little Caledonian metamorphism, typical assemblages are:

ortho-pyroxene-clino-pyroxene-K feldspar-plagioclase  
ortho-pyroxene-clino-pyroxene-olivine.

These assemblages are typical of the granulite facies and in Turner and Verhoogens (1960) classification belong to the higher subfacies, the pyroxene granulite subfacies.

The lower part of the upper Jotun nappe (granite and gabbro sheets) has suffered considerable Caledonian deformation and retrograde metamorphism which have almost obliterated the Pre-Cambrian mineralogy. However, it seems likely that the lower part also suffered a Pre-Cambrian metamorphism in the granulite facies. There is a possibility of a Pre-Cambrian retrograde metamorphism in the upper greenschist or lower amphibolite facies (see page 15), but the age of this metamorphism is uncertain.

##### (2) Basal Gneiss Complex

The typical assemblages of the basal gneiss complex: K feldspar-quartz-plagioclase-biotite-epidote, together with a plagioclase of composition  $An_5$ , suggest that the rocks are in the highest subfacies of the greenschist facies. The muscovite-chlorite gneisses along the basal thrust have crystallised in the lower subfacies of the greenschist facies; the age of this lower greenschist facies metamorphism is uncertain. It may be associated with thrusting (B1), or it may have occurred during later movements along the basal thrust

after the main movement (syn B2 to syn B3 ? ).

No evidence of Pre-Cambrian metamorphism in higher facies has been found by the writer, but the rocks are obviously altered when seen in section (plagioclase, saussuritised, etc.) and Banham (1962) has presented evidence of Pre-Cambrian metamorphism in the almandine-amphibolite facies.

The greenschist regional metamorphism of the basal gneiss complex is something of a problem; the assemblages fit the main Caledonian metamorphism but the biotite foliation strikes E.-W. and is probably a Pre-Cambrian structure. One must conclude that a Pre-Cambrian metamorphism in the greenschist facies took place or else that the metamorphism is a Caledonian metamorphism with mimetic crystallisation parallel to Pre-Cambrian structures.

### Caledonian metamorphisms

At least two main phases of Caledonian metamorphism are found within the area mapped; in addition, evidence suggesting an early dynamic phase has been obtained. Complicating factors include:

1. The main metamorphism (upper greenschist facies) was of long duration with several maxima.
2. Polymetamorphism is not easily discernible in psammites.
3. Strong cataclastic fabrics are common around the base of the upper Jotun nappe.
4. Age relations of fabrics around the basal thrust area are unknown.
5. The chemical control of bulk composition on mineral assemblages is quite marked (e.g. serpentinites).

### First metamorphism

Evidence of a dynamic metamorphism, probably synchronous with B1 deformation has been found and this is discussed

in the next section. This was probably a slate-belt type metamorphism with crystallisation of muscovite and chlorite. Little mineralogical evidence of this now remains.

### Second metamorphism Syn - post B2

The main metamorphism occurred in the highest subfacies of the greenschist facies. In different lithologies, the following assemblages were produced

Quartz-muscovite-K feldspar-biotite (Psammites)

Calcite-muscovite (Limestones)

Hornblende-albite-epidote-garnet (Meta-volcanics)

Biotite-quartz-muscovite-garnet (Pelites)

However, around the serpentinite bodies, the metamorphism was of lower grade, producing chloritisation of the country rock and formation of talc and tremolite by a complementary reaction. This was probably due to an abundance of water. The occurrence of hornblende-garnet in some aureoles shows that this low grade was only localised.

At the base of the upper Jotun nappe, mainly cataclastic effects were produced, but some metamorphism was observed. This was of low grade, probably due to abundance of water and breakdown by cataclasis.

### 3. Third metamorphism pre-syn B3

This retrograde metamorphism occurred throughout the area, but was only minor in its effects. This metamorphism produced the alteration of biotite and garnet to chlorite. The N.-S. shear zones of the upper Jotun nappe may have formed at this time, but are possibly B2 in age.

Later metamorphism is shown by the occurrence of low-grade assemblages in joints.

Fig. 164

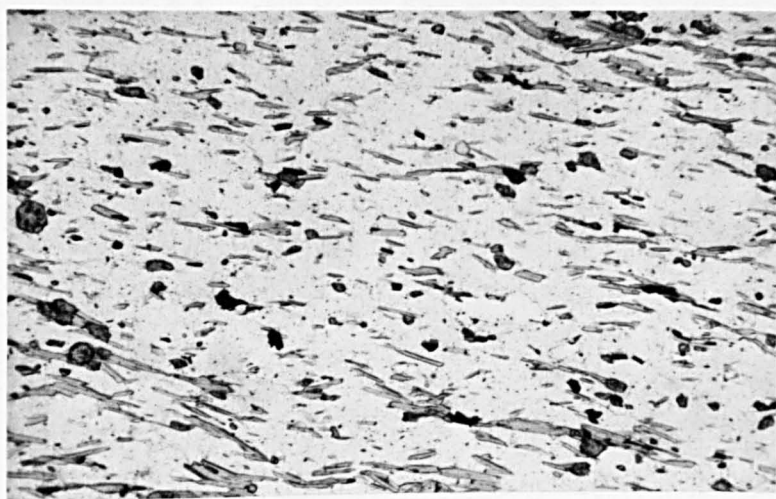
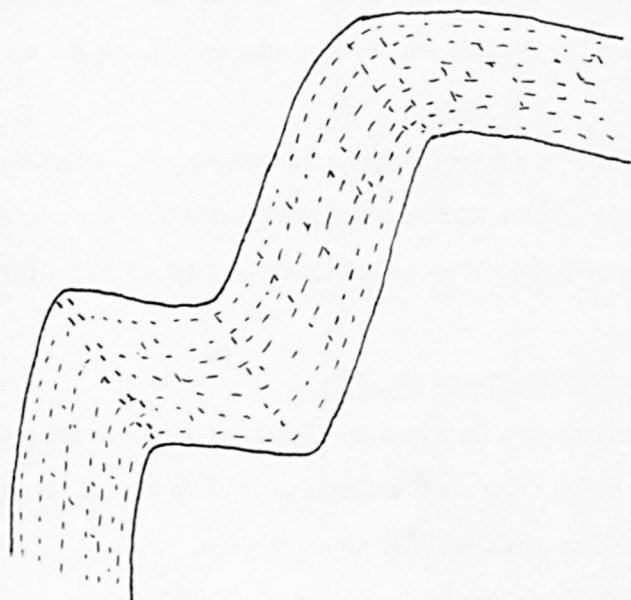


Fig. 165



## 2. Relations of metamorphism and structure

The fabric of a metamorphic rock is composed of inherited and metamorphic elements. Polymetamorphism would be expected to show evidence of earlier fabrics in the total fabric of a metamorphic rock.

In this section, fabrics of some tectonites are described and the relationship of metamorphic crystallisation to folding discussed.

Unfortunately no petrofabrics have been completed, so that no quantitative data on mineral orientations is available.

### B1 fabrics

A typical example of a B1 fabric is the micaceous quartzite from Nettos, described below. In this slide, there is a strong preferred orientation of muscovite flakes, parallel to the axial planes of B1 folds (see Figs 164 and 166).

In view of the recent work of Paterson (personal communication and in press), on the significance of slaty cleavage, it seems probable that the muscovite crystallised parallel to axial planes of folds, during the folding. This evidence suggests a low grade, probably mainly dynamic metamorphism, synchronous with B1 deformation.

### B2 fabrics

The main evidence on B2 fabrics comes from porphyroblasts such as garnet and pyrite. Several garnet-mica-schists have been collected showing the effects of both B2 and B3 folding.

Garnets have been found which in some cases overgrow B2 folds and are obviously post-tectonic (Fig 168); in other cases syn-tectonic garnets with helicitic textures have been found (Fig 169). This suggests that conditions suitable for garnet growth either prevailed for a long time or that two separate maxima are present.

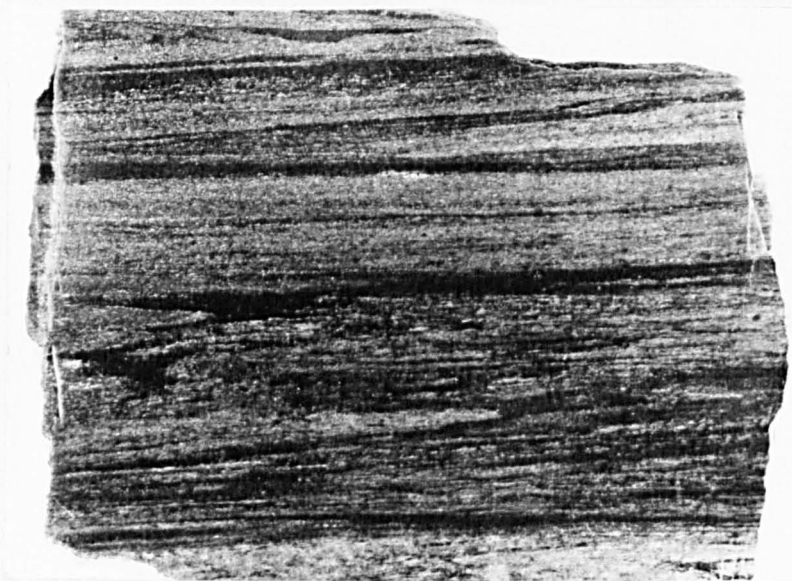


Fig.166. B1 folds, Nettoserter. Note shearing out along axial planes.

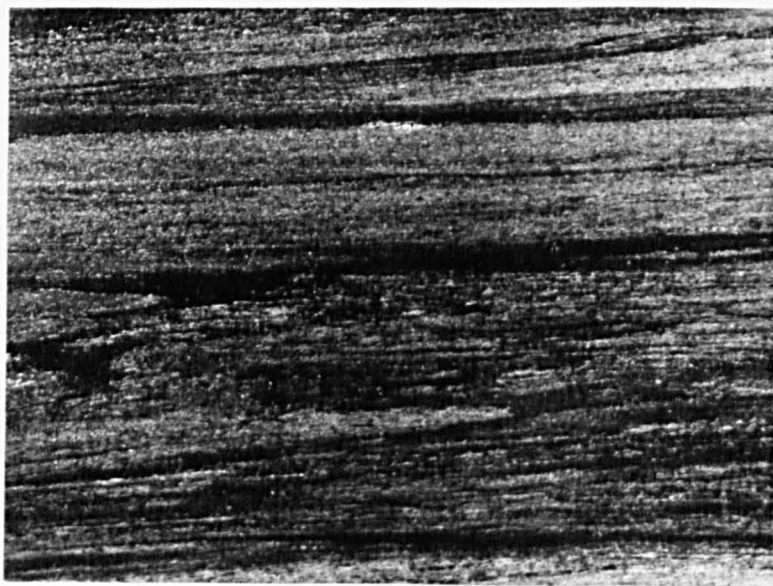
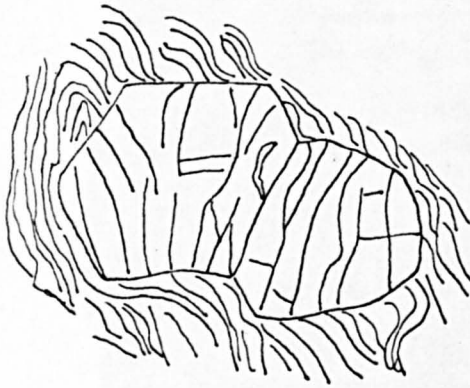


Fig.167. B1 folds, Nettoserter.

Fig 168



post tectonic garnet

Fig169

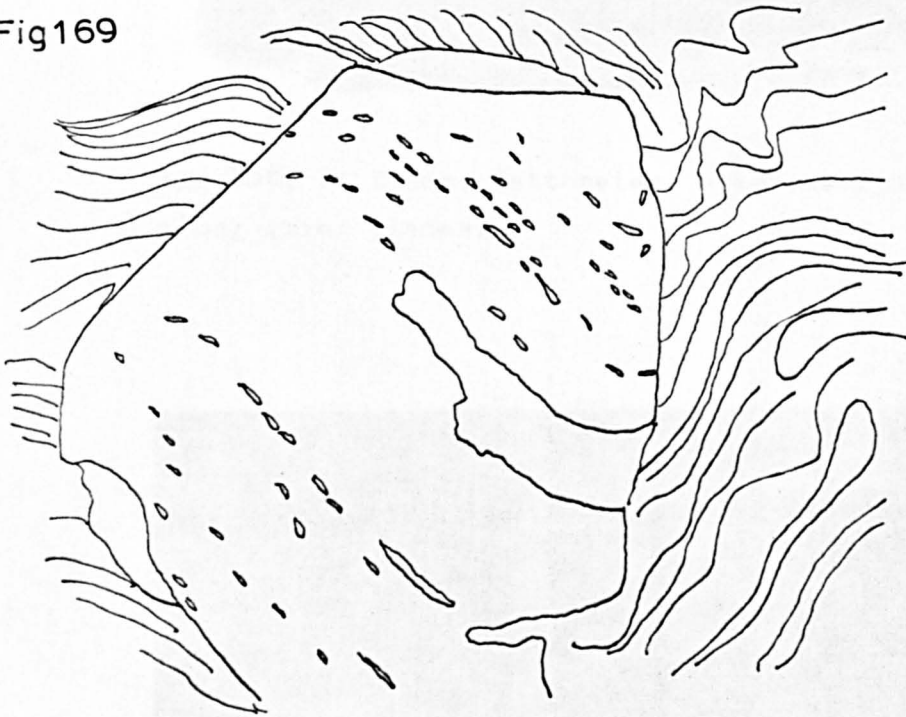
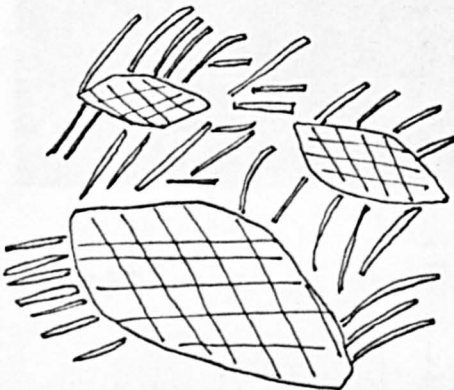


Fig170



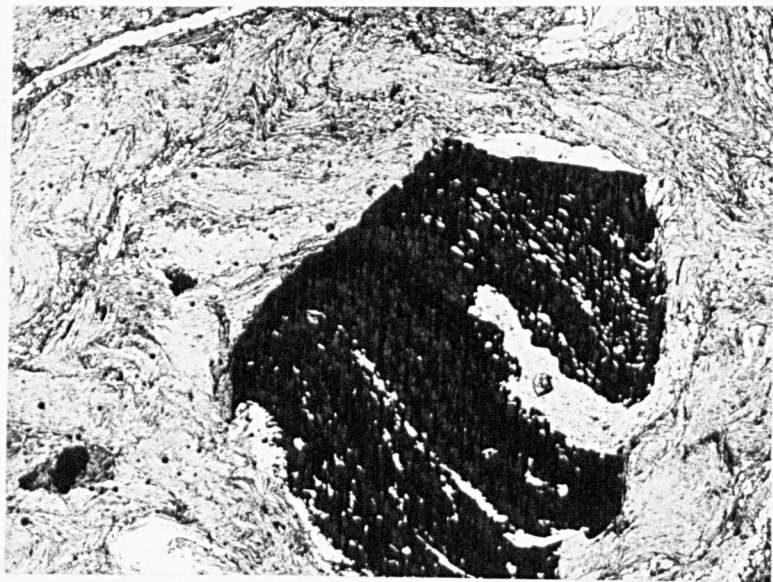


Fig.171. Helicitic texture in garnet.

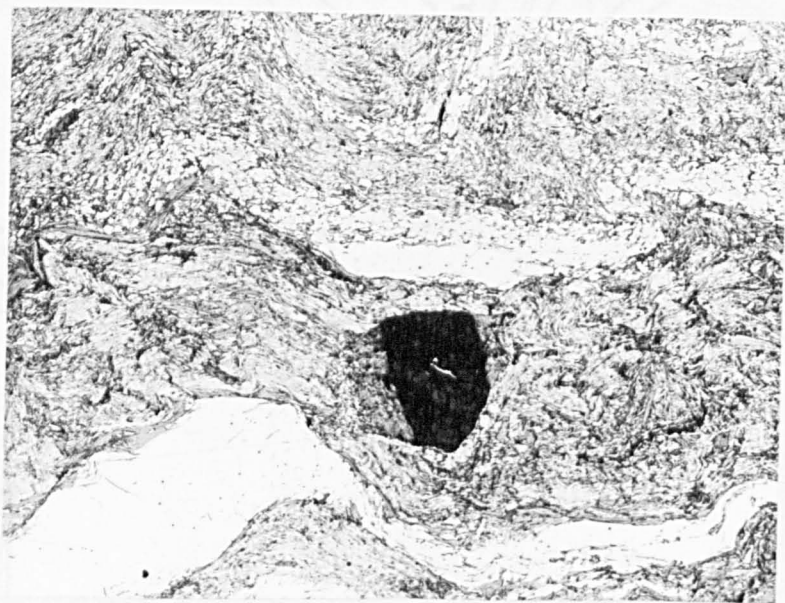


Fig.172. Garnet replaced by chlorite which is later folded.



Other features showing syn and post B2 metamorphism include pressure shadows around pyrite and magnetite grains and two generations of hornblende.

In some amphibolites, a first generation of strongly oriented hornblendes is followed by growth of smaller grains of the same composition, showing little preferred orientation (Fig.170). The first generation is probably syn-tectonic; the second post-tectonic.

The behaviour of muscovite during B2 folding is interesting; some flakes are parallel to compositional layering around a B2 fold; other flakes are parallel to the axial planes (see Fig.165 ). Recrystallisation of muscovite must have occurred.

### B3 fabrics

Several garnet-mica-schists showing the effect of B3 folds have been described. In these, syn or post-B2 garnets are replaced around the rim by chlorite and the chlorite is itself folded by B3 folds (see Fig.172). In some cases the chlorite appears to have formed in pressure shadows.

The chloritisation is probably syn-B3.

The behaviour of micas during B3 folding is complex. Micas with bent cleavage traces are common; but micas are frequently found in domains of strain-slip cleavage, the micas appear to have been rotated into parallelism with the slip-planes and partly recrystallised.

Hornblendes are sometimes bent by B3 folds; elsewhere they have acted as slip surfaces.

### Summary

#### 1. Pre-Cambrian

Metamorphism of the upper Jotun nappe in the granulite facies with a possibility of some retrogression. Metamorphism

of the basal gneiss complex in the upper greenschist facies or above.

## 2. Caledonian

A first metamorphism synchronous with B1 deformation producing slate-belt metamorphism.

A second metamorphism, partly synchronous and partly post B2, producing upper greenschist conditions with growth of garnet; mainly cataclastic deformation at the base of the upper Jotun nappe.

A third metamorphism in the lower greenschist facies, synchronous or before B3 deformation.

## CHAPTER 10.

## GEOLOGICAL HISTORY

In this chapter, an attempt is made to correlate and integrate the stratigraphic evidence with the metamorphic and structural history in order to describe the complete history of the Netto seter area.

It is obvious that the area has had a Pre-Cambrian and a Caledonian history and that these can be considered separately.

### 1. Pre-Cambrian

The North-west Basal Gneiss Complex and the Upper Jotun Nappe had separate Pre-Cambrian histories. It is likely that the Upper Jotun Nappe is a far travelled mass whereas the Basal Gneiss Complex formed the foreland of the Caledonian Geosyncline.

#### (a) Basal Gneiss Complex

The detailed Pre-Cambrian history of the basal gneiss complex is described by Banham (1962). As far as the present writer's work is concerned, the fundamental character of the complex is one of gneisses and foliated granites with a foliation defined by a planar alignment of biotites. This strikes E.-W. and dips at moderate angles to the south. A lineation within this plane is defined by alignment of hornblende prisms and this pitches at  $10^{\circ}$  east.

It is probable that this biotite foliation developed in response to the application of N.-S. compression. During the Pre-Cambrian, the rocks were metamorphosed in the upper greenschist facies or higher.

#### (b) Upper Jotun Nappe

The upper Jotun nappe had a complex Pre-Cambrian history. The place of origin and distance of travel of the nappe are

uncertain; it has probably been thrust either from the west or from the north-west; it may have originated in Greenland.

The rocks of the upper Jotun nappe belong to an igneous complex. The higher part is intermediate and ultramafic and shows evidence of igneous differentiation; the lower part is composed of granites and gabbros. During a Pre-Cambrian metamorphism, the complex was metamorphosed in the pyroxene-granulite facies and a foliation was induced.

A subsequent retrograde metamorphism, which is still later affected by Caledonian movements and which may, therefore, be of Pre-Cambrian age, has brought some of the granulite facies rocks into the amphibolite or upper greenschist facies.

The Pre-Cambrian structural history of the nappe is complex; at least two phases of folding are present, one set with E.-W. axial planes and a later phase with N.-S. axial planes.

Most of the rocks of the upper Jotun nappe have a strong cataclastic texture. This may be entirely due to the thrusting, but may in part be a Pre-Cambrian structure.

### Caledonian

Sedimentation during the Caledonian geosyncline can be divided into three periods

1. Sparagmite group; probably Eo-Cambrian.
2. Main eugeosynclinal succession; psammite group up to upper limestone-pelite group. Probably Cambrian to Ordovician.
3. Feldspathic quartzite group. Ordovician. The possibility that the feldspathic quartzite group represents the Valdres group - molasse type, synorogenic deposits can not be proved on the present evidence.

All three rock groups are affected by the first deformation, B1 and hence must have been deposited before the folding.

### 1. Sparagmite Group

The nature of the sparagmite group, i.e. richness in K feldspar, etc. suggest deposition under foreland conditions.

### 2. Eugeosynclinal succession

Lithological variation within this group is marked.

The succession is essentially psammitic at the base and pelitic at the top but variations occur. Facies variation along the strike is considerable. The presence of meta-volcanic rocks, including pillow lavas and the presence of dunite-serpentinites of alpine-type indicate that the succession is eugeosynclinal.

### 3. Feldspathic quartzite group

This group, consisting of quartzites rather rich in perthitic K feldspar, occurs below the upper Jotun nappe and some evidence has been found of an unconformity at the base of this group (see chapter 3 ).

It is not known whether the sparagmite group owes its present position largely to original unconformity on the basal gneiss complex or to subsequent thrusting. The disturbance at its base is real, but the amount of transport is unknown; the writer prefers to regard it as thrust into place and to leave open the question of the extent of the thrusting.

The supracrustal rocks were thrust over onto the basal gneiss complex and folded. The direction of movement was probably from the west. The fold axial planes and the thrust planes were flat-lying. This constituted the first deformation; a mainly dynamic metamorphism accompanied the deformation and produced slates, etc..

The second phase of folding produced the major structures of the area and was accompanied and followed by the main metamorphism, i.e. that in the highest subfacies of the greenschist facies. The axial trace of B2 folds is N.E. to E.N.E. Deformation was complex,

but the axial planes are fairly constant. The structures probably formed by compression at right angles to their axial planes (i.e. from N.W.-S.E.).

Emplacement of the upper Jotun nappe and accompanying mylonitisation at the base occurred at this time; deformation at the base of the nappe was mainly cataclastic.

Vertical compression produced flat-lying B3 folds and was accompanied and perhaps preceded by a phase of retrograde metamorphism in the lowest subfacies of the greenschist facies. In detail, the trend of B3 folds depends on pre-existing S-surfaces. A tentative suggestion is that they owe their origin to deformation by the weight of upper Jotun nappe rocks overlying the succession. B2 and B3 are not separated by a very large time interval.

E.-W. compression followed, producing kink-bands and warps with conjugate axial planes; the fold axes plunge steeply south.

The last phase of deformation was a rather localised event, producing strain-slip cleavage and kink bands.

Within the mapped area, later movements of a brittle nature are indicated by various joint-suites.

There is no record of any geological events between the Caledonian orogeny and the present except for considerable uplift and erosion. Quaternary glacial deposits are common.

## CHAPTER 11.



## REGIONAL CORRELATIONS

---

In this chapter, it is proposed to review ideas on the large-scale problems of the Scandinavian Caledonides and then to attempt to correlate the lithologies and metamorphic and structural events of the Netto seter area with other parts of Central Norway.

The regional significance of the basal gneiss complex has been discussed fully by Banham (1962) and will not be considered here.

### Outline of the Scandinavian Caledonides (from Høltedahl 1960, Strand 1961)

The N. E. striking Scandinavian Caledonides form the western part of the Scandinavian peninsula. The eastern margin consists of a series of nappes overthrust onto autochthonous Cambro-Ordovician sediments which themselves rest on the Pre-Cambrian of the Baltic shield. The western border is not seen; the Caledonides disappear beneath the sea.

It is possible to distinguish distinct facies type among the sediments of the Caledonian cycle (Eo-Cambrian-Silurian), which were deposited in different parts of the geosyncline and which now occur in distinct parts of the tectonic succession of nappes.

Deposits of so-called "eastern facies" were laid down upon the eastern foreland or in the eastern miogeosynclinal parts of the depositional troughs. Below the marine Cambro-Silurian deposits is the thick psammitic succession of the Eo-Cambrian Sparagmite. In the east the Cambro-Silurian consists of shales and limestones; westwards the amount of calcareous material decreases and the rocks become metamorphosed. Volcanic rocks and Caledonian intrusives are absent in deposits of the eastern facies type.

The other main facies type is the western or eugeo-synclinal facies. Two distinct facies occur within the western facies:

The Trondheim facies and the Nordland facies.

Deposits of the Trondheim facies have thick horizons of basic and acid volcanic rocks and intrusive bodies of peridotite-serpentine, gabbro and trondhjemite.

Sediments of the Nordland facies are mainly pelites and carbonate rocks, although volcanic rocks occur. The stratigraphy is not fully known, but they appear to be a normal succession above the Eo-Cambrian deposits.

Most of the eugeosynclinal deposits can be shown to form nappes and none are believed to be autochthonous.

The Caledonide nappes also contain large amounts of crystalline rocks of Pre-Cambrian age.

#### Caledonide Nappe Structures

In many areas the autochthonous Cambro-Silurian is present, although very thin (0-220 metres). Frequently, however, both Eo-Cambrian Sparagmite and miogeosynclinal Cambro-Silurian have moved over the Archean basement by 'decollement' gliding.

The nappes can be divided into two groups. In the first group, in a lower tectonic position, the nappes are composed of Eo-Cambrian and Cambro-Silurian rocks of the eastern miogeosynclinal sequence. The second group, in a higher tectonic position, are nappes composed of eugeosynclinal rocks of the western facies and crystalline Pre-Cambrian rocks.

Two main nappes of the second group are recognised designated the Lower and Upper Jotun Nappes. The Lower Jotun Nappe is said to comprise a charnockitic core with a cover of eugeosynclinal rocks of the Trondheim facies. The Upper Jotun Nappe is a vast sheet of dimensions 180 Km (N. E. -S. W.) by 85 Km (N.W. -S. E.); it is composed of charnockitic crystalline rocks of a unique type termed the Bergen-Jotun kindred by Goldschmidt (1916)

The lower Jotun Nappe is thrust over the underlying rocks-either Cambro-Ordovician phyllites or Eo-Cambrian sparagmite. Between lower and upper nappes lies a sequence of tectonic sediments, the Valdres Sparagmite. The Valdres Sparagmite is a synorogenic deposit; it is believed to have been derived from rocks of the lower Jotun Nappe, after or during its emplacement. Perthitic feldspars said to be characteristic of the charnockites of the Bergen-Jotun kindred are found within the Valdres Sparagmite.

Both the Jotun Nappes lie in a N. E. trending synclinal depression termed the "Faltunsgaben" by Goldschmidt (1912).

There is a marked unconformity between the Archean rocks of the foreland and the overlying Eo-Cambrian and younger sediments. Within the orogenic belt, however, there is frequently a complete structural conformity between the Pre-Cambrian basement and the Supracrustal rocks. Relations are obscure in many places; in some areas the gneisses have been described as migmatites of Caledonian origin. Granitization of supracrustal rocks producing gneisses has been described by several authors (Ofstedahl 1963). However, in many areas this conformity is only structural and is due to the reworking of parts of the Baltic shield during the Caledonian orogeny.

#### Age of Deformation

The main Caledonian orogeny in the Central part of the mountain chain ended before the beginning of the Devonian, but folding of some Devonian rocks is part of the same cycle. Several phases of folding have been recognised in some areas.

#### Evolution of ideas on Nappe Structures in the Jotunheim

The Jotun Nappes were first described by Brøgger (1893) and although the nappe concept had already been introduced to Scandinavia by the Swedish geologist A. E. Törnebohm, Brøgger did

not interpret the area as a nappe structure. He preferred to interpret the gneisses overlying Cambro-Silurian sediments as a metamorphic boundary. The upward increase in metamorphic grade was postulated as due to the intrusion of igneous rocks above the sediments and later removal of the igneous rocks by erosion.

Bjorlykke (1902) recognised well-marked mechanical contacts with flinty mylonites at the base of the crystalline massifs in the Hardangervidda; at that time he was prepared to accept the nappe theory. However, in later work (1905) he showed that crystalline massifs were situated above either Cambro-Ordovician phyllites or Valdres Sparagmite in all parts of the nappe region but rejected the nappe concept and reverted to Brøgger's original theory. He believed the mechanical contacts to represent only small movements.

Goldschmidt (1916) recognised that the rocks of his Bergen-Jotun kindred had moved along thrust planes to their present position above the sediments, but did not suppose the distance of transport to have been very large. He suggested that the Jotun rocks had moved into their present position along basal thrust planes but were rooted in a synclinal depression at the upper part of Sognfjord- the "Faltungsgraben". The "faltungsgraben" was a strongly marked syncline in the gneiss basement.

Holtedahl (1936) first suggested that the Jotun nappes had been transported over long distances. He suggested that the Jotun rocks were not rooted in the 'Faltungsgraben' but in fact floated on a basal thrust plane above the underlying sediments without any signs of having roots in the present substratum.

Holtedahl's hypothesis has since been accepted by most Scandinavian geologists, although Oftedahl (1961) has tried to reintroduce Goldschmidt's hypothesis.

Since then, however, a gravity survey of the Jotun nappes has been completed by Scott-Smithson (1964). The results of this

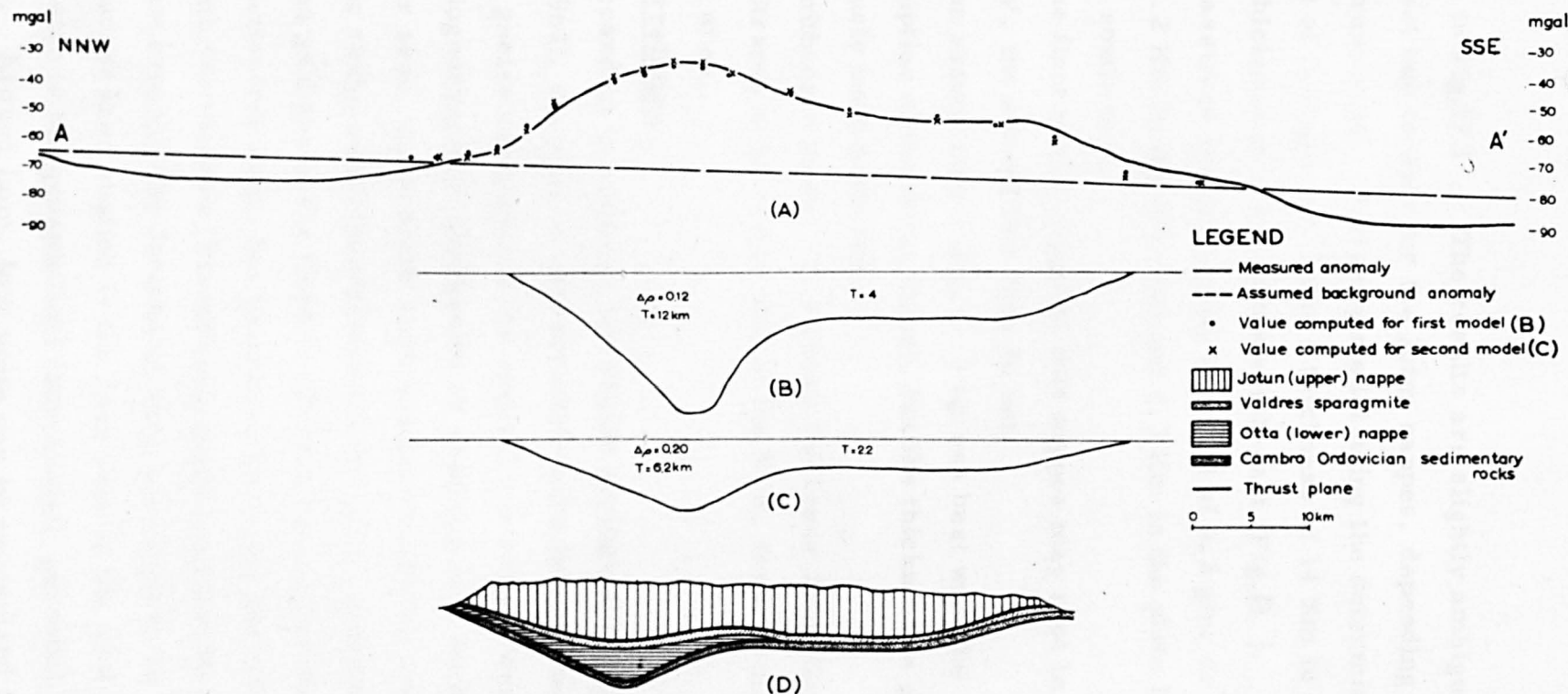


Fig. 2. Profiles through the Jotunheim. A. Bouguer-anomaly profile and the assumed background anomaly. B. Calculated model of the Jotun massif that explains the observed anomalies using a density contrast of 0.12 g/cm<sup>3</sup>. C. Calculated model of the Jotun massif that explains the observed anomalies using a density contrast of 0.20 g/cm<sup>3</sup>. D. Geological interpretation of the gravity model.

work are shown in Fig.173 . The results are slightly ambiguous since he can erect two models for the Jotun nappes, depending on the density contrast used. A gravity model using the determined density contrast of  $0.12 \text{ gm. cc}^{-1}$  has a thickness of 14 Km in the syncline and a thickness of 6 Km to the south-east (Fig.B ). Another model using an assumed higher density contrast of  $0.2 \text{ gm. cc}^{-1}$  shows a thickness of 8.2 Km in the syncline and 4.3 Km in the plate like extension to the south-east.

The first model suggests that nappes may root in the 'Faltungsgaben', the second that they do not.

The second model (fig. C ) agrees best with the geological conception of the Jotun thrust, but the thickness is greater than had previously been supposed.

Smithson's model ( D ) shows the lower Jotun Nappe (Otta Nappe of Strand) to be rather thin in the N. W. towards the present writers area.

### Lithological Correlation

According to orthodox Norwegian geological opinion (Strand 1961, 1964), the area of supracrustal rocks lying between the N. W. basal gneiss complex and the upper Jotun nappe, west of Lom, consists of a miogeosynclinal succession of south-eastern facies. In the Netto seter area, the present work has confirmed the presence of meta-volcanic rocks and demonstrated the presence of alpine-type serpentinites and gabbros in the Cambro-Ordovician succession. Hence, in the Netto seter area, the Cambro-Ordovician succession has affinities with the western (Trondheim) eugeosynclinal facies.

Few areas of the Jotunheim have been studied in any detail. The nearest area studied is the Lom area to the east and here the succession is miogeosynclinal (MacAuslan, personal communication). Around Lom, four units can be recognised from north to south:

Basal gneisses  
 Sparagmites  
 Gneisses of the "base of the Otta nappe"  
 Upper Jotun nappe.

The Cambro-Ordovician sequence of the Nettoseter area has more similarities with the succession of the Sel and Vågå area, east of Lom, established by Strand (1951). This is a eugeosynclinal succession and can be traced into the Trondheim synclinorium. The succession has been fully described by Strand (1951, 1964) and the following revised succession suggested:

Sel micaschist  
 Otta serpentine conglomerate  
 To conglomerate (greenstone conglomerate)  
 Svartkampen group (greenschists, micaschists and  
 greenstones)  
 Heidal group (micaceous quartzites and garnet-mica-  
 schist above basement)

The succession is intruded by saussurite gabbros; slides and thrusts have been recognised.

It can be seen that even over a distance of 35 kms to Lom the succession has changed appreciably and hence detailed correlations are impossible. However, a good general correlation with the Sel and Vågå rocks (and hence the Trondheim synclinorium) can be made. The following similarities are noted.

1. Both successions contain probable thrusts and slides.
2. The general succession Psammites/greenstones/pelites is present in both areas. The absence of the thick conglomerates in the Nettoseter area is only of minor importance, since these are likely to be local deposits.

In the Trondheim synclinorium, three separate orogenies have been recognised, mainly on the basis of conglomerates. These are:

1. Trondheim Orogeny (lower Ordovician), 2. Ekne Orogeny (Upper Ordovician), 3. Horg Orogeny (base of Silurian). The structural significance of these orogenies is unknown.

Postulated correlations between areas of Central Norway can be found in N.G.U. Nr. 164, Pl. 6 and N.G.U. Nr. 208 Pl. 8. At present, the situation can be summarised as follows: While it may be aesthetically satisfying to try to relate the orogenies of the Trondheim area with successive events around Nettos, there is certainly not enough data, at present, to make such a correlation. However a good general lithological correlation can be made with the eugeosynclinal succession of the Sel and Vågå area.

#### Correlation of Metamorphic events

In the Jotunheim, lack of detailed studies on the relationship between folding and metamorphism, prevents a correlation with adjacent areas. At Bygdin, Hossack (1965) found that the main Caledonian metamorphism was immediately after the movement of the upper Jotun nappe. This corresponds with the main greenschist metamorphism in the present area.

#### Structural Correlation

Only three studies involving detailed structural analysis have been undertaken in the Jotunheim. These are

1. Peacey, J. (in Strand 1964)

Prestberget area, Sel and Vaga map area.

2. Hossack, J. (1965)

Bygdin area.

3. MacAuslan, D. (in progress)

Lom area.

Peacey found at least three phases of folding in the Prestberget area.

These were:

F1. Acute isoclinal folds with sharp crests and often intense thinning on the limbs. The axial planes strike W.N.W. and dip steeply to the



N. N. E. The folds plunge 50 slightly south of west.

F2. The orientation is not very different from F1, but the folds are more open with rounded crests. A strong lineation (parallel to fold axes) is present, often a grooving or a rodding.

F3. These are often reclined folds.

Strand correlates F1 with the mise-en-place of the Otta nappe and believes that the main movements to the south and south-east were accommodated by partial movements within the rock and on slides within the nappe complex, as well as movements along the thrust plane.

Strand dates F1 as mid-Ordovician; F3 may be Devonian.

#### Hossack

In the Bygdin area, Hossack found three main phases of folding.

1. N. W. - S. E. trend: synchronous with movement of upper Jotun nappe
2. N. W. - S. E. trend
3. N. E. - S. W. trend.

B1 is a flattening and elongation of conglomerate pebbles and also a direction of folding.

B2 is the major folding

B3 is a cross folding.

#### MacAuslan

In the Lom area, MacAuslan has found a large number of phases of folding; the major folding was E. - W.

It is not possible to make a direct comparison with either Prestberget or Bygdin in view of the distance involved and the different tectonic setting. Further information on the Lom area may permit a correlation.

In all these areas described and possibly along the

Scandinavian Caledonides as a whole (Glomfjell, Soroy, etc.), the first phase has produced very intense acute structures and has been followed by the major fold phase, producing the main geometry of the area.

## CHAPTER 12.

## MINERALOGY

A small amount of work on the composition of the minerals of the area has been carried out and the results are tabulated below. Optic properties of the minerals are incorporated in the petrography.

Insufficient data was obtained to merit a detailed treatment but the work was of some value in determining conditions of metamorphic crystallisation.

### Biotites

Two biotites have been analysed; one from the Hestbrepiggan granite, the other from a schist within the greenstone group. Analysis data and the calculated ion content of each mineral calculated on the anhydrous basis of 22 oxygens per formula unit are presented below. Fig.174 is a qualitative spectrographic analysis of biotite 86.

	<u>63/94</u> (Hestbrepiggan granite)	<u>63/86</u> (greenstone group)
SiO <sub>2</sub>	37.8	35.00
TiO <sub>2</sub>	1.72	2.06
Al <sub>2</sub> O <sub>3</sub>	15.60	16.77
Fe <sub>2</sub> O <sub>3</sub>	8.61	7.12
FeO	19.85	11.16
MnO	0.13	-
MgO	4.80	12.54
CaO	0.91	1.04
Na <sub>2</sub> O	0.90	0.90
K <sub>2</sub> O	7.81	7.30
P <sub>2</sub> O <sub>5</sub>	0.21	-
Total	<u>98.34</u>	

# SPECTROGRAPHIC ANALYSIS

## (QUALITATIVE)

Plate No. 36,37,38.

Work for:

D.R.C.

Date: 11.2.64.

Ag ud	Er nd	Mo ud	Sm nd
Al MC	Eu nd	Na MC	Sn tr
As nd	F nd	Nb ud	Sr ud
Au ud	Fe MC	Nd nd	Ta ud
B ud	Ga nd	Ni ud	Tb nd
Ba mc	Gd nd	Os ud	Te nd
Be ud	Ge ud	P ud	Th nd
Bi ud	Hf nd	Pb ud	Ti tr
Br nd	Hg ud	Pd ud	Tl ud
Ca tr	Ho nd	Pr nd	Tm nd
Cd nd	In ud	Pt ud	U nd
Ce nd	Ir ud	Rb mc	V ud
Cl nd	K MC	Re nd	W ud
Co ud	La ud	Rh ud	Y ud
Cr ud	Li mc	Ru ud	Yb nd
Cs ud	Lu nd	Sb ud	Zn ud
Cu ud	Mg mc	Sc ud	Zr ud
Dy nd	Mn ud	Si MC	

**Final Comments:**

Major Constituents :- Al, Fe, K, Na, Si  
with Ba, Mg, Nb, I.

Trace elements Ca, Sn, Ti.

Sample No.: 63/86

Analyst: A.H.

**Description:**

Biotite with replacement of K by Nb, Na, Ba, Ca and  
replacement of Al by Li.

$(K, Na, Nb, Ba, Ca)_2 (Mg, Fe)_{6-4} (Fe, Al, Li, Ti)_{0-2} (Si, Al)_{2-20-22}$

**Key:**

M. C.  
m. c.  
t. r.

Major constituent  
Minor constituent  
Trace

n. d.  
u. d.

Not determined  
Not detected

(CH, F) 4-2.

Si	6.33		5.283	
Al <sup>4</sup>	1.67	8.00	2.717	8.00
Al <sup>6</sup>	0.74		0.253	
Ti	0.176		0.241	
Fe <sup>3</sup>	0.86		0.810	
Fe <sup>2</sup>	2.19	4.934	1.406	5.561
Mn	0.01		-	
Mg	0.955		2.851	
Ca	0.126		0.177	
Na	0.251	1.684	0.279	1.875
K	1.307		1.419	

The high TiO<sub>2</sub> content is probably responsible for the strong pleochroism. The Mg/Fe<sup>2+</sup> ratio for the biotite from the schist is much higher than that from the granite.

### Hornblendes

Two partial analyses of hornblendes are presented below; both are from amphibolites in the greenstone group. The calculated ion content of each mineral calculated on the anhydrous basis of 23 oxygens per formula unit is given and Fig.17 5 shows tetrahedrally co-ordinated Al<sup>4</sup> plotted against Al<sup>6</sup>, Fe<sup>3+</sup>, Ti.

	<u>63/14</u>	<u>62/21</u>
SiO <sub>2</sub>	45.6	46.4
TiO <sub>2</sub>	0.81	0.85
Al <sub>2</sub> O <sub>3</sub>	10.80	11.46
Fe <sub>2</sub> O <sub>3</sub>	3.10	2.84
FeO	12.40	12.42
MnO	tr.	-
MgO	9.79	8.75
CaO	12.83	10.72

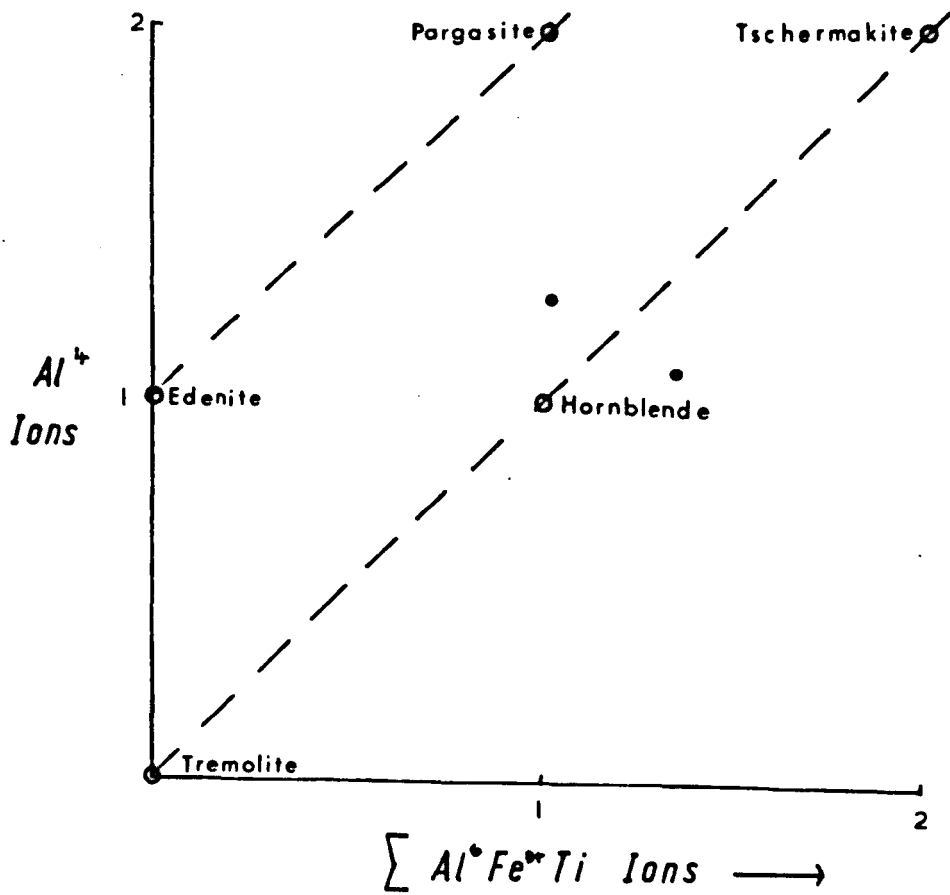


Fig.175 Composition of hornblendes.

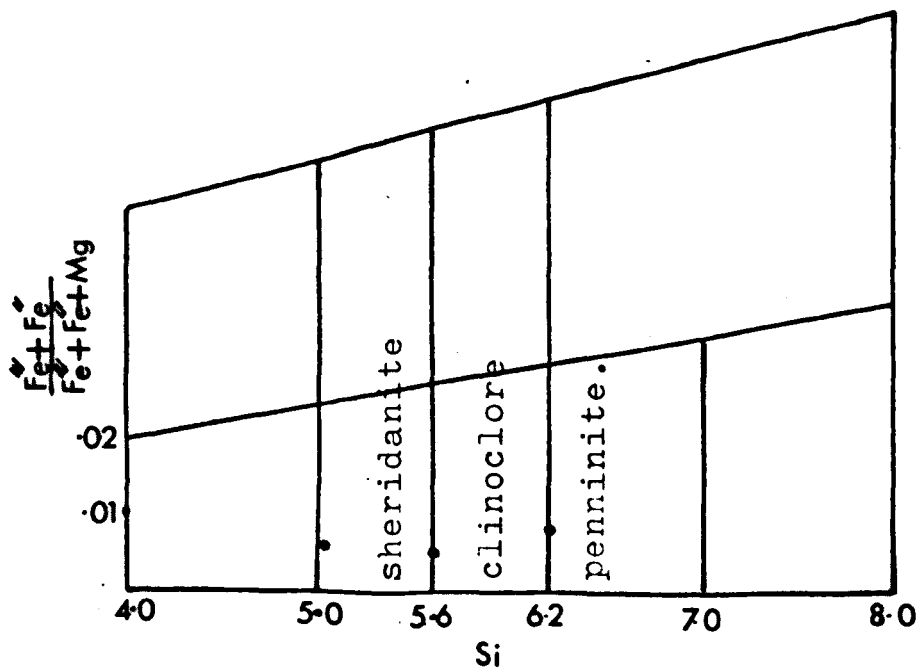


Fig.176. Nomenclature of ortho-chlorites.  
(after Hey 1954).

Na <sub>2</sub> O	2.06		1.62	
K <sub>2</sub> O	0.56		0.53	
P <sub>2</sub> O <sub>5</sub>	0.06		0.01	
Si	6.720		6.927	
Al <sup>4</sup>	1.280	8.000	1.073	8.000
Al <sup>6</sup>	0.593		0.926	
Ti	0.084		0.096	
Fe <sup>3+</sup>	0.336		0.301	
Fe <sup>2+</sup>	1.524	3.704	1.547	4.828
Mn	-		-	
Mg	2.167		1.958	
Ca	2.027		1.711	
Na	0.587	2.625	0.466	2.188
K	0.011		0.011	

The data is consistent with common hornblende.

### Garnets

Two analyses of garnet from garnet-mica-schist are presented below and the calculated ion contents on the basis of 24 oxygens per formula unit given. The garnets are recalculated in terms of percentage end members.

	<u>63/84</u>	<u>63/79</u>
SiO <sub>2</sub>	37.57	38.12
TiO <sub>2</sub>	0.11	0.13
Al <sub>2</sub> O <sub>3</sub>	20.13	20.71
Fe <sub>2</sub> O <sub>3</sub>	0.97	1.21
FeO	33.12	35.51
MnO	0.47	0.21
MgO	4.16	3.97
CaO	0.72	0.51



Si	6.153	6.090	
Al <sup>4</sup>	6.153		6.090
Al <sup>6</sup>	3.833	3.866	
Ti	0.014	0.014	4.019
Fe <sup>3</sup>	0.111	0.139	
Fe <sup>2</sup>	4.528	4.728	
Mn	0.069	0.028	
Mg	1.028	0.946	5.785
Ca	0.125	0.083	

almandine	78.6	81.7
Andradite	2.2	1.4
Grossularite	-	-
Pyrope	17.9	16.4
Spessartine	1.3	0.5

### Epidote

A partial analysis of vein epidote from the basal gneisses is presented below and the calculated ion content on the basis of 13 oxygens given

SiO <sub>2</sub>	38.21	
TiO <sub>2</sub>	0.28	
Al <sub>2</sub> O <sub>3</sub>	23.16	
Fe <sub>2</sub> O <sub>3</sub>	11.60	
FeO	1.11	
MnO	0.12	
MgO	0.66	
CaO	20.46	
Si	3.216	3.216

Al <sup>6</sup>	2.273	
Ti	0.019	3.029
Fe <sup>3</sup>	0.737	
Fe <sup>2</sup>	0.075	
Mn	0.013	2.017
Mg	0.087	
Ca	1.842	

According to Strens (1962) Ca, Si and (OH) proportions in the clinozoisite-pistacite series is virtually constant and the amount of substitution of Fe<sup>3+</sup> for Al<sup>6</sup> is important. The amount of Fe<sup>3+</sup> substituting for Al is approximately 25%, hence the epidote mineral is a pistacite (Winchell 1956).

### Chlorites

Three chlorites from the aureole of the serpentinites were analysed and the results are tabulated below, along with the calculated ion content of each mineral calculated on the anhydrous basis of 28 oxygens per formula unit. Fig 176 shows part of the proposed classification of chlorites (Hey 1954). The chlorites analysed fall between the fields of sheridanite and clinocllore.

	63	68	69
SiO <sub>2</sub>	31.7	28.3	25.9
Al <sub>2</sub> O <sub>3</sub>	12.25	17.89	18.77
Fe <sub>2</sub> O <sub>3</sub>	2.48	1.68	3.03
FeO	3.56	8.18	10.80
MnO	tr.	0.30	0.37
MgO	32.90	29.50	29.00
CaO	0.23	tr.	0.11

Na <sub>2</sub> O	1.43	1.40	1.30
K <sub>2</sub> O	1.10	1.00	1.00
Si	6.22	5.530	5.067
Al	1.78 8.00	2.470 8.00	2.933 8.00
Al	1.04	1.627	1.389
Ti	-	0.000	-
Fe	0.371	0.254	0.436
Fe	0.576	0.134	0.176
Mn	- 11.672	0.054 11.437	0.073 11.352
Mg	9.711	8.648	8.499
Ca	0.056	-	0.018
Na	0.557	0.510	0.508
K	0.297	0.210	0.254

The high content of alkalis is difficult to explain.

The values were rechecked and the sample was examined for impurities such as mica, but this proved negative. It is possible that these are alkaline chlorites but this is difficult to explain in view of the structure.

### Talc

An analysis of talc from the outer zone of a serpentinite body is tabled below and the calculated ion content on the basis of 20 (O) and 4 (OH) per formula unit given.

SiO <sub>2</sub>	62.1	
Al <sub>2</sub> O <sub>3</sub>	1.60	
FeO	3.50	
MgO	25.4	
CO <sub>2</sub>	0.33	
H <sub>2</sub> O	6.6	
Si	7.34	7.35
Al	0.011	
Fe	0.348	
Mg	4.640	4.988

The high water content may be due to adsorbed water.  
Some ferrous iron substitutes for magnesium.

#### Magnesite

Two partial analyses of magnesite are presented below. The total MgO + FeO is very nearly the theoretical ratio MgO/MgCO<sub>3</sub>.

	(A)	(B)
Total Fe as Fe <sub>2</sub> O <sub>3</sub>	8.74	9.31
MgO	34.50	37.00

CHAPTER 13.

## LABORATORY METHODS

### Specimen Collection

During field work, rock specimens were collected for several purposes:

- (1) Rocks considered to be representative of specific lithologies
- (2) Unusual rocks from lithologies of limited occurrence
- (3) Geochemical specimens of selected ultrabasics and amphibolites. Representative samples of fresh rock were collected
- (4) Structural specimens showing interesting minor structures. These specimens were oriented in the field and in some cases three oriented thin sections were cut.

### Microsections

Approximately two hundred and fifty micro-sections of rock specimens were prepared, of which over half were prepared by the writer. The K-feldspar of appropriate slides was stained yellow with sodium cobaltinitrite (Chayes 1952, Bailey and Stewins 1960). Most thin sections were mounted on 2" x 1" slides to facilitate mineral and fabric analysis.

### Preparation of analytical specimens

#### (1) Whole Rock Analysis

Fresh specimens were broken down to 1" fragments using a hydraulic splitter and then crushed by a jaw crusher to a coarse powder. The sample was crushed to a fairly fine powder (80 mesh) by passing through a cone grinder, and the sample was repeatedly quartered until an adequate portion for analysis remained. This was then powdered further in an automatic mortar and by hand to approximately 200 mesh.

## (2) Mineral Preparation

Fresh rock samples were crushed to a coarse powder in the jaw crusher. The powder was elutriated to remove the fine material and dried. The material was then sieved and crushed further until a sample of the required size was obtained. This was found to vary with the separation technique used and individual minerals. Flakey minerals such as chlorite and talc were ground in a mica crusher.

Several separating techniques were used and none were found more than 80% efficient. In the end most samples had to be separated by hand. Techniques used include:

1. "Franz-type" isodynamic magnetic separator. This was useful for separating felsic/mafic fractions
2. Davies non-entraining rotary magnetic separator (model 45V).  
This was much more efficient than the "Franz-type"
3. A symmetric Vibrator Separator. This was useful for separating biotites
4. Heavy liquid methods
  - (a) Bromoform
  - (b) Methylene iodide.

It was not found possible to separate hornblende from biotite by heavy liquid separation.

## Chemical Analysis

Chemical analyses were made according to methods modified after the techniques of Shapiro and Brannock (1952, 56). Spectrophotometric measurements were made on a Hilger and Watts "Uvispek" photoelectric spectrophotometer (H 700-307). Flame photometric measurements were made on a Unicam spectrophotometer SP 900.

(1) Silica

Two methods were used for silica.

The first method was after Shapiro and Brannock (1956) which measures the absorbence of the blue complex resulting from the reduction of the yellow silico-molybdate complex.

The second method (Bloxam 1961) was the yellow complex buffered to pH 3 with chloroacetic acid. The insensitivity of the spectrophotometer at 390 m $\mu$  for this complex can be overcome by using 4 cm. cells.

(2) Alumina

The colorimetric method of Hill (1956) was used throughout this work. This method involves forming a solochrome-cyanine-R-aluminium complex in the presence of sodium mercaptoacetate; the final solution being buffered to pH 6 with ammonium acetate.

(3) Total Iron

Total iron as Fe<sub>2</sub>O<sub>3</sub> was determined by forming a complex with orthophenanthroline in the presence of sodium citrate (Shapiro and Brannock (1956) and measuring the absorption of the resulting orange-red complex at 560 m $\mu$ .

(4) Ferrous Oxide

Two methods were employed, one for whole rock analyses and one for minerals.

For whole rocks the volumetric method of Wilson (1955) was used. This is a back-titration method.

For mineral analyses the micro-colorimetric method of Wilson (1960) was used.

(5) Alkalis Na<sub>2</sub>O, K<sub>2</sub>O

These were determined by flame photometry after



precipitation of iron and aluminium with ammonium hydroxide. Working curves for the spectrophotometer were constructed by Hayward (1965).

(6) Calcium Oxide

Two methods were used and found to be equally satisfactory. In the first method CaO was determined by titration against E.D.T.A. using murexide as an indicator (Shapiro and Brannock 1956).

In the second method CaO was determined by flame photometry (after Hayward 1965)

(7) Magnesium Oxide

Three methods were used at different times.

- (a) Titration with E.D.T.A. using Eriochrome-black-T as the indicator (Shapiro and Brannock 1956).
- (b) Atomic Absorption Spectroscopy.

This was found to be very reliable for small concentrations (0-3 ppm.  $Mg^{2+}$  in solution). Interference by Al was overcome by adding an excess of Sr (2500 ppm.).

- (c) Flame Photometry.

This was fairly accurate for medium concentrations, but useless for small concentrations of  $MgO$ .

(8) Titania  $TiO_2$

Titanium was converted to titanium peroxide and the absorption of the yellow complex measured at 400 m $\mu$  (Shapiro and Brannock 1952).

(9) Manganous Oxide  $MnO$

The method of Shapiro and Brannock (1956) was employed. Manganous oxide was oxidised to permanganate with  $KIO_3$  and the absorption of this compound was measured at 525 m $\mu$ .

(10) Phosphorus Pentoxide  $P_2O_5$ 

A yellow molybdivanadophosphoric acid complex was formed and the absorption measured at 430 m $\mu$ . (Shapiro and Brannock 1952).

(11) Water and  $CO_2$ 

Attempts were made to determine water and  $CO_2$  by the method of Riley (1958) but only partial success was achieved. In the end water and  $CO_2$  combined were determined by heating in a furnace.

(12) Nickel

Ni was determined by the method of Sandell (1950) involving a chloroform separation.

(13) Zinc

A few zinc measurements were made after the method of Burrell (1964, 65). Instrumental peculiarities were marked.

Modal Analysis

The few modal analyses presented in this thesis were made using a Swift automatic point counter and the procedure followed was that of Chayes (1952) and Solomon (1963).

Many rocks were too fine-grained for Modal analysis (Serpentinities) and in others the difficulty of distinguishing quartz from albite prevented modal analysis.

X-ray

X-ray powder photographs of a number of minerals were made. These were taken by Mr. J. Eyett using Iron filtered Co.  $K_{\alpha}$  radiation.

- BAILEY, E.H. & STEWINS, R.E. 1960. Selective staining of K feldspar and plagioclase on rock slabs and thin sections. *Am. Min.* 45, 1020.
- BANHAM, P.H. 1962. Geological Structures and metamorphic history of the Hestbrepiggen area ( Jotunheim Norway). Ph.D. Thesis (1962), Nottingham University.
- BANHAM, P.H. & ELLIOTT, R.B. 1965. Geology of the Hestbrepiggen area ; Preliminary Account. *N.G.T.* 45, 2
- BARTH, T.F.W. 1938. Progressive metamorphism of sparagmite rocks of southern Norway. *N.G.T.* 18, 54.
- BENSON, W.N. 1918. The origin of serpentine. *Am. Jour. Sci.* 46, 693-731.
- BJÖRLYKKE, K.O. 1902. Fra Hardangervidda . *N.G.U.* 34.
- BJÖRLYKKE, K.O. 1905. Det Centrale Norges Fjeldbygning *N.G.U.* 39.
- BLOXAM, A.B. 1961. Photometric determination of silica in rocks and refractory materials. *Anal.* 86, 420.
- BOWEN, N.L. & TUTTLE, O.F. 1949. The system  $\text{MgO-SiO}_2\text{-H}_2\text{O}$  *Geol. Soc. America Bull.* 60, 439-460
- BROGGER, W.C. 1893. Lagfølgen på Hardangervidda og den såkalte "Höifjeldskvarts." *N.G.U.* 11.
- BURRELL, D.C. 1964. Ph.D. Thesis, Nottingham University.
- BURRELL, D.C. 1965. The determination of zinc in amphibolites by atomic absorption spectroscopy. *N.G.T.* 45, 21-31.
- CHAYES, F. 1952. Note on the staining of potassium feldspars with sodium cobaltinitrite. *Am. Min.* 37, 332.
- CHAYES, F. 1956. Petrographic modal analysis. Wiley & Sons Inc. New York.
- CLOOS, E. 1946. Lineation. *Geol. Soc. America Mem* 18.

- De Sitter, L.U. 1958. Schistosity and shear in micro and macro folds. *Geol. en Mijnbouw*, 16, 429-439.
- DONS, J.A. 1960 (Ed) Norwegian guide books.  
Int. Geol. Cong. XX1 Sess. Norden 1960.
- FLEUTY, M.F. 1964. The description of folds. *P.G.A.* 75, 461.
- FLINN, D. 1956. Deformation of the Funzie conglomerate, Feltar, Shetland. *Jour. of Geol.* 64, 480-505.
- FLINN, D. 1962. On folding during three-dimensional progressive deformation. *Q.J.G.S.* 118, 385-433.
- FOSLIE, S. 1931. On antigorite-serpentinites from Ofoten with fibrous and columnar vein minerals. *N.G.T.* 12, 219.
- GJELSVIK, T. 1953. Det nordvestlige gneiss-område i det sydlige Norges alders forhold og tektonisk-stratigraphisk stilling. *N.G.U.* 184.
- GOLDSCHMIDT, V.M. 1912. Die Kaledonische Deformation der Sudnordwegischen Urgebirgstafel. *Vid. Selsk.* 1912, 19.
- GOLDSCHMIDT, V.M. 1916. Übersicht der Eruptivgesteine im kaledonischen Gebirge zwischen Stavanger und Trondheim. *Vid. Selsk.* 1916, 2.
- HAYWARD, A. 1965. M.Sc. Thesis, Nottingham University.
- HESS, H.H. 1933. The problem of serpentinitisation and the origin of certain chrysotile asbestos, talc and soapstone deposits. *Econ. Geol.* 28, 634-657.
- HESS, H.H. 1938. A primary peridotite magma. *Am. Jour. Sci.* 35.
- HESS, H.H. 1955. Serpentine, orogeny and epeirogeny. *Geol. Soc. America Special Paper* 62, 391-408.
- HEY, M.H. 1954. A new review of the chlorites. *Min. Mag.* 30, 277.
- HIGGINS. 1964 Ph.D. Thesis, Imperial College.

- HILL, U.T. 1956. Direct photometric determination of aluminium in iron ores. Anal. Chem 28, 1419.
- HOLTEDAHL, O. 1938. Geological observations in the Oppdal-Sundal-Trollheimen district. N.G.T. 18, 29.
- HOLTEDAHL, H. 1950. Geological and petrological investigations in the north-west part of the Oppdal Quadrangle. B.U. 1949, 7.
- HOLTEDAHL, C. 1960 (Ed) Geology of Norway. N.G.U. 208.
- HUBBERT, M.K. & RUBEN, W.W. 1959. Role of fluid pressure in mechanics of overthrust faulting. Bull. Geol. Soc. America. 70, 115-166.
- HOSACK, J. 1965. Ph.D. Thesis, University of Edinburgh.
- KRUMBEIN, W.C. 1959. Trend Surface Analysis. Jour. Geophys. Res. 64, 823-34.
- LANDMARK, K. 1948. Geologiske undersøkelser i Luster-Bøverdalen. B.U. 1948. 1.
- LANDMARK, K. 1951. Tverfolding i den kaledonisk fjellkjede. N.G.T. 29, 241.
- MCCIRNEY, A.R. & BEST, M. 1961. Experimental deformation of viscous layers in oblique stress fields. Geol. Soc. America. Bull. 72, 495-498.
- MEHNERT, K.R. 1939. Die meta-konglomerate des Wiesenthaler Gneiszes im Sächsischen Erzgebirge. Min. Petr. Mitt. 50, 194.
- NADAI, A. 1950. Theory of flow and fracture of solids Vol 1. MCGRAW-HILL, N.Y.
- OFTEDAHL, C. 1964. The nature of the basement contact. N.G.U. 227.
- PATERSON, M.S. & WEISS, L.E. 1962. Experimental folding in rocks. Nature 195, 1046-1048.

- PETTIJOHN, F.J. 1949. Sedimentary rocks. Harper & Bros. N.Y.
- RAMBERG, H. 1962. Contact strain and folding instability of a multilayered body under compression. Geol. Rdsch. 51, 405-439.
- RAMBERG, H. 1963(a). Strain Distribution and Geometry of Folds. Bull. Geol. Inst. Uppsala. 42, pt 4.
- RAMBERG, H. 1963(b). Fluid Dynamics of Viscous Buckling Applicable to Folding of Layered Rocks. Bull. Amer. Assoc. Petr. Geol. 47, 484-505.
- RAMSAY, J.G. 1956. The Supposed Moinian Basal Conglomerate at Glen Strathfarrar, Inverness-shire. Geol. Mag. 93, 32-41.
- RAMSAY, J.G. 1958. Superimposed folding at Loch Monar, Inverness-shire and Ross-shire. Q.J.G.S. 113, 277-307.
- RAMSAY, J.G. 1960. Deformation of early linear structures in areas of repeated folding. Jour. of Geol. 68, 75-83.
- RAMSAY, J.G. 1962 (a) The Geometry and Mechanics of Formation of Similar Type Folds. Jour. Geol. 70, 309.
- RAMSAY, J.G. 1962 (b) Interference Patterns produced by Superposition of Folds of Similar Type. Jour. Geol. 70, 466-481.
- RAST, N. 1956. The Origin and Significance of Boudinage. Geol. Mag. 93, 401-409.
- REITAN, P.H. & GEUL, J.J.C. 1958. On the formation of a carbonate bearing ultrabasic rock at Kviteberg, Lyngen, Northern Norway. N.G.U. 205.
- REKSTAD, J. 1914. Fjeldstroket mellem Lyster og Böverdalen. N.G.U. 69.
- RILEY, J.P. 1958. Simultaneous determination of water and carbon dioxide in rocks and minerals. Anal. 83, 42.
- SANDELL, E.B. 1950. Chemical Analysis 3. Colorimetric

Determination of traces of Metals 2<sup>nd</sup> Ed.

Interscience Publications Inc.

SANDER, B. 1912. Über Einige Gesteinsgruppen des Tauern Westendes. Jahrb. Geol. Bundesanstalt 62, 219-287.

SCHIEFERDECKER, A.A.G. 1959. Geological Nomenclature.

Roy. Geol. & Min. Soc. Neth Gorinchem.

~~SMITHSON~~ SMITHSON, S. 1964. Foreløpige resultater av tyngdemålinger over Jotun-dekkene.

Saertrykk av Tidsskrift for Kjemi, Bergvesen og Metallurgi 5, 77-101.

SHAPIRO, L & BRANNOCK, W.W. 1952. Rapid analysis of silicate rocks. Am. Geol. Surv. Circ. 165.

SHAPIRO, L & BRANNOCK, W.W. 1956. Rapid Analysis of Silicate Rocks. Am. Geol. Surv. Bull. 1036.

SHOULS, M.M. 1958. The Geology of the Metamorphic Rocks near Sotaset, Norway. Ph.D. Thesis, Nottingham University.

SOLOMON, M. 1963. Counting and sampling errors in modal analysis by point counter. Jour. Pet. 4, 367.

STRAND, T. 1949. On the gneisses from a part of the N.W. gneiss area of southern Norway.

STRAND, T. 1951. Sol and Vågå map areas. N.G.U. 178.

STRAND, T. 1953. The relationship between the basal gneisses and the overlying metasediments in the Surnadal area. N.G.U. 184, 100.

STRAND, T. 1961. The Scandinavian Caledonides-a review. Am. Jour. Sci 259, 161.

STRAND, T. 1964. Geology and structure of the Frestberget area. N.G.U. 228

STRAND, T. 1964. Otta-dekket og Valdres-gruppen i strøkene langs Løverdalen og Leirdalen. N.G.U. 228.

- STRENS, R.G.J. 1962. Ph.D Thesis, Nottingham University.
- TALIAFERRO, N.L. 1943. The Franciscan-Knoxville problem  
Am.Assoc. Petr. Geol. Bull. 27, 109-219.
- TURNER, F.J. 1948. Evolution of the Metamorphic Rocks.  
Geol. Soc. America. Mem. 30.
- TURNER, F.J., GRIGGS, D.T., CLARK, R.H. & DIXON, R.H. 1956.  
Deformation of Yule Marble.  
Geol. Soc. America. Bull. 67, 1259.
- TURNER, F.J. & VERHOOGAN, J. 1960. Igneous and Metamorphic  
Petrology. McGraw-Hill. N.Y.
- TURNER, F.J. & WEISS, L.E. 1963. Structural Analysis of  
Metamorphic Tectonites. McGraw-Hill. N.Y.
- WAARD, D.D.E. 1959. Anorthite content of plagioclase in  
basic and pelitic crystalline schists as  
related to the metamorphic zoning in the  
Ursu massif, Timor. Am. Jour. Sci. 257, 553.
- WEISS, L.E. & MCINTYRE, D.B. 1957. Structural geometry of  
the Dalradian rocks of Loch Leven.  
Jour. Geol. 65, 575.
- WILEY, P.G. 1960. The system  $\text{CaO-MgO-FeO-SiO}_2$  and its  
bearing on the origin of ultrabasic and basic  
rocks. Min. Mag. 32.
- WILSON, G. 1953. Mullion and rodding structures in the  
Moine Series of Scotland. P.G.A. 64.



## ACKNOWLEDGEMENTS

The writer wishes to thank all those who have contributed to the preparation of material for this thesis.

Firstly, to Professor W.D. Evans for making facilities available in the Department of Geology, University of Nottingham. Secondly, to Dr. R.B. Elliott who supervised the work and whose advice and discussion have been invaluable. Thirdly, to Dr. P.H. Banham of the University of London, who introduced the writer to the Jotunheim in 1961 and who has provided much advice and discussion, both in the field and in the laboratory. To Mr. Graham Precious and Mr. Frank Nixon, undergraduates from the Department of Geology, University of Nottingham, who acted as field assistants.

Professor J.G. Ramsay allowed the writer to use unpublished data on the "sedimentary shape factor of deformed conglomerates", and provided interesting and useful discussion on factors involved in conglomerate deformation.

I would like to thank my colleagues at Nottingham and elsewhere for stimulating and useful discussions on a wide range of topics.

The assistance of Mr. T. Foster in the preparation of microsections and Mr. J. Eyett for considerable photographic assistance is greatly acknowledged.

The final geological map was prepared by Mr. Gordon Smith to whom the writer is indebted.

Finally, the assistance in preparation of this thesis given by Miss Sheila Hicks was of great value.

This work was carried out during a three year tenure of a D.S.I.R./S.R.C./N.E.R.C. studentship, for which the writer is duly grateful.

THE GEOLOGY OF THE COUNTRY AROUND NETTOSETER,  
HÖYDALEN, NORWAY

---

by D.R. COWAN, B.Sc.

A B S T R A C T

The area is part of the north-west Jotunheim mountains in southern Norway and consists of three main rock units; Granitic rocks of the Basal Gneiss Complex outcrop in the north of the area; supracrustal rocks of presumed Eo-Cambrian to Ordovician age in the central part and the Upper Jotun Nappe outcrops in the south.

Previous work in the area (mainly by Nottingham workers) had shown that the supracrustal rocks were thrust onto basal gneisses. The detailed structure of the supracrustal rocks, the relationship of the Upper Jotun Nappe to underlying rocks and structure and the metamorphic history were unknown and little detailed petrography and chemistry of the supracrustal rocks had been carried out.

The writer, by means of detailed structural analysis, with petrographic, chemical and mineralogical studies, has attempted to reconstruct the detailed metamorphic and structural history of the supracrustal rocks.

The stratigraphy and a description of the lithologies with field relations, petrography and chemistry are given and a special

study made of amphibolites and dunite-serpentinites.

The structure of the area is complex; Pre-Cambrian structures from the Basal Gneiss Complex and Upper Jotun Nappe and five phases of Caledonian deformation (excluding joints) are recognised. Orientation and symmetry of folds are discussed.

Occurrences of conglomeratic structures are described; these are B-tectonites, essentially tectonic inclusions formed by disruption of continuous layers.

A quantitative study of fold styles is presented and folding is discussed in kinematic terms; the second Caledonian deformation (B2) is complex.

A movement picture is suggested for each main phase of deformation. A quantitative fold description is considered and B2 folding is discussed from theoretical and experimental points of view.

The metamorphic history of the area is described; three Caledonian metamorphisms and several Pre-Cambrian phases described.

A tentative geological history is presented and some of the broader aspects of the work discussed.

Mineral analyses are presented and a brief description of the methods used given.

